LATE PLEISTOCENE-HOLOCENE SEDIMENTATION, BURIED RIVER CHANNEL MORPHOLOGY AND SEISMIC STRATIGRAPHY OF INNER CONTINENTAL SHELF OFF GOA, WEST COAST OF INDIA

Thesis submitted to the

GOA UNIVERSITY

for the award of the degree of

DOCTOR OF PHILOSOPHY

IN

MARINE SCIENCES

By

Kanchan Mani Dubey

Under the guidance of

Dr. A. K. Chaubey

GOA UNIVERSITY

Taleigao Plateau,

Goa

July 2019

LATE PLEISTOCENE-HOLOCENE SEDIMENTATION, BURIED RIVER CHANNEL MORPHOLOGY AND SEISMIC STRATIGRAPHY OF INNER CONTINENTAL SHELF OFF GOA, WEST COAST OF INDIA

Thesis submitted to the **Goa University** for the award of the degree of

DOCTOR OF PHILOSOPHY

IN

MARINE SCIENCES

By

Kanchan Mani Dubey

Under the guidance of

Dr. A. K. Chaubey
Former Chief Scientist
(CSIR-National Institute of Oceanography, Dona Paula, Goa)

July 2019

सर्वतीर्थमयी माता सर्वदेवमय: पिता।
मातरं पितरं तस्मात् सर्वयत्नेन पूजयेत्।।

(पद्मपुराण सृष्टिखंड, 47/11)

Dedicated to
My Mummy and Papa

For my Guru

गुरुर्ब्रह्मा गुरुर्विष्णुर्गुरुर्देवो महेश्वरः ।
गुरुःसाक्षात् परब्रह्म तस्मै श्रीगुरुवे नमः॥

(आदिशंकराचार्य गुरुस्तोत्रम्)

Declaration

As required under the Goa University guidelines, I state that the present thesis entitled "**Late Pleistocene-Holocene sedimentation, buried river channel morphology and seismic stratigraphy of inner continental shelf off Goa, west coast of India**" is my original research work carried out at the CSIR-National Institute of Oceanography, Goa and no part thereof has been submitted for any other degree or diploma in any university or institution. The literature related to the problem investigated has been cited. Due acknowledgements have been made wherever facilities and suggestions have been availed of.

Kanchan Mani Dubey
Ph.D. Student
Goa University

Certificate

This is to certify that the thesis entitled **"Late Pleistocene-Holocene sedimentation, buried river channel morphology and seismic stratigraphy of inner continental shelf off Goa, west coast of India"** submitted by **Mr. Kanchan Mani Dubey** for the award of the degree of Doctor of Philosophy in the Department of Marine Sciences, embodies original research work under my supervision. The thesis or any part thereof has not been previously submitted for any degree or diploma in any university or institution. Research material obtained from other sources has been duly acknowledged in the thesis. Any text, illustration, table etc. used in the thesis from other sources, have been duly cited and acknowledged.

Dr. A. K. Chaubey
Former Chief Scientist
CSIR-National Institute of Oceanography
Dona Paula, Goa-403004

Acknowledgements

I would like to express my thanks and indebtedness to all those who have supported, helped, and encouraged me throughout this long journey. First and foremost, I would like to express my indebtedness and heartfelt gratitude to my research supervisor, **Dr. Anil Kumar Chaubey**, Former Chief Scientist, CSIR-National Institute of Oceanography, Goa, for his support, valuable advice, inspiring guidance, constant encouragement and patience from introduction of research topic to the completion of the thesis. It would not have been possible to complete this research work without his constant motivation, provoking discussions, critical comments and support during the course of work at NIO, Goa. He has always remained so kind, affectionate and caring to me.

I take this opportunity to express my sincere thanks to Prof. Sunil Kumar Singh, Director, CSIR-NIO as well as former directors Dr. S.W.A. Naqvi, Dr. S. Prasanna Kumar and Dr. V.S.N. Murthy for supporting me to carry out research and avail the facilities of NIO.

I profusely thank Dr. S.M. Karisiddaiaih, Dr. P.S. Rao and Shri T. Ramprasad (Former Chief Scientists, CSIR-NIO, Goa) for generously devoting their time for editing the thesis and providing fruitful suggestions. I am also thankful to Dr. R. Nigam (Former Deputy Director, CSIR-NIO, Goa), Dr. S.D. Iyer, (Former Chief Scientist, NIO, Goa) Dr. K Srinivas (Principle Technical Officer, CSIR-NIO, Regional center, Visakhapatnam), Dr. R. Saraswat (Senior Scientist, CSIR-NIO, Goa), Dr. V. Yatheesh (Senior Scientist, CSIR-NIO, Goa), and Dr. Jacob Jensen (Scientist, CSIR-NIO, Goa), for their time to time critical comments and useful suggestions.

I am truly obliged to my Departmental Research Committee (DRC) members, Prof. K.S. Krishna (Centre for Earth, Ocean and Atmospheric Sciences, University of Hyderabad), Prof. G. N. Nayak (Department of Marine Sciences, Goa University), for their critical comments and valuable suggestions during different stages of my research work.

I place on record my gratitude to Prof. H.B. Menon, Dean School of Earth Ocean and Atmospheric Sciences, Goa University as well as former heads Prof. C.U. Rivonkar and Prof.

V.M. Matta for all the official support required for smooth conduction of the research work at Department of Marine sciences, Goa University.

Further, I am grateful to entire survey and Instrumentation team including Mr. V.P. Mahale (Senior Scientist, CSIR-NIO, Goa), Mr. G. Walker, Mr. S.S. Gaonkar, (Former Principle Technical Officers, CSIR-NIO, Goa), Mr. D.K. Naik, Mr. A. Sardar, (Principle Technical Officers, CSIR-NIO, Goa), Mr. G.M. Tirodkar, Mr. C. Vaz, (Senior Technical Officers, CSIR-NIO, Goa) for the technical support and co-operations provided during the survey program. Special mention to Mr. P Marathe, Mr. V. D. Khedekar, and Mr. D Gracias, for introducing me with practical aspect of marine geophysical surveying and training me for the same. I express thanks and appreciations to Mr. M.M. Milind, B.H. Patole, Ramesh T. and Kuldeep Kumar for their technical support provided onboard RV Sindhu Sadhana. I also acknowledge Masters and all the crew of RV Sindhu Sadhana and boatmen of MFB Falguni for their assistance during the surveys.

I acknowledge University Grant Commission (UGC), New Delhi for financial support through an award of UGC-CSIR (NET)-JRF/SRF to carry out the research work. I also thank Mr. V. Krishna Kumar, Mr. Tejesh Marihal, Mr. Thavapandian P., Mr. Rohit M. Dhavjekar, and all office staff at CSIR-National Institute of Oceanography, Goa and Yashwant Naik and all office staff at Department of Marine sciences, Goa University, Goa for their assistance and timely administrative support.

A research cannot be completed without the active support of the colleagues and fellows, both present and the past. I have learnt several things and received fruitful comments while discussions. I got their support in all the possible ways at various stages of my research work. They have always remained warm and affectionate to me. A special appreciation goes to my loving friends and lab-mates Mr. Rajeev Yadav, Mr. H Dattaram, Mr. S.P. Balooni, Mr. Pankaj Kumar, Dr. Sujata Raikar, Akhil Mishra, Shravan Kumar, Pitchika Vinay Kumar, Vimal Maurya, Dhruv Singh, Vijay, Roopesh T. Naik, Sripad R. Bandodakar Pabitra Singha, Chandan Kumar Mishra, Pankaj Prasad, Ramanand Yadav, Lalit Arya, and Trilochan Kumar for their support, care and encouragements. I am also thankful to Govind Joshi, Dr. Soumya Mohan, Aditi Mitra, Kalpna Chandel, Mintu Chowdhury, and other friends from NIO for their support and motivation. I would also like to acknowledge my close friends Rajwant Singh and Abhishek Singh for moral support and motivation.

I am, indeed, short of words to express my inner-feeling to my beloved family members. On this occasion, I remember my mother Mrs. Radha Dubey who remained with me in different faces (Mrs. Suman Dubey, Mrs. Urmila Patel). I always felt her around me and received her blessings. I express my heartfelt gratitude to my father Mr. Mata Prasad Dubey who devoted his entire life to make me reach at higher destinies. He always stood behind me for all important decisions, particularly for pursuing PhD after the Master's Degree. I am highly indebted to him for giving me constant encouragements and moral support throughout the course of work. Therefore, I dedicate this thesis to him.

I am hugely grateful to my younger brothers Anupam, Vivek, Rohit, and My Sister-in-law Mrs. Deepika Dubey for their affection, continuous support and encouragements. I express deep sense of gratitude to my beloved sisters Arati and Nisha. My many special thanks are also due to my wife Mrs. Beenu K. M. Dubey for her patience and support which was a continuous source of inspiration to continue this work. In the last, I would also like to acknowledge my sweet little baby and bundle of joy "Siddhiksha". She joined me in this journey recently after the thesis submission.

Contents

List of Figures

List of tables

Preface

The sedimentary records from continental shelves of the world normally represent an ideal archive to study various sedimentary processes as well as for deciphering past fluctuations in climate system and possible forcing mechanism. Late Quaternary is characterized by a succession of several relative sea-level fluctuations of high amplitude. Therefore, modern continental shelves have evolved under the effect of sea-level fluctuations. In each cycle of sea-level, as the shelves flooded, coastal environments progressively migrated landward forming various sedimentary units over a wide area of the shelves. Similarly, as the shelves emerged, coastal environment progressively migrated seaward leaving exposed shelves for various erosion processes. Thus, these sedimentary units are well recorded on the seafloor/sub-seafloor and testify the complex interplay between depositional and erosion processes during consecutive transgression and regression. At lowered sea-level, one of the important features formed on the shelf is fluvial incisions. These incised valleys provide evidence of paleo-flow conditions which can be linked with paleo-climatic variations. Incised valleys are also important as they provide accommodation for the low stand and early transgressive sedimentation in shelf environments. They also protect entrained sediments from removal by subsequent transgressive erosion. Therefore remnants of such preserved valley-fill succession are key elements for inferring processes that create, modify and preserve continental shelf sequence stratigraphy. Such shelf deposits associated with the sea-level changes are widely studied using High Resolution Shallow Seismic (HRSS) techniques with long sediment core data and interpreted within the framework of sequence stratigraphic concepts. In general, incision signatures of older cycles are buried deeper in the sedimentary strata. Therefore, due to unavailability of high-cost long cores, multi-cycle channel incisions have been less studied in comparison to widely-preserved single cycle (simple) incised valleys. Globally, “simple” incised valleys of the Late Pleistocene-Holocene from different continental margins have been well studied and revealed important geomorphologic as well as stratigraphic information. Later, these pieces of information have been linked to create the evolutionary history of continental shelves and paleo-environmental variations through the last glacial period. Similar studies of polycyclic channel incision system, capable of providing better and longer history of continental shelf evolution, are lacking globally.

The western continental margin of India is a passive margin, and is characterized by i) a wide continental shelf having NW-SE trend, ii) a remarkably straight shelf edge limited by ~130 m isobath, iii) a narrow continental slope bounded between ~130- 2000 m isobaths, and iv) deep sedimentary basins. The shelf is ~300 km wide in Kutch-Saurashtra area and gradually narrows down southward to ~50 km in Kerala offshore area. Complementary to this, the continental slope is narrow in the north but widens towards the south. The shelf area is comprised of mainly five shelf sub-basins, namely Kutch, Saurashtra, Bombay, Konkan and Kerala offshore basins.

The hinterland area of Saurashtra and a part of Bombay offshore basins are covered by Deccan trap basalt, whereas the adjacent land area of Konkan and Kerala basins along with a part of Bombay offshore basin is the pediment of Western Ghats. The average height of Western Ghats is ~1100 m from mean sea-level. Numerous long and short but fast flowing rivers and estuaries originate from the Western Ghats and flow parallel to each other. These drainage systems have been the main erosional agent of the Western Ghats and spreading the eroded terrigenous sediments on the inner continental shelf of the west coast of India.

The western continental shelf, having an area of ~310000 km^2, is divided into three units: inner, middle and outer shelf. The inner shelf is smooth with gently sloping topography (gradient 1:800) and extends up to 55-60 m water depth in the north and narrows down to 25 m water depth off Cochin. Surficial sediment sample analyses of different studies revealed that nearshore area (up to 5-10 m water depth) between Saurashtra and Quilon is mostly covered by terrigenous sand and up to ~60 m water depth it is dominantly covered by silty clay (Rao and Wagle, 1997 and references therein). Whereas, deeper region is dominantly covered by relict carbonate sands. It is worth to mention that sedimentation rates are not uniform on the inner continental shelf. Normally, high sedimentation rates have been observed near river mouths.

HRSS studies in the west coast of India are mostly focused on the geomorphology of the continental shelf which revealed presence and the distribution of several surface/subsurface geomorphologic features like sand ridges, wave cut terraces, pockmarks and gas-charged sediment. At spars locations between Goa and Mangalore, buried channel incisions have also been reported. These incision signatures are buried under 10-15 m thick Holocene sediments and presumably represent relict extensions of rivers that crossed the shelf at lowered sea-level positions during the Late Pleistocene. Early seismic studies on the continental shelf also revealed a prominent subsurface reflector at ~35 m below the seabed off the mouth of Narmada

and Tapti rivers. The same reflector becomes shallow towards the south and occurs at ~15 m below the seabed off Cochin. Later, recent seismic stratigraphic studies revealed that seabed and this base reflector form a wedge like sediment package. This wedge-shaped sediment package thickens towards shore and pinches out around 50 m water depth. The wedge is characterized by low amplitude, continuous and parallel reflectors extending seaward which downlap against the base reflector.

Although considerable work has been carried out on the western continental shelf of India, using shallow seismic techniques, most of them were focused only on the geomorphological aspects. A few of them have reported channel incision signature at sparsely located seismic tracklines, and recognized seismic units within the late-Quaternary deposits on the western continental shelf of India. A combined geomorphologic and stratigraphic study using HRSS technique, which is capable to decipher evolutionary history of the continental shelf and paleo-environmental variations through geological past, is still lacking in India. Present study utilized geomorphologic and stratigraphic approaches and is based on well-oriented high resolution shallow seismic profiles to decipher multi-cyclic incisions of the Late Pleistocene, and to understand evolutionary history of the present inner continental shelf of Goa, west coast of India.

Objectives

Keeping the present understanding in view, following objectives are formulated to address during the present research work:

1. Spatial distribution and sedimentation rate of the Holocene sediment.
2. Palaeo-river channel pattern, their distribution, channel dimensions, and palaeo-flow estimates.
3. Development and evolution of palaeo-river channels in conjunction with sea level changes during the Late Pleistocene-Holocene.
4. Sedimentary architecture and Late Pleistocene-Holocene evolution of the present continental shelf.

The result obtained in this study is expected to establish the Holocene sedimentation rates, Late Pleistocene evolution of paleo-river channels and their role in evolution of the present inner continental shelf of the study area.

Study Area

The study area is located on the continental shelf of the central west coast of India and lies between Karwar in the south and Tiracol in the north. In the offshore, it extends up to ~60 m water depth. Chapora, Baga, Mandovi, Zuari, Sal and Talpona are the rivers of the study area which originates from the Western Ghats and have been continuously depositing sediments on the nearby continental shelf. The sediments load carried out by these rivers predominantly belongs to the erosion of the Western Ghats which is composed of basalts, charnockites, granite gneiss, khondalites, leptynites and metamorphic gneisses with detached occurrences of crystalline limestone, iron ore, dolerites, anorthosites, residual laterite and bauxite ores.

The research work carried out in the present study form the thesis which has been presented in nine chapters. Chapter wise brief summary of the thesis is given below:

Chapter 1 emphasizes on general background and motivation of the present research. It includes a brief description of relevant research work carried out on other continental shelves and compares with the present status of the similar studies on western continental shelf of India. Further, the chapter contains statement of the problem and objectives of the study, study area and significance of the present study.

Chapter 2 synthesizes previous relevant research on the western continental shelf of India. In light of existing knowledge, this chapter includes the description of tectonic framework, surface and subsurface morphology, climate and coastal circulation, and sediment distribution on the western continental shelf of India. It also includes, the description of hinterland geology and geological settings of the study area.

Chapter 3 deals with HRSS dataset and published results utilized in the present study. The chapter describes the methodology used for seismic stratigraphic analysis. It gives the details of acquired sediment core data. Further, it describes methodology for computation hydraulic parameters of observed channel incision signature, which have been used later in chapter 6 for comparing the hydrologic environment of the two glacial periods. It also discusses the computation methodology of the Holocene sediment thickness and sedimentation rates as well methodology for preparation of respective gridded data.

Chapter 4 describes the new methodology which has been developed in this study to find out approximate age and total period of non-deposition and erosion of a subaerial unconformity in absence of long sediment core data. The methodology developed is based on the base level concept for river channel and correlate observed subaerial unconformities with available sea-level curve. It also presents stratigraphical analysis of high resolution seismic sections to accomplish one of the objectives of the present study. The analysis includes identification of different seismic units, their bounding surfaces and prominent subaerial unconformities. Total eleven seismic units and three sub-seismic units with corresponding bounding surfaces have been identified on the basis of their seismic attribute. Out of the eleven bounding surfaces three surfaces (S6, S7, and S9) has been identified as subaerial unconformities. Further, the identified unconformities are correlated with the global sea-level curve to find out corresponding glacial period (lowest stand of the cycle) of their formation and corresponding period of non-deposition and erosion.

Chapter 5 discusses briefly, how the 4th order sea-level variations have affected deposition and erosion processes on the inner continental shelf of the study area. Further, it emphasizes on the Holocene sediment distribution and sedimentation rate pattern. Holocene sediment distribution is not uniform in the study area. It varies along as well as orthogonal direction to the present coastline. This chapter examines the probable causes for the non-uniform sedimentation.

Chapter 6 emphasizes on the buried channel morphology and their evolution during the Late-Pleistocene. Based on the observed subaerial unconformities, incision signatures have been differentiated according to their glacial period of formation. The inner continental shelf of the study area contains incision signatures related to three phases of incisions. This chapter also describes the methodology developed for interpolation of plan view morphology of each phase of incision. The interpolation methodology is based on the analysis of shape, size and infill reflector characteristic of incision signatures. Using the described methodology, plan view morphology of each phase of incision has been deduced. This chapter also includes quantitative analyses of the incision signatures. The analyses mainly comprise estimation of aspect ratio, mean channel discharge, channel flow velocities, and channel bed shear strain of each phase of incision. It also includes calculations of dominant slope and channel sinuosity. Further, it discusses evolution of these buried channels on the inner continental shelf and compares paleo-

climatic variations during different glacial periods of the Late Pleistocene. Further, this chapter describes roles of these paleo-channels on evolution of inner continental shelf of the study area.

Chapter 7 deals with paleo-coastline features such as paleo-beaches/sandbars and beach rocks. The results of the present study suggest the presence of paleo-coastline at ~55 m water depth. The chapter also describes occurrence and distribution patterns of gas-charged sediment zones in the study area. Based on the confining layers and depth of occurrences, gas-charged sediments are categorized in two zones. Distribution of gas-charged sediment Zone-1 is restricted to a specific region between ~8 and 30 m water depths. Whereas, gas charged sediments Zone-2 is distributed in the entire study area between 20 and 45 m water depths. The chapter also discusses probable sources of organic material which are responsible for formation of these gas-charged sediment zones.

Chapter 8 presents the Late-Pleistocene Holocene evolutionary history of inner continental shelf off Goa. It summarizes the evolutionary history of the continental shelf of Goa in three stages i.e. Stage -1, Stage-2, and Stage-3. Stage-1 describes the evolution during ~325 kyr to 200 kyr BP. Whereas Stage-2 and Stage-3 describe the evolution during ~200 kyr to 120 kyr BP and ~120 kyr BP to present, respectively.

Chapter 9 includes the conclusions drawn from the present doctoral work. Major conclusions of the study are as follows:

I. Identified eleven distinctively visible seismic units (U1 to U11) and three sub-seismic units (U6a, U7a and U9a) in the inner continental shelf of Goa.

II. Identified three subaerial unconformities namely S6, S7 and S9 and correlated with sea-level curve. Oldest subaerial unconformity (S6) was exposed during ~330-220 kyr BP and youngest one (S9) was exposed during ~110-7 kyr BP, whereas subaerial unconformity S7 was exposed during ~195-125 kyr BP.

III. Bounding surface 'S11' has been identified as Holocene transgressive surface. This surface with seabed confines the Holocene sediments.

IV. Holocene sediments have accumulated in a lens-shaped wedge. The thickness of the Holocene sediment wedge increases seaward upto ~30 m water depth, beyond it decreases sharply and reduces to a minimal value at ~50 m water depth.

V. Pinch out of Holocene sediment wedge at deeper water depth signifies that the terrigenous sediment influx beyond 50 m water depth is negligible whereas, in the nearshore region it is due to wave base erosion.

VI. Agonda headland region acted as a depo-center for the Holocene sediments where maximum Holocene sediment thickness of 15.7 m has been observed. Minimum sediment thickness in the study area is 0.75 m at ~50 m water depth offshore Canacona.

VII. Paleo-channel incisions on the inner continental shelf are differentiated into three phases of incisions: Phase-1, Phase-2 and Phase-3. Youngest channel incisions are carved between ~110 kyr BP and ~10 kyr BP and belongs to Phase-3 incisions. Phase-2 incisions are carved during ~320-125 kyr BP, whereas, Phase-1 incisions are older than ~330 kyr BP.

VIII. With each passing sea-level cycle, channel incisions became more sinuous and their areal extent increased. The buried channel had evolved from straight river type (Phase-1) to ingrown meander (Phase-2) and then similar to anastomosing type (Phase-3).

IX. Unlike Phase-2 and Phase-1, Phase-3 incisions are incised in multiple estuarine and low energy fluvial condition.

X. Comparison of computed hydraulic parameters of Phase-2 and Phase-3 incisions reveals that Phase-3 incisions took place in lower hydraulic energy condition than the Phase-2 incisions

XI. Phase-2 channels had ~33% more mean bank full discharge than that of the Phase-3 channels. The mean depths of the Phase-2 incisions are almost double than the Phase-3 incisions.

XII. Hydrologic environment associated with penultimate and prior to penultimate glacial periods was also stronger than that of last glacial period. Our study suggests that Indian summer

monsoon was stronger during the formative stage of Phase-2 (MIS 6 & 8) incisions than that of Phase-3 (MIS 2 & 4) incisions.

XIII. Paleo-coastline (during post LGM transgression) is interpreted at ~55 m water depth and this coastline is more or less parallel to the present coastline. Paleo-coastline hs preserved signatures of paleo-beaches and paleo-surf zone sand bars which are more frequently observed in the south of Sada headland region and are located ~35 km away seaward from the present coastline.

XIV. Two different types of gas-charged sediment zones are identified on the inner continental shelf off Goa, central west coast of India. Zone-1 has limited areal extent between ~8 and 30 m water depth in the sheltered basin of the study area. Zone-2 is distributed in the entire study area mostly between ~20 m and ~45 water depth. Associated source organic material and gas-charged sediment in Zone-1 is younger (Holocene) than the associated organic material and gas charged sediment in Zone-2 (Late Pleistocene).

The present study reveals that the inner continental shelf of Goa contains preserved signatures of compound incised valley. Methodology used in this study by integrating qualitative and quantitative seismic geomorphology provides a valuable procedure for gaining insight into the evolutionary history of drainage system in absence of long sediment core data. Moreover, the study also provides comparison of hydrologic regimes associated with prevailing environment during the last two glacial periods.

Chapter 1
General Background

1.1 Introduction

Continental shelves are the gently sloping land mass extension that are partially submerged under the sea water and are confined between coastline and continental shelf break, with seafloor gradient of the order of 1:1000 (Singh and Jammu, 2008). The width of continental shelves varies from region to region, from a few tens of meters (tectonically active western coast of North and South America) to hundreds of kilometers (~1300 km, western coast of Siberia). Though they encompass only ~8.9% ($32x10^6$ km^2) of total area of the oceans (Harris et al., 2014), still they are the most significant part of the world ocean as far as socio-economic uses are concerned. They are very useful for navigation, recreation, and production of renewable energy from wave, tidal currents and wind (Barrie and Conway 2014). Continental shelves contain valuable living and non-living resources. They (i) provide ~95% of the total marine fish catches, (ii) contain largest reservoirs of oil and gas (~30% of all petroleum extracted from both land and sea), and (iii) also contain valuable mineral resources (Roberts and Hawkins, 1999; Harris et al., 2015).

The continental shelves had initially formed due to disintegration of the Pangaea supercontinent. Subsequently, they evolved due to the complex interaction of endogenous (e.g. geodynamics) and exogenous (e.g. climate) processes (Fig. 1.1) through the geological past (Chiocci and Chivas, 2014). Overall physiography, i.e. width and slope of the continental shelves, is controlled by geodynamics, particularly tectonics. Whereas climate determines overall sediment type and sediment supply. Further, complex interplay between sediment supply sources (such as fluvial and estuarine channel system) and prevailing hydrodynamics (e.g. waves and currents) control sediment distribution as well as surface sedimentary structure of continental shelves of the world.

The Quaternary Period (the most recent 2.6 million years of Earth's history) is extremely important as compared to 4.5 billion years of the Earth history because it is the interval during which humans evolved and it includes the present. Quaternary evolution of continental shelves of the world was primarily controlled by climate-driven eustatic changes. The shelves during the Quaternary underwent dramatic environmental changes, with repetitive cycles of emergence and submergence, displacement of the shoreline, and consequent alternation of sedimentation and erosion. Events of the Quaternary are preserved in sediments of continental shelves with a greater degree of completeness and temporal resolution than those of any earlier geologic period of comparable length. Therefore, studies of these sedimentary archives are being carried out by diverse and growing groups of researchers worldwide. The present study focuses on inner continental shelf of Goa, west coast of India using high-resolution shallow seismic reflection data.

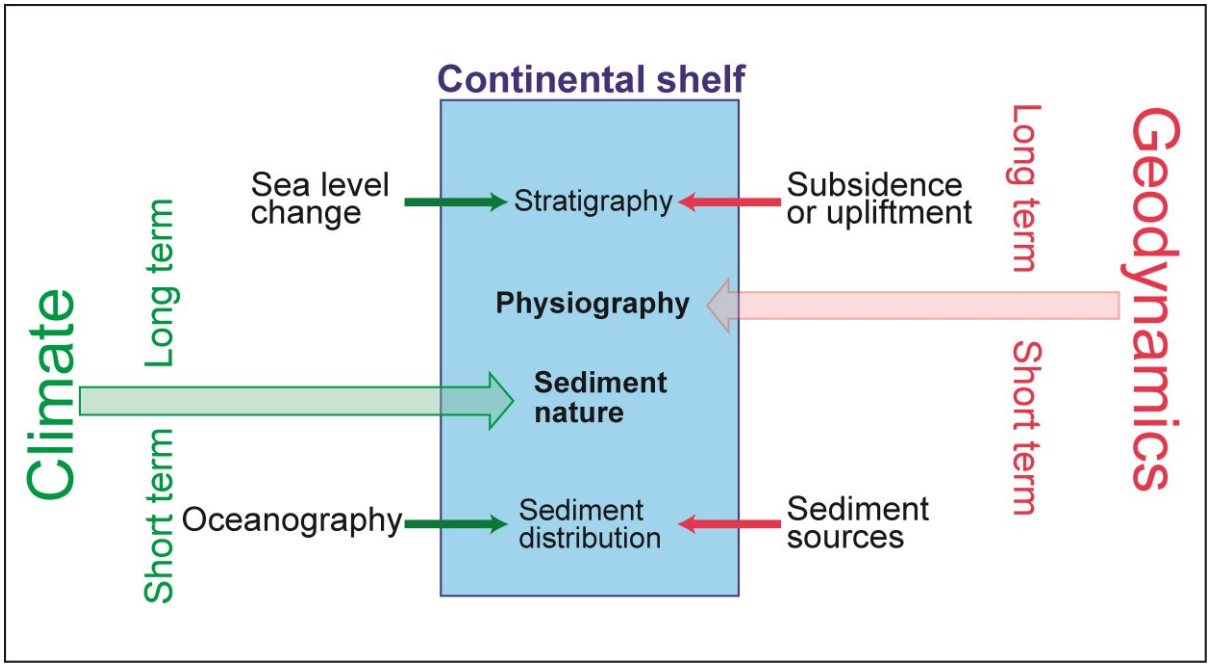

Figure 1.1 Schematic diagram depicting processes (endogenous and exogenous) controlling sedimentation on continental shelves, on both short- and long-term geological timescales (Chiocci and Chivas, 2014).

1.2 Quaternary evolution of continental shelves

Quaternary continental shelves are evolved under combined effect of tectonics, eustasy, climate, deposition and erosion processes working in coastal region. Conceptual models illustrating evolution of continental shelf over a cycle of sea-level change is shown in Figure 1.2. Figure 1.2A illustrates initial sea-level, shoreline position, and erosional fluvial channels

on coastal plain and sediment deposition on the continental shelf. In response to sea-level fall, shoreline migrates seaward (Fig. 1.2B). A new coastal plain (i.e. submerged seabed of continental shelf) becomes available for various sub-aerial erosion processes (fluvial, glacial and Aeolian). At the same time, it gives rise to a variable accommodation space seaward which controls grain size gradation of sediment and their layer geometry. One of the important geomorphic responses of the sea-level fall is fluvial incision. As the sea-level falls, incision starts. Fluvial channels which were debouching at higher shoreline position earlier, incise deeper extent of the exposed continental shelf. In response to further sea-level fall, incision extends further deep in the exposed shelf strata. The magnitude of fluvial erosion of the exposed continental shelf is again highly controlled by the base level (i.e. sea-level), physiography of the shelf and hydrodynamic condition of the channel. Physiography of the continental shelf is controlled by the basement tectonics, whereas climatic condition mainly controls hydrodynamic energy of the channel. In an intense humid climatic condition, high energy fluvial channel can extensively erode and alter the exposed shelf. On a favorable physiographic and climatic condition, erosion capacity of a fluvial channel increases with sea-level fall. On the other hand, with enlarged catchment area, fluvial channel system dumps huge amount of terrigenous sediment over submerged part of continental shelf which further get dispersed and deposited by autocyclic processes (longshore and cross-shore drift currents, littoral current, etc.) as per prevailing accommodation space. Autocyclic processes are generated within the sedimentary system and are responsible for local to regional scale changes such as ripple migration, delta switching, lateral migration of beach-barrier bars etc. (Beerbower, 1964). In general, autocyclic processes do not cause any significant physical or chemical sedimentological changes (geological formation level) in the strata. They also do not change sedimentary architecture of basins significantly (Beerbower, 1964).

In case of a stable sea-level condition, formation of shoreline features (such as beach/barrier sand bar, river delta, wave cut terraces etc.) takes place on deeper extent of the shelf. During the subsequent sea-level rise following the glacial maximum (Fig. 1.2C), shoreline migrates back to landward and coastal plain submerges. As a result, various millennial scale sedimentary bodies are formed over a wide area of shelves. The coast line transgression causes burial of channel incisions and other features below a new set of sedimentary layers with some alteration due to wave action of the transgressive sea. Channel-filling with terrigenous sediments typically begins with base-level (i.e. sea-level) rise, preserving all evidences of climatic and geodynamic variations. Buried channels may also contain sediment deposits of subsequent highstand sea-

level (Zaitlin et al., 1994). Preservation of these signatures on continental shelves again depend on physiography of shelf, sediment supply sources and rate of sea-level rise.

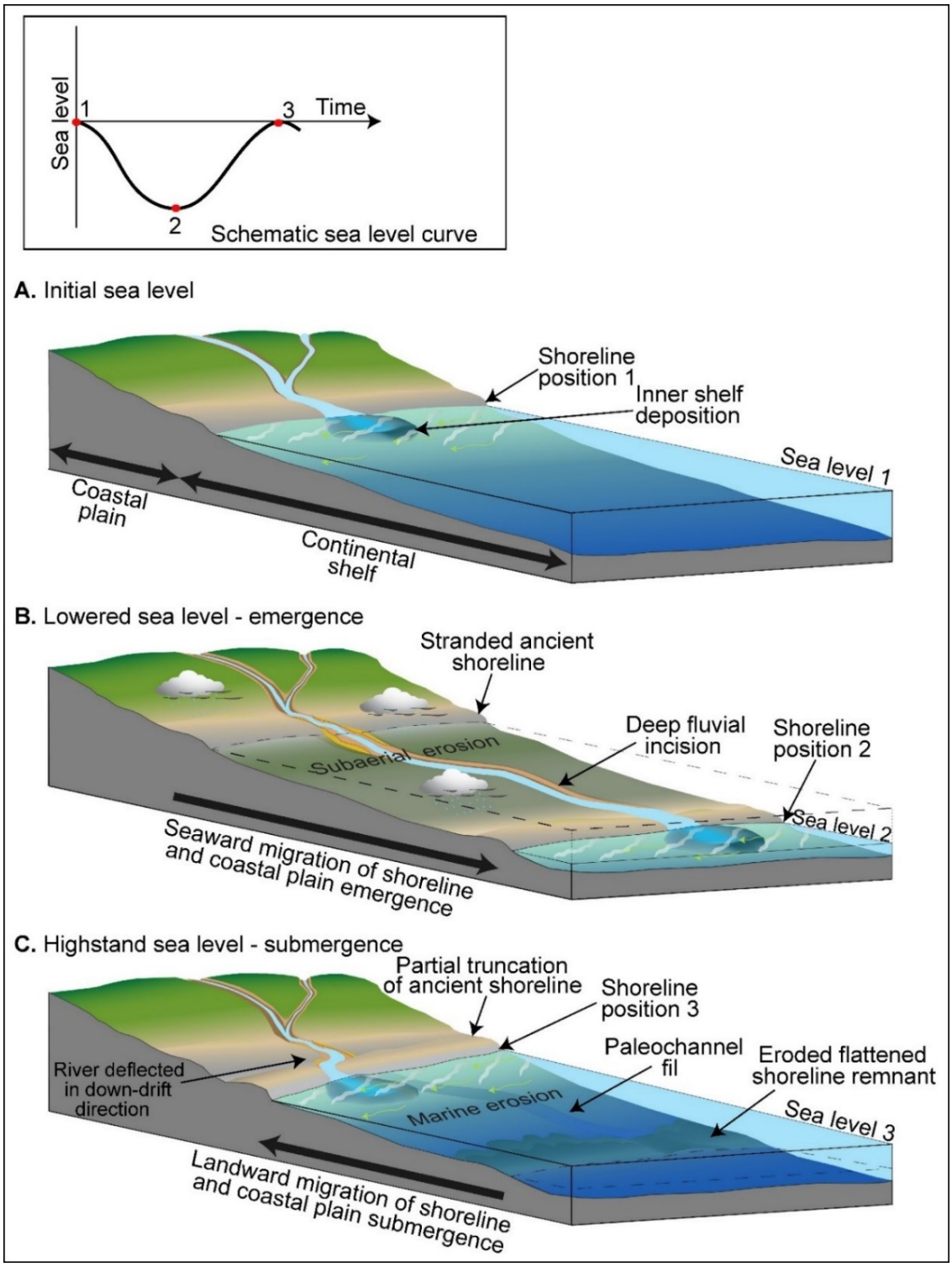

Figure 1.2 Conceptual models illustrating evolution of continental shelf over a cycle of sea-level change (modified from Schwab et al., 2009). Annotations 1, 2 and 3 on schematic sea-level curve correspond to (A) initial sea-level, (B) lowered sea-level, and (C) highstand sea-level, respectively.

The Quaternary Period has experienced several climate driven glacio-eustatic sea-level fluctuations (Fig. 1.3). These fluctuations have gross cyclic period of 80 to 100 kyr (Waelbroeck et al., 2002; Siddall et al., 2003; Rehak et al., 2010) and maximum amplitude of the order of ~120 m. Continental shelves have gone through several cycles of emergence and submergence due to these glacio-eustatic sea-level fluctuations during the Quaternary. As a result, continental shelves of the world contain preserved signature of "Simple incised valley", and "Compound incised valley".

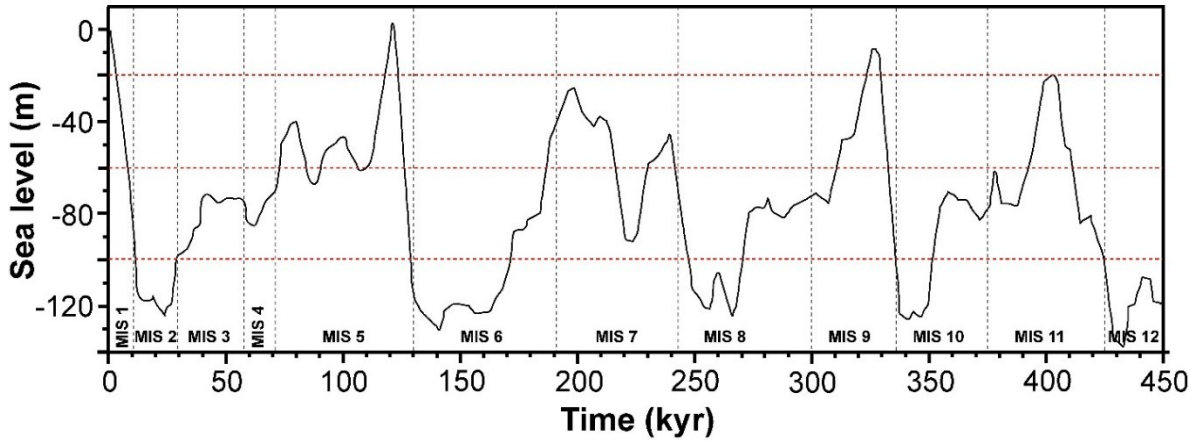

Figure 1.3 Sea-level curve of the last 450 kyr (modified by Rehak et al., 2010 from Siddal et al., 2003). Marine Isotopic Stages (MIS) have been added following Lisiecki and Raymo (2005).

Persevered fluvial channel incision signatures on continental shelves corresponding to one glacio-eustatic sea-level cycle are referred as "Simple incised valley" (Zaitlin et al., 1994). The continental shelves containing signature corresponding to only one glacio-eustatic sea-level cycle are due to zero preservation potential for incision signature of previous sea-level cycles (Labaune et al., 2010). On the other hand, preserved channel incision signatures corresponding to several glacio-eustatic sea-level cycle are observed on several continental shelves worldwide. Such multi-cycle (poly-cycle) incised valleys are referred as "Compound incised valley".

1.3 Geophysical studies of the Quaternary continental shelves of the world

Remnants of incised valley-fill succession on continental shelves of the world are key elements for inferring processes that create, modify, and preserve continental shelf sequence stratigraphy on one hand and for providing alternatives for several onshore mineral resources on the other hand. The incised valleys protect entrained sediments from removal by subsequent transgressive erosion. Moreover, channels of these incised valleys play a key role in redistribution of terrigenous sediment in the form of potential economic heavy mineral (i.e.

ilmenite, magnetite, cassitertite, chromite, rutile, zircon, and gold) deposits (Chiocci and Chivas, 2014). Further, gravels and relict shelf sand bodies are useful for construction and glass industries, respectively (Chiocci and Chivas, 2014). Globally, continental shelves are reported for existence of fresh water aquifers which are now looked upon as potential drinking water source for coastal cities (Post et al., 2013; Morgan et al., 2018). Therefore, investigations of such preserved valley-fill succession have academic as well as socio-economic importance.

Globally, shelf sedimentary deposits associated with the sea-level changes and tectonic activity are widely interpreted within the frame work of sequence stratigraphic concepts. Since, most of these deposits are highly variable with respect to their vertical as well as areal extent, extrapolation of stratigraphic information from sediment core data over entire area is not advisable. Therefore, sedimentary architecture of continental shelves is best studied using High Resolution Shallow Seismic (HRSS) data and long sediment cores. Some of the well studied continental shelves of the world are Northwest European shelf (Lericolais et al., 2003; Chaumillon et al., 2010; Menier et al., 2010; Traini et al., 2013; Menier et al., 2016), Northeastern Australian shelf (Fielding et al., 2003), New Jersey shelf (Nordfjord et al., 2005, 2006), Western South Huanghai shelf (Xianghuai et al., 2011), South African shelf (Green, 2009), Sunda shelf in South East Asia (Hanebuth et al., 2009), Hong Kong shelf (Bahr et al., 2005), Mississippi-Alabama shelf (Greene et al., 2007), Roussillon shelf (Tesson et al., 2010, 2011, 2015) and western Long Island shelf, New York (Liu et al., 2017). In general, erosional and depositional signatures corresponding to older glacio-eustatic cycles of the Quaternary are buried deep in sedimentary strata. Therefore, due to unavailability of high cost long cores, "compound incised valleys" have been less studied in comparison to widely-preserved "simple incised valleys". Globally, simple incised valleys of the Late Pleistocene-Holocene from different continental margins, such as Northwest European shelf (Lericolais et al., 2003; Chaumillon et al., 2010; Menier et al., 2010; Traini et al., 2013; Menier et al., 2016), Northeastern Australian shelf (Fielding et al., 2003), New Jersey shelf (Nordfjord et al., 2005, 2006), Western South Huanghai shelf, (Xianghuai et al., 2011), South African shelf (Green, 2009), Sunda shelf in South East Asia (Hanebuth et al., 2009) have been well studied and have revealed important geomorphologic as well as stratigraphic informations. Later, these informations have been linked to create evolutinary history of continental shelves and paleo-environmental variations through last glacial period. However, only a limited number of similar studies worldwide, capable of providing better and longer history of continental shelf evolution, have hitherto focussed on compund incised velley system. Incised valleys on the continental

shelf of Hong Kong (Bahr et al., 2005), Mississippi-Alabama (Greene et al., 2007), Roussillon shelf (Tesson et al., 2010, 2011, 2015), and western Long Island, New York (Liu et al., 2017), are examples of best studied compound valley incisions which were formed over tectonically passive and minimal subsidence shelf setting. Studies dealing with mutli-cyclic channel incisions on continental shelves of India are still lacking.

The present study is focused on the inner continental shelf of Goa, west coast of India. Closely spaced, well-oriented high-resolution shallow seismic profiles are utilized to decipher the Late Pleistocene-Holocene stratigraphic features and to investigate roles of endogenic and exogenic processes during the Holocene sedimentation. It also aims to evaluate roles of multi-cyclic incisions during the Late Pleistocene and provide a better understanding of evolutionary history of the inner continental shelf of Goa.

1.4 Geophysical studies on western continental shelf of India

For the past fifty years, a large number of geological and geophysical studies have been carried out on the western continental shelf of India. First systematic geological study of the continental shelf of western India started during International Indian Ocean Expedition (IIOE) between 1962 and 1965. During 25th cruise of INS Kistna, surface sediment samples from the continental shelf were collected to analyze grain size and carbonate content (Nair and Pylee, 1968). Later, Nair et al. (1978) reported surface sediment distribution pattern and carbonate content with respect to water depth of the continental shelf between Vengurla and Manglore. The study was based on 129 surface sediment samples from the shelf and 5 rock samples from the hinterland. The sediment samples were acquired at a sampling interval of 10 km along several tracklines spaced at 20 km interval. After 1980, most of the geological studies concentrated in near shore region at very shallow water depth and were focused on the sediment distribution pattern, micro-organism and coastline morphology. In fact, early seventies to mid-eighties, majority of the near shore geological studies were limited between ~15 m water depth and coastline, and were mostly based upon surface sediment sample analysis. These geological studies were basically focused to map and analyze continental shelf sediment types and their distribution.

In mid-eighties, focus of geological studies turned on paleo-environment and sea-level related studies. Nigam (1988) reported cyclic monsoonal variations of the last 100 years based on percentage abundance of benthic foraminifera in grab sediment sample recovered from Kali

River mouth zone (22 m water depth). The study lead to other paleo-climatic studies using sediment samples acquired from the western continental shelf of India (Nambiar et al., 1991; Nambiar and Rajagopalan 1995; Manjunatha and Shankar, 1992; Nigam et al., 1995; Pandarinath et al., 1998, 2001; Khare et al., 2008). These climatological studies have also reported the Holocene sedimentation rates at different locations on the western continental shelf of India based on ^{14}C dating of sediment samples. Kale and Rajaguru (1985) identified transgressive and regressive sea-level events during the Neogene and Quaternary based on land based fossil and archeological records, and drill-well results of Oil and Natural Gas Corporation Limited. One of the important outcomes of the study was the Holocene sea-level curve for the west coast of India. Nigam et al. (1992), based on analysis of ooides and benthic foraminifera records of a 26.5 m long sediment core, reported the sea-level transgression between 14500 year BP and 10000 year BP. The sediment core was recovered from the continental shelf of Mumbai at 75 m water depth. Later, Hashimi et al. (1995) regenerated a new Holocene sea-level curve for the west coast of India based on radiometric dating of organic material (peat and woods), microorganism (benthic foraminifera), sediments (littoral concrete, ooids carbonates, sand, shell etc.) from surface sediment samples acquired from different water depths.

As far as high-resolution geophysical studies are concerned, between mid-seventies to early nineties, most of the studies in near shore region were limited to investigate seabed and sub seabed characteristics for development of coastal based industries (Almeida, 1977a, 1977b, 1977c; Siddiquie, 1976a, 1976b; Rao, 1977). These were carried out at fringe locations off Mumbai, Gujarat, Karwar, Mangalore etc. However, in the beginning of the eighties, Siddiquie et al. (1980) reported presence of gas charged sediment zones in the inner continental shelf of Mumbai. These gas charged sediment zones were reported based on the observed acoustic masking in the high resolution seismic sections and was a milestone as far as geophysical studies over the continental shelf of west coast of India is concern. Findings of this study motivated researchers for a well-planned geophysical investigation of western continental shelf of India using high resolution seismic reflection technique. Later, Siddiquie et al. (1981a, b) reported and mapped zones of acoustic masking (i.e. gas charged sediment zones) from the southern continental shelf of Gulf of Khambhat and off shore Maharashtra and Kerala. Thereafter, gas charged sediment zones on the continental shelf were reported and discussed by many other researchers (Karisiddaiah et al., 1993; Veerayya et al., 1998; Karisiddaiah and Veerayya 2002). Rao (1989) reported seabed characteristics of the continental shelf between Malvan and Mangalore using side scan sonar imagery and bathymetry data. His study revealed

smooth inner continental shelf (up to 40-50 m water depth) covered with fine grain sediments, and a non-depositional and erosional outer shelf depicting undulating topography. The outer shelf is comprised of algal and oolitic ridges, and self-edge with isolated algal ridges. Till 1990 geophysical studies were largely limited to the investigation of gas charged zone, seabed characteristics and shallow sub-seabed sediment assemblage using echo-sounding, seabed sonography and shallow seismic reflection profiling. During nineties, a number of investigations reported geomorphological features such as submarine terraces/wave cut terraces, sand ridges, paleo-beaches (Vora and Almeida 1990; Wagle et al., 1994; Rao and Veerayya 1996; Subba Raju et al., 1996; Vora et al., 1996; Wagle and Veerayya 1996). Some of these studies explained formation of geomorphologic features such as wave cut terraces, sand ridges etc. due to sea-level fluctuations (Wagle et al., 1994; Vora et al., 1996; Wagle and Veerayya, 1996; Vora, 1997). Fluvial channel incision signatures off Vengurla, west coast of India were first reported by Subba Raju et al. (1991) using high resolution seismic data. Thereafter presence of incision signatures on the western continental shelf of India have been reported from sparse locations based on few seismic tracklines (Karisiddaiah et al., 2002; Mazumdar et al., 2009; Michael et al., 2009). Shareef et al. (2016) mapped plan view morphology of buried Bharathppuzha River from the incision signature on the inner continental shelf of Munambam, Kerala.

First ever attempt on seismic sequence stratigraphic study on the western continental shelf of India was carried out by Karisiddaiah et al. (2002) who reported sequence stratigraphic characteristics of continental shelf between off Coondapur (near Bhatkal) and Kasargad (near Mangalore). Based on the analysis of high-resolution seismic data acquired along seven tracklines, they reported the Late Pleistocene-Holocene sedimentary sequence which is composed of nine seismic units that were possibly controlled by high-frequency sea-level fluctuations. In absence of long sediment core data, they tried to correlate few of the recognized seismic units with available sea-level curve and concluded that those seismic units were deposited during the last glacial period. In another study by Mazumdar et al. (2009), based on the high resolution shallow seismic profiles, taken from the continental shelf off Betul, a wedge-shaped sediment package characterized by low amplitude, continuous, parallel reflectors extending seaward up to a water depth of 50 m was reported. The sediment wedge thickens towards shore and pinches out at ~50 m water depth (~24.5 km off the Goa coast). The weak reflectors within the wedge downlap against a planar surface referred to as maximum flooding surface.

1.5 Statement of problem and objectives of the study

As discussed in previous sections, evolutionary history of recent geological past (Quaternary) of present western continental shelf of India is very little known due to lack of high-resolution geophysical investigations. Though a foundation had been laid, a combined geomorphologic and stratigraphic studies using high-resolution shallow seismic data to investigate the Quaternary evolutionary history of the western continental shelf and paleo-environmental variations through geological past, is still lacking in India. The role of allogenic processes such as fluvial channel incision, climatic variation and eustasy in the evolutionary history of the western continental shelf of India were never investigated. Further, studies dealing with compound incised valley on both the continental shelves of India are still lacking.

The main goal of the present study is to map stratigraphic and buried geomorphic features of the inner continental shelf of Goa and to decipher the Late Quaternary evolutionary history. The study, based on closely-spaced and well-oriented high-resolution shallow seismic profiles, utilizes integrated geomorphologic and stratigraphic approaches to investigate roles of endogenous and exogenous processes for shelf sedimentation. It also seeks to evaluate the role of multi-cyclic incisions of the Late Pleistocene and provide a better and deeper understanding of evolutionary history of the present inner continental shelf of Goa, west coast of India. Keeping current understanding in view, following specific objectives are formulated for the present study:

(i) Spatial distribution and sedimentation rate of the Holocene sediment.
(ii) Paleo-river channel pattern, their distribution, channel dimensions, and paleo-flow estimates.
(iii) Development and evolution of paleo-river channels in conjunction with sea-level changes during the Late Pleistocene-Holocene.
(iv) Sedimentary architecture and Late Pleistocene-Holocene evolution of the present continental shelf.

1.6 Study Area

The study area (Fig. 1.4) is located on the inner continental shelf of the central west coast of India and lies between Karwar in the south and Tiracol in the north. In the offshore, it extends up to ~60 m water depth.

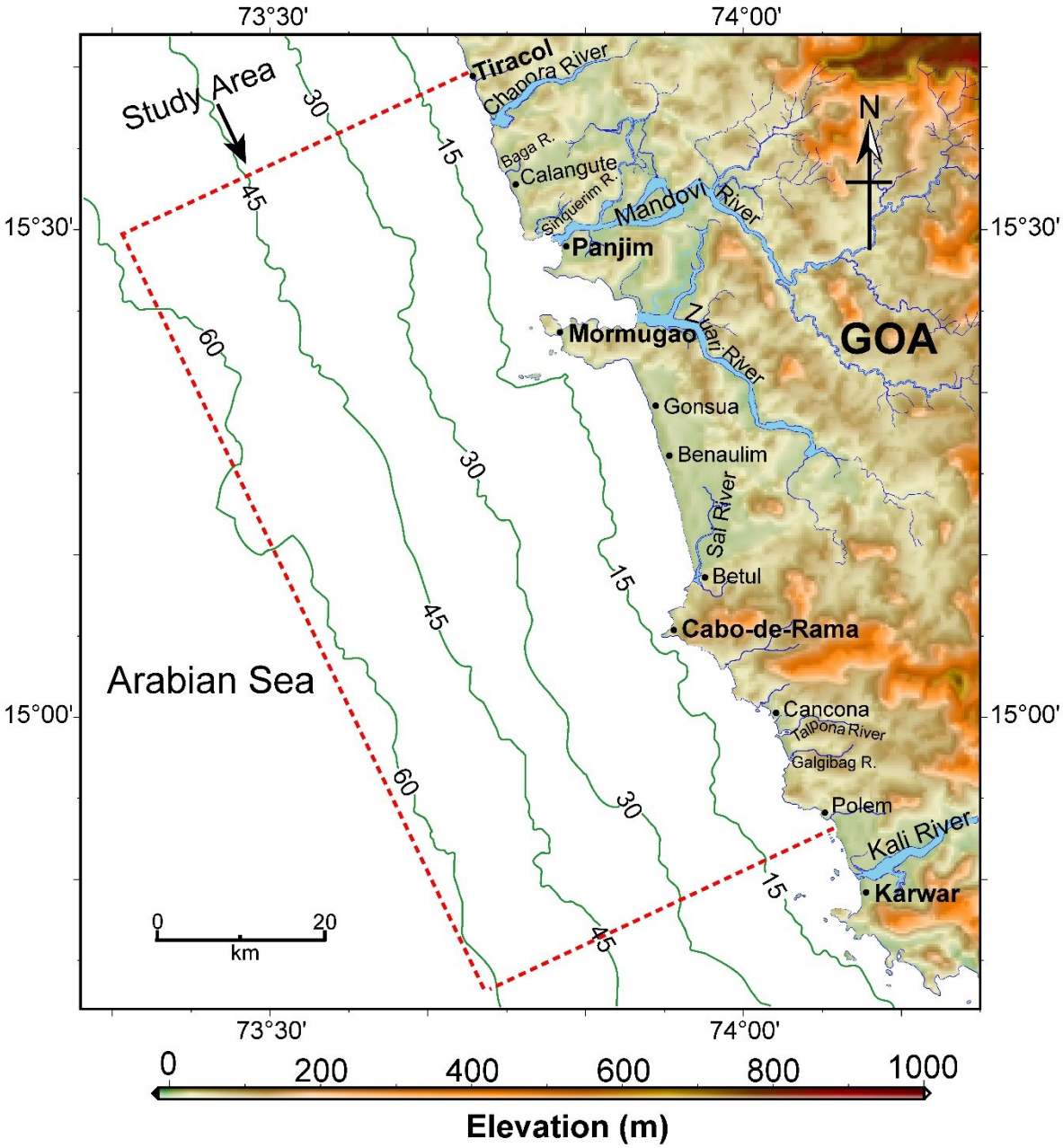

Figure 1.4 Map depicting study area (red dashed line) on the continental shelf of Goa. Isobaths are shown with solid green contour lines and annotated values on the contours are in meter. The relief map and bathymetric contours are generated using grid data of GEBCO (GEBCO_2014 version 20150318, Weatherall et al., 2015).

Chapora, Baga, Mandovi, Zuari, Sal and Talpona are the rivers of the study area which originate from the Western Ghats and have been continuously depositing sediments on the nearby

continental shelf. The sediment load carried out by these river predominantly belongs to erosion of Western Ghats which is composed of basalts, charnockites, granite gneisses, khondalites, leptynites, and metamorphic gneisses with detached occurrences of crystalline limestone, dolerites, anorthosites, residual laterite and bauxite (Gokul et al., 1985).

1.7 Significance of the study

Study of Holocene sediment distribution pattern enable to understand processes which play the key role in long-term sediment deposition on the inner continental shelf. Previous sedimentological studies from the study area and nearby region revealed that the Holocene sediment in the inner continental shelf is composed of clayey material (Mazumdar et al., 2009; Pandarinath et al., 2001). Therefore, investigating the Holocene sediment and preparing a thickness map provide an estimate of total volume of clay deposits in the study area.

As far as stratigraphic study is concerned, present study provides an alternative methodology (discussed in Chapter 4) to assign age of subaerial unconformities through the study of long sediment cores. This methodology is useful in the study of "compound incised valleys" in the absence of costly long sediment core data to a certain extent.

Combined analyses of geomorphologic and hydrological properties of river channel incisions of different glacial periods provide keys to decipher large scale paleo-environmental changes. It can also be used as a means to provide a context for observed historical trends to predict near future conditions in a changing climate (Blum and Tronqvst, 2000). Further, the mapped buried paleo-channels can be useful in predicting the incident potential hazard of submarine engineering.

Worldwide presence of potential offshore fresh/brackish water aquifer on continental shelves (Post et al., 2013) asserts the fact that channel incisions do not just erode the exposed shelves but also alters sediment distribution and therefore may provide suitable site for occurrence of offshore aquifers (Morgan et al., 2017). Some of these aquifers are thought to be well connected with onshore recharge sites (Hathaway, 1979; Johnston, 1983; Oteri, 1988; Malone et al., 2003; Person et al., 2003, 2011; Grasby et al., 2009; Zhang et al., 2011; Varma and Michael 2012; van Geldern et al., 2013), while some of these are not connected (Kastner et al., 1990; Mora 2005). With growing demands of drinking water supply, these aquifers are now looked upon as

the major alternative source. Coastal states of India suffer from scarcity of drinking water during summer season. Mapped buried paleo-river channel on the continental shelf of Goa could be used as a candidate site for mitigation of water scarcity as it lays the foundation for future investigations of offshore freshwater aquifers.

Chapter 2
Geological Framework

2.1 Introduction

Geologically, the continental shelf together with the continental slope and continental rise forms the continental margin (Fig. 2.1). The continental crust forms the bedrock of the continental shelf, while the oceanic crust forms the bedrock of the abyssal plains. Continental margin extends till Ocean-Continent Boundary. There is a legal as well as geological definition for a continental shelf (Fig 2.1). The legal definition of a continental shelf is provided under Article 76 of the United Nations Convention on the Law of the Sea. It states that the continental shelf of a coastal State comprises "the seabed and subsoil of the submarine areas that extend beyond its territorial sea throughout the natural prolongation of its land territory to the outer edge of the continental margin, or to a distance of 200 nautical miles from the baselines from which the breadth of the territorial sea is measured where the outer edge of the continental margin does not extend up to that distance" (Smith and Taft, 2000). Geologically, the continental shelf is defined as "a zone adjacent to a continent (or around an island) which extends from the low water line to a depth at which there is usually a marked increase of slope towards oceanic depths" (IHO, 2008). In brief, a continental shelf is an integral part of a continent that extends underwater to the shelf break. Throughout this thesis, the term continental shelf is used in geological sense and not in legal sense.

Present chapter synthesizes previous relevant research on the western continental shelf of India. In the light of existing knowledge, it describes the surface and subsurface morphology of the western continental shelf and sediment distribution over it. This chapter also describes the regional hinterland geology, southwest monsoon and coastal circulation in the Arabian Sea. Along with regional information, it tries to bring out the relevant geological information of the study area too.

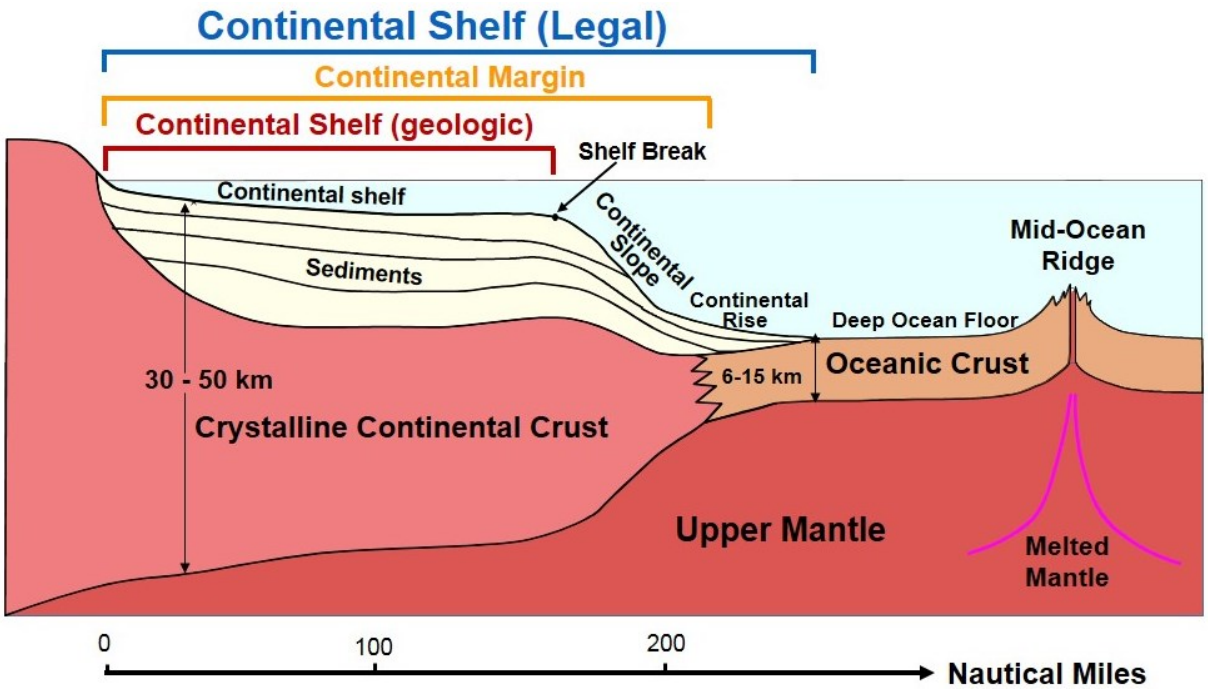

Figure 2.1 Schematic diagram depicting legal and geologic aspects of a continental shelf of a passive continental margin (Modified from J-P Levy, 2000 and Symonds et al., 2000).

2.2 Regional tectonic settings

Western continental shelf of India is a part of passive continental margin of India in the Arabian Sea. The Western Continental Margin of India (WCMI) trends NNW-SSE and extends from Kutch in the north to Cape Comorin in the south. The tectonic features of the WCMI are closely linked to the evolutionary history of the Indian subcontinent, from its breakup with Gondwanaland to its northward drifting and ultimately collision with the Eurasian plate (Bhattacharya and Chaubey, 2001; Bastia and Radhakrishna, 2012). The major portion of the Indian Peninsula is a shield area which comprised of exposed Precambrian igneous rocks such as gneisses, schists, charnockites and metamorphosed sedimentary rocks (Kumar, 1985). While the central-west part of peninsula is covered by younger Cretaceous to earliest Paleocene Deccan continental flood basalt (Gombos et al., 1995). As far as evolutionary history of the WCMI is concerned, it experienced multiple phases of extensional tectonics in the geological past and evolved in three distinct phases. In the first phase, Madagascar separated from Seychelles-Laxmi Ridge-India during the Late Cretaceous under the influence of the Marion mantle plume (Norton and Sclater 1979; White and McKenzie 1989). Second major tectonic phase was the rifting between Seychelles-Laxmi Ridge and India during end of the Late Cretaceous (Bhattacharya et al., 1994, Bhattacharya and Yatheesh, 2015; Ramana et al., 2015). Third and final tectonic phase which influenced the WCMI was rifting and subsequent drifting

of Seychelles from Laxmi Ridge-India during the Early Paleocene (Naini and Talwani, 1983; Miles and Roest, 1993; Chaubey et al., 1998, 2002; Dyment, 1998; Royer et al., 2002; Torsvik et al., 2013; Bhattacharya and Yatheesh, 2015). The last two phases of rift/drift scenario were contemporaneous with the volcanic eruption by the Reunion mantle plume, which resulted in the eruption of Deccan Continental Flood Basalt province (DCFB) on the central-western India (Mahadevan, 1994) as well as continental flood basalt on the Praslin island on the Seychelles micro-continent (Devey and Stephens, 1991) at ~65 Ma (Fisk et al., 1989). The volcanism emplaced numerous magmatic intrusives/extrusives within the crust of WCMI and played a major role in reshaping WCMI and modified the crustal geometry of the region. In a recent study, Kumar and Chaubey (2019) suggested that flood basalt carpeted the entire northwest continental margin of India extending up to the Laxmi-Laccadive ridges except some isolated basement-high features. Apart from the Rèunion hotspot activity, another geodynamic event, the Indo-Eurasian continental collision resulted in (i) slowing down spreading rates across the Carlsberg, Central and Southeast Indian ridges, (ii) plate boundary re-organization, and (iii) Himalayan orogeny which had profound effects on sedimentation in the Arabian basin and western continental margin of India.

The WCMI is a classic example of an elevated passive continental margin with a well-defined escarpment, the Western Ghats. Typical to the divergent continental margins it also has its subsidence history. Studies on the WCMI show that rapid subsidence of the WCMI started in the Late Cretaceous (~60 Ma) which through Oligocene slowed down with the cooling (Mohan, 1985; Agrawal, 1990; Agrawal and Rogers, 1992; Whiting, 1994; Gombos et al., 1995). Whiting (1994) has prepared subsidence curves for 27 wells located at western continental margin of India. The subsidence curves show a characteristic Late Oligocene to early Miocene (~24 ± 5 Ma) rapid increase in subsidence rate superposed on the long-lived, slow thermal subsidence. The magnitude of this excess subsidence increases seaward from the coast, ranging from a few meters to >2000 m near the shelf edge. He suggested that the excess subsidence was the combined result of margin progradation and Indus fan loading. The effect of margin progradation decrease southward in general. Corresponding to this excess sediment load in outer shelf-slope region low relief high elevation features of flexural uplift in Saurashtra Basin have been identified. A comparatively recent study reveals that there is no geomorphological evidence of rapid flexural uplift or neo-tectonic activity (except Koyna region) since Tertiary Period (Kale and Shejwalker, 2008). It also reveals that the flexural uplift has almost ceased in the coastal region of Konkan Basin and concludes that the entire western Deccan Basalt

Province area belongs to the class of low tectonic activity from the Tertiary Period. However, continental shelf of west coast of India is considered as tectonically quiescent passive shelf with minimal subsidence during the Quaternary (Whiting, 1994; Faruque and Ramachandran, 2014).

The western continental shelf is comprised of several subsurface ridges and horst-graben complexes which were evolved during the three stages of rifting and subsequent drifting mentioned above. Some of the structural trends of the western continental shelf of India were considered to be mainly controlled by the Precambrian structural grain of the western Indian shield (Biswas, 1987; Kolla and Coumes, 1990; Subrahmanyam et al., 1995). It is considered that three dominant Precambrian orogenic trends namely, NW-SE to NNW-SSE Dharwar trend, the NE-SW Delhi-Aravali trend, and ENE-WSW to E-W Satpura trend controlled the tectonic framework of west coast of India (Fig. 2.2) during the evolution of the WCMI (Biswas, 1987). Geophysical evidence reveal extension of structural and tectonic trends from the Indian subcontinent to the continental shelf of the WCMI (Bhattacharya and Subrahmanyam, 1986; Biswas, 1987; Biswas and Singh, 1988; Kolla and Coumes, 1990; Rao, 1984; Singh and Lal, 1993; Subrahmanyam et al., 1993). Singh and Lal (1993) observed that several structures in the shelf region along the Konkan-Kerala basin have continuity from the mainland.

The transverse arches, from north to south, are Saurashtra, Bombay, Vengurla and Tellicheri arches which divide the shelf into five offshore sub-basins, namely the Kutch, Saurashtra, Bombay, Konkan, and Kerala basins (Biswas and Singh, 1988). The NE-SW trending Saurashtra arch separates the Kutch offshore basin from the Saurashtra offshore basin in the north (Biswas, 1987). Further, the ENE-WSW trending Vengurla arch separates the Konkan basin in south from Ratnagiri basin in the north (Singh and Lal, 1993). Tellicherry arch separates Konkan basin from Kerala basin, whereas Bombay high separates offshore Saurashtra basin from Ratnagiri basin. The physiography of the western continental shelf is largely affected by the horst graben structures and varies through these sub-basins. The Quaternary continental shelf of the WCMI evolved due to the complex interaction of glacio-eustatic sea-level fluctuations and sedimentary processes.

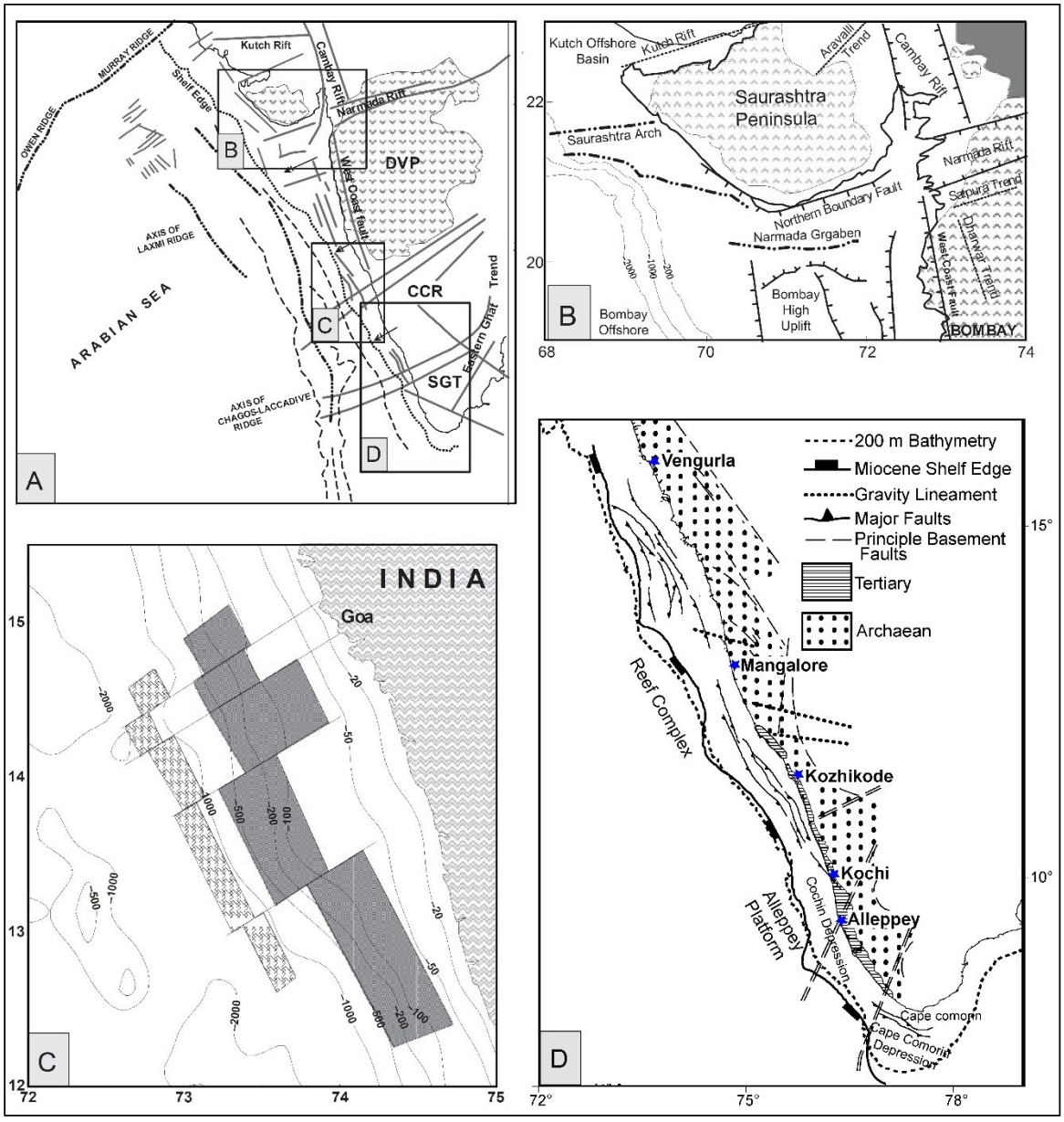

Figure 2.2 Map showing major structural trends on Indian subcontinent, and continuation of onshore structural trends into the western continental shelf of India (adopted from Bastia and Radhakrishna, 2012). (A) Structural trends (Kolla and Coumes, 1990). (B) Extension of Narmada-Son lineament into the offshore (Bhattacharya and Subrahmanyam, 1986). (C) Structural offsets in the central part of the margin (Subrahmanyam et al., 1993). (D) Structural continuity into the shelf areas of the Konkan-Kerala basin (Modified from Singh and Lal, 1993 and Bastia and Radhakrishna, 2012).

2.3 Regional physiography

The western continental margin of India is characterized by (i) a wide continental shelf having NW-SE trend, (ii) a remarkably straight shelf edge, (iii) a narrow continental slope bounded between 200 and 2000 m isobaths and, (iv) deep sedimentary basins. The continental shelf on the WCMI extends from Sir Creek in the north to Kanyakumari in the south (Fig. 2.3). The

western continental shelf, having area of about 310000 km^2, is divided into two parts: inner and outer shelf (Faruque and Ramachandran, 2014). The inner continental shelf extends from coastline to 55-60 m water depth in the north and narrows down to 25 m water depth off Cochin. The seabed of the inner shelf is smooth with a gentle slope of 1:7000 - 1:3300 (Wagle et al., 1994; Wagle and Veerayya, 1996; Rao and Wagle, 1997) and is carpeted with recent clayey silt and silty clay sediments with high organic matter and low carbonate content. The outer continental shelf extends from ~60 m water depth to shelf break and is commonly interrupted by shore-parallel ridges and reefs with a relief of 2-18 m (Nair, 1975). The seabed topography is rough and is carpeted with relict carbonate sediments, coarse sands with low organic matter and high carbonates. A narrow transition zone that lies between inner and outer continental shelf, displays uneven seabed topography with small scale buried pinnacles between 2 and 10 m thick sediments and textural differences in surficial sediments (Rao, 1989). This narrow transition zone is also considered by several researchers as mid-continental shelf (Wagle and Veerayya, 1996; Wagle et al., 1994; Rao and Wagle, 1997; Faruque and Ramachandran, 2014), where detailed geological and geophysical investigations are still lacking.

The physiography of the western continental shelf basin varies considerably through its sub-basins (Fig. 2.3). The shelf width in the Kutch basin varies from ~140 km off Kori creek to ~100 km off Dwarka. Further southward in the Saurashtra offshore basin, it increases from ~200 km off Diu to a maximum of ~340 km off Daman (Faruque and Ramachandran, 2014). Fifty Fathom Flat (FFF) is one of the most prominent topographical feature of the Saurashtra offshore basin and is centered about 18º 30' N and 71º 36' E. It is located roughly between 90 and 260 km from the coast. It is nearly oval shape and has almost flat topography (water depth ~90 m) covering an area ~28000 km^2. Basinal highs (Bombay and FFF) in the Kutchh-Saurashtra region contribute to smooth and even topography of the shelf region. The gradient of the westward dipping shelf in this region progressively becomes flatter southward and varies from 1:394 to 1:3050 (Faruque and Ramachandran, 2014). Due to presence of basement faults and folds, the shelf break close to the Saurashtra sub-basin occurs at ~180 m. The shelf edge in this region is remarkably straight but does not follow the coastline. Further south, width of the continental shelf between Daman and Ratnagiri region gradually decreases and reaches to ~90 km off Ratnagiri (Nair, 1975). The inner shelf in this region is moderately smooth with a gentle gradient ranging between 1:695 and 1:325. The shelf break near Ratnagiri sub-basin occurs between 130 and 180 m.

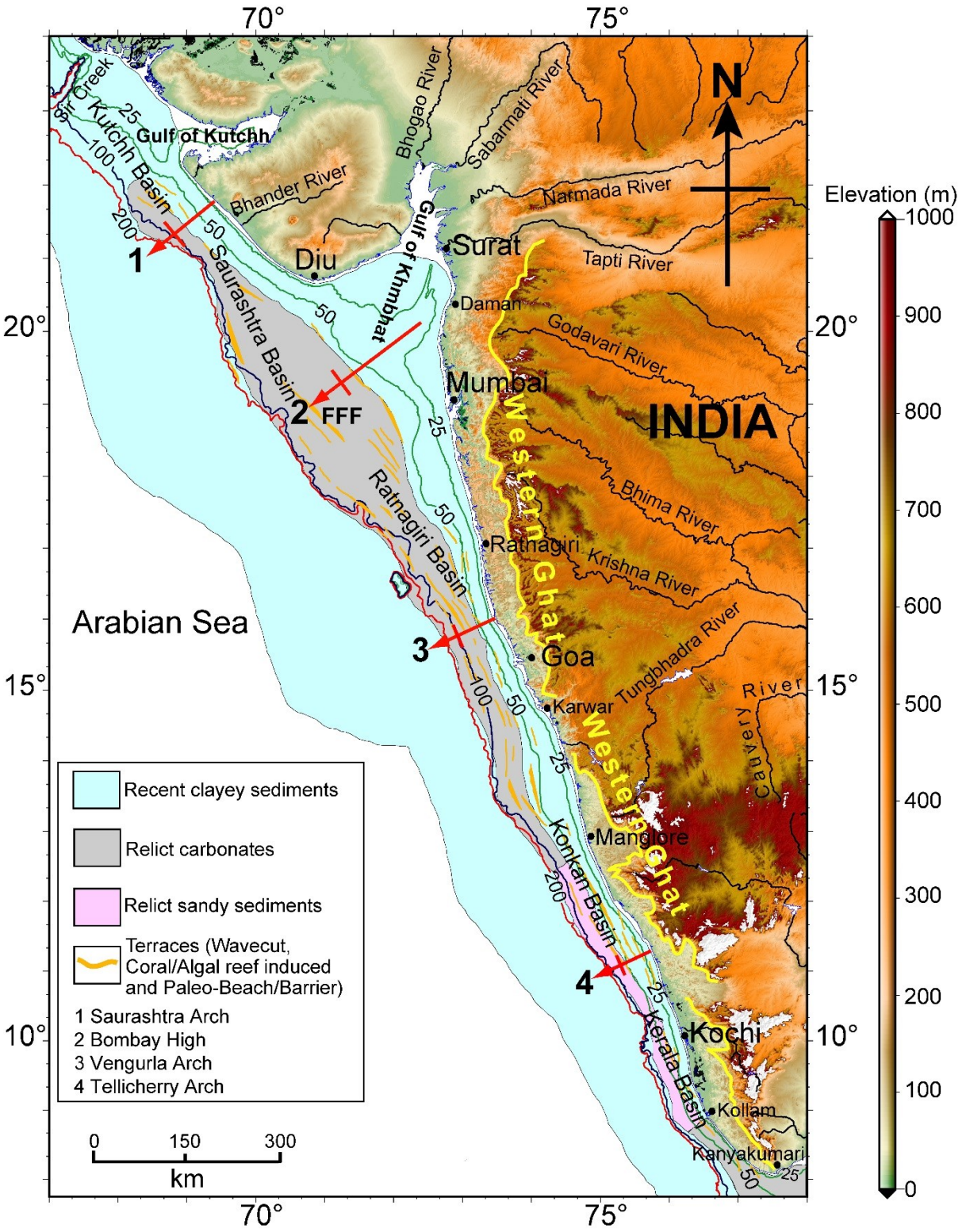

Figure 2.3 Map depicting surface sediment and terraces on the western continental shelf of India along with topography of hinterland. Solid green lines represent 25 and 50 m isobaths. Solid blue and red lines represent 100 m and 200 m isobaths, respectively. The relief map and bathymetric contours are generated using grid data of GEBCO (GEBCO_2014 version 20150318, Weatherall et al., 2015). Surface sediment and submarine terraces of the region were adopted from Kessarkar et al. (2003) and Wagle et al. (1994), respectively.

The width of continental shelf near the Konkan sub-basin region again increases to ~120 km off Goa, ~130 km off Karwar, ~140 km off Udupi (Nair et al., 1978; Rijil, 2011) and decreases southward thereafter. The inner continental shelf in this region is smooth and is limited to ~50 m water depth (Nair et al., 1978). Outer shelf (beyond ~50 m water depth) is again uneven due to the occurrence of submarine terraces. The submerged terraces off Karwar between 75 and 92 m water depth correspond to the stillstand of global lowered sea-level during the early Holocene (Vora and Almeida, 1990; Vora et al., 1996; Rao et al., 2003). Further southward the width of continental shelf narrows down to 80 km off Mangalore (Karnataka). The shelf break near Konkan sub-basin region occurs between ~90 and 130 m water depth (Nair et al., 1978; Rijil, 2011). Further southward, the width of continental shelf near Kerala sub-basin continues to narrow down to ~73 km off Kozhikode to 60 km off Quilon (presently Kollam) in Kerala (Rao and Wagle, 1997; Rijil, 2011). Inner continental shelf in this region is smooth and limited to ~25 m water depth off Kochi (Rao and Wagle, 1997). Submarine terraces in this region occur beyond ~35 m water depth in the outer continental shelf. Submarine terraces observed between ~55 to 60 m water depths extend ~200 km between off Mangalore and Kochi. Continental shelf break in this region occurs between ~60 m and 95 m water depth (Rijil, 2011). As a whole, width of the western continental shelf narrows down from north to south. Contrary to it, width of the continental slope widens from north to south (Biswas, 1982).

2.4 Climate and coastal circulation

Except Kutch region, the entire west coast of India experiences tropical wet climate, whereas Kutch region experiences semi-arid climate. Maximum temperature of the northern part of India in summer (March-June) rises beyond 45°C. This abnormal heating of northern main land of India and northward shift of Intertropical Convergence Zone (ITCZ) causes seasonal wind reversal (Pant and Parthasarathy, 1981; Goswami et al., 1984). The seasonal wind reversal between June and September is known as Indian summer monsoon and is responsible for 55-60% of total annual rainfall of India.

The Arabian Sea circulation is greatly affected by strong seasonal monsoon wind pattern. During the southwest monsoon (June-September), surface current with a mean speed of 50 cm/s covering up to ~150 km in the coastal Arabian Sea, prevails in a clockwise/southerly direction. Whereas during the northeast monsoon (November to February), the current is replaced by a northerly flow with a mean speed of only about 15 cm/s (Varadachari and Sharma 1967). An underwater current is also reported to exist during southwest monsoon between 100 and 250 m

water depth (Shetye et al., 1990, 1991). In addition, wave activity is also higher during this season.

Studies of Indian summer monsoon variations revealed that the monsoonal activity has been varying in the geological past with different time scale (Rostek et al., 1993; Thamban et al., 2002; Clift et al., 2008; Banakar et al., 2010; Patnaik et al., 2012; Saraswat et al., 2013). Though, intensification of rainfall in Indian subcontinent is related with the formation of Himalaya during the Miocene, first signature of seasonal variability in rain (i.e. monsoon) is reported in the Late Miocene (Clift et al., 2008). Various records (from South China Sea, Indian Ocean, and Himalayan region) provide evidence for southwest monsoon variation in the Pliocene and Quaternary. Pliocene monsoon variation was majorly controlled by northern hemisphere glaciation, whereas the Quaternary monsoon variations were influenced by glacial-interglacial cycles (Patnaik et al., 2012). Analysis of sediment core record from the Arabian Sea and Indian Ocean indicated several fluctuations of monsoonal rainfall intensity during the last 100 kyr (Rostek et al., 1993; Banakar et al., 2010). Thamban et al. (2002) reported discrete events of humidification at ~28,000 and 22,000 years BP. Their study further revealed that after last glacial maxima, precipitation and terrigenous input increased considerably between 15.6 kyr BP and 14.5 kyr BP, indicating a regional climatic augmentation during the early de-glaciation (Thamban et al., 2002; Saraswat et al., 2013). Further, these studies revealed commencement of the Holocene with intensified southwest monsoon which lasted till the mid-Holocene (Patnaik et al., 2012). Later it became relatively weak after 5,600 years BP and apparently interrupted by intervals of enhanced monsoon activity (Thamban et al., 2002; Banakar et al., 2010; Saraswat et al., 2013).

2.5 Sediment distribution

Western continental shelf of India is carpeted with recent coarse grain sands up to ~10 m water depth followed by clayey silt and silty clay up to ~50 m water depth (Fig. 2.3) on the inner shelf between Saurashtra and Quilon (Wagle et al., 1994: Rao and Wagle, 1997). Between 50 to 100 m, the continental shelf is usually covered with relict calcareous sands and beyond 100 m up to the slope again it is covered with clayey sediment with admix of recent terrigenous sediment (Rao and Rao, 1995; Rao and Wagle, 1997; Kessarkar et al., 2003). The inner continental clayey sediment zone generally extends up to 60 m water depth off the major rivers and narrow down to 25 m in the south-western part (Rao and Wagle, 1997). This zone is widest on the continental

shelf off Narmada and Tapti and narrows down to the south. It is 40 km wide off Saurashtra, 175 km off Tarapur, 80 km off Bombay, and 40 km off Ratnagiri, 45 km off Goa and Bhatkal and 25 km off Cochin. The sediment on the inner continental shelf is terrigenous in nature and numerous long and short but fast flowing rivers originating from Western Ghats, are the main source of these sediments. These rivers are typical monsoon rivers which lose their sediment transport capacity after SW summer monsoon. The seasonal variation of the terrigenous sediment supply attributes to the sedimentation pattern on the inner continental shelf of west coast of India. During post-monsoon and pre-monsoon seasons there is no significant sediment transport to the inner shelf (Nair et al., 1978). The major source for the clayey sediments on the continental shelf between Saurashtra and Goa is Deccan traps. Whereas, between Goa to Kanyakumari it was suggested to be derived from older gneissic rocks of western Dharwar gneisses (Rao and Rao, 1995). Outer shelf, beyond 50 m water depth till the shelf edge, is predominantly carpeted by relict carbonate sands (50-80% carbonate) between Saurashtra and Kanyakumari except Mangalore and Kollam (Nair, et al., 1978; Wagle et al., 1994; Kessarkar et al., 2003). Between Mangalore and Kochi, it is predominantly carpeted by relict terrigenous sands (Rao and Rao, 1995). Occurrence of Pisolitic limestone and beach rocks at various depths on the outer shelf revealed the formation of the surficial sediment in shallow water or sub-aerial environment during the last glacial period (Rao, 1990). Shelf edge to slope, seabed is again carpeted by recent terrigenous clayey sediments with 20-40% carbonate content (Kessarkar, et al., 2003). In northern region up to off Goa, it is carpeted by admix of Deccan Trap and Indus River derived terrigenous sediment and in southern region, it is carpeted by terrigenous sediments derived from western Dharwar gneisses.

The geophysical investigations on the continental shelf have revealed a prominent subsurface reflector (Siddique et al., 1981a, b; Rao and Wagle, 1997). This reflector has been reported to occur at ~35 m below the sea bed off the mouth of Narmada and Tapti rivers. Further southwards, the same reflector becomes shallower and occurs at ~25 m below the sea bed off Mumbai and ~15 m below the sea bed off Cochin. The sediments above this reflector are considered to be deposited during the Holocene (Siddique et al., 1981a, b; Rao and Wagle, 1997). Buried features such as palaeo-channels and wave cut terraces have been reported between Daman and Goa.

Sedimentation rates are not uniform throughout the continental shelf. Normally near the river mouth zones, high sedimentation rates have been observed. The high sedimentation rates in the

north corroborate with the high sediment flux derived from larger rivers and lesser sedimentation rate in the central and SW part suggest less sedimentation rates on the shelf. The clay accumulation rate is 19 mm/year at the mouth of the Narmada and Tapti rivers. It is about 5-7 mm/year in the nearshore region at 20-36 m water depth (Borole et al., 1982), and about 1.8-2.5 mm/year in the offshore region of Bombay at about 50-52 m water depth (Borole et al., 1982; Manjunatha and Shankar, 1992). Towards south the rate observed are low and vary from 0.45 to 0.72 mm/year in the inner shelf sediments off Mangalore (at 35-45 m depth)(Manjunatha and Shankar, 1992; Pandarinath et al., 1998), 0.54 to 2.6 mm/year off Karwar at 20-35 m (Nigam et al., 1992; Caratini et al., 1994; Pandarinath et al., 2001).

2.6 Regional hinterland geology

The hinterland area of Saurashtra and Ratnagiri offshore basin is covered by Deccan trap basalt, whereas Konkan and Kerala basin along with a part of Ratnagiri offshore basins are covered by western Precambrian terrain i.e. Dharwar craton and Southern Granulite Terrain (SGT) (Wadia, 1975; Kumar, 1985; Subrahmanya, 1987) (Fig. 2.4). The area is characterized by 35-65 km wide low lying (50-100 m) strip of coastal plains which is at places, interrupted by westward undulating table lands (100-500 m). These coastal plains are comprised of estuarine mudflats, mangroves, saltpans and sandy beaches and covered by Quaternary alluvium. The coastal plain is followed by a steeper higher terrain of the Western Ghats (Figs 2.3 & 2.4). Western Ghats 'mountain range' is the most prominent inland mega-geomorphological feature adjacent to the west coast of India. It is believed that formation of this mega geomorphological feature developed as a continental edge during the time of separation between India and Seychelles microcontinent following the Deccan flood basalt eruption during the Late Cretaceous (Widdowson 1997; Subrahmanya 1998; Gunnell and Fleitout 2000; Chand and Subrahmanyam 2003). It runs parallel to west coast along the north-south direction, and extends up to ~1500 km (Kale and Shejwalkar, 2008). It starts from south of the Tapti River in the north and ends at Kanyakumari district of Tamilnadu in the south and covers an area of ~160000 km2. Western edge of Deccan continental flood basalt constitutes the Ghats from south of Tapti River to Goa, and thereafter older western Dharwar craton shield and Kerala Khondalite Belt of SGT constitutes the Ghats till Kanyakumari. Anamudi is the highest peak of the Western Ghats located in Kerala and its height is 2695 m from mean sea-level. Average height of the Western Ghats ~1000 m.

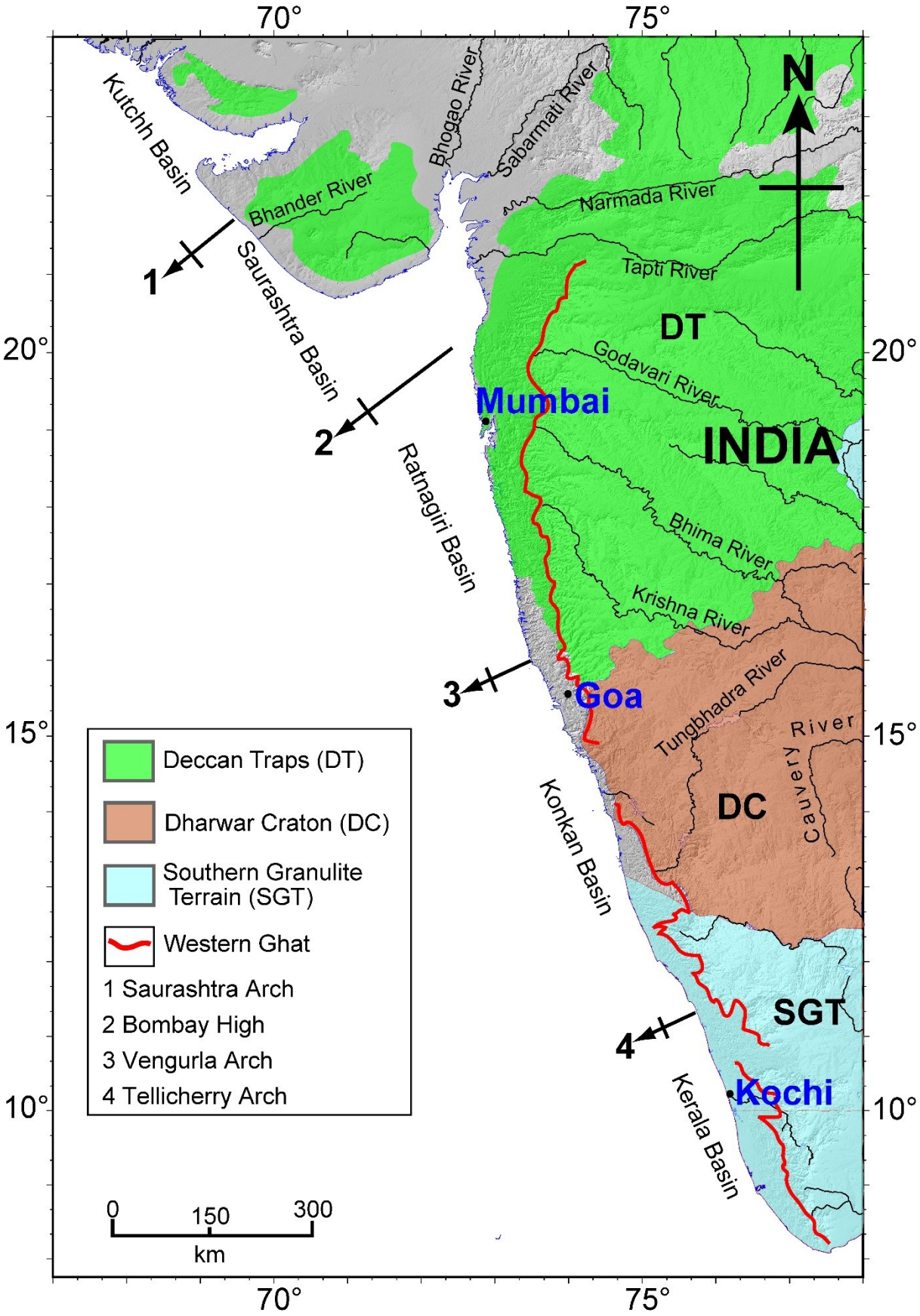

Figure 2.4 Map depicting hinterland geology of the western continental shelf of India (Modified from Bastia and Radhakrishna, 2012 and Kumar and Chaubey, 2019).

Flood basalt is the main constituent of the Deccan trap which was erupted during the Late-Cretaceous (Biswas, 1987; Malod et al., 1997) is supposed to lie upon Precambrian western Dharwar craton (Gokul et al., 1985; Kumar, 1985; Dessai, 2011). Whereas the Dharwar craton is comprised of numerous sub parallel supracrustal belts which are basically made up of severely metamorphosed volcanic and plutonic igneous and sedimentary rocks such as greenstone (metabasalt), granitic gneiss, Quartz-sericite schist, Quartz-chlorite-biotite schist (Gokul et al, 1985; Kumar, 1985; Devaraju et al., 2007, 2011; Dessai 2011). Similar to Dharwar Craton SGT is also comprised with numerous supracrustal belts which basically comprised of severely metamorphosed plutonic igneous and sedimentary rocks (Cenki and Kriegsman 2005). A narrow strip of coastal plain generally separates Western Ghats from the Arabian Sea, except at few places (Fernandes, 2009; Dessai, 2011). At few places it extends up to the Arabian Sea and stand tall as headlands. With an average height of ~ 1000 m, Western Ghats act as a barrier for SW monsoon winds and forms as one of the rainiest region in the world. Maximum precipitation (>3000 mm) occurs during the southwest monsoon (June to September) which is ~90% of the annual precipitation (Thamban et al., 2002). Numerous long and short rivers and estuaries originate from the Western Ghats escarpment and flow parallel to each other. Godavari, Krishna, Tungabhadra and Cauvery are the major eastward flowing rivers originating from Western Ghats and debouching into the Bay of Bengal. Narmada and Tapti are two major rivers which originate from Satpura and Vindhyan trends and debouch into the Arabian Sea in the Gulf of Khambhat. Whereas, Mahi, Mondovi, Zuari, Kali, Sharavati, Gangavali, Netravathi, Pamba, Bharathppuzha, and Periyar are few major westward flowing rivers which originates from Western Ghats and debouch into the Arabia Sea. These rivers, comparatively smaller than the eastward flowing Western Ghats rivers, flow through the steeper slope of the Western Ghats and, are main erosional agents for the Western Ghats. These drainage systems have been continuously eroding the Ghats and spreading the eroded terrigenous sediments on the inner continental shelf of west coast of India. Due to high seasonal variation in precipitation, most of these typical monsoon drainage channels are seasonal and show heavy run-off during the monsoon season and remain sluggish in rest of the years.

2.7 Geological setting of the study area

Geographically study area is located on the inner continental shelf of Goa, central west coast of India between latitudes 14°40' N and 15°40' N and longitude 73°24' E and 74°05' E where water depth varies from ~8 m to 60 m (Fig. 2.4). It includes ~105 km of the entire Goa coastline.

Physiographically, from east to west, inland area of Goa is divided into three major parts: (i) the Western Ghats (hilly region), (ii) central table land (undulating terrain) and, (iii) coastal plain (Fernandes, 2009). The N-S trending high imposing hills of the Western Ghats constitute the eastern most part of Goa. Average height of the ghat in Goa is ~1000 m (Dessai, 2011). The Western Ghats in Goa region is primarily constituted by Goa group of Dharwar supergroup (Fernandes, 2009; Dessai, 2011) except north-eastern part of the region where the Deccan flood basalt is the main constituent of the Western Ghats. The basal rocks of the Ghat are made of metavolcanics with intercalations of metasediments overlain by a larger proportion of clastics, dominated by greywacke (GSI, 1996). The supracrustal rocks are mainly composed of basalts, charnockites, granite gneisses, khondalites, leptynites, and metamorphic gneisses with detached occurrences of crystalline limestone, dolerites, anorthosites, residual laterite, banded ferruginous quartzite and bauxite (Gopalkrishnan, 1976; Harinadha Babu et al., 1981; Gokul et al., 1985; Devaraju et al., 2010; Dessai, 2011). The NW-SE trending undulating central table lands are usually capped by dismembered laterite. The central table lands with an elevation range of ~100-400 m separate the Western Ghats hills from the coastal plain (Krishnan, 1968; Gokul et al., 1985; Fernandes, 2009; Dessai, 2011). Some of the table land extend till coastline in the form of headlands. Aguada, Sada and Cabo-de-Rama are major headlands made up of meta-sediments, meta-basites and subvolcanic rocks of Sanvordem and Barcem formations of Goa. The northern headlands of Goa are particularly made up of erosion resistive dolerite rocks and have major controls on the coastline physiography (Fernandes, 2009). The western most part of inland area of Goa is characterized by low lying (height variation ~50-100 m) coastal plain. Supracrustal rocks in coastal plain adjacent to the study area is mainly composed of metamorphosed sediments, greywacke, basites, banded haematite quartzites, granites and older gneissic rocks of Vageri, Bicholim, Sanovordem, Barcem formations and Chandranath granite gneisses (Fernandes, 2009; Dessai, 2011). These formations are shown in Figure 2.5. The supracrustal rocks are overlain by recent alluvium deposits in the form of sandy beaches, sand dunes, tidal mudflats, estuarine alluvium, saltpans, and marshes. Coastal plains are often interrupted by NW-SE trending table lands in the central region.

Tiracol, Chapora, Mandovi, Zuari, Sal, Talpona and Galgibag are important rivers flowing through Goa and carry terrigenous material from high lands of the Western Ghats to the continental shelf of Goa in the Arabian Sea. All the rivers that flow within the coastal state of Goa are estuarine due to tidal impact. Though tides dominate, fresh water also enters in the estuaries by rivers and rivulets that join them at the upstream. Further, Mhadei is the freshwater

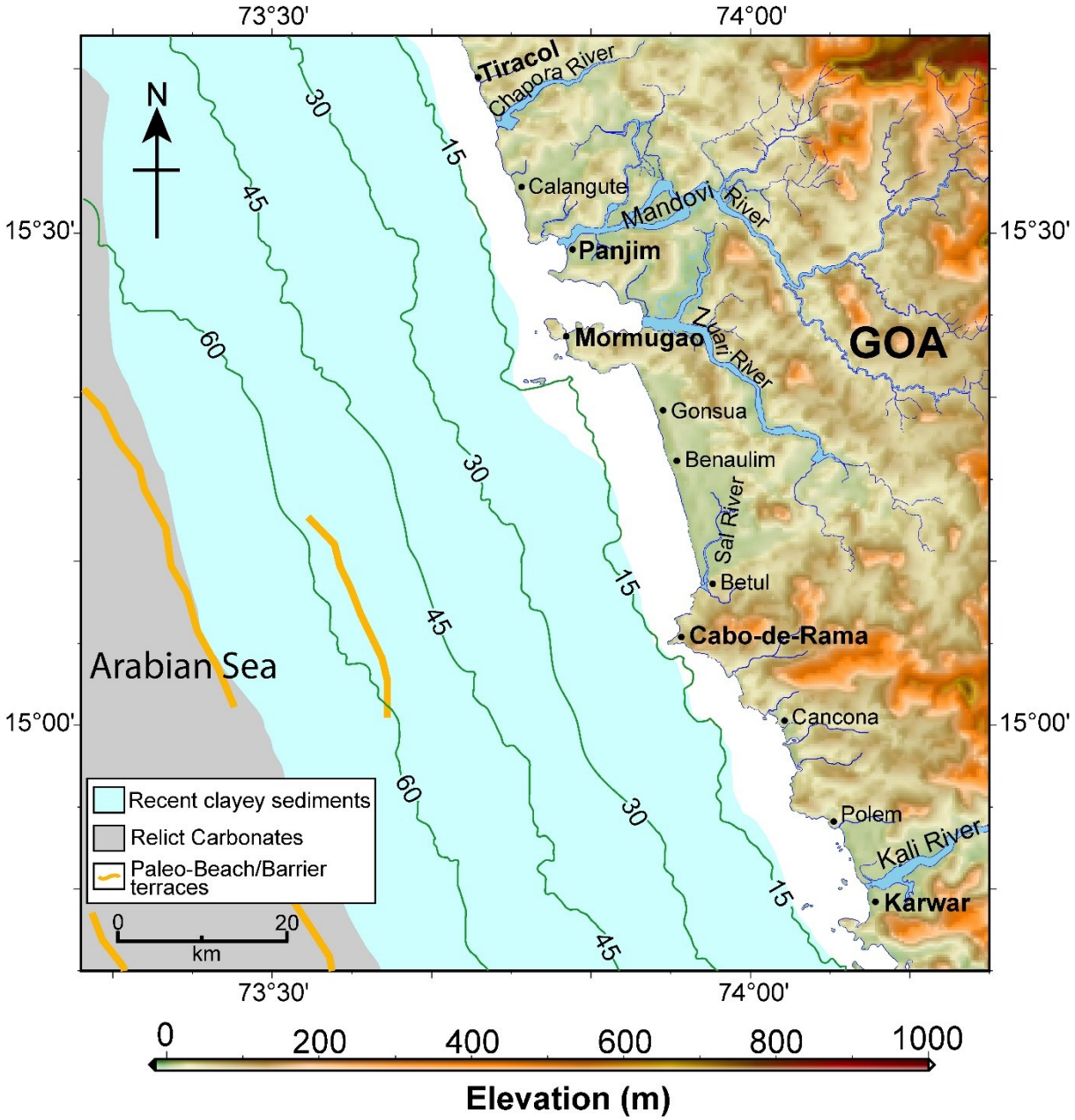

Figure 2.5 Map of study area. Isobaths corresponding to 15, 30, 45 and 60 m water depths are shown with solid green lines. Prominent features and present river drainage pattern are shown on the relief map of adjacent land area. The relief map and bathymetric contours were generated using grid data of GEBCO (GEBCO_2014 version 20150318, Weatherall et al. 2015). Surface sediment and submarine terraces distribution of the region were taken from Kessarkar et al. (2003) and Wagle et al. (1994), respectively.

stream, originates in the Western Ghats in Karnataka, and joins the Mandovi (Shetye et al., 1995). Therefore, in this thesis, the major estuaries are also referred as river. Mandovi and Zuari are the largest estuaries of Goa, each with ~50 km long main course (Shetey et al., 1995). Mandovi and Zuari with ~1896 km^2 and 917 km^2 catchment area, respectively, constitute largest river basin of Goa and drains water from more than half of the total area of Goa (~3700

km^2). Gano, Valvat, Dicholi, Kudnem, Mhapsa, Mhadei and Khandepar are the main tributaries of Mandovi estuary (Shetye et al., 1995; 2007). Whereas, Kushavati, Uguem and Guloli are the main tributaries of Zuari estuary (Shetye et al., 1995; 2007). Annual run-off for Mandovi and Zuari at Panaji and Marmugao Bay, respectively have been estimated ~ 6000 MCM and 2190 MCM (1 MCM = 1 Million Cubic Meter) (Shetye et al., 2007). Most of the run-off occurs during June to September (summer monsoon season) with peak daily run-off greater than 150 MCM. Heavy rainfall in the monsoon season (June-September) on the slopes of the Western Ghats leads to heavy run-off in the catchment area of these estuaries. Due to the heavy runoff, the salinity of these estuaries at the mouth zone fall drastically to ~2‰ which causes flocculation in the tidal zone only (Nair et al., 1978). Though the flocculation occurs, these estuaries remain the main agents for the terrigenous sediment supply to the continental shelf of Goa. They carry most of their annual terrigenous sediment supply during the monsoon season and contribute insignificantly in rest of the season (Nair et al., 1978; Shetye et al., 2007). Longshore current drift plays a major role in further dispersion of these sediments (Veerayya et al., 1981).

The inner continental shelf of the study area is marked by an even and gentle topography (Nair et al., 1978; Rao, 1989; Wagle et al., 1994). Whereas the outer shelf is characterized by uneven topographic variations due to occurrence of several small and large scale pinnacles (~5 m height) and terraces in the region. From ~50 to 70 m water depth, the outer shelf is dominated by small scale sand bar and algal ridges, whereas it is dominated by carbonate terraces beyond ~70 m water depth (Nair et al., 1978; Rao, 1989; Wagle et al., 1994). In the nearshore region of the study area between shoreline and ~10 m water depth, it is predominantly covered by beach sands and muddy sand (Veerayya et al., 1981) followed by silt and clayey-silt or silty-clay with carbonate content less than 20% up to ~50 m water depth (Nair et al., 1978: Mazumdar et al., 2009).

It is mostly covered by calcareous sands with 50-75% carbonate content between 50 and 100 m water depth (Nair et al., 1978). Beyond 100 m water depth, presence of admixture of recent sand silt and clay sediments are reported which show ~80 % carbonate content (Nair et al., 1978; Rao and Wagle, 1997; Wagle et al., 1994; Kessarkar et al., 2003). The surface current in this region are expected to play the key role at these depths for the observed sediment distribution pattern (Nair et al., 1978). Holocene sediments in the study area are reported to be deposited as a wedge-shaped sediment package (Karisiddaiah et al., 2002; Mazumdar et al.,

2009). This wedge-shaped sediment package thickens towards shore and pinches out at ~50 m water depth, and is bounded by a planar surface referred as maximum flooding surface (Karisiddaiah et al., 2002; Mazumdar et al., 2009).

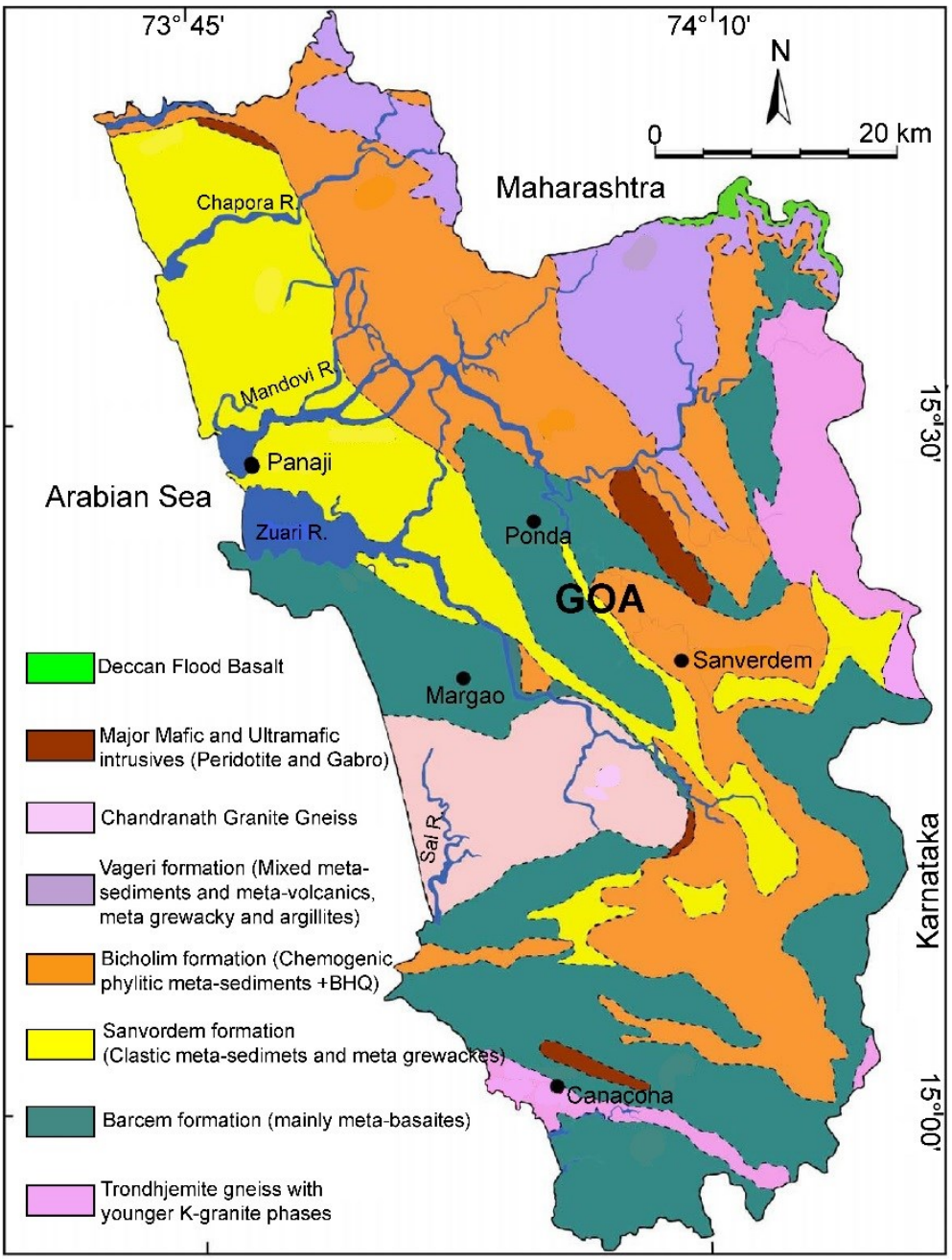

Figure 2.6 Geology of Goa (adopted from Dessai, 2011 and Fernandes, 2009).

Chapter 3
Data and Methodology

3.1 Introduction

The present study is primarily based on single channel High Resolution Shallow Seismic (HRSS) data. Besides, bathymetry and sediment data are also utilized for this study. Bathymetry and high resolution shallow seismic data (Table 3.1) were acquired onboard the *Coastal Research Vessel Sagar Sukti* (Cruise nos. SASU-194, SASU-196) and *Mechanized Fishing Boat Falguni* during 2009-10 and 2014, respectively. Sediment samples were collected at three locations (GC-01, GC-02 and GC-03) using gravity corer onboard *Research Vessel Sindhu Sadhana* during 2017 (Fig. 3.1). The bathymetry and seismic data were acquired along parallel tracklines spanning orthogonal to the coast at one nautical mile line spacing between ~8 and 60 m water depth of the study area. A total ~1650 line kilometer of HRSS data, acquired along 50 parallel tracklines (Fig. 3.1), are used in this study. In addition, published sedimentological data and sea-level curves for the Late Quaternary (eustatic) and the Holocene (west coast of India) are used to assign the age of interpreted seismic sequence boundaries.

Table 3.1 Details of bathymetry and HRSS data utilized in the study.

Cruise ID	Surveyed trackline ID	Echo-sounder used	Seismic system used	Number of tracklines
SASU-194	SaSu-24 to SaSu-34	Deso-17 DS	Sparker system	11
SASU-196	SaSu-35 to SaSu-51	Deso-17 DS	Sparker system	17
GK	GK-01 to GK-22	Atlas Deso-30	Sparker system	22

Present chapter describes the details of types and sources of data used in this study. It presents the minutia of acquisition, processing and interpretation methodology of the HRSS and single beam bathymetry data. The chapter also provides an overview of computation methodology for hydraulic and geomorphic parameters of buried channel, sediment thickness and sedimentation rates. Besides, it also describes methodology used for computation of thickness and sedimentation rate of the Holocene sediments, and preparation of grid data of sediment thickness, sedimentation rate and the Holocene transgressive surface.

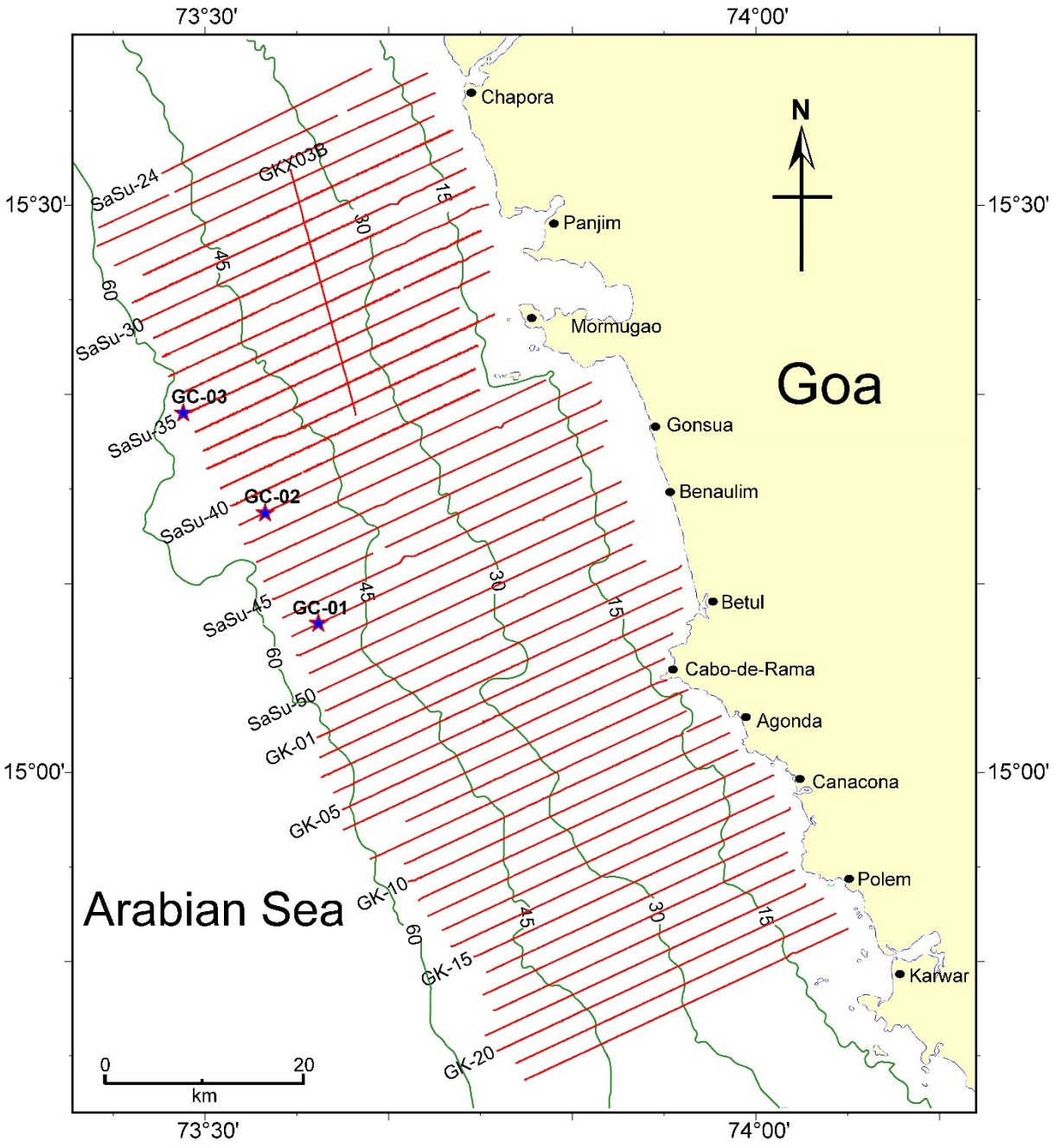

Figure 3.1 Map depicting survey tracklines along which high resolution shallow seismic and bathymetry data were acquired. Stars denote locations of sediment core. Annotated values on isobaths (solid green contours) are in meter.

3.2 Types and sources of data

3.2.1 High resolution shallow seismic data

High resolution shallow seismic data were acquired using sparker seismic system with multi-tipped sparker squid as seismic source. It is one of the most convenient energy source for HRSS data acquisition from the continental shelf because it is easy-to-deploy and cost-effective, and has ability to work in very shallow water depth with least environmental impact compared to other implosive seismic sources. Moreover, it is capable of providing a better penetration to sedimentary assemblage and can deliver a very good interpretable seismic section after application of few simple processing steps. Details of acquisition and processing of shallow seismic data are presented in the following sub sections:

3.2.1.1 Acquisition of shallow seismic data

Sparker seismic system was comprised of energy source CSP D700, multi-tips squid spark array SQUID 500, data acquisition unit Octopus 760 and a 20 element hydrophone steamer with 0.25 m hydrophone spacing. Energy source unit was set to supply 300 J per shot through multi-tipped sparker squid and the seismic signal received through the hydrophone streamer was recorded at 24 kHz sampling frequency rate for 500 ms record length (Table 3.2). The multi tipped sparker squid was towed ~15 m behind the vessel/boat, whereas hydrophone streamer was towed ~20 m behind the vessel/boat. Each shot was geo-referenced using a Differential Global Positioning System (DGPS). DGPS manufactured by Trimble (Model 4000 SE) along with the differential beacons (operating in 283.5 to 325 kHz band) were used for navigation and positioning during the survey. The system, being differential, overcomes the error caused by disturbances in ionosphere-troposphere and other errors. The system comprised of two Pro Beacon GPS receivers. The Pro Beacon receiver used advanced digital signal processing technique to track and demodulate the signals from DGPS's radio beacon. The navigation data were logged using windows based HYPACK® software during the survey. The HYPACK® software provides tools to (i) design survey tracklines, (ii) navigate along the planned tracklines, (iii) provide position data to other geophysical systems (echosounder and sparker system), (iv) log raw position and depth data and, (v) realize the quality control in real time navigation. Continuous monitoring of navigation data quality was carried out online using display system both at recording room and wheel house of the vessel/boat. Online monitoring of navigation data also helped to keep the vessel/boat speed limit ~4 knots (~7.4 km/h) during the data acquisition.

Table 3.2 Sparker seismic system and acquisition parameters.

HRSS energy source unit		
CSP-D 700 with SQUID-500 (4-electrode, multi tips sparker array)	Shot rate	2 per second
	Energy	300 J
	Operator voltage	3500 volt
	Source (Squid) towed behind vessel	20 m
	Source (Squid) depth	0.5-1.0 m
HRSS signal receiver unit		
Single-channel streamer	Length	4.5 m
	Number of hydrophones	20 element hydrophone array
	hydrophone spacing	0.25 m
	Streamer towed behind the vessel/boat	25 m
	Receiver depth	On the sea surface
HRSS signal recording unit		
OCTOPUS-760 D	Data format	SEG-Y
	Recording length	500 ms
	Sample rate	40 µs (24 kHz)
Navigation system		
DGPS (Trimble)	Operating frequency band	283.5 to 325 kHz
	Data logging software	HYPACK®
Vessel speed		~ 4 knot

3.2.1.2 Processing of shallow seismic data

Acquired seismic data was processed at CSIR-National Institute of Oceanography, Goa using seismic data processing software package SeisSpace®ProMAX® of Landmark Solutions, USA. The objective of seismic data processing was to reduce artefacts (secondary bubble effect, short-path multiples, etc.) and produce an interpretable seismic section. Major processing steps involved in the processing are resampling, frequency filtering, deconvolution, and gain correction. The data was resampled at 0.1 ms interval and stored in an internal format of SeisSpace®ProMAX®. Major processing steps (Table 3.3) have been described in the following sub-sections.

Table 3.3 Major processing steps and parameters used for processing the high resolution shallow seismic data.

Processing step	Parameters used
Resample	0.1ms
Band-pass filter	'Ormsby' band pass filter applied in frequency domain with 25% zero padding for FFT, and corner frequency (Hz) of 100 -125 -1100 -1200.
Deconvolution	Minimum-phase spiking, Operator length=8.0 ms, pre-whitening=0.1%.
Band-pass filter	'Ormsby' band pass filter applied in frequency domain with 25% zero padding for FFT, and corner frequency (Hz) of 100-125-2200-2500.
Automatic Gain Control (AGC)	AGC Scalar: RMS, Operator length: 100 ms, Scalar application: centred.

- ***Resampling***

Seismic data were resampled to reduce data size for easier and less time-consuming data handling and processing. To resample the data with adequate resampling rate, frequency characteristic of the raw data was analyzed using interactive spectral analysis tool of SeisSpace®ProMAX® 2D. Interactive spectral analysis tool plots dB power distribution over entire frequency range of acquired data. Power spectrum of entire traces of raw data reflects frequency notching due to ghost and bubble effect. It was more severe beyond 2500 Hz frequency. Therefore, firstly an 'Ormsby' band pass filter with corner frequency of 100-125-2200-2500 Hz was applied and afterwards data was resampled with 0.1 ms sampling rate (corresponding Nyquist frequency = 5000 Hz). Applied band pass filter works as anti-aliasing filter as well as rectify low and high- frequency noises from data. After resampling, power spectrum of the data was re-analyzed to verify the output.

Resampled data was first subjected to trace editing and top muting. Later, it was subjected to band-pass filtering, deconvolution and gain corrections to improve seismic reflectors.

- ***Band-pass filter***

Band-pass filters are commonly used in seismic processing to remove low and high frequency noises (Yilmaz, 2001). The entire seismic data along each surveyed track was re-analyzed using interactive spectral analysis tool to find out dominant frequency as well as frequency band in the data. The analysis indicated frequency band of 100-1200 Hz. Accordingly, an 'Ormsby' band-pass filter with corner frequency of 100-125-1100-1250 Hz was applied to the data. The same band pass filter was again applied to the data after application of spiking deconvolution

tool. Application of band pass filter after deconvolution tool aims to remove extra noise added by the deconvolution process.

➢ ***Deconvolution***

Deconvolution compresses basic seismic wavelet in recorded seismogram, attenuates reverberation and short-period multiples, and thus increases temporal resolution (Yilmaz, 2001). Trace by trace spiking deconvolution was applied to the data using "Spiking/Predictive Decon" tool of SeisSpace®ProMAX®. An operator length of 8 ms and time gate of 0-250 ms were used during application of the deconvolution operator to the data. Pre-whiting noise of 0.1% was added during the processing. Complete removal of reverberation and multiples are difficult from seismic data acquired by single channel sparker seismic system. However application of deconvolution tool considerably reduces reverberation as well as short-period multiples, and noticeable improvement is observed in the seismic section (Fig. 3.2).

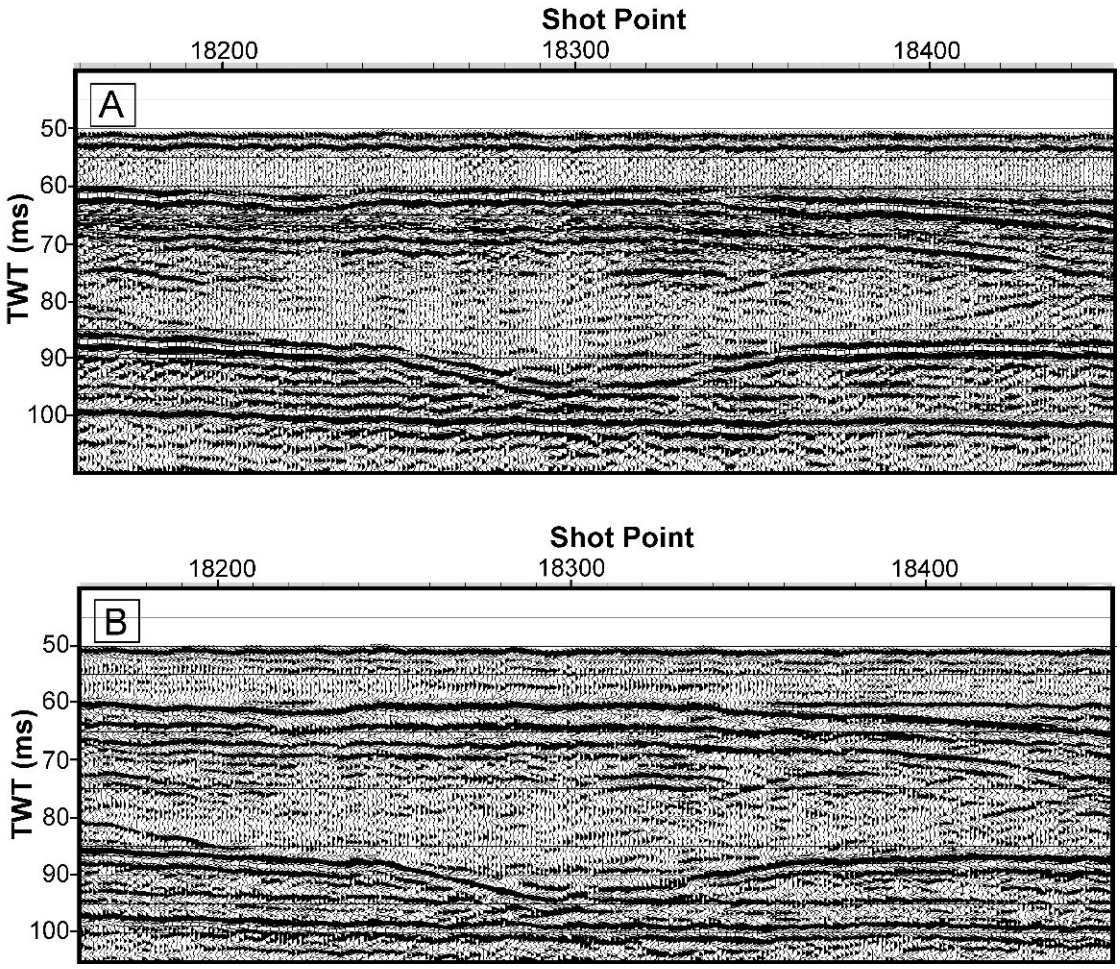

Figure 3.2 High resolution shallow seismic sections: (A) after resampling and, (B) after application of deconvolution.

➢ ***AGC***

Automatic Gain Correction (AGC) is applied to the data using AGC tool of the SeisSpace®ProMAX®. AGC scalar (RMS) and operator length (100 ms) in central application mode were applied to the data. This was carefully applied mainly for trace amplitude balancing with a purpose to enhance seismic section visualization without any distortion.

The processed seismic data revealed a dominant frequency band ranging from 800 to 1200 Hz with a central frequency of ~1000 Hz. Considering P-wave velocity of 1583 m/s (Krishna et al., 1989) in shallow sediments of the study area, the processed seismic data revealed vertical resolution of ~40 cm. Vertical seismic resolution is the minimum distance required to distinguish two close by seismic reflectors so that both can be defined separately rather than as one reflector. Apart from these major processing steps, SeisSpace®ProMAX® was also used to extract navigation data from the SEG-Y header files of the HRSS data. The navigation data were later used for generating different types of map after layout corrections.

3.2.2 Acquisition and processing of bathymetry data

The bathymetry data were acquired along with HRSS data using single-beam echo-sounders which were calibrated using the bar check method. The echo-sounder was interfaced with the navigation system for digital depth logging. The data was processed using HYPACK® data acquisition software. The data processing involves removal of spurious depth (spikes) data and draft corrections. Later, processed bathymetric data was used to generate grid for bathymetry at 500 m grid interval. The gridded data was used to generate bathymetric contours of the study area and analyze the Holocene sediment thickness and sediment distribution pattern in the study area.

3.2.3 Acquisition and processing of sediment sample data

Three sediment cores (GC-01, GC-02 and GC-03) were collected using gravity corer onboard *Research Vessel Sindhu Sadhana* during cruise SSD-039 in July 2017. The cores were acquired between 55 and 60 m water depths in the study area. Details of these sediment cores are presented in Table 3.4.

The sediment cores were collected using 6 m long steel barrel and 560 kg additional weight. The barrel accommodates 6 m core liner. The gravity corer barrel along with plastic core liner

Table 3.4 Details of sediment cores collected for the present study.

Core ID	Core length (m)	Location	Water Depth (m)
GC-01	2.26	73.6199211° E, 15.138998° N	54.5
GC-02	0.53	73.5702313° E, 15.236446° N	55.6
GC-03	0.57	73.4854666° E, 15.317605° N	60.4

was fired at required locations to collect sediment samples. Recovered sediment samples were preserved onboard lab facility of the *Research Vessel Sindhu Sadhana.* Later, sediment samples were processed in Micropaleontology laboratory of CSIR-National Institute of Oceanography, Goa. The collected sediment samples were processed for (i) carbon 14 dating and (ii) grain size analyses. Sediment samples recovered from each sediment core were sub-sampled at 1 cm interval for carbon dating purpose. From selected sub-samples, benthic foraminifera and carbonate samples were extracted following the standard methodology for extraction. Later, these samples were dated using ^{14}C technique in the Department of Geology and Mineralogy, University of Cologne, Germany and Inter University Accelerator Centre, New Delhi. The ^{14}C dates were calibrated using "Marine13" dataset (Reimer et al., 2013) and Calib 7.1 software (Stuiver et al., 2017) considering a reservoir correction ΔR for the eastern Arabian Sea of 177±73 years. Calib 7.1 is an online software based program which facilitate calibration of radio carbon dates and marine reservoir correction. Further, sediment samples recovered from GC-01 were sub-sampled at 0.5 cm interval for coarse fraction analysis following the standard methodology.

3.2.4 GEBCO bathymetry and elevation data

Present study also utilizes the General Bathymetric Chart of the Oceans (GEBCO) data for generating various maps. The GEBCO_2014 bathymetry and elevation data (Weatherall et al., 2015) is a digital bathymetric and elevation model of the global ocean floor and land topography prepared by combining ship-borne depth soundings with interpolations guided by satellite-derived gravity data. GEBCO_2014 (version 20150318), an updated version of GEBCO_08, provides bathymetric and topographic data with 30 arc-second grid spacing. For the present study, the gridded bathymetry and elevation dataset was downloaded from the GEBCO website (https://www.gebco.net) and subsequently required data were retrieved for the study area and adjoining hinterland.

3.2.5 Published sea-level curves and sedimentation rate

Apart from HRSS, bathymetry and sediment sample data, present study also utilizes published sea-level curves and sedimentation rates. The study utilizes the Holocene sea-level curve (Hashimi et al., 1995) of west coast of India (Fig. 3.3) to compute the Holocene sedimentation rates at any locations of the study area and to prepare its spatial distribution map. It also uses global sea-level curve (Rehak et al., 2010) to assign age for identified stratigraphic layers due to the absence of long sediment core data from the study area.

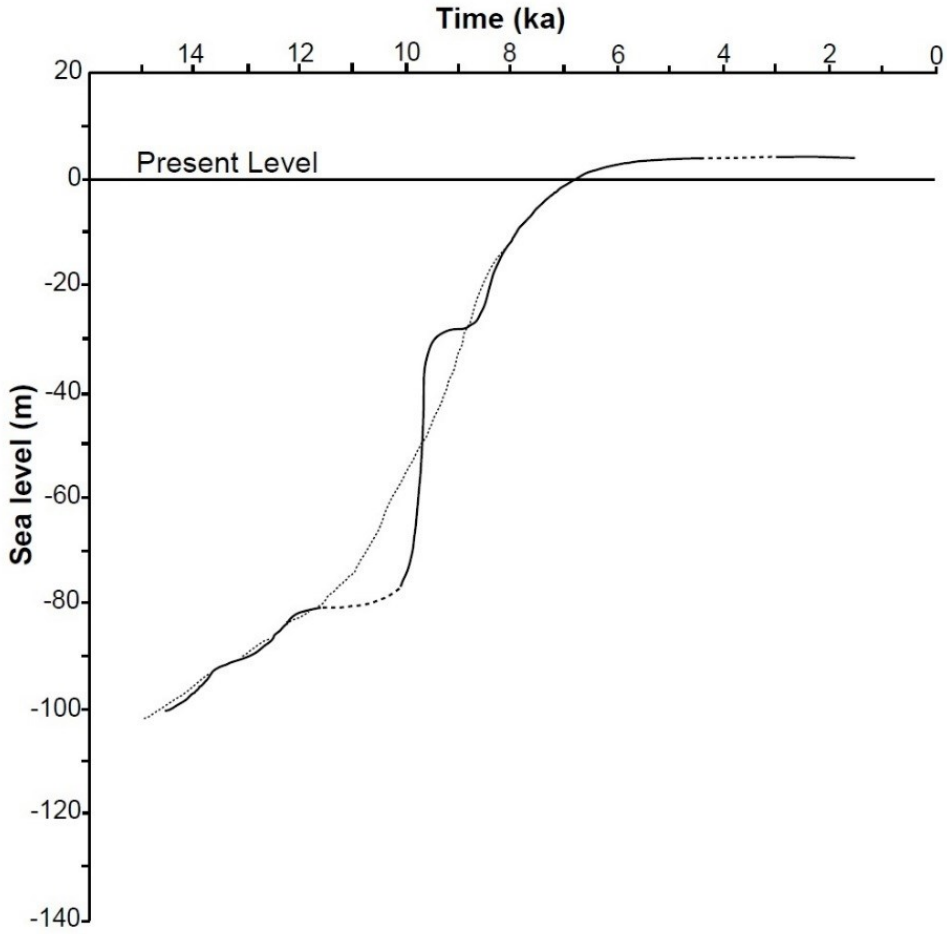

Figure 3.3 The Holocene sea-level curve of west coast of India (Hashimi et al., 1995). Dotted points represent a generalized envelop of the proposed sea-level curve. Dashed line on the broken sea-level curve indicates lack of data.

Further, published sedimentation rates (Nigam and Nair, 1989; Nambiar et al., 1991; Caratini et al., 1994; Nigam and Khare, 1995; Pandarinath et al., 2001) from the study area and nearby region are used to compare with the Holocene sedimentation rates obtained from the present study and to draw important inferences. The compiled details of published sedimentation rates are presented in Table 3.5.

Table 3.5 Details of sediment samples and sedimentation rates (around the study area) published by various researchers.

Sl. no.	Area	Core no.	Location and (water depth)	Depth in the core	Dating technique & (material)	Age (yrs BP)	Sedimentation rate (mm/yr)	References
1	Off Karwar	GV 3713	14.88° N; 73.965°E (20 m)	26 cm	Excess ^{210}Pb (sediment)	100	2.6	Nigam and Nair, 1989; Nigam and Khare, 1995
2	Off Karwar	SK-148/14	14.84° N; 74.0° E (22 m)	2.58-2.59 m	^{14}C (o.m.)*	4190 ± 110 (Calibrated)	0.62 (4190 yr BP to present)	Pandarinath et al., 2001
3	Off Karwar	SK-148/14	14.84° N; 74.0° E (22 m)	5.35-5.36 m	^{14}C (c.w./p.)**	9280 ± 150 (Calibrated)	0.54 (9280-4,190 yr BP)	Pandarinath et al., 2001
4	Off Karwar	SK-27B/8	14.83° N; 73.990 E (22 m)	1.30-1.35 m	^{14}C (o.m.)*	2220 ± 40 (Calibrated)	0.60 (2220 yr BP to present)	Caratini et al., 1994
5	Off Karwar	SK-27B/8	14.83° N; 73.990 E (22 m)	1.40-1.45 m	^{14}C (o.m.)*	2020 ± 40 (Calibrated)	0.70 (2020 yr BP to present)	Caratini et al., 1994
6	Off Karwar	SK-27B/8	14.83° N; 73.990 E (22 m)	2.25-2.30	AMS ^{14}C (Shell)	2220 ± 70 (Calibrated)	1.02 (2220 yr BP to present)	Caratini et al., 1994
7	Off Karwar	SK-27B/8	14.83° N; 73.990 E (22 m)	3.00-3.05	^{14}C (o.m.)*	3510 ± 60 (Calibrated)	0.86 (3510 yr BP to present)	Caratini et al., 1994
8	Off Karwar	SK-27B/8	14.83° N; 73.990 E (22 m)	4.45-4.50	^{14}C (o.m.)*	4325 ± 65 (Calibrated)	1.03 (4325 yr BP to present)	Caratini et al., 1994
9	Off Karwar	SK-44/13	14.74° N; 74.05° E (25 m)	3.00-3.04	^{14}C (o.m.)*	3780 ± 210 (Calibrated)	0.80 (3780 yr BP to present)	Caratini et al., 1994
10	Off Karwar	SK-44/13	14.74° N; 74.05° E (25 m)	4.50-4.55	^{14}C (o.m.)*	6370 ± 170 (Calibrated)	0.58 (6370-3780 yr BP)	Caratini et al., 1994

11	Off Karwar	SK-44/13	14.74° N; 74.05° E (25 m)	4.55-4.60	^{14}C (o.m.)*	6200 ± 90 (Calibrated)	0.73 (6200 yr BP to present)	Caratini et al., 1994
12	Off Karwar	PC-1490	14.67° N; 73.99° E (33.7 m)	5.78-5.80	^{14}C (c.w./p.)**	8620 ± 300 (Uncal.)	0.67 (8620 yr BP to present)	Nambiar et al., 1991
13	Off Karwar	PC-1459	14.6° N; 74.23° E (17.7 m)	3.02-3.10	^{14}C (Shell)	3410 ± 90 (Uncal.)	0.89 (3410 yr BP to present)	Nambiar et al., 1991
14	Off Karwar	PC-1464	14.43° N; 74.21° E (25 m)	4.20-4.38	^{14}C (c.w./p.)**	9630 ± 120 (Uncal.)	0.44 (9630 yr BP to present)	Nambiar et al., 1991
16	Off Honnavar	SK-148/13	14.4° N; 74.0° E (50 m)	1.67-1.69	^{14}C (c.w./p.)**	9790 ± 120 (Calibrated)	0.17 (9790 yr BP to present)	Pandarinath et al., 2001
17	Off Honnavar	SK-148/13	14.4° N; 74.0° E (50 m)	1.99-2.00	^{14}C (c.w./p.)**	9990 ± 120 (Calibrated)	1.6 (9990-9790 yr BP)	Pandarinath et al., 2001
18	Off Honnavar	SK-148/13	14.4° N; 74.0° E (50 m)	2.20-2.22	^{14}C (c.w./p.)**	10010 ± 120 (Calibrated)	11.0 (10010-9990 yr BP)	Pandarinath et al., 2001
19	Off Honnavar	SK-148/13	14.4° N; 74.0° E (50 m)	2.72-2.74	^{14}C (o.m.s.)***	10760 ± 130 (Calibrated)	0.69 (10760-10010 yr BP)	Pandarinath et al., 2001
20	Off Mangalore	RVG/207	(41 m)	0.50-0.60	^{14}C (o.m.)*	1330 ± 80 (Calibrated)	0.45 (1330 yr BP to present)	Pandarinath et al., 1998
21	Off Mangalore	RVG/207	(41 m)	0.90-0.10	^{14}C (o.m.)*	2090 ± 80 (Calibrated)	0.53 (2090-1330 yr BP)	Pandarinath et al., 1998
21	Off Mangalore	SS/MG/02	(45 m)	0-70 mm	Excess ^{210}Pb (sediment)		0.56	Manjunatha and Shankar, 1992
*Organic Material, **Carbonized woods and peats, ***Sediment enriched with black fine organic material.								

3.3 Methodology

Single-beam bathymetry and HRSS data were acquired with an aim to map underlying stratigraphic and geomorphologic features of the shelf strata of the study area. Processed HRSS data were analyzed and interpreted for seismic sequence stratigraphy, buried paleo-channel morphology and other sub-surface formation scale morphological features along with geo-acoustic features. In order to convert Two Way Travel time (TWT) into depth (m) following formula is used:

$$D = (V_p * TWT)/2$$

Where, D is the computed depth in meter, V_p is the P-wave velocity in m/s, and TWT is in milliseconds. P-wave velocity of 1500 m/s in water column and 1583 m/s in sediments (Krishna et al., 1989) are used to convert two way travel time into depth. In the following sub-sections, adopted methodologies for analyses and interpretation of seismic data are presented.

3.3.1 Method of seismic stratigraphic analysis

The sequence stratigraphic analysis is carried out following methods suggested by Vail et al. (1977) and Catuneanu et al. (2009). The method used in the high resolution sequence stratigraphic analysis involves identification of depositional sequences, stacking pattern of strata and key stratigraphic surfaces. The technique of seismic sequence analysis involves dividing the processed seismic sections into seismic sequences according to their internal reflection pattern, boundary geometry and structure produced by the reflected P-waves. Sequence stratigraphic surfaces mark change in depositional environment which in turn causes high contrast variation in acoustic impedance. In a high resolution seismic section, beds which have contrasting acoustic impedances stand out as strong reflectors. Therefore, in HRSS section strong reflectors generally indicate the sequence stratigraphic surfaces. High resolution sequence stratigraphic framework provides freedom to choose any of the stratigraphic surface as the bounding surface. In the present study, sub-aerial unconformities have been chosen as the sequence bounding surface because recognizing subaerial unconformity with lenticular seismic facies are easier to identify and correlate with the sea level curve. Seismic sequence bounded by two subaerial unconformities were further analyzed and divided into system tracts based on other marked stratigraphic surface. System tracts were further subjected to seismic facies analysis. Seismic facies analysis is the description and geological interpretation of seismic reflector parameters such as reflection pattern, continuity, amplitude and frequency.

Seismic reflection parameters such as continuity, amplitude and frequency may differ (Fig. 3.4) for each system tract. The reflection pattern reveals a gross stratification pattern from which depositional and erosion environment with variation in accommodation space for a system tract can be inferred.

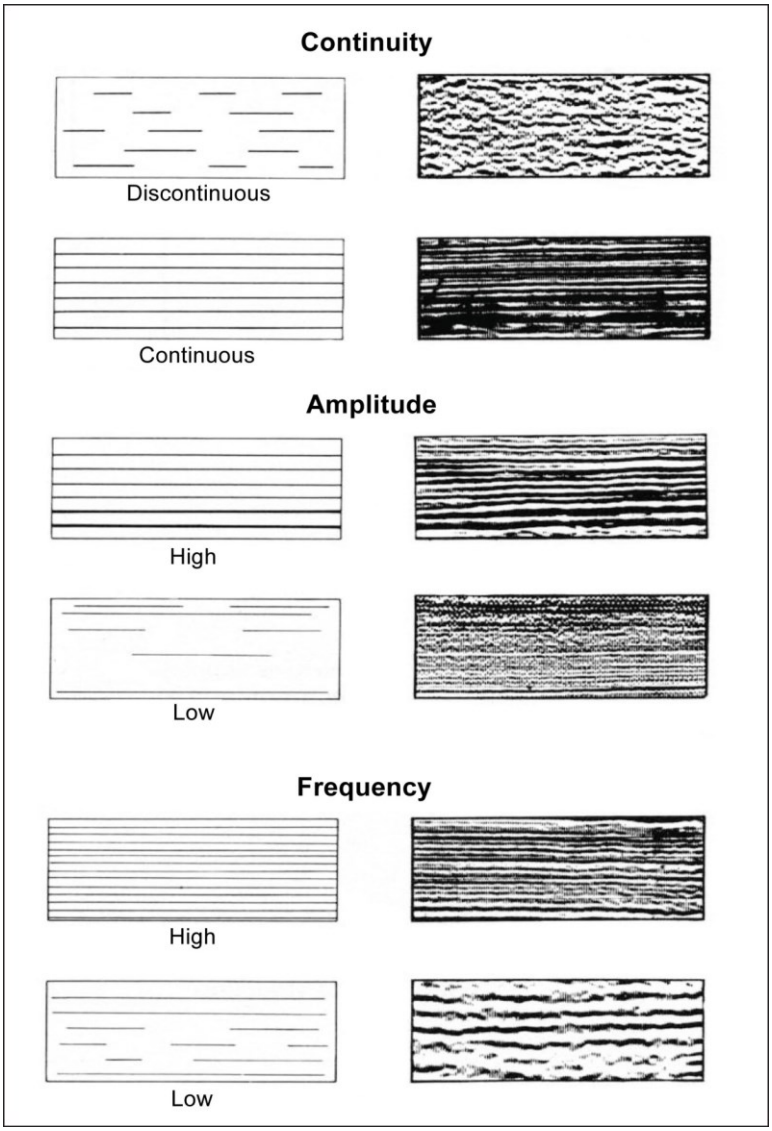

Figure 3.4 Seismic reflection parameters (continuity, amplitude and frequency) used in seismic sequence stratigraphic analysis (Vail et al., 1977).

The reflection patterns can be divided grossly into two subgroups such as (i) simple reflection patterns, (ii) reflection patterns at sequence boundaries. The types of seismic reflection patterns are given in Table 3.6. The reflection continuity is closely associated with continuity of strata itself. Reflection amplitude indicates the velocity-density contrast of individual interfaces/reflectors.

Table 3.6 Types of seismic reflection patterns.

1	**Simple seismic reflection patterns**		
1.1	Parallel / Even	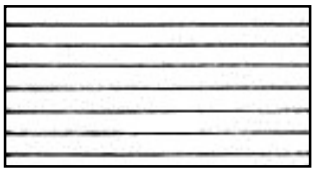	Relatively parallel reflectors: Deposition in static accommodation space (highstand generally) and uniform sediment supply with periodic high and low energy deposition.
1.2	Sub parallel	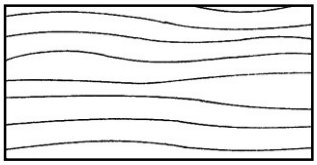	Sub parallel reflectors: Deposition in higher frequency accommodation space variation which might be resonated with non-uniform environment with non-periodic high and low energy deposition. Or deposition in non-uniform environment with non-periodic high and low energy deposition
1.3	Divergent		Divergent reflectors gradually spread out in the down dip direction: May indicate decrease in accommodation space and continuous increase in sediment supply
1.4	Lenticular	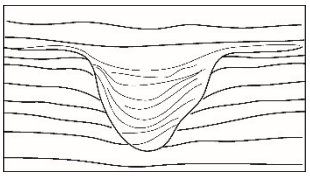	Lenticular reflection pattern: represents channel incision essentially formed during the lowered sea-level. Infill reflector may represents the sediment deposition of varied environment.
1.5	Chaotic	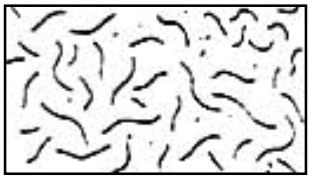	Chaotic reflection patterns: are indicative of unconsolidated, non-stratified coarse grain sediment deposits, deposited very near to the shore in wave action zone in very high energy condition.
1.6	Hummocky	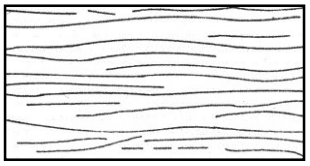	Hummocky reflection pattern: may represent partially stratified, coarse grain sediment deposits intercalated with fine clay and silt material. Usually formed in deeper region where authigenic sediment supply surpasses fine grained terrigenous sediment supply

1.7	Reflection free			Reflection free: indicate deposition of homogenous fine grain sediment material. The Holocene clay and silt deposits show normally reflection free zones in seismic section.
2.	**Seismic reflection patterns at sequence boundaries**			
2.1	Upper Boundary	Top lap	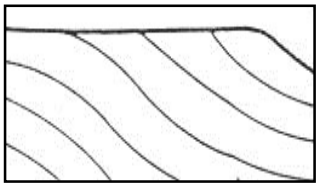	Reflectors are convergent or tangential to the upper boundary of the seismic sequence. Deposition occurs near the wave base of appreciable energy.
2.3	Lower Boundary	Onlap	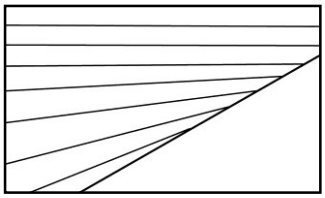	Reflectors are flat to dipping upward and thinned at up dip termination on a dipping stratigraphic surface. Onlapping is a result of slow marine transgression after a brief stand still. It reflects the retrogradation of strata.
2.4		Downlap	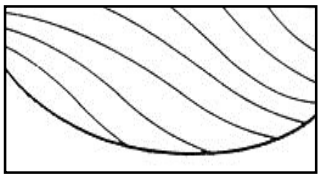	Reflectors dipping downward and thinned at its down dip termination along a gently dipping stratigraphic surface. Downlap forms towards the seaward end of the depositional sequence. It is due to lower terrigenous sediment supply and reflects progradation of strata.
2.5	Concordance		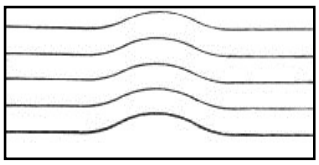	Reflectors are conformable to the bounding surfaces of the seismic sequence. It is the result of slow and uniform deposition with low energy.

3.3.2 Computation of Holocene sediment thickness

The Holocene sediment thickness at each location is computed using following formula:

$$T = (TWT_{Holocene\_TS} - TWT_{seabed})\, V_{p(sed)}/2$$

Where, T is the Holocene sediment thickness in meter. $TWT_{Holocene\_TS}$ is the two way travel time corresponding to Holocene_TS reflector in milliseconds, TWT_{seabed} is the two way travel time corresponding to seabed reflection in milliseconds, and $V_{p(sed)}$ = 1583 m/s, is P-wave velocity in sediments (Krishna et al., 1989). Holocene_TS refers to the Holocene Transgressive Surface.

3.3.3 Computation of Holocene sedimentation rates

Since transgressive surfaces are the results of sea-level transgression, every point on this surface across the shore is the locus point of shoreline trajectory and denotes the mean sea-level during transgression. Considering this logic, the Holocene sea level curve (Hashimi et al., 1995) is used to date each point of this surface. For this purpose, the Holocene sea-level curve has been digitized using 'Surfer13' software and database of depth (m) of paleo sea-level with respect to present mean sea-level, and corresponding time in kilo years was generated. Later, this depth versus time data was merged with the XYZ data of Holocene_TS of every tracklines using a MATLAB code developed for this study (Fig. 3.5). Later this data was merged with the sediment thickness data and used to compute sedimentation rate corresponding to each shot number using following formula;

$$R = T/t$$

Where, R: sedimentation rate (mm/year) at a given location, T: sediment thickness in meter, t: time (kyr) extracted from the sea-level curve.

```
clear all
% xyz = xlsread('xyz.xlsx');
% zt=xlsread('zt.xlsx');

xyz=load('X-HOL_TS.txt');
tz=load('Y-Sealevel.txt');



for i=1:length(xyz)
    for j= 1:length(tz)
        diff(i,j)=abs(xyz(i,3)-tz(j,2));

    end
            [minNum, c] = min(diff(i,:));
           merg(i,1)=xyz(i,1);
           merg(i,2)=xyz(i,2);
           merg(i,3)=xyz(i,3);
           merg(i,4)=tz(c,2);
           merg(i,5)=tz(c,1);
end

 merg=merg';
fileID = fopen('XY-HOL_TS_ZT.txt','w');
fprintf(fileID,'%10.8f %10.8f %10.5f %10.5f %10.5f\n\r',merg);
fclose(fileID);
```

Figure 3.5 MATLAB code used for merging xyz data of the Holocene_TS with zt data of the digitized Holocene sea-level curve data.

3.3.4 Quantitative geomorphic analyses

River channels are the surface manifestation of interaction between water and the landscape. Under the effect of prevailing climatic condition, different types of landscape give rise to river channel with different morphological features. Morphological features of rivers are controlled by topographical as well as lithological character of the landscape. River channels are classified (Rosgen, 1994) based on morphological characteristics of land (physiography, lithology) and rivers (number of active channels, entrenchment, aspect ratio of cross-section, sinuosity of plan form, and channel slope) (Fig. 3.6).

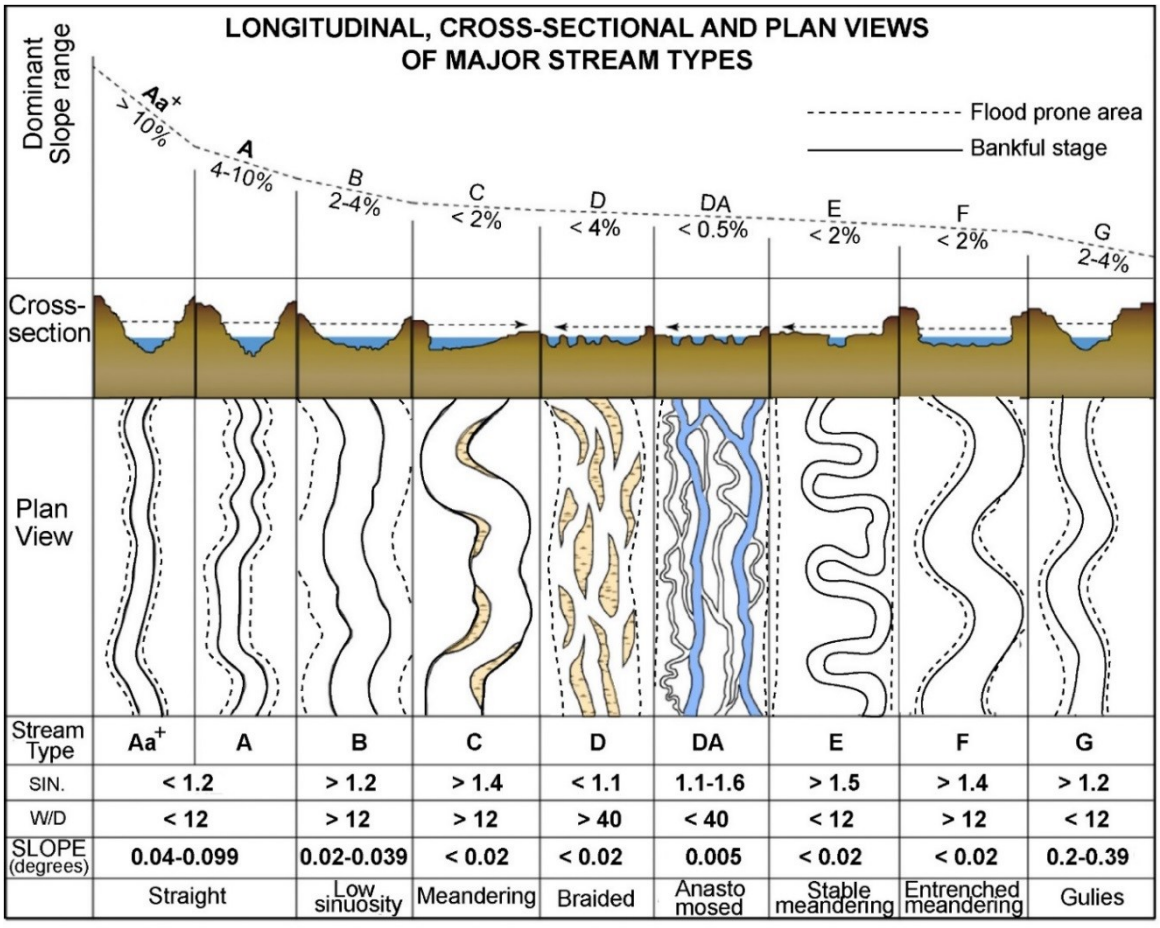

Stream Type	Aa^+	A	B	C	D	DA	E	F	G
SIN.	< 1.2		> 1.2	> 1.4	< 1.1	1.1-1.6	> 1.5	> 1.4	> 1.2
W/D	< 12		> 12	> 12	> 40	< 40	< 12	> 12	< 12
SLOPE (degrees)	0.04-0.099		0.02-0.039	< 0.02	< 0.02	0.005	< 0.02	< 0.02	0.2-0.39
	Straight		Low sinuosity	Meandering	Braided	Anasto mosed	Stable meandering	Entrenched meandering	Gulies

Figure 3.6 Schematic diagram showing morphological characteristics (longitudinal, cross-sectional and plan views) of major types of stream channels (modified after Rosgen, 1994). SIN: Sinuosity, W/D: Width to depth ratio.

Though present study focuses on buried river channel morphology, it still utilizes the Rosgen's river classification system to describe the delineated buried channels with respect to their plan form. It may be mentioned here that the Rosgen's classification of existing in-land river system need not be in full agreement with the classification of offshore buried channel system because they are delineated based on their remnant incision signature only. Further quantitative

geomorphologic analyses of the channel incision signatures provide a tool to compare hydrological environment during different periods of incision.

Paleo-discharge of buried channel system of the present study area is estimated using empirical hydraulic equations (Sternberg, 1972; Dury, 1976; Friedrichs, 1995) for modern rivers and estuaries on the basis of preserved paleo-channel geometry assuming uniformitarianism. Morphologic parameters such as width (w), mean depth (d_{mean}), maximum depth (d_{max}), aspect ratios (w/d_{mean}) and cross-sectional area (A) of channel incision have been estimated from observed incision signature in the HRSS section (Fig. 3.7A).

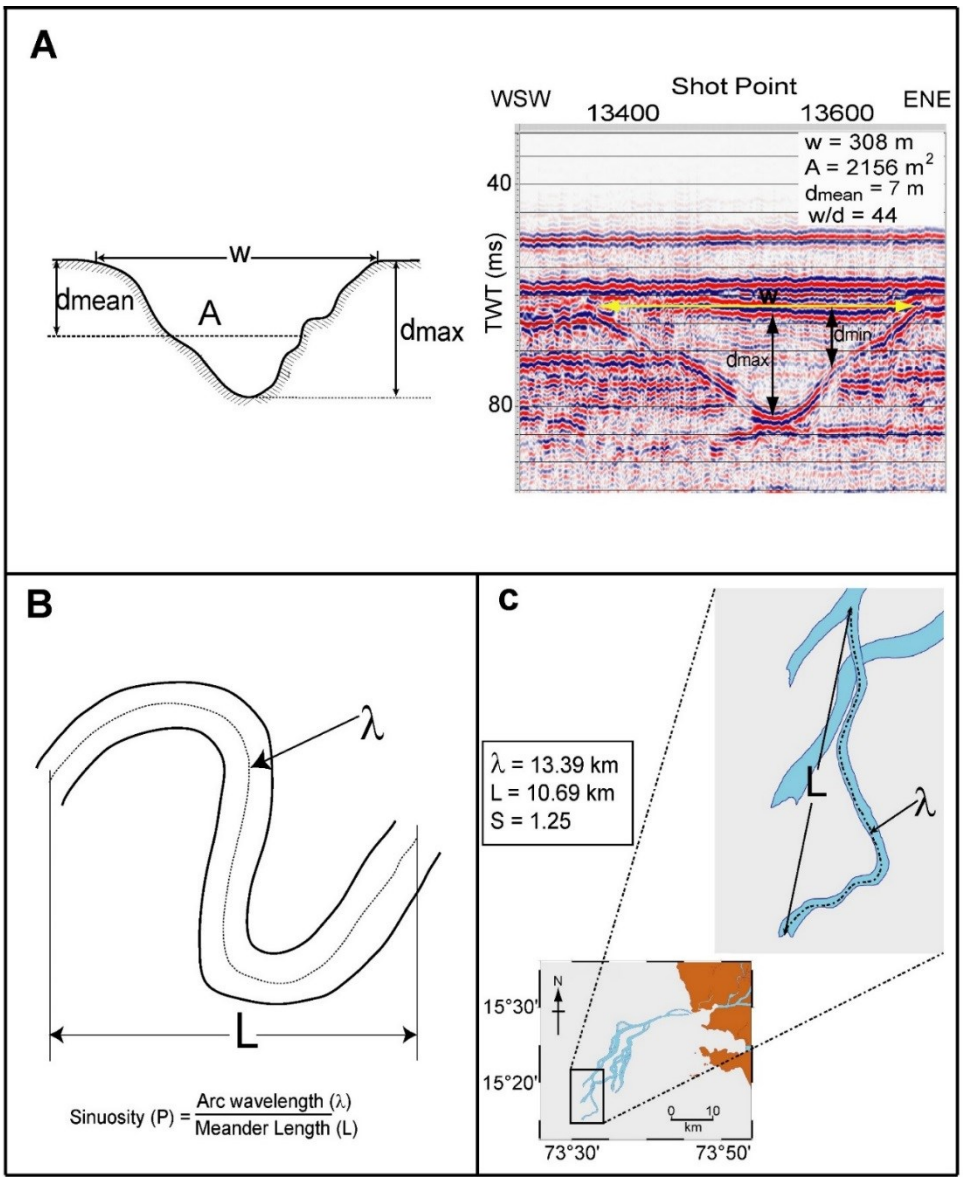

Figure 3.7 Channel pattern properties used for computation of aspect ratio, sinuosity and paleo-hydraulic parameters. Illustation to calculate **(A)** aspect ratio from channel geometry, and **(B)** sinuosity of channel pattern. **(C)** A channel section showing interpolated plan view morphology of channel incision and its sinuosity.

Further, sinuosity (S) and slope gradient (SD) are computed from interpolated plan view morphologies (Fig. 3.7B, C) of incised channel using following relationship (Leopold et al., 1964; Dury, 1976):

$$S = \lambda/L$$

$$SD = (W_{S1}-W_{S2})/L$$

Where, L: Meander length, λ: Path length, W_{S1}: Water surface level at position 1 in incised channel, W_{S2}: Water surface level at position 2 in the same incised channel.

The geomorphic parameters are measured only for those incisions which were traversed by seismic survey tracklines orthogonally. Whereas parameters like slope gradient, meander length, path length and channel sinuosity have been calculated from interpolated plan view morphologies of incised channel sections.

Since mapped channel incisions might have been carved in varied environmental condition from fully estuarine to fully fluvial condition, therefore, computation of water discharge for both fluvial and estuarine cases are considered here. For fluvial system, following empirical equation provided by Dury (1976) is used:

$$Q = 0.83A^{1.09} \quad \text{---------- (1)}$$

For tidal system, following empirical equation provided by Friedrichs (1995) is used:

$$Q = A^{\alpha} \quad \text{---------- (2)}$$

Where, Q is water discharge and A is cross-sectional area corresponding to bank full discharge.

Following Friedrichs (1995), α=0.96 is used for computation in the present study. The value of α is based on previous studies of worldwide modern tidal channels (Friedrichs, 1995).

Further mean flow velocity for both fluvial and tidal incisions is calculated using continuity equation:

$$Q = A\ v \quad \text{---------- (3)}$$

Where, v is the mean velocity.

3.3.5 Generation of gridded data

Gridded data for sediment thickness and sedimentation rates during the Holocene_TS were generated using XYT (longitude, latitude and sediment thickness) dataset of the sediment thickness and XYR (longitude, latitude and sedimentation rate) dataset of sedimentation rates, respectively. Similarly, gridded data for depth of occurrence of the Holocene_TS was generated using XYZ (longitude, latitude and depth of TS with respect to mean sea-level) dataset of the Holocene_TS. Generic Mapping Tools (GMT) provides triangulate and surface tools for gridding of the data. For this study, a Combination of "blockmean" and "surface" tools were chosen to generate the above mentioned gridded data at a grid interval of 20 arc-second (one-third of the trackline spacing). Surface tool utilizes minimum curvature methodology of interpolation. Surface along with tension (T) and convergence (C) parameter provides better geologically reliable interpolations. It is worth to mention here that the 'blockmean' tool is essentially used to remove spurious data in generation of the gridded data. In order to find out error in gridded datasets of the Holocene sediment thickness, the Holocene sedimentation rates and the Holocene_TS, percentage Root Mean Square Error (RSME) is considered in this study. Percentage RMSE is defined as:

$$\% \text{ RMSE} = 100\text{x}(\text{RMSE})/ (\text{Total range})$$

Percentage RMSE for the Holocene sediment thickness, the Holocene sedimentation rates and the Holocene_TS gridded datasets are found to be 0.29, 2.76 and 0.12, respectively (Table 3.7). Further, a grid filter ('grdfft' tool of the GMT) has been applied to generate final grid data to avoid spatial aliasing of features smaller than 2 nautical miles (i.e. less than 3.7 km in size). Application of grid filter sets sensitivity limit of the grid data for spatial variations of geomorphological features to ~3.7 km.

Table 3.7 Details of variables for computation of percentage RMSE.

Holocene sediment thickness (m)				**Holocene sedimentation rate (mm/yr)**				**Holocene_TS (m)**			
Min	**Max**	**Range**	**RMSE**	**Min**	**Max**	**Range**	**RMSE**	**Min**	**Max**	**Range**	**RMSE**
0.08	15.7	14.9	0.043	0.05	1.64	1.59	0.044	12	60	48	0.058
% RMSE		0.29		% RMSE		2.76		% RMSE		0.12	

The gridded datasets were used to prepare the Holocene sediment thickness, sedimentation rates and the Holocene_TS maps which are utilized to analyze spatial distribution of the Holocene sedimentation pattern in the study area and discussed in details in Chapter 5.

Chapter 4
Sedimentary Architecture

4.1 Introduction

Sedimentary architecture of a continental shelf is mainly controlled by sea-level changes, climate and tectonics. The resulting deposits (systems tracts in sequence stratigraphy) may be preserved in continental shelf sediments. Sequence stratigraphy is the most efficient tool to decipher evolutionary history between depositional layers. High resolution seismic and sediment sample data are required to analyze the stratigraphic features of a sedimentary basin. On the basis of facies analysis, different system tract and bounding surfaces can be identified in high resolution seismic sections. Further, these system tracts and bounding surfaces can be put in older to younger order using stratigraphic cross correlation. Karisiddaiah et al. (2002) have reported sequence stratigraphic characteristics of western continental shelf between Coondapur (near Bhatkal) and Kasargad (near Mangalore). Based on analysis of high resolution seismic data acquired along seven tracklines, they reported that the Late Pleistocene-Holocene sequence is composed of nine seismic units corresponding to sedimentary bodies that were possibly controlled by high-frequency sea-level fluctuations. In absence of long sediment core, they attempted to correlate few of the recognized seismic units with the then available sea-level curve and concluded that those seismic units were deposited during the last glacial period and during the Holocene. In another study, a wedge shaped sediment package characterized by low amplitude and continuous parallel reflectors extending seaward up to a water depth of ~50 m was reported (Mazumdar et al., 2009). The sediment wedge thickens towards shore and pinches out at ~50 m water depth. The weak reflectors within the wedge downlap against a planar surface was referred as maximum flooding surface.

The above two stratigraphic studies (Karisiddaiah et al., 2002; Mazumdar et al., 2009) are reported from fringe locations of the western continental shelf of India. Though a foundation had been laid through these studies, an integrated geomorphologic (sub-surface) and

stratigraphic study using HRSS data, is still lacking in India. Further, though sequence stratigraphic analysis of sedimentary strata can provide their relative age of formations, still it requires ground truthing through studies of long sediment core to put these system tract and bounding layers in geo-chronological order. The high operational cost of long sediment cores prohibits the stratigraphic studies on a massive scale over continental shelves. In order to overcome this problem an alternate methodology is developed in this study to put the interpreted stratigraphic record of the study area in geo-chronological order. Further, integrated geomorphologic (sub-surface) and stratigraphic studies are capable of providing a clear picture of paleo-environmental variations through the geological past, and evolutionary history of the continental shelf. This chapter discusses a new methodology to assign the age of Subaerial Unconformities (SU) using sea-level curve. It also emphasizes on sequence stratigraphic analysis using high resolution shallow seismic data.

4.2 A new method for assigning age of SU

The new methodology explains sub-aerial unconformities within the geological time scale, in absence of age of stratigraphic layers derived from study of long sediment cores. It involves identification of subaerial unconformities and its correlation with sea-level curve to find out the period of formation of the subaerial unconformities. Since it does not involve any dates from sediment sample, it provides approximate period of formation and hence approximate period of non-deposition and erosion at any location on the subaerial unconformity. The methodology is described in detail in the following section.

4.2.1 Correlation of subaerial unconformities with sea-level curve

Subaerial unconformities are the surface of erosion and non-deposition formed in lowered sea level condition under the effect of different erosion processes active in the past (Zaitlin et al., 1994; Zecchin and Catuneanu, 2013). It is an exposed surface over which channel incision takes place. Such subaerial unconformities are identified as the seismic horizon containing channel incision signatures (Catuneanu et al., 2011). In this study, it is considered that a channel incision at a particular location started as soon as surface got exposed due to lowering of sea level. In response to further sea-level fall, channel incised deeper and migrated laterally. The incision potential of a channel increases on steeper surface, and longitudinal profile get readjusted. Incision potential is directly related with gradient of surface, base level, and lithology for a given hydrological regime. It varies throughout the course of a channel and is higher at middle

course. In mature condition, incision potential for vertical entrenchment almost ceases to zero at lower course as the channel flows very close to the base level. However, channel widening may take place depending upon flow velocity. Therefore, base level of river channel is defined as the lowest limit up to which a river can erode (Davis, 1902; Schumm, 1968, 1993; Marr et al., 2000) when incision potential becomes negligible.

The deepest entrenchment in a subaerial unconformity is identified to find out sea-level at the mature stage of the channel incision. Thus sea-levels at the time of initiation, maturity and complete burial of an incision have been estimated from seismic section. Further, estimated sea-level values from seismic section have been correlated with available sea-level curves to get complete lifespan of incisions and hence total period of non-deposition and erosion of an observed subaerial unconformity. It may be noted that deepest incision in the same subaerial unconformity for entire area is used for this analysis.

Therefore, to find out the time of commencement and complete burial of a particular incision and to identify respective glacial period from sea-level curve, following methodology has been developed for this study and illustrated in schematic diagram shown in Figures 4.1 (I) and (II):

(i) Identified subaerial unconformities have been marked in each seismic section of the study area and correlated from section to section. Further, they have been annotated in younger to older order. For example, subaerial unconformity "SU-1" is younger than "SU-2" because "SU-1" is cross cutting "SU-2" (Fig. 4.1 (II)).

(ii) Sea-levels for initiation and complete burial of a channel incision in a subaerial unconformity have been estimated from seismic section. For example, incision "A" in "SU-1" is at a depth of Z_1 mbsl (meter below present sea-level) (Fig. 4.1 (II)). This suggests that incision "A" was initiated during sea-level fall, when the sea-level was at least Z_1 m below present sea-level. It got completely buried in subsequent sea-level rise, when it rose again up to this level (i.e. Z_1 mbsl).

(iii) Sea-level at the time of mature stage of the channel is estimated considering that channel started aggrading, when base level reached at least up to the maximum entrenchment level of an incision. For example, maximum entrenchment of incision 'A' is Z_4 m (Fig. 4.1 (II)). This indicates that at this location, channel started aggrading when sea-level was at Z_b mbsl $\{Z_b \geq (Z_1 + Z_4)\}$.

(iv) Integrated the information obtained from seismic section steps (i), (ii), (iii), and correlated with the sea-level curve to obtain a period of non deposition and erosion at the location of incision. For example, incision 'A' initiated when sea-level was at “a”, i.e. ~t_3 kyr BP (Fig. 4.1 (I)). It got matured when the sea-level reached to “b”, i.e. ~t_2 kyr BP and then it got buried when sea-level reached to “c”, i.e., ~t_1 kyr BP. From these information, it has been estimated that SU-1 was exposed at this location for a period of ~(t_3-t_1) kyr between ~t_3 kyr BP and ~t_1 kyr BP (Fig. 4.1 (II)). Similarly, it can be estimated that SU-2 was exposed for a period of (t_7-t_5) kyr between ~t_7 kyr BP and ~t_5 kyr BP at location of incision “C”.

To estimate total period of non-deposition of a subaerial unconformity, sea-levels for deepest entrenchment in that subaerial unconformity have been correlated with the available sea-level curve (Figs. 4.1 (I) and (II)). For example, "SU-1" is younger than "SU-2 " and deepest incision “A” got matured when sea-level was ≥ (Z_1+Z_4) mbsl (Fig. 4.1 (I)). Correlating these information with sea-level curve, it can be concluded that "SU-1" started emerging at ~t_4 kyr BP due to the sea-level fall and was completely exposed at ~t_2 kyr BP for a period of ~(t_4-t_2) kyr (Fig. 4.1 (I)).

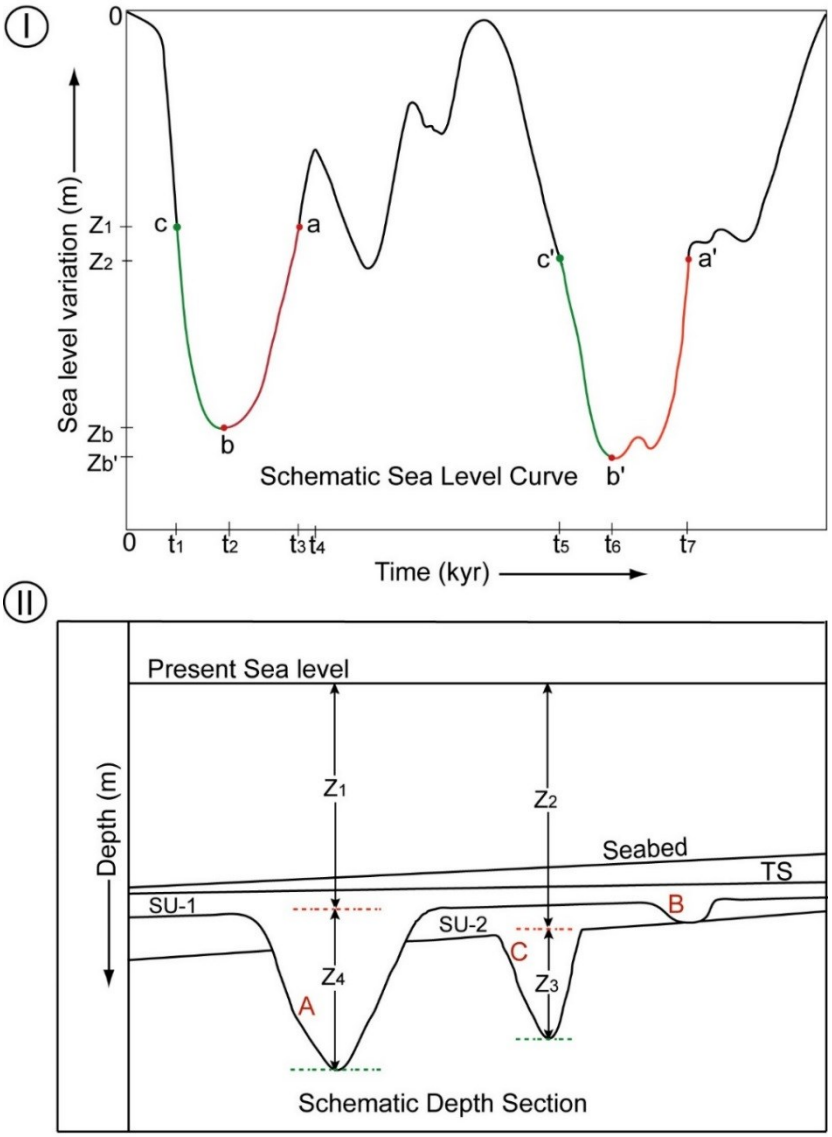

Figure 4.1 Schematic diagrams showing **(I)** Sea-level curve, and **(II)** Depth section depicting seabed, Transgressive Surface (TS), subaerial unconformities (SU-1, SU-2) and channel incisions A, B and C. In the schematic sea-level curve, points a, b, and c show sea-levels at which incision A initiated, got matured and completely buried, respectively. Similarly, points a', b' and c' show sea-levels at which incision C initiated, got matured and completely buried, respectively. **ab** and **a'b'** (shown with red color in Fig. 4.1(I)) depict time period when channel was mostly degradational. **bc** and **b'c'** (shown with green color in Fig. 4.1(I)) depict time period when channel was mostly aggradational.

4.2.2 Limitations of the methodology

The methodology developed here provides a time period of non-deposition and erosion on a subaerial unconformity which can always be calibrated at later stage with few sediment sample dates. But in absence of sediment sample dates, it is obligatory to understand pros and cons of the methodology to get optimum results. This methodology is based on few considerations on

channel incision, sea-level curve and base level concept. The limitations of the new methodology and the scope of error are discussed below:

(i) It uses sea-level curve to obtain age of subaerial unconformities, therefore an accurate relative sea-level curve of a study area is a requisite. A normalized relative sea-level curve which encompasses effect of basin tectonics provides sea-levels with an accuracy of ±5 m (Rehak et al., 2010). Therefore at a point where sea-level is varying with minimum rate (generally at peaks of interstadials and glacials), it may cause millennial scale error in age estimation. Correlation of several incision signatures with sea-level of a study area may reduce this error significantly. Another problem with this method is unavailability of relative sea-level curve for a study area. In this case, eustatic sea-level curve may be used for tectonically passive continental margins where thermal subsidence on continental shelf is in sub meters. Otherwise corrections for tectonic movement (i.e. upthrust and downthrust) must be incorporated before correlating with eustatic sea-level.

(ii) Subaerial unconformities are generally reworked by Transgressive Ravinement Surface (TRS) during subsequent sea-level rise. TRS may significantly rework incision signature in subaerial unconformities. The extent of erosion may depend on the shape of shoreline geometry and rate of shoreline transgression. On a low gradient continental shelf, reworking may cause erosion of few meters thickness of sedimentary strata. Still the error in age estimation will be less than the error discussed in (i) above.

(iii) It assumes that incision starts with emergence of shelf strata due to lowering of sea-level. In fact, it is not always true because there may be lag to initiate incision in response to base level change. It may be noted that configuration of river inlet and coastline varies with decadal scale, which may introduce error in age estimation of the order to 10 years. If river migration takes place on the exposed shelf, it leaves its migratory signatures in the sediment assemblage which can be mapped through the HRSS data. Therefore this assumption also does not generate significant error in age estimation.

(iv) The requirement of complete mapping of subaerial unconformity in orthogonal direction of shoreline is another important aspect of this methodology. Tracking same subaerial unconformity in different seismic sections, generated along tracklines parallel to a coast, may mislead. Therefore, it is suggested that at least few seismic sections, generated along tracklines perpendicular to the coast, must be used for mapping subaerial unconformities.

In the present study, HRSS data have been acquired along parallel tracklines orthogonal to the coast. The study area is known to remain tectonically quiescent passive shelf during the Quaternary (Whiting, 1994; Faruque and Ramachandran, 2014). Therefore global sea-level curve for the Quaternary is confidently used and correction for vertical tectonic movement is ignored. On the basis of above discussed factors it can be summarized here that proposed methodology is capable enough to provide time period of formation, erosion and non-deposition of a subaerial unconformity with a possible error of less than 1 kyr.

4.3 Sedimentary architecture of the study area

Processed HRSS sections reveal certain characteristic features of the sedimentary architecture of the study area. One such prominent feature is lens shaped sediment package bounded by the seabed on top. It is comprised of low amplitude (nearly transparent), continuous and parallel reflectors which pinch out at ~50 m water depth (Fig. 4.2 A & B). Remarkably, this sediment package does not show any signature of aerial or subaerial erosion (Fig. 4.2 A). The weak reflectors within this sediment package downlap against a reflector at ~50 m water depth. Below this reflector, two more characteristic features of the study area can be easily observed. One of these is located in nearshore region up to ~35 m water depth and display very little penetration of seismic energy along with scanty diffraction patterns. Low penetration with scanty diffraction pattern suggests that the region is made up of coarse grain, poorly stratified sediments with rocky patches. It is evident that these rocky patches were the primary sources of coarser sands and have acted as a structural barrier for allogenic sedimentary processes in the past. Other characteristic feature is located in deep water region of the study area and displays decent amount of penetration with several continuous and seaward dipping reflectors having high amplitudes. These seaward dipping reflectors suggest presence of stratified sedimentary layers in this region which are conspicuous result of allogenic and autogenic processes. Further, some of these seaward dipping reflectors contain numerous buried channel signatures which are incised during low stand sea-level conditions. Although recurrent incisions have altered stratal surfaces to such an extent that signatures are indistinguishable but at places prominent subaerial unconformities can be easily differentiated. HRSS sections of the study area are further examined for seismic facies analysis to investigate terminations and stacking patterns of the reflectors along with their seismic attributes. Results of the analysis are discussed in the following sections.

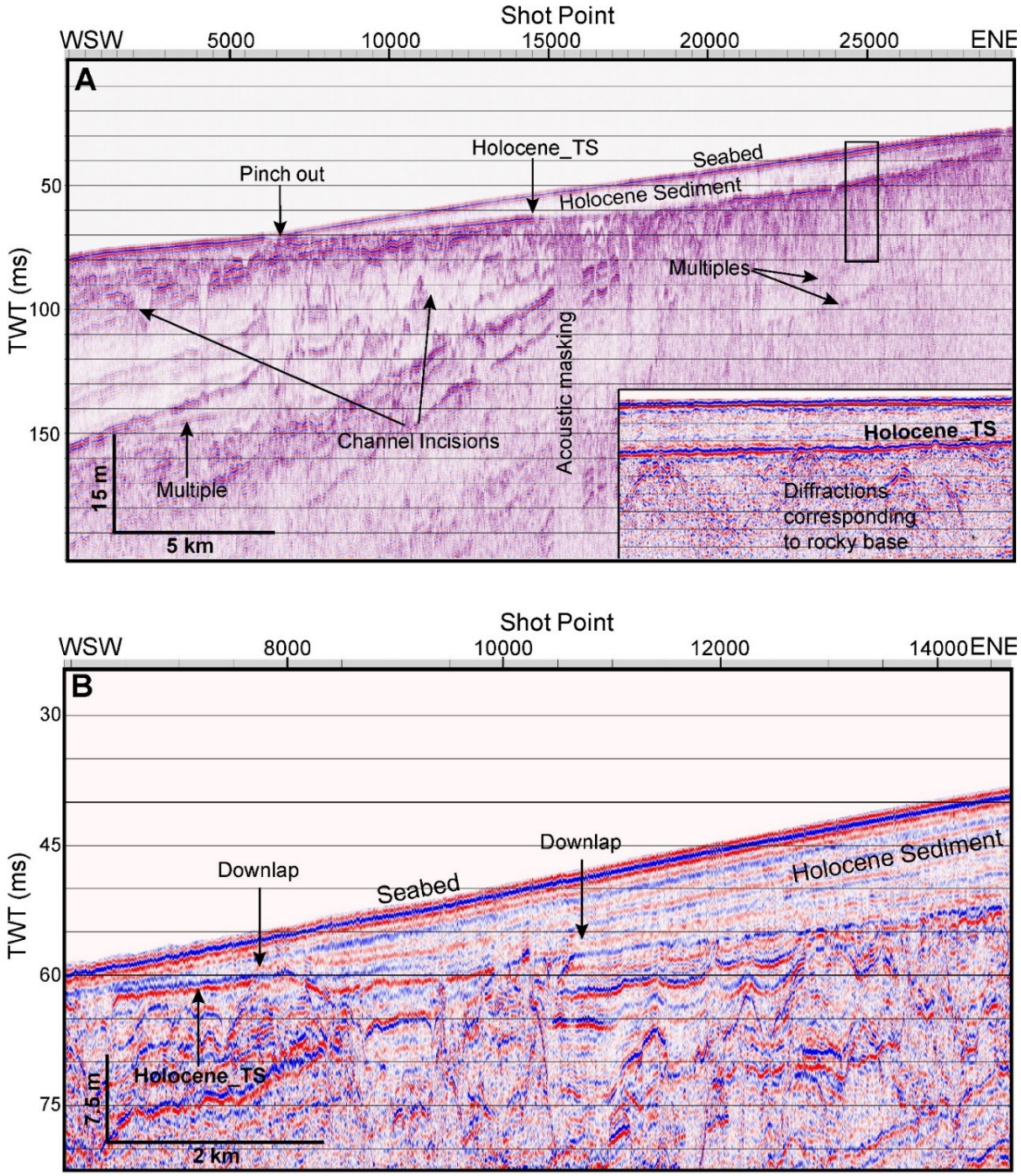

Figure 4.2 (A) Seismic sections along trackline SaSu-36, showing general characteristic of sedimentary architecture of the study area. An enlarged seismic section of the rectangular box, depicting rocky signature, is shown in lower right corner of the figure. (B) Seismic section along part of the trackline GK-14, showing downlapping of Holocene sedimentary strata over Holocene MFS (see Fig. 3.1 for locations). MFS: Maximum Flooding Surface.

4.4 Seismic facies analysis

Based on the seismic facies analysis eleven seismic units (U1 to U11) and corresponding bounding surfaces (S1 to S11) are identified. In addition, three sub units (U6a, U7a, and U9a) separated by corresponding transgressive surfaces (S7a and S8a) have also been identified.

Seismic characteristics of units and surfaces are described in Table 4.1. Each unit is composed of one seismic facies that does not have significant lateral variations. In the following sections, seismic stratigraphy from younger to older order is described in terms of their geometry and stacking pattern:

(i) Seismic unit 11 (U11)

The unit U11 is the youngest and upper most seismic unit. It is bounded by S11 as well as by S1 (locally) at the bottom and seafloor at the top (Figs. 4.3 A & B). It lies above (i) U10 in deeper region (water depth more than 53 m), (ii) U9a between water depth 8 and 53 m, and (iii) U1 locally in shallow region. This unit is a lens shaped seismic unit. Maximum thickness of this unit is ~16 ms which is observed at ~35 m water depth. Thickness of this unit pinches out at ~50 m water depth due to significantly less terrigenous sediment supply at this level. It is truncated by igneous rock outcrops near the shore. This unit is made up of continuous and parallel reflectors having very low amplitude (nearly transparent). Remarkably, this sediment package does not show any signature of aerial erosion (Fig. 4.2 A). The weak reflectors within this lens shaped unit downlap on the planer surface. This reflector (downlap surface) becomes feeble shoreward and sometimes not easily identifiable. This particular characteristic of this reflector indicates that there is not much contrast in acoustic impedance across this reflector in the shallower region. It means that the sedimentary layer, responsible for this reflector, is formed in stable depositional environment. On correlation with the available Holocene sea-level curve this reflector has been identified as a transgressive surface (Fig. 4.2 B) which is formed due to sudden rise in sea-level during mid-Holocene, is termed as Maximum Flooding Surface (MFS). Reflector corresponding to MFS, seems to merge with another prominent reflector S11 at ~50 m water depth. In comparison to reflector corresponding to MFS, this reflector, overlying numerous channel incision signatures, is very easily identifiable in every seismic section and seems to rework underlying surface.

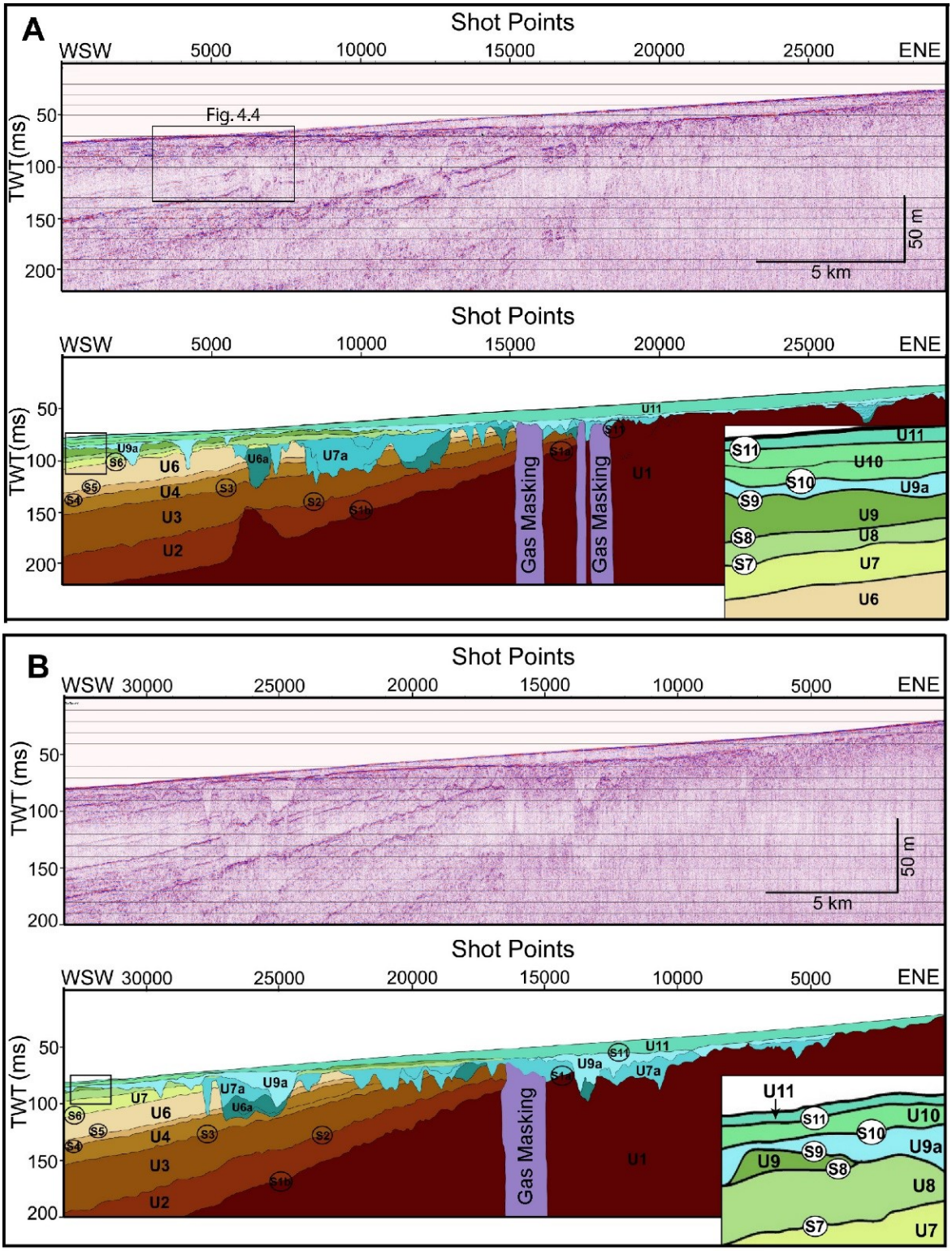

Figure 4.3 Seismic image and interpreted section along tracklines (A) SaSu-36, and (B) SaSu-27, showing seismic units U1 to U11 with bounding surfaces S1a & b to S11. Insets (rectangular blocks) in interpreted sections are enlarged at lower right corner of corresponding interpreted section. Location of tracklines SaSu-36 and SaSu-27 is shown in Fig. 3.1. Enlarged seismic image and interpreted section of inset (rectangular block marked on seismic image in Fig. 4.3 A) is shown in Fig. 4.4.

Correlation with Holocene sea-level affirms that this reflector is formed due to wave erosion during initial Holocene transgression and should be termed as Holocene TS or Holocene Transgressive Ravinement Surface (TRS). For this study, this surface is termed as Holocene TS. The Holocene TS, overlying numerous buried channels, differentiates Holocene sediments with the Late Pleistocene sediments. The seismic facies suggest well bedded fine grained deposits (clayey and silty). S11 have been previously identified as Maximum Flooding Surface (MFS) formed due to sea-level rise after last glacial maximum during the Holocene-Pleistocene transition (Mazumdar et al., 2009). Technically U11 should contain sedimentary deposits during the Holocene transgression (i.e. TST) and highstand normal regressive deposits (HST) but the thickness of TST and bounding surface MFS is not noticeable everywhere. It can be observed in a few locations of the study area only. Therefore, U11 contains Holocene sediment deposits which are largely characterized by High Stand System Tract (HST).

(ii) Seismic unit 10 (U10)

The seismic unit U10 lies directly below U11 and is bounded by S11 (Holocene-MFS) on top and S10 at bottom (Figs. 4.2 A & B). It is limited in deeper region of the study area and is never observed in shallow region (≤ 53 m water depth). The maximum thickness of U10 varies from ~2 ms to ~6 ms along the coast, and its thickness increases basin wards reaching to ~6 ms. This unit is made up of continuous, parallel, low to medium amplitude reflectors. At places, reflectors at upper part of this unit show chaotic to hummocky pattern with moderately high amplitude reflectors and hinder the reflection from underlying strata (detailed discussion in Chapter 7). The reflectors of this unit onlap S10. Available Holocene sea-level curve for west coast of India (Hashimi et al., 1995) suggests that sea-level rose in stages after Last Glacial Maximum (LGM). Also, submarine terraces which are markers of prolonged shallow water condition have been reported at ~92 m, ~84 m, ~71 m, ~65 m, ~55 m, and ~31 m on the western continental shelf of India (Nair, 1975; Wagle et al., 1994). Therefore, on the basis of reflection pattern of this aggrading sediment unit, it is interpreted that this unit was deposited during late Pleistocene, post LGM when sea-level rise was very slow or a brief standstill period existed around this water depth and is characterized as TST (Transgressive System Tract). The mounded reflection pattern with moderately high amplitude reflectors are interpreted as sand bars/ paleo-beaches which are accreted in coastal depositional environment during this very slow rise or stand still period and nearby river being the sand source.

Table 4.1. Characteristics of the seismic units (U1 to U11) and bounding surfaces (S1a to S11) recognized on the data with their seismic descriptions.

Seismic Units	Descriptions of seismic facies and reflection terminations	Seismic images showing labeled seismic units and bounding surfaces
U11	Low amplitude, parallel, continuous reflection configuration. **Base:** Downlaps on S11 **Top:** Seafloor	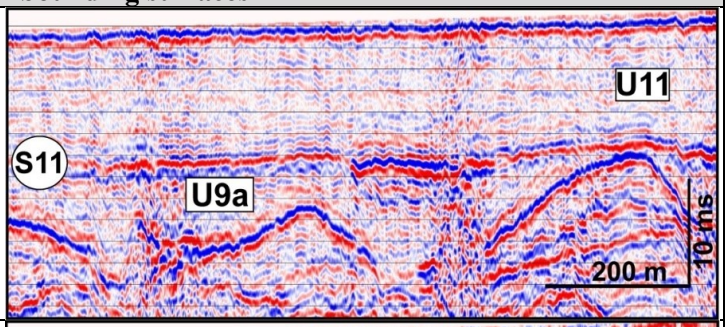
U10	Low to medium amplitude, parallel, continuous reflection configuration. **Base:** Onlaps onS10 **Top:** Concordant with S11	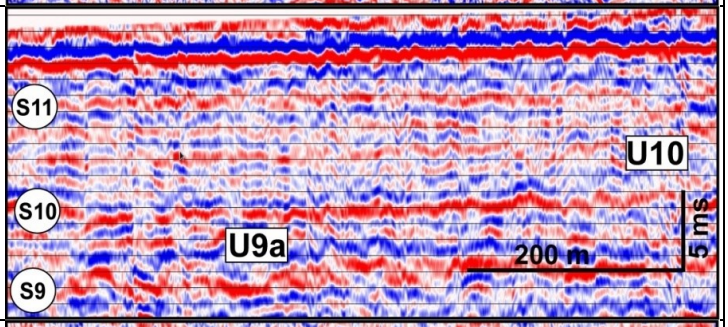
U9	High amplitude, parallel, continuous and wavy reflection configuration **Base:** Concordant with S8 **Top:** Eroded, and bounded by S9	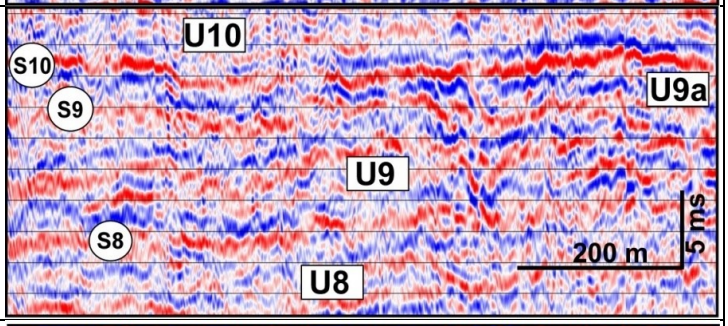
U8	Reflection pattern is not clear. **Base:** Concordant with S7 **Top:** Concordant with S8	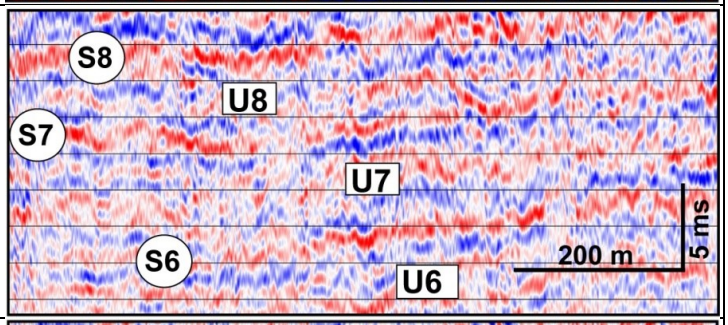
U7	Low to medium amplitude, parallel, slightly wavy configuration. **Base:** Concordant with S6 and S7a **Top:** Eroded by S7	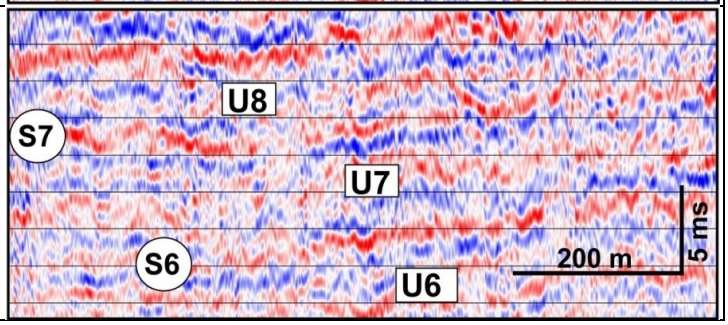

U6	Low amplitude, continuous, parallel configuration. **Base:** Concordant with S5 **Top:** Eroded by S6	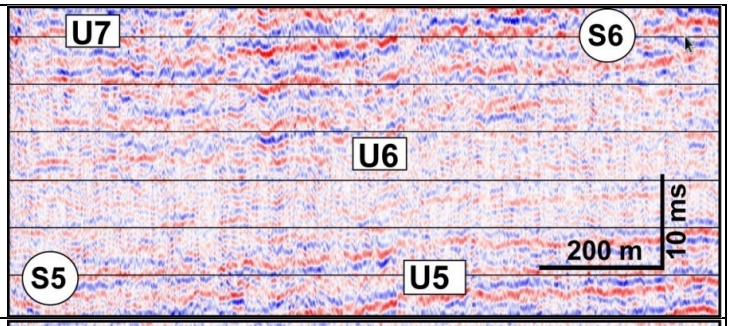
U5	Low to medium amplitude, continuous, parallel, slightly wavy configuration. **Base:** Concordant with S4 **Top:** Concordant with S5	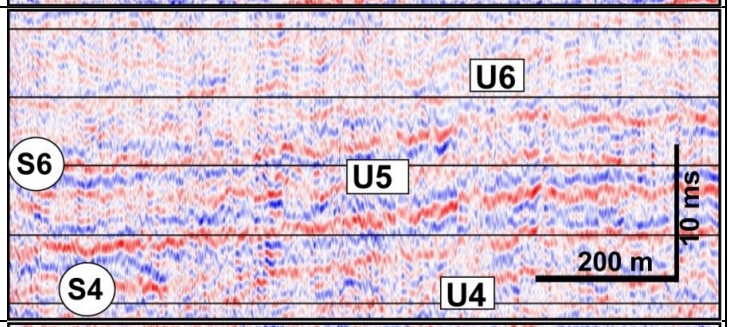
U4	Very low amplitude, highly continuous, parallel configuration. **Base:** Concordant with S3 **Top:** Concordant with S4	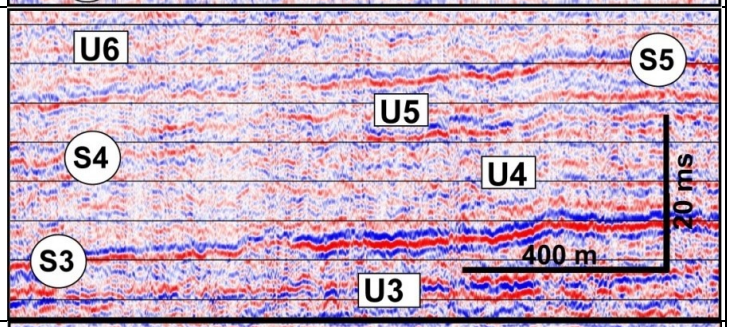
U3	Very low amplitude, continuous, parallel configuration. **Base:** Concordant with S2 **Top:** Concordant with S3	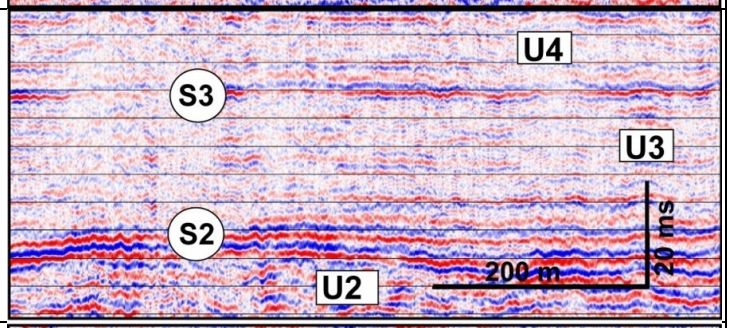
U2	Low frequency, low amplitude, highly continuous, parallel configuration **Base:** Concordant with S1b, S1b is an acoustic basement, below this only multiples are visible **Top:** Concordant with S2	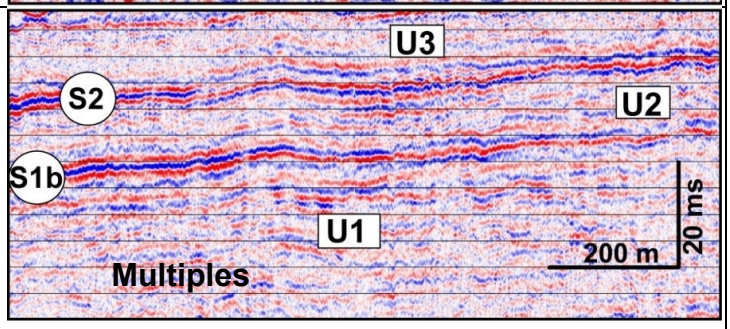

U1	High amplitude chaotic with diffraction pattern **Base:** not determined **Top:** Eroded by S1a, it is upper boundary of basalt	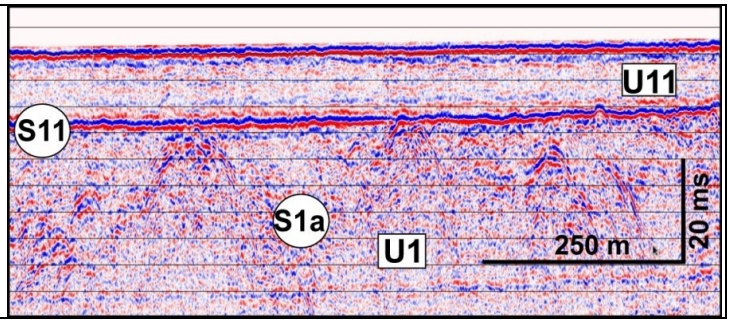

(iii) Seismic unit 9a (U9a)

U9a is bounded by S9 at its bottom and S10 on its top in deeper region (water depth >53 m), whereas it is bounded by S11 in shallower region (water depth <53 m) (Figs. 6A & B). This seismic unit consists of low to high amplitude reflections and reflection configuration varies across the study area from divergent to mounded infill reflectors in deeper region. Whereas, complex fills are mostly found in shallow region. The unit S9 is a surface which contains lenticular incision signatures which have been incised in low stand sea-level during Last glacial period and represents subaerial unconformity. Correlation of S9 with sea-level curve has been discussed in details later in Section 4.3.3. The unit S9 seems to merge with S11 at ~55 m water depth. Aspect ratios of incision as well as infill signatures indicate variable environment during initiation (mostly estuarine environment) up to mature (fluvial environment) stages of incisions. For example, vertical entrenchment of ~26 m (using V_p = 1583 m/s for sediment assemblage and 1500 m/s for water column) at 60 m depth of incision (Fig. 4.4) and chaotic reflection pattern at the base of incision indicate fluvial environment deposition of coarser sediment in high energy condition. Whereas, divergent to mounded infill reflectors indicate fluvial to transition zone environment. Therefore, S9 represents a polygenic, surface.

(iv) Seismic unit 9 (U9)

The seismic unit U9 is bounded on top by S9 and by S8 at its bottom (Figs. 4.3 A & B). It lies below U9a and is a prograding unit. Thickness of U9 increases basin ward. The seismic unit U9 is made up of continuous, parallel and medium to high amplitude reflectors. Since top of the unit is eroded by fluvial incision it has been interpreted that this unit contains high stand to low stand sediment deposits.

(v) Seismic unit 8 (U8)

Seismic unit U8 lies directly above U7 & U7a and is bounded by S8 on top and S7 as well as S8a at its bottom (Figs. 4.3 A, & 4.4). Its thickness is ~4-5 ms and seismic reflectors within this

unit are not very clear except the bounding layers. Since U8 lies just above U7a, it is interpreted that U8 was deposited during sea-level rise and contains transgressive to high stand deposits. S8a represents a transgressive surface which bounds the infill reflectors of U7a at its top.

(vi) Seismic unit 7a (U7a)

The seismic unit U7a is bounded by S7 at its bottom and by S8a on its top (Figs. 4.3 A & B). This seismic unit consists of low to high amplitude reflections and reflection configurations vary across the study area from divergent to complex infill reflectors. Similar to S9, S7 also contains lenticular incision signatures which have been incised during low stand sea-level and represents subaerial unconformity. Correlation of S7 with sea-level curve has been discussed in details in Section 4.3.3. Vertical entrenchment on this surface reaches up to ~35 m. Similar to S9, aspect ratios of incision as well as infill signatures on S7 also indicate variable environment incision and deposition. Therefore, S7 is also a polygenic surface.

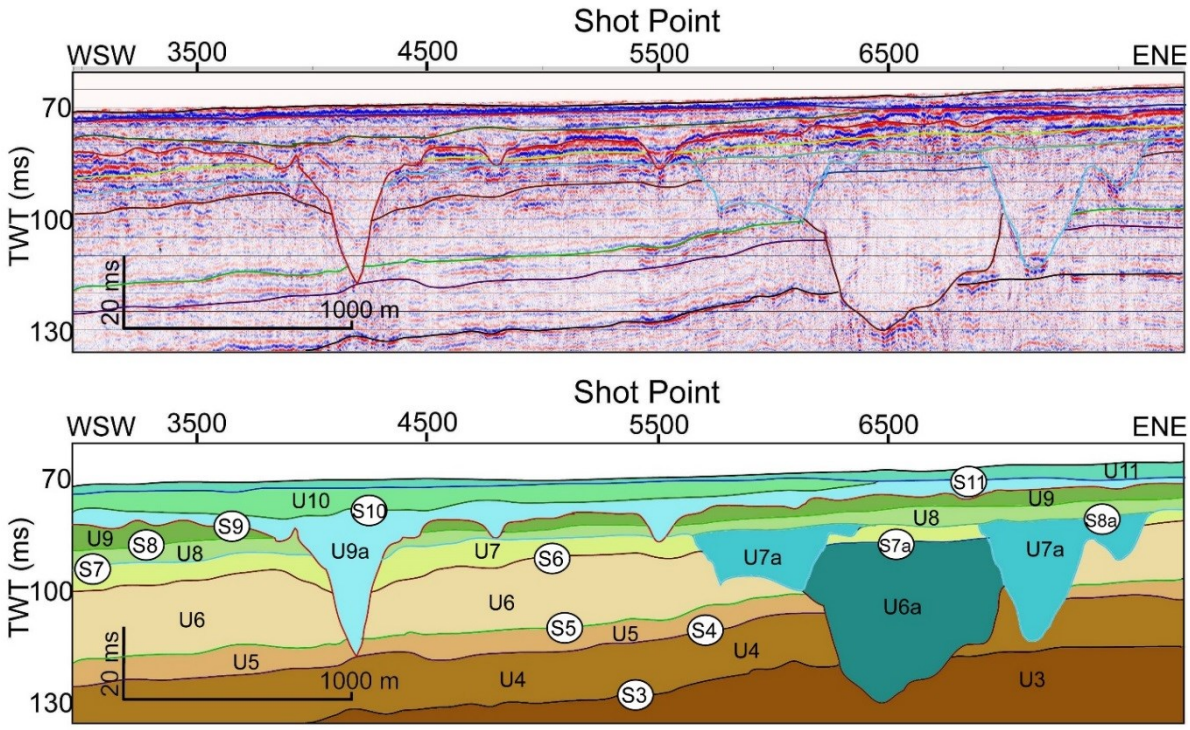

Figure 4.4 Enlarged seismic image and interpreted section of part of SaSu-36, showing seismic units (U3 to U11) and corresponding bounding surfaces (S3 to S11). S7a and S8a are transgressive surfaces which bound seismic units U6a and U7a, respectively.

(vii) Seismic unit 7 (U7)

Seismic facies of unit U7 shows parallel, wavy, continuous and low to medium amplitude reflectors. It is bounded by S7 at top and S6 at its bottom. Thickness of this unit increases basin

ward. The seismic facies suggest well-bedded fine grained deposits. U7 is eroded by channel incisions and the erosion surface is S7.

(viii) Seismic unit 6a (U6a)

Seismic unit U6a is bounded by S7a at its top and S6 at its bottom (Figs. 4.3 A & B). Here S6 contains the lenticular incision signatures which was incised during low stand sea-level and represents subaerial unconformity. Correlation of S6 with sea-level curve is discussed in details in Section 4.3.3. Similar to unit U7a, this seismic unit also consists of low to high amplitude reflections and reflection configuration vary across the study area from divergent to complex infills and interpreted to contain both fluvial and estuarine deposits. Thus, S6 also represents a polygenic surface. In general, incision signatures on S6 are reworked by channel incision on S7. Some of them can be easily differentiated in a seismic section (Fig. 4.3 A), whereas, other reworked signatures are differentiated based on section to section correlation.

(ix) Seismic unit 6 (U6)

The unit U6 is made up of parallel, continuous and very low amplitude (nearly transparent) reflections. It is bounded by S6 at its top and S5 at its bottom. Thickness of this unit increases basin ward. The seismic facies suggest well-bedded fine grained marine sedimentary deposit. Top of U6 is eroded by channel incisions and the erosion surface is S6.

(x) Seismic unit 5 (U5)

The seismic unit U5 is made up of continuous, parallel and medium amplitude reflections. It is bounded by S5 at top and S4 at the bottom. Thickness of this unit does not vary considerably (Figs. 4.3 A & B). Both the bounding surfaces do not contain incision signature, though U5 is eroded by younger channel incisions at places. The seismic facies suggest well-bedded fine grained deposits.

(xi) Seismic unit 4 (U4)

The unit U4 is made up of continuous, parallel and low amplitude reflectors. It is bounded by S4 at its top and S3 at its bottom. Thickness of this unit also increases seaward. Both the bounding surfaces do not contain incision signature, though U4 is eroded by younger channel incisions at places. The seismic facies suggest well-bedded fine grained complete marine sediment deposits and was never exposed for subaerial erosion.

(xii) Seismic unit 3 (U3)

Seismic unit U3 is bounded by S3 at its top and by S2 at its bottom (Figs. 4.3 A & B). It is characterized by concordant, continuous, and medium to low amplitude reflections. Both the bounding surfaces of this unit also do not contain incision signature, though top of the seismic unit U3 is eroded by younger channel incisions at places. This unit is interpreted as well bedded marine sedimentary deposit and was never exposed for subaerial erosion.

(xiii) Seismic unit 2 (U2)

Seismic unit U2 onlaps on unit U1. It is bounded by two concordant surfaces, S1b at its bottom and S2 at its top. Its seismic facies shows low frequency, low to medium amplitude, discontinuous, parallel to sub-parallel and slightly wavy reflectors. Its thickness increases seaward. This unit has been interpreted as oldest marine sedimentary deposit which might be overlying Precambrian crystalline rocks.

(xiv) Seismic unit 1 (U1)

The seismic unit U1 is the lower most unit identified on seismic section, in which no basal boundary is visible. Its seismic facies normally shows high amplitude reflection with diffraction pattern. At places high amplitude chaotic reflections are also observed. It outcrops near the present day coastline where it has been well studied and identified as Precambrian basal rocks (Fernandes, 2009; Dessai, 2011). The upper boundary of U1 is (i) a clear erosion surface (S1a) from coastline to 40 m water depth and marks the rocky basement, and (ii) the acoustic basement (S1b) beyond 40 m water depth. It is expected that some sediment assemblage is present below the acoustic basement.

4.5 Estimation of age of subaerial unconformities

As mentioned earlier, three subaerial unconformities S9, S7 and S6 are identified, where S9 is the youngest. All the three subaerial unconformities have seaward dipping character. These subaerial unconformities are reworked in the shallower region due to periodic incisions S9, S7 and S6 which are distinctively observed at ~70, ~75 and ~80 mbsl, respectively at the western boundary of the study area. The deepest incision observed at S9 is ~26 m which is located at ~69 m below the present sea-level (Fig. 4.5). This suggest that the deepest incision on S9 resulted due to lowering of sea-level at least up to ~95 m below present sea-level.

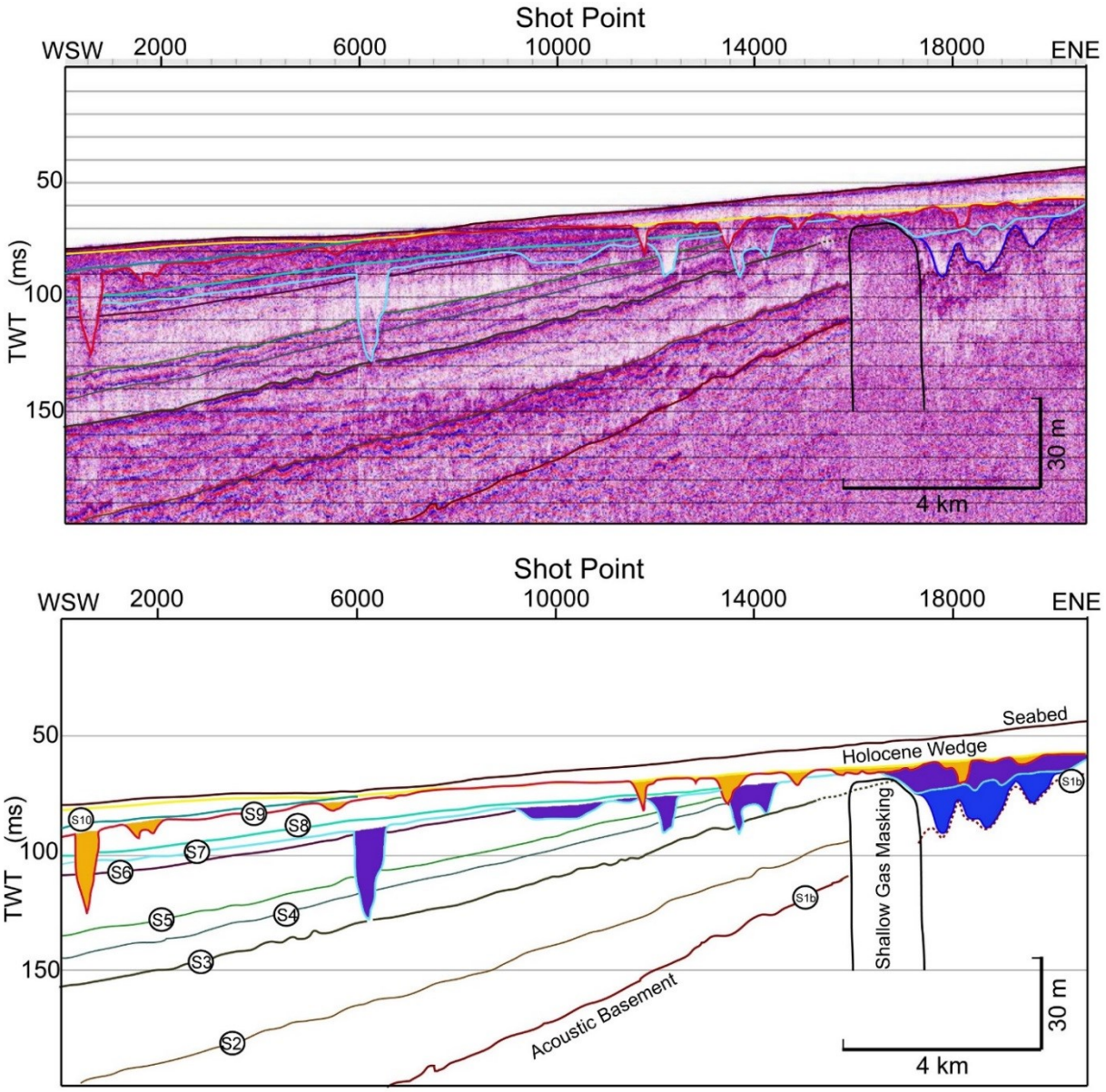

Figure 4.5 Seismic image and interpreted seismic section along trackline SaSu-38, showing two prominent subaerial unconformities (S7 and S9) and bounding surfaces of different seismic units in the study area.

Similarly, the deepest incision observed at S7 is ~35 m which is located at ~64 m below present sea-level. It means that the deepest incision on S7 resulted due to lowering of sea-level at least up to ~99 m below present sea-level. Subaerial unconformity S6 is although not as evident as S9 and S7, but at some places there are clear evidences of this unconformity. As it is shown in Figures 4.3A and 4.4, a very thin layer of marine sediment differentiates the incision on S7 from incision on S6. The deepest incision observed at S6 is also ~35 m which is located at ~68 m below present sea-level. This indicates that the deepest incision on S6 resulted due to lowering of sea-level at least up to ~103 m below present sea-level. It may be mentioned here

that S6 and S7 might have been altered by corresponding transgressive surfaces (S7a and S8a) too. Integrating above information and correlating with available sea-level curve (Siddall et al., 2003; Rehak et al., 2010), it is interpreted that S9 was exposed in the study area for ~105 kyr in last glacial period during ~115-10 kyr BP (Fig. 4.6). Although a thin layer of deposition is expected in the study area due to higher order sea-level fluctuations between ~90 and ~70 kyr BP (Fig. 4.6), clear signature of that layer is not observed in the seismic sections. It appears that this layer was completely eroded due to wave base erosion during subsequent lowering of the sea-level. Similarly, it is interpreted that S7 was exposed for ~70 kyr in penultimate glacial period during ~195-125 kyr BP. The channel incision on subaerial unconformity S7 took place during the low stand sea-level of MIS 6. Similarly, S6 was exposed for ~105 kyr between ~320 kyr BP and ~215 kyr BP and the channel incision took place during low stand corresponding to MIS 8. Correlation of subaerial unconformities with sea-level curve allows us to further assign period of formation of some of the identified seismic units within the limit of the study area. The oldest subaerial unconformity identified in the study area is S6. It started emerging with sea-level fall during ~320-250 kyr BP and got completely exposed at ~280 kyr BP, therefore, seismic unit U6 is interpreted to be older than ~280 kyr BP (Fig. 10). The seismic unit U6a contains sediment deposited by incised channels, which is interpreted as aggraded due to subsequent sea-level rise during ~250-215 kyr BP. Sea-level rise from ~80 mbsl caused the marine sedimentary deposition on S6. The surface S7 emerged due to sea-level fall during ~195-140 kyr BP and was completely exposed in the study region between ~185-125 kyr BP. Since unit U7 is bounded by S6 at its bottom and by S7 at its top, therefore, U7 is interpreted to contain sediment deposited during ~220-185 kyr BP. Whereas, U7a got deposited during ~140-125 kyr BP. Similarly, U8 contains sediment deposits during the sea-level rise between ~125-120 kyr BP. In the subsequent sea-level fall, S9 started emerging and got completely exposed at ~70 kyr BP in the study area, therefore unit U9 is interpreted to be deposited during ~115-70 kyr BP. Similar to unit U8, seismic unit U10 was deposited due to post glacial sea-level rise during the Pleistocene-Holocene transition. U11 have been found to be deposited during the Holocene and are considered as high stand deposits (Karisiddaiah et al., 2002; Mazumdar et al., 2009).

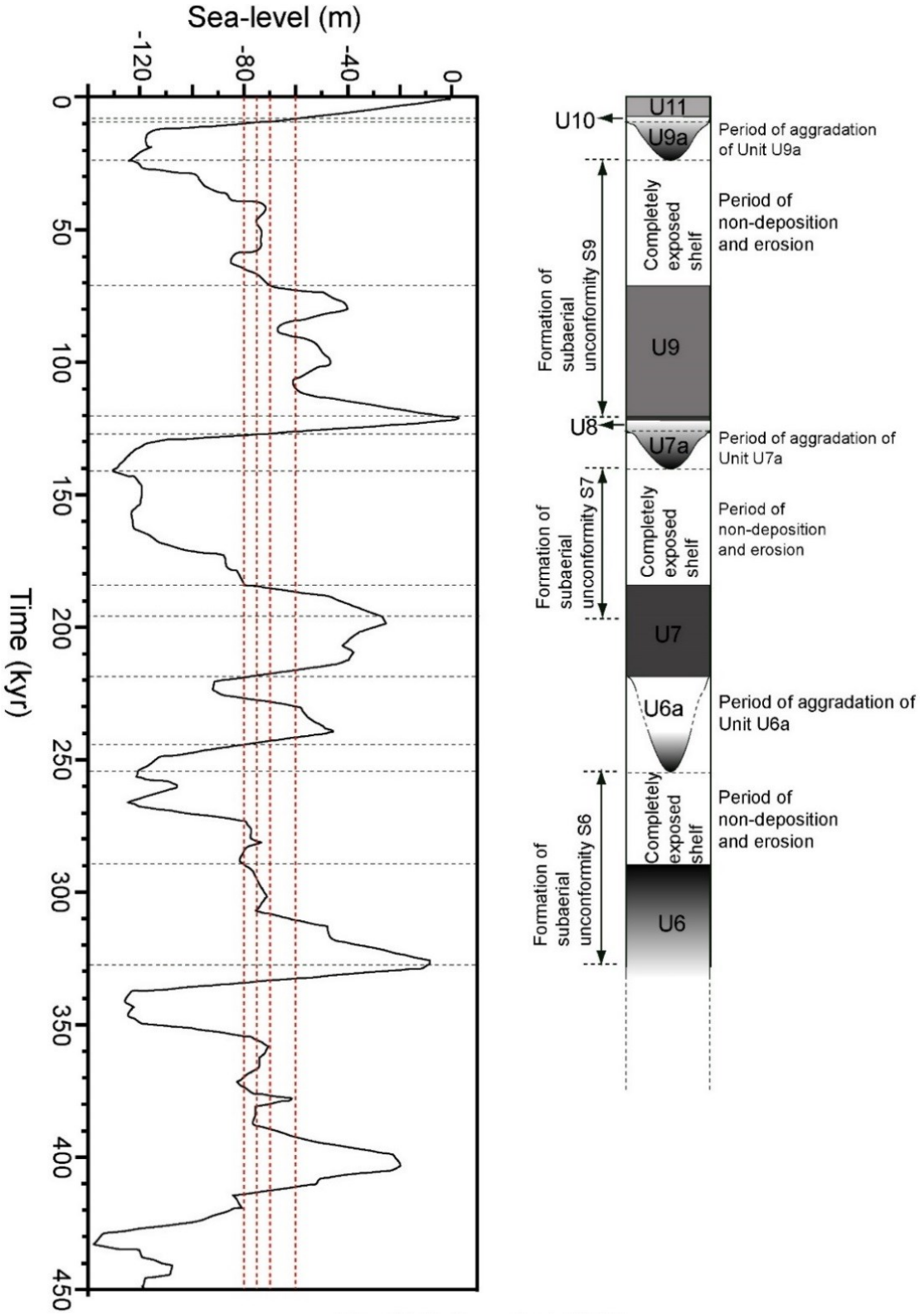

Figure 4.6 Correlation of sea-level curve of the last 450 kyr (modified by Rehak et al., 2010 from Siddal et al., 2003) with inferred seismic stratigraphy. U6 to U11 represent seismic units.

4.6 Discussion

Sedimentary architecture of the inner continental shelf of Goa reveals a lens shaped sediment wedge (U11). As correlated in section 4.4.3, this sediment assemblage was deposited during Holocene transgression and high stand normal regression after LGM. Similar transgressive and high stand sediment deposits after Penultimate Glacial Maxima (PGM) or older glacial period are also expected to be present. But careful analysis reveals absence of seismic signature of such transgressive and high stand sediment assemblage in the inner continental shelf of Goa. The sediment deposits corresponding to high stands of pre-LGM may be present in small pockets trapped around rocky patches very near to shoreline. This observation suggest that during each sea-level fall (forced regression), high stand sediment deposits got washed away by wave & tidal scouring and transported to deeper region by cross-shore currents.

Based on the sediment supply, modern continental shelves can be grouped as highly sediment starved, moderately sediment starved and highly sediment supplied shelf (Catuneanu et al., 2011; Zecchin and Catuneanu, 2013). In a highly sediment starved shelf, a sediment cover of prograding calcareous (biogenic, shell bed) sediment assemblage is expected beyond pinching out of terrigenous sediment seawards. Thickness of this calcareous sediment increases seaward. In a moderately sediment starved shelf, a shore detached mud accumulation in the outer part of the shelf is expected. In the present study, presence of terrigenous sediment stops predominant growth of calcareous sediment (shell bed). Whereas, in case of highly sediment supplied shelf, an aggrading terrigenous sediment cover over entire shelf is expected. The inner continental shelf of Goa depicts a lens shaped wedge which pinches out at ~50 m water depth, signifying negligible terrigenous sediment supply beyond 50 m water depth. Based on sediment sample data, several researchers (Hashimi et al., 1978; Nair et al., 1978; Rao et al., 1991; Rao and Rao, 1995; Rao and Wagle, 1997; Kessakar et al., 2003) have reported calcareous sediment (mostly biogenic) with trace amount of terrigenous clay on the outer shelf between Gulf of Kutch and Mangalore. Presence of modern terrigenous clay on the slope region and their transport from hinterland across outer shelf have been confirmed (Kessarkar et al., 2003). In light of the results of the present study and sediment distribution on the outer shelf, it is suggested that continental shelf of Goa is a moderately sediment-starved continental shelf.

Presence of prominent subaerial unconformities corresponding to 4^{th} order sea-level variations reveals that unlike simple valley, inner continental shelf of Goa have been incised multiple

times (like a compound valley system) during the Late Quaternary. Ancestral rivers of Goa had extensively altered the sedimentary architecture of the inner continental shelf of Goa. Signatures of channel incision corresponding to three glacial maxima are well preserved. Bounding surfaces below S6 do not have any incision/erosion signatures, well stratified concordant reflector within these units indicate marine depositional environment. Absence of topsets in these older unit also indicate that highstand sediment deposits were completely washed away during each subsequent sea-level fall. This may be due to high gradient of the inner continental shelf of Goa prior to 330 kyr.

4.7 Conclusions

The application of seismic and stratigraphic concepts to seismic data allows to conclude that the present continental shelf of Goa is a moderately sediment starved type shelf. Terrigenous sediment deposition ceases at ~50 m water depth. There are eleven distinctively visible seismic units (U1 to U11) and three sub-seismic units (U6a, U7a and U9a) in the inner continental shelf of Goa. Further, a new methodology is developed in this study to explains sub-aerial unconformities within the geological time scale in absence of age of stratigraphic layers derived from study of long sediment cores of river base level concept on incision signatures and corelation with sea-level curve. It allows to assign period of formation of some of the seismic units. The sedimentary strata on the inner continental shelf contains preserved channel incision signatures corresponding to more than three glacial periods. It allows to conclude that under the effect of glacio-eustatic sea-level variations, inner continental shelf of Goa has evolved as compound incised valley through the Late-Pleistocene.

Chapter 5
Holocene Sedimentation

5.1 Introduction

Present chapter is interconnected with the previous chapter and emphasizes on the spatial distribution of the Holocene sediment thickness over the inner continental shelf of Goa. It also tries to scrutinize and determine the major factors responsible for the observed sedimentation pattern. It discusses briefly, how the 4^{th} order sea-level variations along with other coastal constraints have affected depositional processes on the inner continental shelf. Further, it computes the Holocene sedimentation rates and its spatial distribution pattern over the inner continental shelf of Goa using the Holocene sea-level curve (Hashimi et al., 1995) of the west coast of India.

5.2 Holocene Sedimentation

Based on the sequence stratigraphic analysis of the High Resolution Shallow Seismic (HRSS) data (discussed in Chapter 4), seismic unit U11 is interpreted to embody the Holocene sediment assemblage of the study area. U11 is bounded by seabed on top and by S11 at bottom. Bounding surface S11 is interpreted as the Holocene Transgressive Surface (Holocene_TS) which separates the Holocene sediments from the Late-Pleistocene sediments in the study area except at deeper region (beyond ~50 m water depth). At deeper depth, bounding surface S11 separates units U10 and U11. It may be mentioned here once again that unit U10 is inferred to be deposited during initiation of the Holocene epoch. These two surfaces (seabed and S11) cover almost the entire Holocene deposits in the study area. Therefore, both the bounding surfaces (S11 and seabed) have been digitized from every seismic sections using seismic data processing software SeisSpace®ProMAX®. The digitized data have been used to generate corresponding grid data and to investigate key factors responsible for the observed Holocene sediment distribution in the study area. The grid data is used to prepare the Holocene sediment thickness map, and an equivalent shoreline trajectory map (map depicting depth variation of the Holocene_TS (S11)).

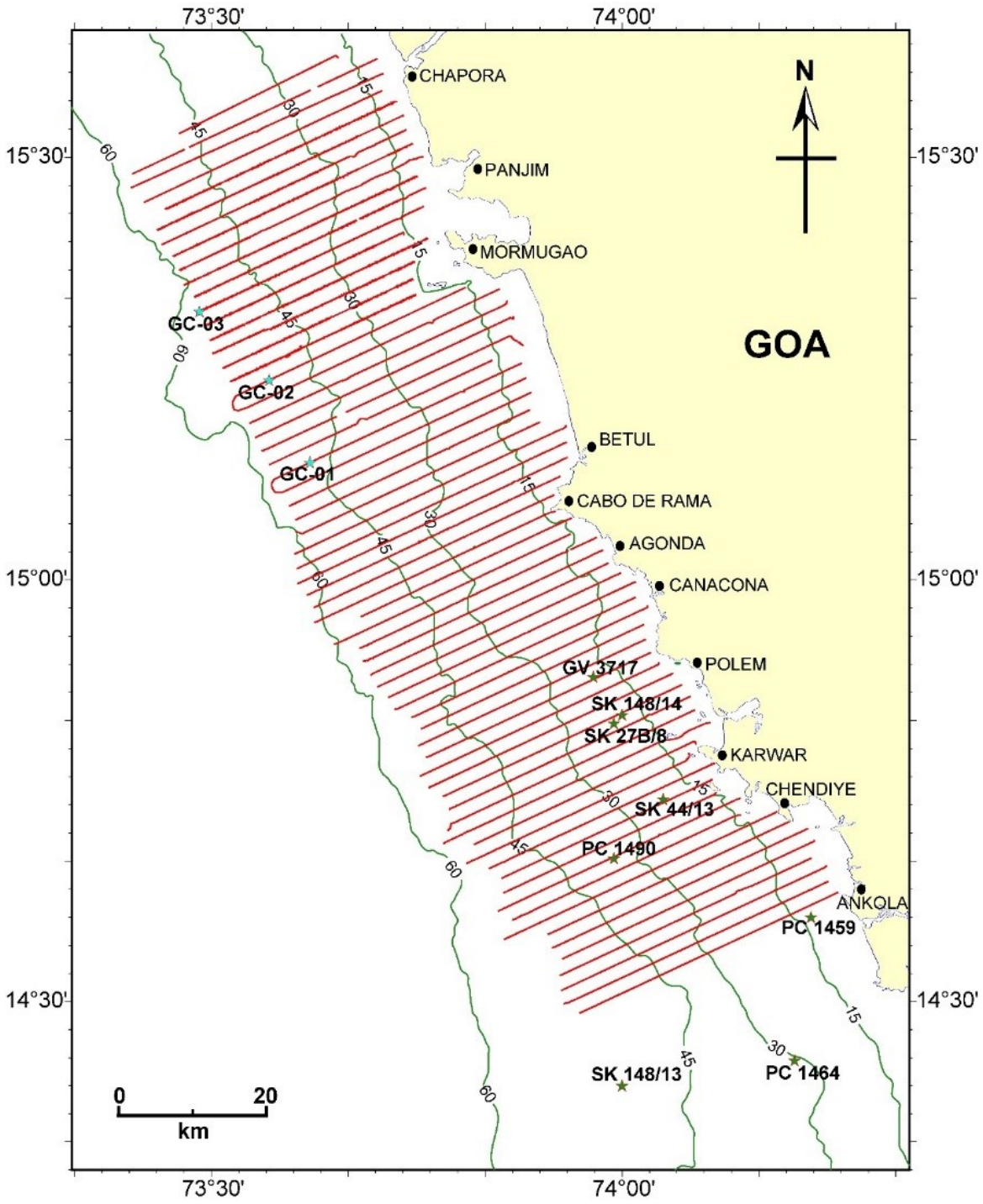

Figure 5.1 Seismic tracklines which are used for preparation of the Holocene sediment thickness and sedimentation rates. Solid red lines represent tracklines along which HRSS data were acquired. Solid green lines represent isobaths along which water depth is annotated in meter. Green stars denote location of sediment cores compiled from previous studies. Cyan stars denotes location of sediment cores collected for the present study.

It may be noted here that the Mandovi and Zuari rivers are major source of terrigenous sediment in the study area. The Kali River in Karnataka, located in the immediate vicinity of the study area, might have also played an important role in contributing the sediments into the study area.

It is a major river of Karnataka which debouches into the Arabian Sea near Karwar and roughly forms an inland geological boundary between Goa and Karnataka. It is a typical west coast river and has comparable properties in hydrological aspect with the Mandovi and Zuari rivers of Goa. Therefore, sediment thickness map was prepared for extended area of the inner continental shelf located between off Chapora in the north and off Ankola in the south. For this purpose, seismic data along 17 tracklines between off Polem and off Ankola have been added to the existing seismic data of the study area (Fig. 5.1). In the following sections, primary observations and analyses of spatial distribution of the Holocene sediment thickness and sedimentation rates are described.

5.2.1 Holocene sediment thickness map

Holocene sediment thickness map (grid interval 20 arc seconds) is generated using gridded sediment thickness data. The data is sensitive to spatial variations of any geomorphological features (in sediment thickness) larger than ~3.7 km (see Chapter 3 for details).

As discussed earlier in chapter 4, the Holocene sediments are deposited in a lens shaped wedge i.e. the sediment thickness decreases basinward as well as shoreward. Holocene sediment thickness is truncated by outcrops of igneous rocks towards shore. Whereas, pinching out of the sediments in deeper region (~50 m water depth) occurs due to significantly less terrigenous sediment supply. The thickness map also revealed two conjoint zones of high sediment accumulations (Fig. 5.2). These two zones are located offshore between Betul and Polem, and almost enveloped by 35 m isobath (Fig. 5.2). These zones have ~3 to 5 m more thick sediment than other region between off Chapora and off Ankola, at similar water depth.

The Holocene sediment thickness varies from 0.8 to 15.7 m on the inner continental shelf between Chapora and Ankola (Fig. 5.2). In general the thickness increases from coastline to ~20 m water depth. Beyond 20 m water depth, it continuously decreases and becomes almost invariable (~2.0 m) beyond ~50 m water depth. In order to analyze variation of the sediment thickness along the present day isobaths, sediment thickness data have been extracted along isobaths and profile plots are generated (Fig. 5.3). It is observed from the analyses of these profiles that the Holocene sediment thickness decreases from Chapora to Ilha-De-Grande Island along 15 and 20 m isobaths. Beyond Ilha-De-Grande Island, it first increases up to Karwar and then again decreases sharply further southward. A sudden decrease in the sediment thickness can be observed between offshore Betul and Canacona, suggesting a low sedimentation zone.

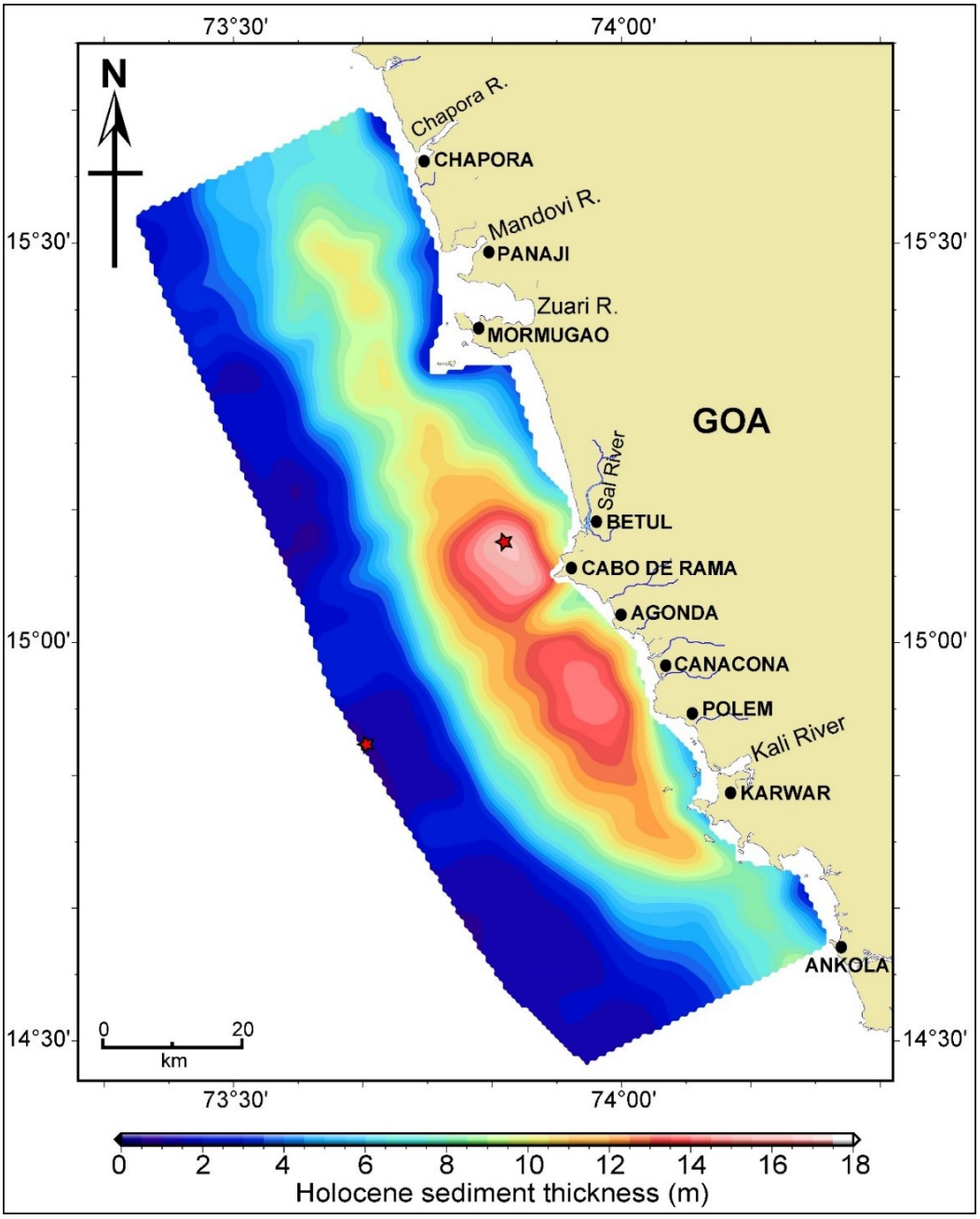

Figure 5.2 The Holocene sediment thickness map depicting thick sediment deposits close to coast between Betul and Karwar. Red stars denote maximum and minimum sediment thickness locations.

The sediment thickness along 25, 30, 35 and 40 m isobaths show a continuous increase of sediment thickness from Chapora to Canacona and sharply decreases south of Canacona (Fig. 5.3). The sediment thickness along 45 m isobath does not display any significant trend and is almost invariable (~2.0 m) along 50 m isobath. Further analysis of gridded sediment thickness data reveals an average sediment thickness of ~6.4 m deposited during the Holocene on the inner continental shelf between Chapora in the north and Ankola in the south. Numerical computation based on the gridded data reveals a total volume of ~32.09 km^3 of the Holocene

sediment deposited over 5014 km^2 area on the inner continental shelf between Chaopra and Ankola.

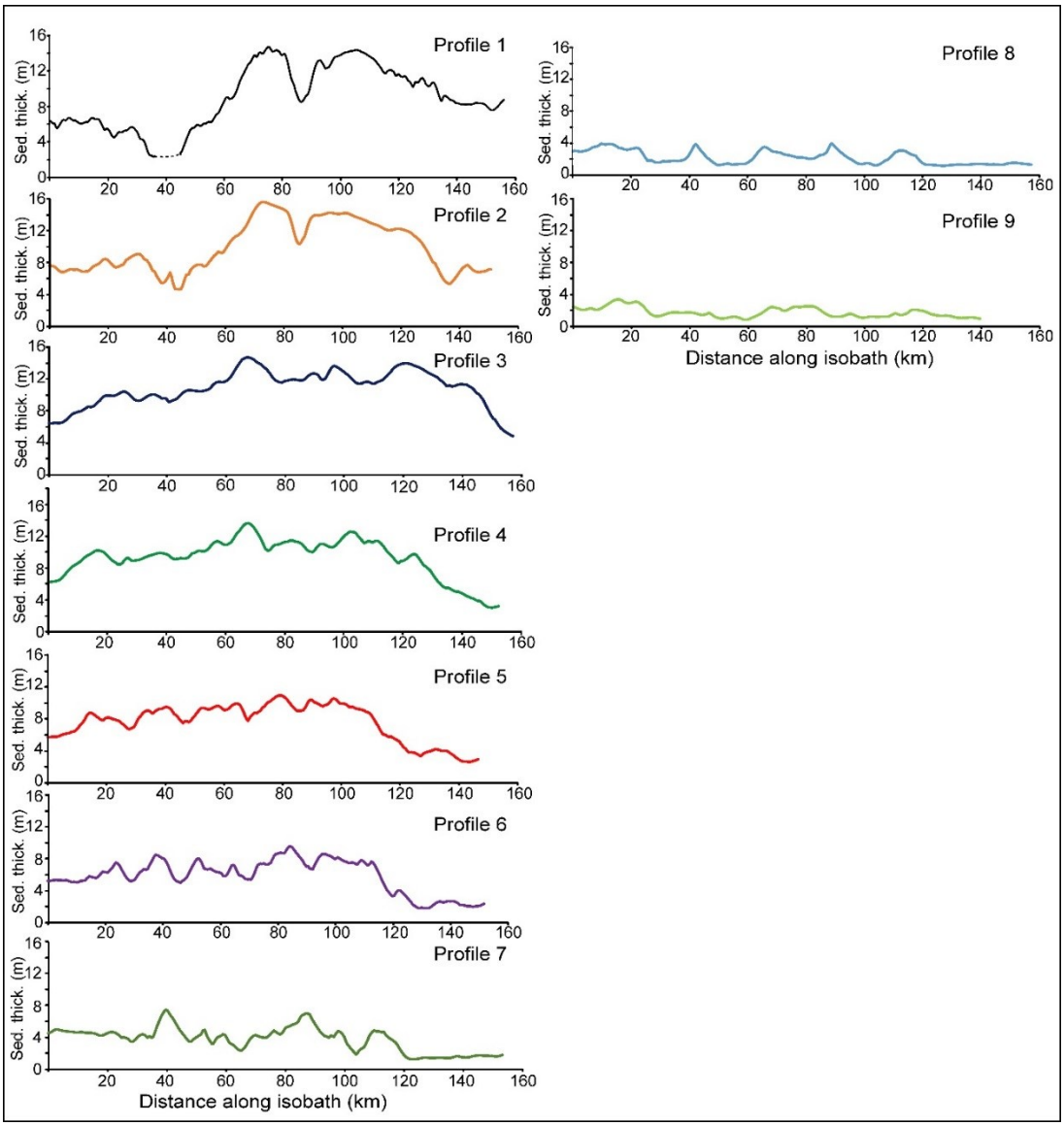

Figure 5.3 Holocene sediment thickness profiles along isobaths. Profiles 1 to 9 represent sediment thickness variations along 15, 20, 25, 30, 35, 40, 45, 50 and 55 m isobaths, respectively.

5.2.2 Holocene Sedimentation rate

Gridded data for the Holocene sedimentation rate are used to prepare a map depicting mean sedimentation rate and its pattern on the inner continental shelf between Chapora and Ankola (Fig. 5.4). Similar to the sediment thickness map, it also revealed two anomalous zones located offshore Betul and Cancona. These zones are enveloped by 35 m isobath and show anomalously high sedimentation rates. The analysis revealed that mean sedimentation rate during the Holocene varied from 0.05 mm/yr near location 14.837222° N, 73.681667° E to 1.64 mm/yr

near location 15.119167° N, 73.8575° E. Similar to the sediment thickness pattern, mean sedimentation rate during the Holocene also increases up to 20 m water depth, beyond 20 m water depth it continuously decreases with depth and becomes almost invariable (~0.2 mm/yr) after 50 m water depth. Sedimentation rate variation along isobaths also show similar trend as of sediment thickness.

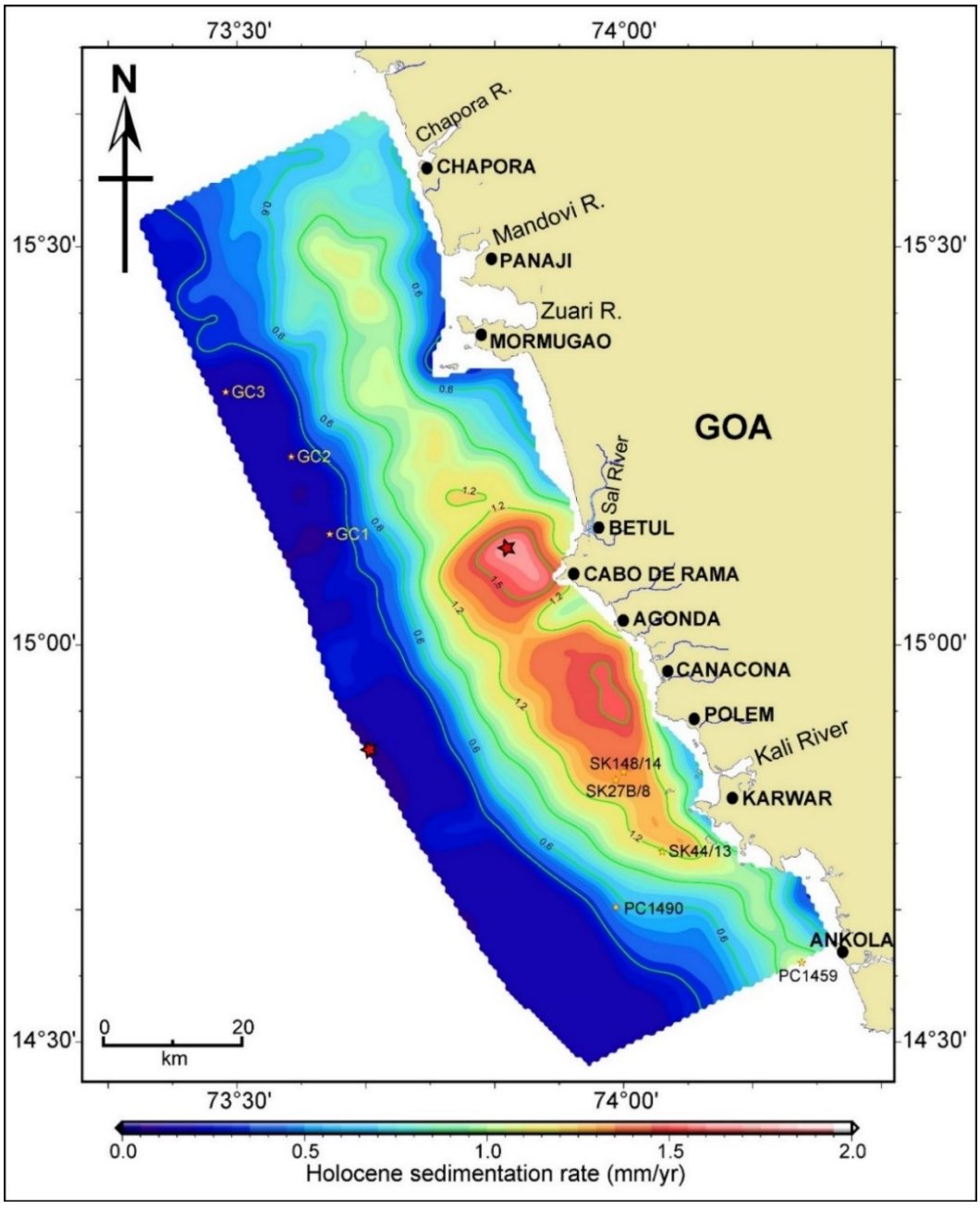

Figure 5.4 Map depicting mean sedimentation rate during the Holocene. Solid green lines are contours for sedimentation rates which are annotated in mm/yr. GC-01, GC-02, and GC-03 are the sediment cores collected for this study. SK148/14, SK27B/8, SK44/13, PC1490 and PC1459 are sediment cores acquired during previous studies. Red stars denote maximum and minimum locations of sedimentation rates.

5.2.3 Sedimentation rate from core data

Three sediment cores namely GC-01, GC-02 and GC-03 were collected from the inner continental shelf of Goa between ~55 and 60 m water depths during cruise SSD-039 of *Research Vessel Sindhu Sadhana* during July 2017. As mentioned in Chapter 3, the sub-samples of these sediment cores were dated using ^{14}C technique in the Department of Geology and Mineralogy, University of Cologne, Germany. Details of the sediment cores and calibrated ages are presented in Table. 5.1.

Table 5.1. Details of sediment cores, material used for dating and radiocarbon dates.

Core ID & core length	**Location & water depth**	**Depth in core (cm)**	**Material used for ^{14}C dating**	**Measured ^{14}C age (Years BP)**	**Calibrated ^{14}C age (Years BP)**
GC-01 (2.26 m)	73.6199211° E, 15.1389980° N (54.5 m)	26-27	Carbonate / foraminifera	1211±22	612±22
		76-77		2087±24	1465±24
		99-100		2452±26	1895±26
		125-126		5441±30	5637±30
		222-223		6766±41	7113±41
GC-02 (0.53 m)	73.5702313° E, 15.2364460° N (55.6 m)	44-45	Carbonate / foraminifera	3106±26	2711±26
GC-03 (0.57 m)	73.4854666° E, 15.3176050° N (60.4 m)	10-11	Carbonate / foraminifera	3130±25	2738±25
		55-56		4297±26	4190±26

Mean sedimentation rates from the deepest sample of the cores GC-01, GC-02 and GC-03 are calculated which are 0.31, 0.16 and 0.13 mm/yr, respectively. Further, a depth versus age curve for these cores has been plotted for comparative analysis (Fig. 5.5). The curve revealed that although the cores GC-01 and GC-02 are located at almost same water depth (~55 m), sedimentation rates at these locations are inconsistent with each other. GC-01 show anomalously higher sedimentation rate than the GC-02 for the same depth interval. The sediment core GC-03, which was collected from ~60 m water depth, also does not show any similarity with the GC-01 and GC-02. Mean sedimentation rate from the gridded data at the respective locations of GC-01, GC-02, and GC-03 are 0.22, 0.16, and 0.14 mm/yr. The mean sedimentation rates derived from the grid data at these locations are quite comparable with the mean sedimentation rate obtained from the sediment cores GC-02 and GC-03.

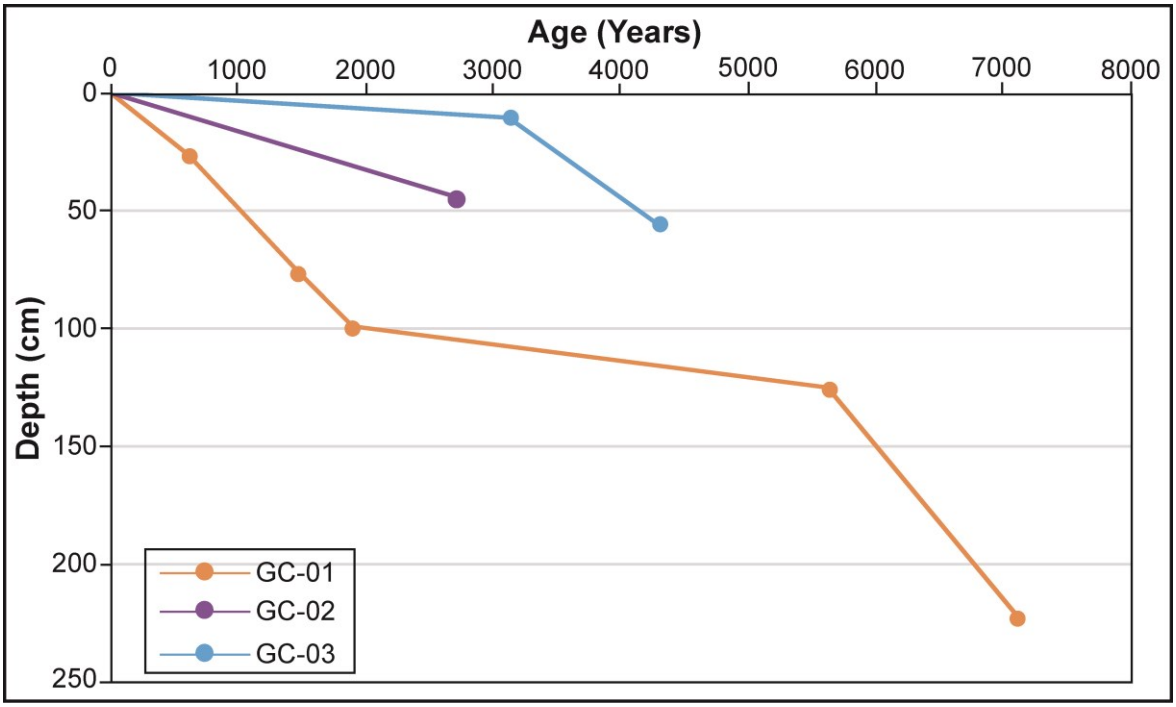

Figure 5.5 Depth (in sediment core) versus calibrated age curve for sediment cores GC-01, GC-02 and GC-03. Cores GC-01 and GC-02 were collected at ~55 m water depth, whereas core GC-03 was collected at ~60 m water depth. (Location of the cores are given in Fig. 5.1).

5.3 Analysis of observed sediment thickness pattern

Interestingly, two conjoint anomalous sediment thickness zones located between off Betul and off Polem are far away from the two major terrigenous sediment sources, Mandovi-Zuari and Kali rivers. Though several small estuaries (Sal, Talpona and Galgibag) and creeks debouch into the inner continental shelf of Goa (nearby anomalous zones), still high accumulation of the Holocene sediments in this zone is unusual. In fact, mouth zones of Mandovi-Zuari, and Kali rivers also do not show any abnormal high sediment accumulation. It is generally believed that in coastal region outside the surf zone, distribution of sediments over the continental shelf are controlled by coastal currents (i.e. longshore and cross-shore) along with major sediment sources (i.e. estuaries and creeks) and nearshore morphology. The anomalous sediment thickness zones observed in this study can be explained with the following three possible ways:

(i) Sediments are supplied predominantly from distant larger sources and coastal currents along with nearshore geomorphology played key roles at local scale,

(ii) Sediments are supplied predominantly from close-by sources and coastal currents along with nearshore geomorphology played key role, or

(iii) Sediments are supplied predominantly from close-by sources and nearshore geomorphology have played key roles with very limited role of coastal currents.

Narmada and Tapti are two largest rivers of west coast of India which supply large amount of terrigenous material into the Arabian Sea in the north. Previous geophysical and geological studies on western continental shelf of India revealed that the maximum Holocene sediment thickness decreases from ~35 m near mouth of Narmada and Tapti rivers in the north to ~15 m off Cochin in the south (Siddique et al., 1981a, b; Rao and Wagle, 1997). Therefore, it is expected that the sediment thickness between off Chapora and off Ankola should also show similar trend. However, the sediment thickness does not show such trend, instead it first increases and then decreases southward. Also, maximum Holocene sediment thickness observed in the study area, except at the anomalous zones, is only ~11 m which is less than the sediment thickness reported off Cochin (~15 m). Therefore, the observed Holocene sediment thickness pattern discards the possibility of distant sediment sources and coastal currents as key players for accumulation of anomalous sediment thickness mentioned above. Previous sedimentological studies on the western continental shelf (Hashimi et al., 1978; Kessarkar et al., 2003) also revealed that the sediments deposited over the shelf is mostly transported from the hinterland area through cross-shore coastal currents and discards the major role of longshore coastal currents.

As mentioned, two conjoint zones of anomalous sediment accumulation are located in the south of the Mandovi - Zuari river mouth zone and north of the Kali river mouth zone. Considering north-south coastal currents during the monsoon in this area, thick sediment deposits are expected in the south of each river, as these rivers supply most of the sediment during the monsoon season (Nair et al., 1978; Shetye et al., 1995, 2007). The present study does not show high sediment accumulation in the south of the Kali river mouth zone, though two conjoint zones of anomalous sediment accumulation are found south of Mandovi - Zuari river mouth zone. Therefore it is obvious here that the role of coastal longshore current is limited (i.e. they do not play major role) for the observed sediment deposit pattern between off Chapora and off Ankola.

It will now be shown that nearshore morphology (Basin characteristics and shoreline configuration) and paleo-fluvial processes had played significant role in the observed sediment deposit pattern between off Chapora and off Ankola. In the following paragraphs, a detailed discussion is presented on this aspect:

Continental shelf basin of Goa had been significantly reworked by wave action during the Holocene shoreline transgressions. The coastal processes such as fluvial and tidal erosion

together with wave action have also contributed significantly in reshaping the basin. In this case transgressive surfaces across the coast may act as the equivalent shoreline trajectory and hence can reveal effective basin characteristics. Therefore, the Holocene transgressive surface (S11) is digitized and a gridded database for depth variation of Holocene_TS is prepared using Generic Mapping Tools (discussed in chapter 3). This gridded data is further used to prepare a depth variation map of Holocene_TS (Fig. 5.6).

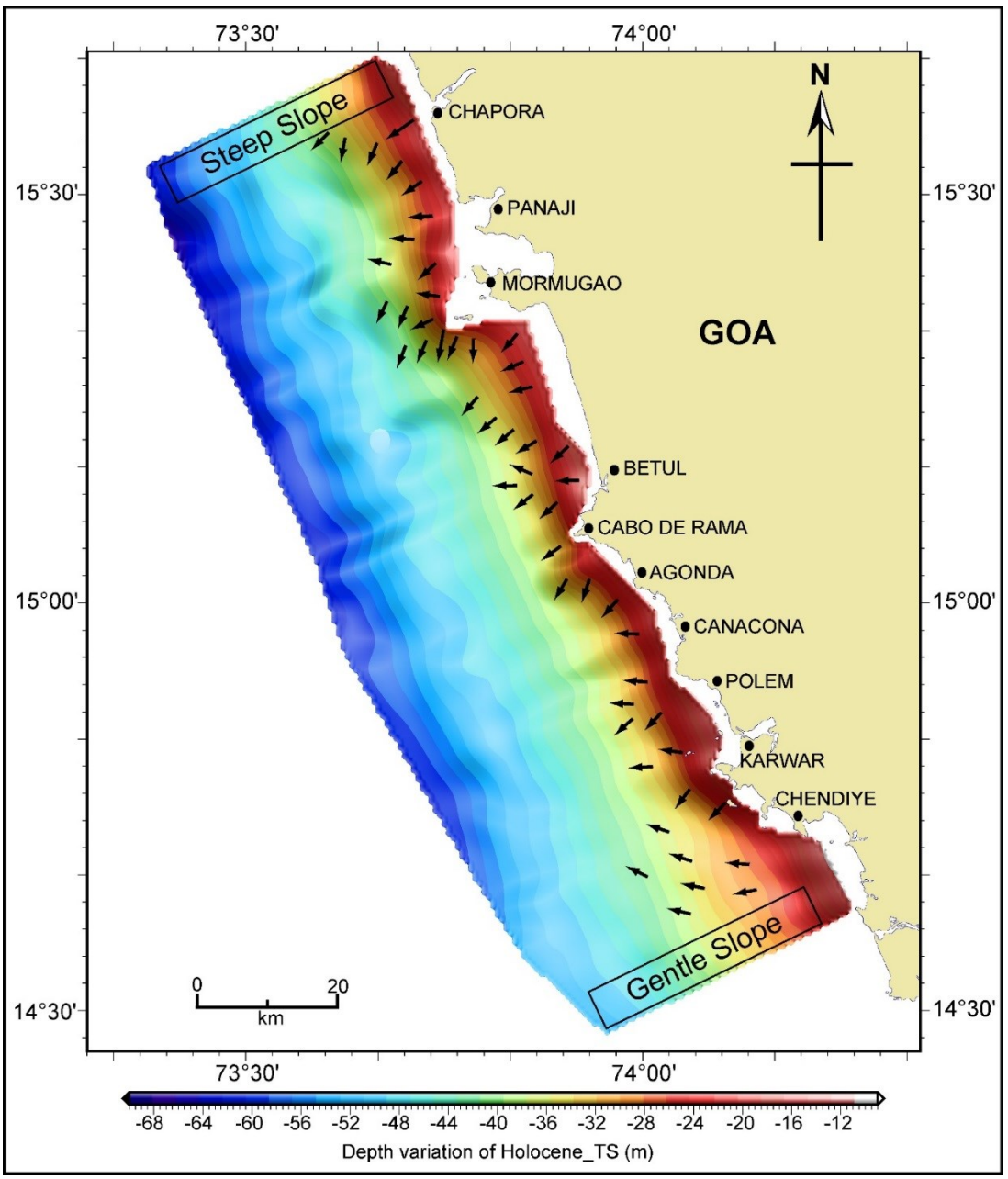

Figure 5.6 Map depicting depth variation of the Holocene_TS on the inner continental shelf between off Chapora and off Ankola, central west coast of India. Small arrows shows approximate sediment movement direction under the effect of gravitational pull in absence of longshore coastal currents.

Further to analyze the Holocene_TS (effective sedimentary basin) characteristics, depth to Holocene_TS are extracted along 6 transects each, parallel as well as orthogonal to the present coastline using the gridded data and profile plots are generated (Figs. 5.7 & 5.8). The Holocene_TS depth profiles, parallel to the coastline, are sub-divided into 8 zones (A to H) to investigate offshore extension of land features and their impact on the basin structure (Fig. 5.7). The Holocene_TS depth variation map reveals several prominent characteristic features of the inner shelf basin which are described in the following paragraphs using the Holocene_TS depth profiles (Fig. 5.6).

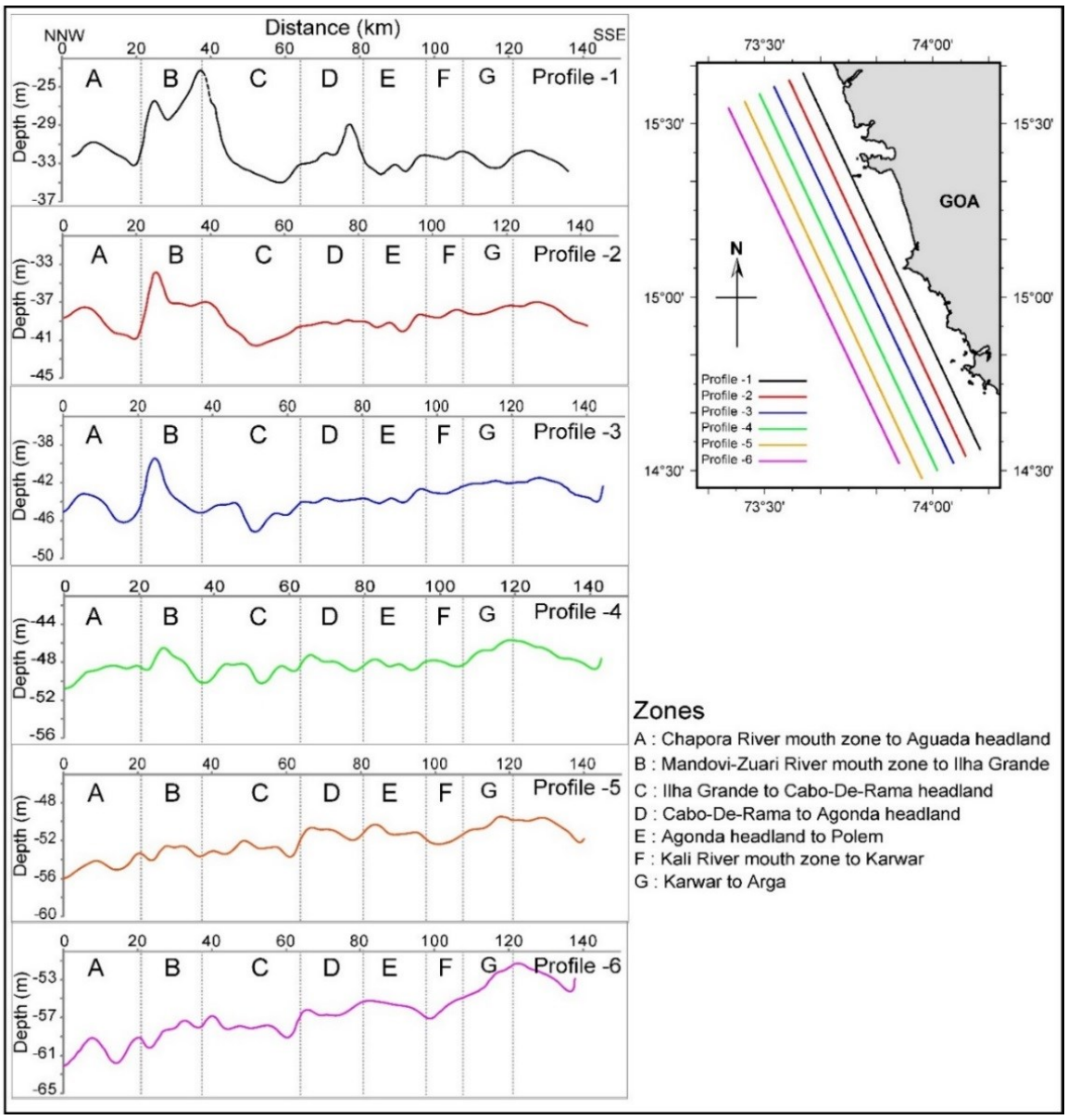

Figure 5.7 Depth profile of the Holocene transgressive surface along six parallel transects. These transects are parallel to the present coastline and shown in the inset map. Depth profiles are divided into 8 zones (A-H) to analyze impact of hinterland features.

Depth profile of Holocene_TS (Profile-1) did not reveal any noticeable trend except in zones B and D (Fig. 5.7). Zone B, located in the vicinity of Mandovi-Zuari river mouth and Ilha-De-Grande Island, is an elevated zone with ~8-10 m relief. Whereas zone D which lies in the vicinity to the Cabo-De-Rama and Agonda headlands, is an elevated zone with a relief of ~4-5 m. Zone-B revealed offshore extension of Mandovi-Zuari mouth area and Ilha-De-Grande island platforms. Zone-D also revealed offshore extension of Cabo-De-Rama headland. Extent of Mandovi-Zuari mouth zone can be observed till Profile-4. Thus the elevated zone observed in Zone-B divided the inner shelf basin into two parts i.e. northern and southern, while Zone-D affects the basin locally and creates a barrier for the sediment movement across it (up to ~35 m present water depth). The elevated Zone-B creates dips towards Zone-C with an average gradient of 1:800 (comparable to inner shelf gradient). Whereas, shallowest peak in Zone-D dips towards Zone-C with an effective gradient of 1:2000. Zone-B and Zone-D together form a local basin in Zone-C at shallower depth.

Further analysis of depth profile along other transects revealed a noticeable northwestward dipping trend. This trend became progressively more prominent towards the deeper region (Fig. 5.7). Though the dip in northwestward direction is very gentle (Maximum dip is of the order of 1:10000) and may not contribute much in deeper region for sediment deposition, it might have affected the direction of sediment movement in the initial stage of transgression. This gentle dip, together with Zone-D (with an effective gradient of ~1:800 southeastward) form a local basin southward of Zone-D for sedimentation.

The depth profiles of Holocene_TS, orthogonal to the present coastline, reveals that average dip of the Holocene shoreline trajectory varies from ~1:770 in the north to ~1:1215 in the south (Fig. 5.8), implying flatter Holocene_TS in the south as compared to the north. This suggests a concave coastline in the initial stage of coastline transgression, which might have been interrupted by extensions of local land features. Interestingly, depth profile of the Holocene_TS orthogonal to the coast also revealed concave nature of the Holocene-shoreline trajectory (Fig. 5.8). The concavity of the shoreline trajectory varies through entire region between off Chapora and off Ankola. It initially increases southward but again starts decreasing off Polem to further southward. In the northernmost part, additional accommodation space (vertical) of ~4 m was created due to concavity of the Holocene_TS, whereas in southernmost part, this space was reduced to ~2 m. Interestingly, the central region between off Betul and off Canacona, additional accommodation space of ~8 m was created due to concavity of the Holocene_TS

(Fig. 5.8). This elucidates deeper Holocene_TS in the central region as compared to the northern as well as southern region.

Remarkably, the central region (located between off Betul and off Canacona) have been found to have maximum Holocene sediment thickness (Fig. 5.2). Fluvial processes during the last glacial period and erosion by wave action during sea-level transgression might have played major roles for variable concavity of the Holocene_TS. Presence of ancestral Mandovi-Zuari river channel in the northern basin (discussed in chapter 6) and ancestral Kali river in the southern basin might have caused erosion of ~2-4 m of sedimentary strata. Whereas, concavity of the Holocene_TS in the central region of the southern basin is anomalous as there is no larger river in this region which can cause erosion of ~8 m of sedimentary strata. High resolution shallow seismic sections were reanalyzed to explain the anomalous concavity of the Holocene_TS. The analysis revealed anomalous erosion of subaerial unconformity S9 (Fig. 5.9). Further analysis of the HRSS sections revealed that this anomalous erosion is related with paleo-fluvial processes which were active during the episodic sea-level transgression in the early Holocene. For example, HRSS section along SaSu-51 revealed anomalous coastward truncation of S9 (Fig. 5.9). This anomalous truncation was caused by a channel inlet which was active in nearby region when sea-level was at ~55 m below the present sea-level. Presence of these channel inlet provided an alternate route to sea water to ingress further deeper into the exposed land leaving a coastal sedimentary island behind. Initially, tidal current through the channel caused predominant erosion of the inlet and played an important role in widening of the channel landward. At the same time shoreward portion of the island was supplied excess sediment from the tidal inlet which caused flat shoreface and lowered littoral drift. These processes together caused anomalous erosion of the island on one side and excess sedimentation on the other side. As a result, the flat shoreface was preserved. Later, sea-level rise coupled with wave action widened the inlet zone which facilitated extensive erosion of larger area and generated a local deeper basin.

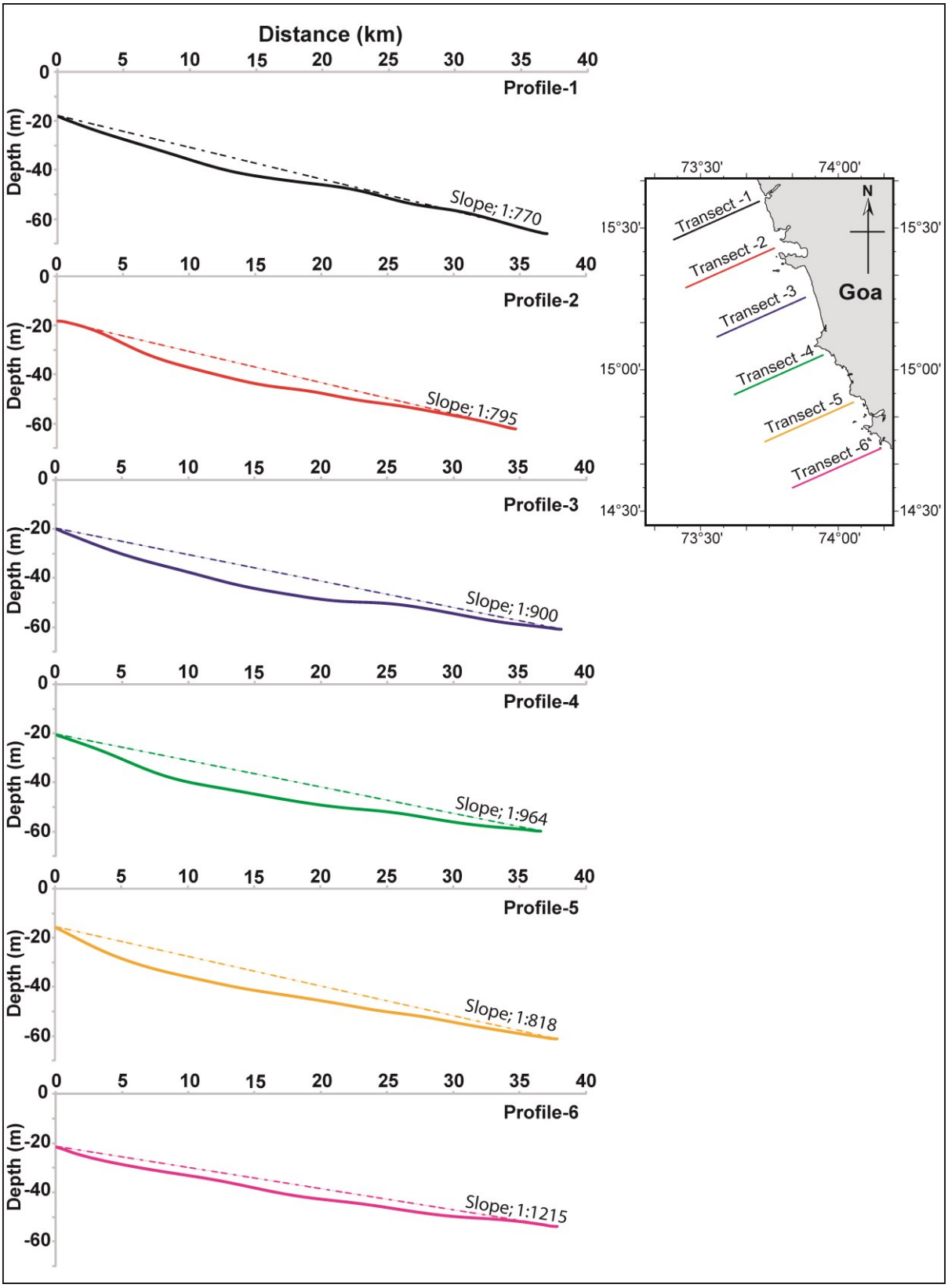

Figure 5.8 Depth profile of the Holocene transgressive surface (representing Holocene-shoreline trajectory) along six transects. These transects are orthogonal to the present coastline and are shown in the inset map. Dotted lines are drawn to indicate approximate gradient of the Holocene transgressive surface.

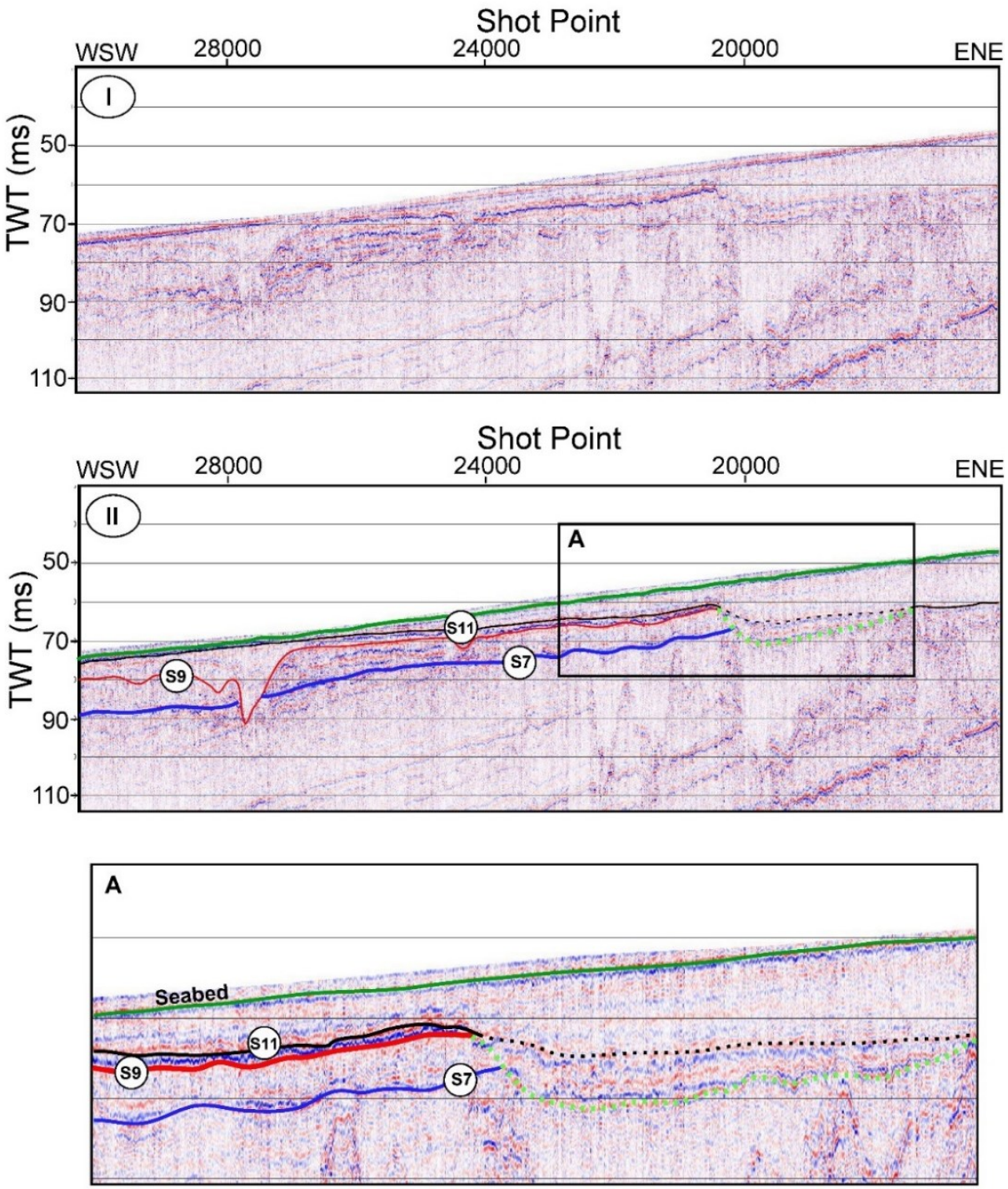

Figure 5.9 HRSS sections along SaSu-51, (I) un-interpreted seismic section, (II) interpreted seismic section, depicting prominent bounding surfaces and truncation of S9, (A) enlarged section of the box in section (II). S9 and S7 are prominent subaerial unconformities of the study area (discussed in chapter 4), S11 is the Holocene transgressive surface. Dotted green line shows reworked subaerial unconformity in tidal environment. Dotted black line indicates effective transgressive surface.

This explains the anomalous concavity of the Holocene_TS along the trackline SaSu-51. A map depicting areal distribution of anomalous truncations of subaerial unconformity S9 is presented

in Figure 5.10. Interestingly, these anomalous truncations are found in the same zone where anomalous sediment thickness (in the central region) is observed. The local deeper basin was formed under the influence of paleo-coastal processes with its conducive gradient attracted progressively more sediment for deposition. Further, the Holocene_TS profiles orthogonal to the coast revealed steeper gradient of the Holocene transgressive surface near the coastline which progressively became gentler seaward (Figs. 5.6 & 5.8). The Holocene sea-level curve of west coast of India (Hashimi et al., 1995) reveals that the sea-level rise took place in stages. A near standstill condition prevailed at ~28 m below the present sea-level (Fig. 5.11). The Holocene_TS at shallower depth was transgressed by the sea after the standstill. The gradient of the Holocene transgressive surface of shallower region explains major sediment (coarser) movement under the effect of gravitational pull (Fig. 5.6). The sediment movement under the effect of gravitational pull is in agreement with higher sediment accumulation zones.

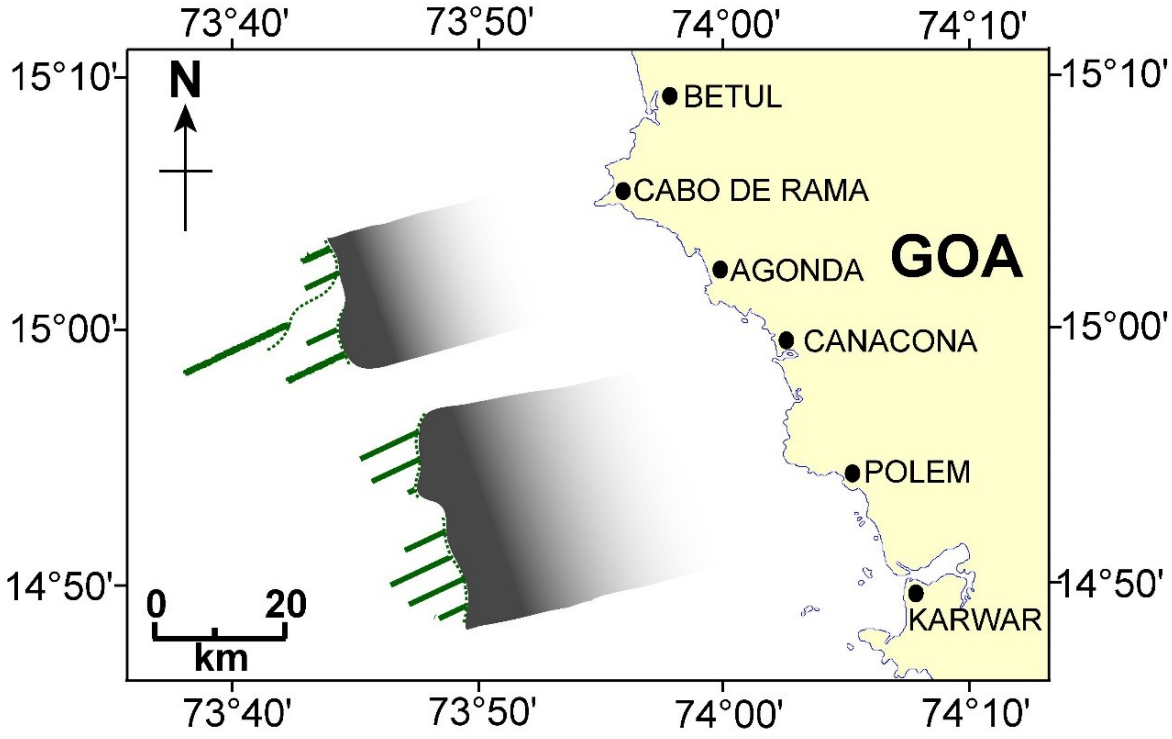

Figure 5.10 Map showing locations, where anomalous truncation of subaerial unconformity (S9) took place. Solid green lines represent remains of the subaerial unconformity. Shaded with gradient (black regions) shows locations where extensive erosion induced by tidal inlet channel took place.

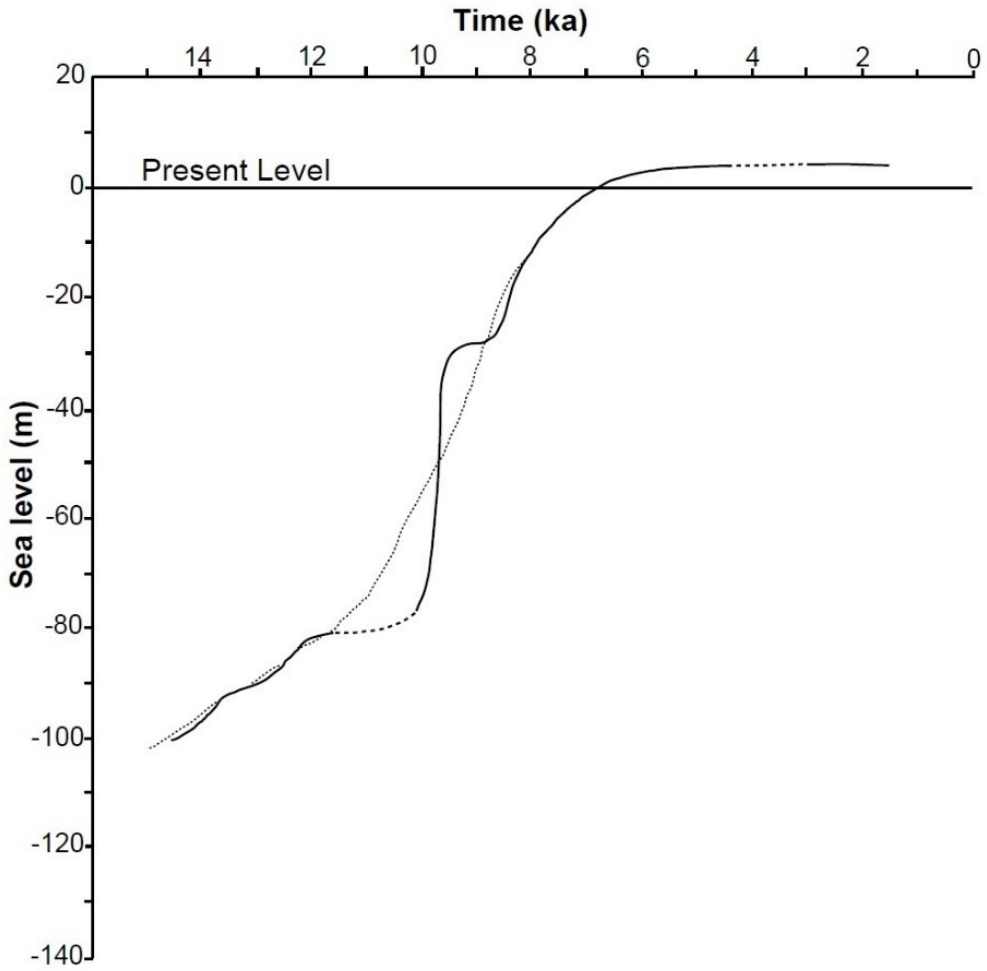

Figure 5.11 The Holocene sea-level curve of west coast of India (Hashimi et al., 1995). Dotted points represent a generalized envelop of the proposed sea-level curve. Dashed line on the broken sea-level curve indicates lack of data.

Fast flowing rivers and channel inlets debouching in the central region (i.e. between off Betul and off Canacona) of the inner continental shelf basin have narrow and smaller estuary (Sal, Talpona and Galgibag) which allows most of the sediment load to reach in the Arabian Sea. On the other hand Mandovi-Zuari and Kali rivers have wider and larger estuary zone which effectively filter coarser sediment in upper zone of the estuary and allow finer sediment only to reach in the Arabian Sea. This in turns explain low sediment thickness near the mouth zone of Mandovi-Zuari and Kali rivers. It is worth to note here that the sea-level has not varied much from last ~7.0 kyr BP and took ~1-1.5 kyr to attain the present sea-level after the standstill at ~28 m (Fig.11). This indicates that location and configuration of river mouth zone have not varied much in the last ~7.0 kyrs. Therefore, most of the mid to late Holocene sediment were deposited in the same conditions.

From above analysis it may be concluded here that present coastline configuration, nearshore morphology along with paleo-fluvial and tidal processes have played important roles in the observed Holocene sediment thickness distribution pattern in the study area. Most of the sediments in the study area were derived from nearby sediment sources (nearby estuary or rocky headland). The analysis of this study undermines the role of longshore coastal currents (outside the surf zone) and distant sediment sources as being important reason of the observed sediment thickness distribution pattern.

5.4 Comparison of sedimentation rates with previous studies

Several researchers (Nambiar et al., 1991, 1995; Manjunatha and Shankar, 1992; Nigam et al., 1995; Pandarinath et al., 1998, 2001; Khare et al., 2008) have reported sedimentation rates at different locations on the inner continental shelf of west coast of India. These sedimentation rates were reported based on the ^{14}C dating of sediment samples. Details of sediment core, sample dates and sedimentation rates are compiled from the earlier studies and presented in Table 5.2. Five sediment cores (GV-3717, SK-27B/8, SK-44/13, SK-148/14, PC-1490) are located off Karwar between 22 and 34 m water depth and three sediment cores (SK-148/13, PC-1459, and PC-1464) are located on the inner continental shelf south of study area (Fig. 5.1). Though, the gridded data for sedimentation rates allows to compare mean sedimentation rates at respective locations of the sediment cores, four out of five sediment cores (GV-3717, SK-27B/8, SK-44/13, SK-148/14) could not be compared as these sediment cores are short i.e. do not reach till the base of Holocene. For example sedimentation rate at core locations GV-3717 (water depth 20 m) was estimated as 2.7 mm/yr for the last 100 years. Though a high sedimentation rate is expected at this location (near Kali river mouth), the information extracted from merely 100 year old sample cannot be generalized for the entire Holocene. Similarly, the deepest dated samples from SK-27B/8, SK-44/13 and SK-148/14 are from 4.5, 4.6 and 5.36 m below the seabed, respectively. Whereas the Holocene sediment base (i.e. Holocene_TS) interpreted from the HRSS data lies at ~10 to 13 m below the seabed at these locations. Simple extrapolation of sedimentation rate to the entire Holocene is unjustifiable due to significant variation in depositional environment during Holocene transgression. The deepest dated sample in core SK-148/14 is found to be 9280±150 yr BP which gives an impression of the Holocene base at 5.36 m from the seabed. High resolution shallow

Table 5.2 Details of sediment samples and sedimentation rates (around the study area) published by various researchers.

Sl. no.	Area	Core ID.	Location (water depth)	Depth in the core	Dating technique & (material used)	Age (yr BP)	Sedimentation rate (mm/yr)	Reference
1	Karwar	GV 3713	14.880° N; 73.965°E (20 m)	26 cm	Excess ^{210}Pb (sediment)	100	2.6	Nigam and Nair, 1989; Nigam and Khare, 1995
2	Karwar	SK-148/14	14.84° N; 74.00° E (22 m)	2.58-2.59 m	^{14}C (o.m.)*	4190 ± 110 (Calibrated)	0.62 (4190 yr BP to present)	Pandarinath et al., 2001
3	Karwar	SK-148/14	14.84° N; 74.00° E (22 m)	5.35-5.36 m	^{14}C (c.w./p.)**	9280 ± 150 (Calibrated)	0.54 (9280-4.190 yr BP)	Pandarinath et al., 2001
4	Karwar	SK-27B/8	14.83° N; 73.99° E (22 m)	1.30-1.35 m	^{14}C (o.m.)*	2220 ± 40 (Calibrated)	0.60 (2220 yr BP to present)	Caratini et al., 1994
5	Karwar	SK-27B/8	14.83° N; 73.99° E (22 m)	1.40-1.45 m	^{14}C (o.m.)*	2020 ± 40 (Calibrated)	0.70 (2020 yr BP to present)	Caratini et al., 1994
6	Karwar	SK-27B/8	14.83° N; 73.99° E (22 m)	2.25-2.30 m	AMS ^{14}C (Shell)	2220 ± 70 (Calibrated)	1.02 (2220 yr BP to present)	Caratini et al., 1994
7	Karwar	SK-27B/8	14.83° N; 73.99° E (22 m)	3.00-3.05 m	^{14}C (o.m.)*	3510 ± 60 (Calibrated)	0.86 (3510 yr BP to present)	Caratini et al., 1994
8	Karwar	SK-27B/8	14.83° N; 73.99° E (22 m)	4.45-4.50 m	^{14}C (o.m.)*	4325 ± 65 (Calibrated)	1.03 (4325 yr BP to present)	Caratini et al., 1994

9	Karwar	SK-44/13	14.74° N; 74.05° E (25 m)	3.00-3.04 m	^{14}C (o.m.)*	3780 ± 210 (Calibrated)	0.80 (3780 yr BP to present)	Caratini et al., 1994
10	Karwar	SK-44/13	14.74° N; 74.05° E (25 m)	4.50-4.55 m	^{14}C (o.m.)*	6370 ± 170 (Calibrated)	0.58 (6370-3780 yr BP)	Caratini et al., 1994
11	Karwar	SK-44/13	14.74° N; 74.05° E (25 m)	4.55-4.60 m	^{14}C (o.m.)*	6200 ± 90 (Calibrated)	0.73 (6200 yr BP to present)	Caratini et al., 1994
12	Karwar	PC-1490	14.67° N; 73.99° E (33.7 m)	5.78-5.80 m	^{14}C (c.w./p.)**	8620 ± 300 (Uncal.)	0.67 (8620 yr BP to present)	Nambiar et al., 1991
13	Karwar	PC-1459	14.6° N; 74.23° E (17.7 m)	3.02-3.10 m	^{14}C (Shell)	3410 ± 90 (Uncal.)	0.89 (3410 yr BP to present)	Nambiar et al., 1991
14	Karwar	PC-1464	14.43° N; 74.21° E (25 m)	4.20-4.38 m	^{14}C (c.w./p.)**	9630 ± 120 (Uncal.)	0.44 (9630 yr BP to present)	Nambiar et al., 1991
16	Honnavar	SK-148/13	14.40° N; 74.00° E (50 m)	1.67-1.69 m	^{14}C (c.w./p.)**	9790 ± 120 (Calibrated)	0.17 (9790 yr BP to present)	Pandarinath et al., 2001
17	Honnavar	SK-148/13	14.40° N; 74.00° E (50 m)	1.99-2.00 m	^{14}C (c.w./p.)**	9990 ± 120 (Calibrated)	1.6 (9990-9790 yr BP)	Pandarinath et al., 2001
18	Honnavar	SK-148/13	14.40° N; 74.00° E (50 m)	2.20-2.22 m	^{14}C (c.w./p.)**	10010 ± 120 (Calibrated)	11.0 (10010-9990 yr BP)	Pandarinath et al., 2001
19	Honnavar	SK-148/13	14.40° N; 74.00° E (50 m)	2.72-2.74 m	^{14}C (o.m.s.)***	10760 ± 130 (Calibrated)	0.69 (10760-10010 yr BP)	Pandarinath et al., 2001
*Organic Material **Carbonized woods and peats ***Sediment enriched with black fine organic material								

seismic sections near the core location assertively reveal ~11 m sediment thickness (Fig. 12). Further, samples in cores SK-27B/8 and SK-44/13 have been dated as 4325±65 yr BP and 6200±90 yr BP, respectively. It may be noted that all the three cores (SK-148/14, SK-27B/8 and SK-44/13) are located between 22 and 25 m water depth and have recovered core length ranging between 4.5 and 5.36 m, signifying anomalous variation in dated age. Considering the results of the present study and sample dates from cores SK148/14, SK-27B/8 and SK-44/13, it is opined that the dated carbonized woods might have not formed in-situ condition and hence the dated age are not representing age of the corresponding sedimentary layer. It is surmised that the carbonized woods might have been formed in the flood plains of the Kali river and subsequently drifted to core location during the sea-level transgression.

Sediment core PC-1490 which is located off Karwar at ~34 m water depth (Fig. 5.1) has a core length of 5.80 m (Table 5.1). The carbonized woods and peats from sub sample at 5.78-5.80 m core depth were dated and their uncalibrated age was estimated to be 8620±300 year BP (Pandarinath et al., 2001). The uncalibrated age was calibrated in this study using the Calib 7.1 computer program based on IntCal13 data. The calibrated age is found to be 9675±300 yr BP. As per HRSS data, the Holocene base (i.e. Holocene_TS) is found to be ~5-6 m below the seabed at the same water depth. Projection of core PC-1490 on the nearest HRSS section (Fig. 5.13) reveals that the core penetrated the entire Holocene sedimentary strata and landed at the base of seismically interpreted Holocene layer. Further, a comparison was also made between mean sedimentation rates obtained from dated sediment sample and gridded data of the present study. The mean sedimentation rate obtained from the calibrated age of dated samples comes out to be 0.59 mm/yr which is in agreement with the mean sedimentation rate of 0.54 mm/yr obtained from the present study. It revealed that the Holocene base is at comparable depth.

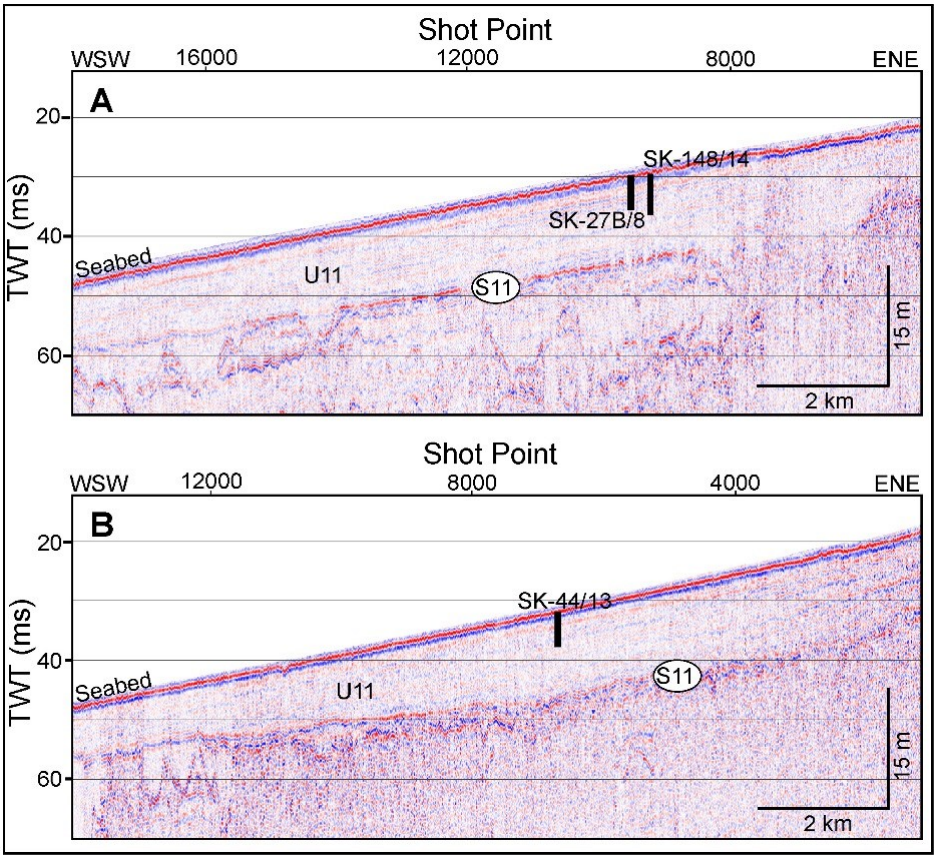

Figure 5.12 Sediment cores projected on nearby seismic sections. Cores SK-27B/8 and SK-148/14 are projected on part of seismic section GK-21. Whereas, core SK-44/13 is projected on part of seismic section GK-28. S11 and U11 indicate the Holocene transgressive surface and sedimentary unit, respectively.

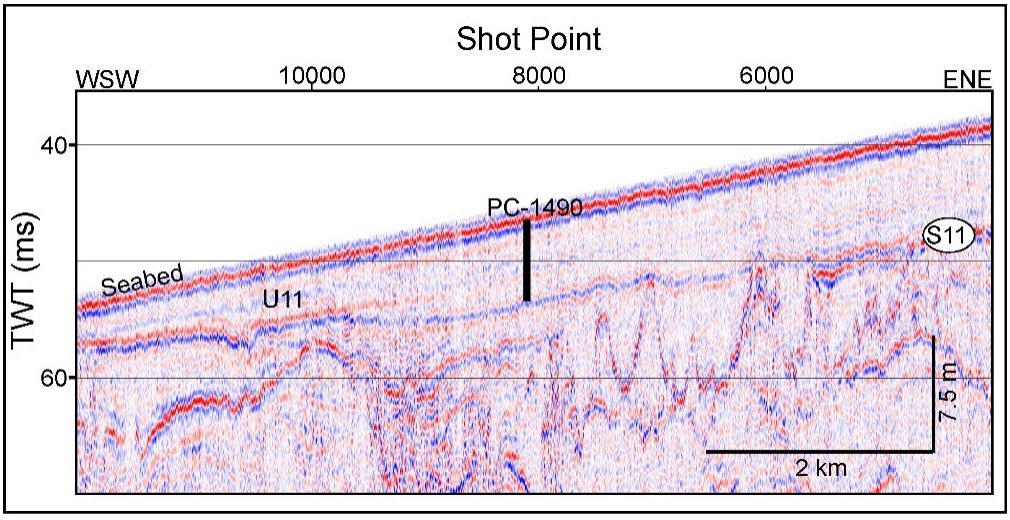

Figure 5.13 Sediment core projected on nearby seismic sections. Core PC-1490 is projected on part of seismic section GK-30. S11 and U11 indicate the Holocene transgressive surface and sedimentary unit, respectively.

Sediments cores GC-01, GC-02 and GC-03 were acquired from the study area with an aim to verify the Holocene base and sedimentation rates obtained from the gridded data generated from

Holocene_TS and sea-level curve. Unfortunately the cores did not penetrate the sedimentary strata and reach up to the Holocene base. Therefore, comparison of sedimentation rates cannot be made as envisaged. However SK-148/13, which is located at ~50 m water depth and slightly south of off Ankola, revealed mean sedimentation rate of 0.2 mm/yr during the Holocene (Table. 5.1). The sedimentation rate is again in good agreement with the rates determined (0.2 mm/yr) in the present study.

5.5 Conclusions

Sequence stratigraphic analysis of the HRSS data allowed to map the Holocene sediment thickness along the tracklines, which further facilitated to generate gridded data for the Holocene sediment thickness, Holocene_TS and Holocene sedimentation rates. Generated gridded data of sediment thickness revealed that a total of ~32.09 km^3 volume of sediment were deposited on the inner continental shelf between off Chapora and off Ankola, central west coast of India. The Holocene sediment thickness varies from 0.78 to 15.67 m. The thickness increases from coast to ~20 m water depth and thereafter decreases to ~2 m at 50 m water depth. Sediment thickness map revealed two conjoint anomalously high sedimentation zones which are located between offshore Betul and Canacona. Along the coast up to 40 m water depth, the thickness initially increases from offshore Chapora to offshore Cancona and thereafter decreases sharply southward. Beyond 45 m water depth, it does not show any significant trend. Analysis of the Holocene_TS and sediment thickness distribution pattern carried out in this study rejects roles of distant terrigenous sediment sources and longshore currents for the observed Holocene sediment deposition on the inner continental shelf of the study area. Further, it establishes hinterland sediment source, present coastline configuration, nearshore geomorphology along with paleo-fluvial and tidal processes as the key players for the observed sediment thickness distribution pattern. The gridded data of sediment thickness and sedimentation rate provide a clearer picture of the sedimentation pattern between off Chapora and off Ankola. Comparison of mean Holocene sedimentation rates of this study with previous sedimentological studies revealed that the sedimentation rates estimated from the gridded data of the present study are reasonably very good. Distribution pattern of the Holocene sedimentation rates and the Holocene sediment thickness on the inner continental shelf between off Chapora and off Ankola are useful outcomes of this study, which can be used for future sedimentological and climatological studies.

Chapter 6
Buried Channel Morphology

6.1 Introduction

River channel systems, a result of interaction between water and the landscape, are very dynamic geomorphologic features which are constantly striving for the equilibrium. Base level plays a key role for equilibrium between water flow and sediment transport. Changes in the hydrological regime and base level disrupt equilibrium which becomes evident from changes in channel morphology. Remnant of once active river or stream is known as paleo river channel and if it is buried under sediments, it is called as buried river channel. Buried channels, preserved as morphological sedimentary entities, provide ample track records of changes in the hydrological regime.

Buried river channel system, incised during low stand of sea-level, is an important geomorphic feature on continental shelves as it provides accommodation for low stand and early transgressive sedimentation in shelf environments. They also protect entrained sediments from removal by subsequent transgressive erosion. Therefore remnants of such preserved valley-fill succession are key elements for inferring processes that create, modify and preserve continental shelf sequence stratigraphy. Study of buried incised channel systems can provide a broader understanding of variables affecting deposition, erosion and preservation of shelf strata. Seismic sequence stratigraphic analyses of sedimentary architecture (discussed in Chapter 4) of the study area revealed that the inner continental shelf of Goa contains buried river channel incision signatures corresponding to more than three cycles of fourth order sea-level fluctuations. Studies of such polycyclic channel incision system alongwith sequence stratigraphic analyses are capable enough to provide better and longer history of continental shelf evolution and offer clues to compare hydrological regime of different glacial periods during their formative stage.

Mandovi and Zuari are the two largest rivers of Goa (see section 2.7 in chapter 2). Considering the present geomorphological and hydrological properties of Mandovi-Zuari and other smaller rivers of Goa, it is expected that the ancestral rivers of Mandovi and Zuari might have extensively incised the inner continental shelf of the study area in the geological past. Therefore, delineation of buried channels of these rivers may offer better constraints for investigation of the role of channel incision in the evolutionary history of the inner continental shelf of Goa. Successful delineation of buried geomorphological properties of a channel system requires closely spaced High Resolution Shallow Seismic (HRSS) tracklines. In this study, HRSS data along tracklines spaced at one nautical mile are collected to map buried river system carved by ancestral rivers of Mandovi and Zuari. The tracklines of high resolution shallow seismic data utilized for the above mentioned purpose are shown in Figure 6.1.

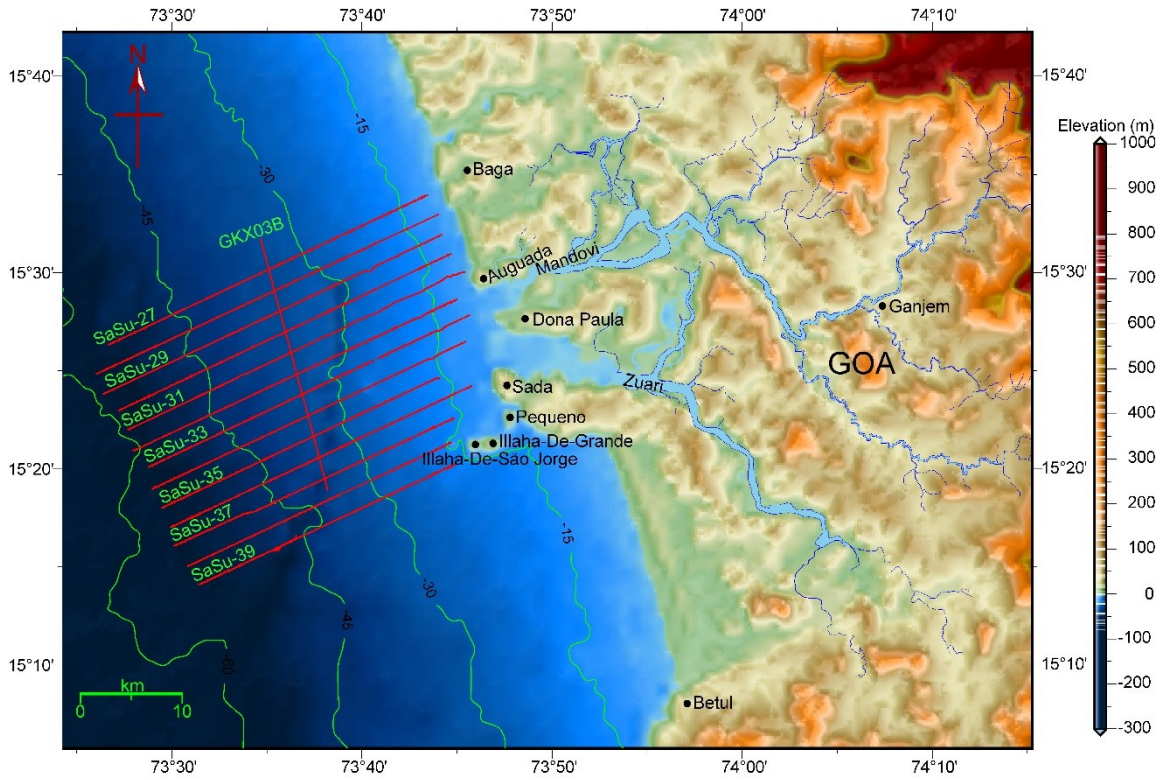

Figure 6.1 Location of high resolution shallow seismic tracklines (solid red lines), superimposed on bathymetry, on the inner continental shelf of Goa, central west coast of India. Solid green curves are isobaths and annotated values on it refer to water depth in meter. Prominent features and present river drainage pattern are shown on the relief map of adjacent land area. The relief map was generated using grid data of GEBCO (GEBCO_2014 version 20150318, Weatherall et al. 2015).

Present chapter is based on the geomorphological analysis of observed channel incision signatures in the study area. It also describes detailed geomorphologic analysis of buried channel incision signatures and offers evolutionary history of buried channels. Further it presents inferences drawn on the paleo-environmental variations based on the comparison of hydrologic properties of channel incisions of different glacial periods. It will be shown later in this chapter that the interpreted channel incisions are carved by the ancestral Mandovi and Zuari rivers.

6.2 Morphologic analysis of observed incision

6.2.1 Cross-sectional morphology

Morphologic features, such as channel dimension, shape and aspect ratio of different parts of a river system, provide useful information which can be used to interpret channel characteristics and its evolutionary history. Incision dimension is useful to differentiate between main and tributary channels, whereas, aspect ratio (width to depth ratio) of incisions is important to differentiate between tidal and fluvial environment at the mature stage of incisions (Leopold et al., 1964; Rosgen, 1994; Nordfjord et al., 2005). V-shaped incision takes place due to higher energy condition and are generally found at upper stage (far above the base level) of a river (Rosgen, 1994) or at lower stage in case of sudden fall in the base level (Begin et al., 1981; Schumm, 1993). U-shaped channel cross-sections are mostly found in lower-middle to lower stage of a river channel due to the reduced incision potential (Leopold, 1964; Rosgen, 1994). Further, V-shaped incision gets modified to U-shaped incision due to periodic incision and deposition in due course of time. Cross section of a straight river channel normally has symmetrical flanks (cc' in Fig. 6.2), whereas, the same at meandering part of river has asymmetrical flanks (bb' and dd' in Fig 6.2). Similarly, erosion and deposition in a channel is dependent on the shear stress generated by the flow profile of a river (Leopold, 1964; Paola et al., 1992; Iwuoha et al., 2016). Shape of the cross section can provide a clue about energy condition of channel during its formative stage whereas, infill reflections can indicate about energy condition during aggradation of a river. Therefore, shapes of a channel and infill reflection characteristics of each observed incision can be useful to interpret energy condition, qualitative lifespan, and channel migration.

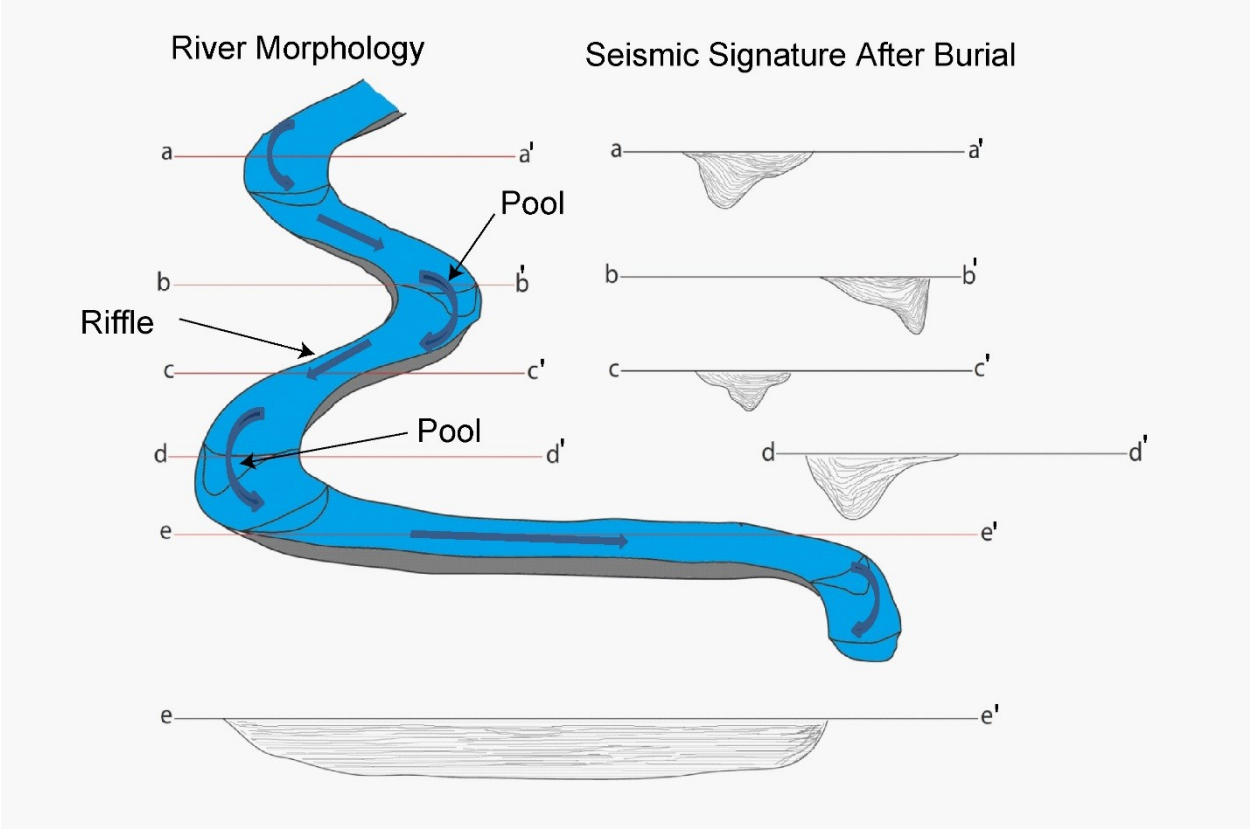

Figure 6.2 Schematic diagram showing channel geometry of different features of a buried meandering channel and its expected signature in seismic section with respect to orientation of seismic trackline. The degree of alignment or perpendicularity of the incision with respect to the trackline can be inferred from infill signature pattern. Incisions having flow direction across the seismic tracklines will show infill signature following the bed geometry, whereas incisions having flow direction along the tracklines will show infill signature parallel to velocity profile. Tracklines a-a', b-b', c-c' and d-d' cross the river channel orthogonally, whereas, e-e' traverses along the river channel.

In light of the above, incision signatures observed in the present study have been analyzed, and detailed analyses are presented for representative incision signatures of the study area (Fig. 6.3). The incision signatures A1, A2, A3 and A4 in Figure 6.3(I) are observed at ~50 m water depth and are buried ~15 m below seabed. Incision A1 is ~900 m wide with maximum entrenchment of ~37 m (mean depth ~30 m). It is U-shaped with almost symmetrical flanks and nearly transparent infill signature. These observations suggest that the incision might have started (i) when the sea-level was at least ~65 m (50 m water depth + 15 m overburden) below the present sea surface, and

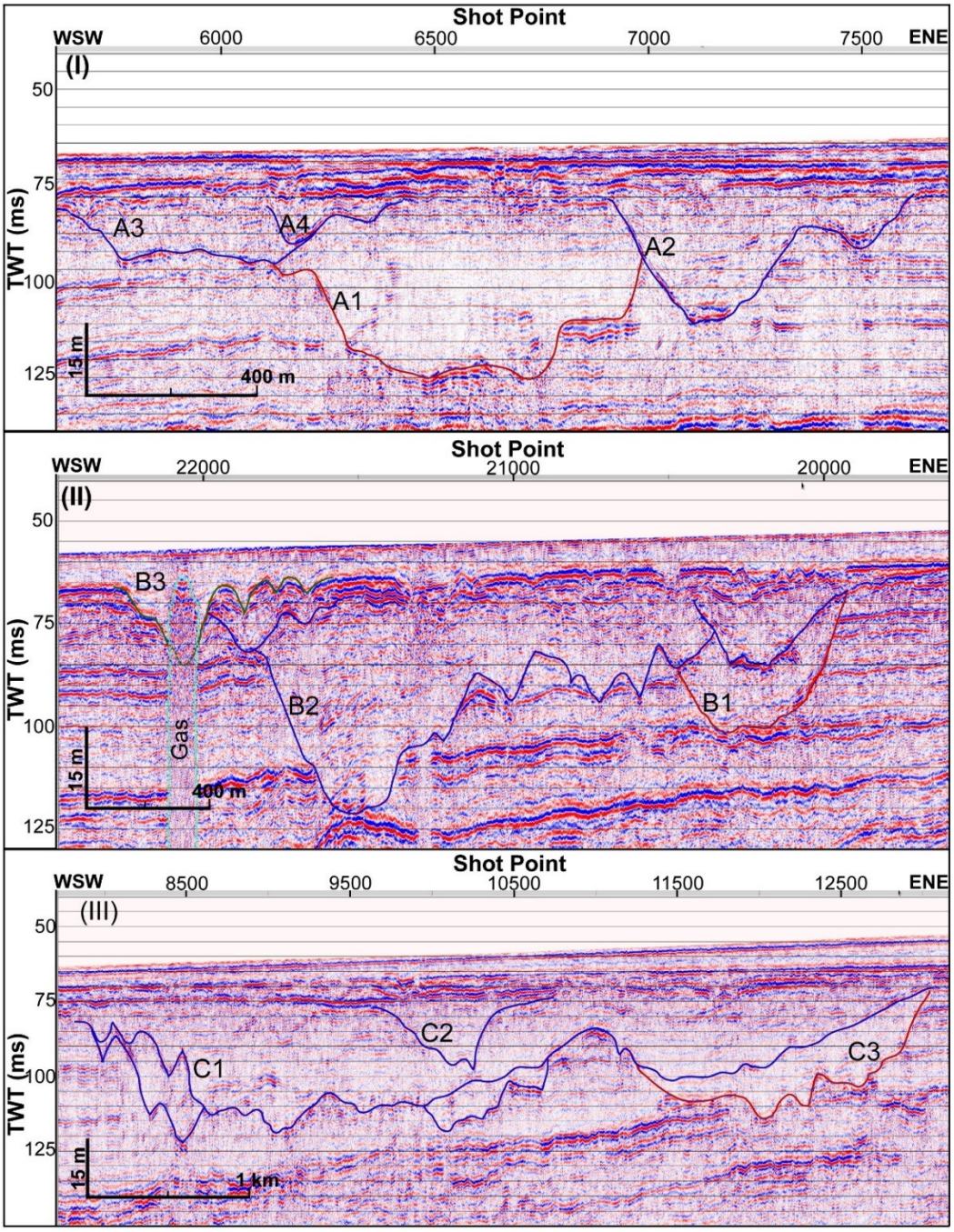

Figure 6.3 Part of interpreted seismic section along trackline **(I)** SaSu-36, showing channel incision signature during 320-125 kyr BP (Phase 2). A1, A2, A3 and A4 represent channel incisions indicating that seismic tracklines traversed orthogonal to river channel at those locations. **(II)** SaSu-35, showing channel incision signature during 320-125 kyr BP (Phase 2) and 110-10 kyr BP (Phase 3). B1 & B2 represent Phase 2 incisions, whereas, B3 represents Phase 3 incisions. **(III)** SaSu-36, section showing signature of Phase 2 channel incision, indicating that seismic trackline traversed along flow direction of river channel. Details of Phase 1, 2, 3 and corresponding time duration are presented in Section 6.3.

(ii) in the estuarine environment itself, which rapidly migrated to fluvial environment. Also, it attained its mature state (i.e. maximum entrenchment level) when the sea-level was at least 102 m (65+37) below the present sea surface. U-shape and nearly transparent infill signatures

suggest that river was at its mature condition for longer time and subsequently buried due to sea-level rise in low energy condition. Whereas, V-shape of incision A2 suggests that it was active for shorter period than that of incision A1. Comparison of shapes and infill signatures of A1 and A2 indicate that both the incisions got buried in response to sea-level rise, under different energy regimes. Incision A2 got buried under higher energy condition than that of incision A1. Incision A3 is boxcar- shaped and has almost symmetrical flanks. In incision A3, infill signature is chaotic and superimposed by diffraction pattern in the upper part (Fig. 6.3(I)). Incision shape and chaotic infill signature indicate that the incision A3 might have taken place as a result of few extreme flood events and got buried in similar energy condition, probably due to lateral adjustment (avulsion) of the river channel. Further, diffraction pattern in the upper infill indicates that the channel was capable of carrying large grain size sediment. Avulsion of rivers due to extreme flood event have been reported around the world and well-studied, e.g. avulsion in Koshi river in India (Sinha et al., 2014), Thomson river in Australia and Yellow river in China (Zheng et al., 2017). The cross section geometry of avulsion channel has higher width to depth ratio than the older (parent) channel (Brizga and Finlayson, 1990). For example, avulsion channel of Koshi River was generated during extreme flood event in August 2008. It is more than 100 m wide and ~1 to 2 m deep (higher aspect ratio) box-car shaped channel in the lower stage (Sinha et al., 2014).

Higher rate of sedimentation than erosion results in aggradation of river bed. Further, for higher sedimentation rate, it is necessary that the flow discharge rate must be equal or below a critical discharge rate (Miller et al., 1977; Begin et al., 1981; Ribberrink and van der Sande, 1985; Flemings and Jordan, 1989; Paola et al., 1992; Paola, 2000; Iwuoha et al., 2016). Therefore, in an exposed marine alluvial plain, the river bed is expected to be smooth, and turbulent flow is least expected during the aggradation. In view of the above, it is considered that burial of the observed channels took place during the laminar flow in low energy condition. In this condition, sedimentation across flow direction is much affected by river bed geometry than flow velocity and follows the bed geometry. Whereas, sedimentation along flow direction is much affected by mean flow velocity and are parallel to the direction of flow. Therefore, infill seismic signature across and along the buried channel should show parallelism to the river bed geometry and flow direction respectively. In this study, incision dimension, shape and infill reflection configuration are used to interpret degree of alignment of river flow direction with respect to seismic trackline. For example, in case of incisions A1, A2, A3 and A4 (Fig. 6.3(I)) infill signature follows the bed geometry. Therefore, it can be interpreted that flow direction of buried

channel at this location was more or less orthogonal to the seismic trackline. In case of incision C1, which is ~5000 m wide and ~36-38 m deep, infill signature is nearly transparent with an indication of parallel stratification (Fig. 6.3(III)). It can be interpreted that the seismic track line traversed the buried river channel along the flow direction of the channel on the basis of infill reflection pattern and exceptionally larger width of the incision (Figs 6.2 and 6.3(III)). Deeper entrenchments at both ends suggest sinuous thalweg. Incisions showing seismic signatures of a channel section flowing orthogonal to seismic tracklines are further examined for symmetricity of flanks. If the incision is asymmetrical, it can be interpreted that the water was flowing on a curved path during meandering of river. Steeper flank represents cut bank, while gentle flank represents point bar or slip off slope bank. Asymmetric incisions, having cross-flow characteristics and migratory behavior, are also identified. For example, incision B2 is V-shaped with asymmetrical flanks (Figs. 6.2 and 6.3(II)). Infill reflection signatures are transparent to low amplitude and follow river bed morphology. V-shape and infill signature suggest that seismic trackline traversed the incised river perpendicular to flow direction. The asymmetrical shape suggests that river channel was flowing on a curved path (meander) and have migrated with time. Both lateral as well as vertical migration signatures can be observed in the seismic section (Fig. 6.3(II)). The direction of lateral migration is from ENE to WSW i.e. from shallower to the deeper region of exposed shelf. The incision became deeper with lateral migration. It is interpreted that deepest part of the incision was a pool of the sinuous river channel. The river course was meandering with center of curvature towards shallower region of exposed shelf. In response to the higher rate of sea-level lowering and varied hydrodynamic condition, the channel has adjusted its course towards deeper region of the exposed shelf with increasing entrenchment depth.

After cross-sectional geomorphic analyses, channel incisions of different age of formation are differentiated based on the cross-cutting relation of observed channel incisions with each other and subaerial unconformities. For example, cross cutting relationship of incisions A1, A2 and A3 reveals that the incision A1 is older than incisions A2 and A3. Further, a signature of marine deposition can be seen just above the incision A1, but it is absent in incision A2 (Fig. 6.3(I)). This suggests that the incision A2 took place during subsequent sea-level lowering after complete burial of the incision A1. Therefore, it can be interpreted that incision A1 and incisions A2, A3 were formed in two different glacial periods. This information is later used to find out the age of channel initiation and its complete burial history using the methodology

described in Section 4.2 of Chapter 4. Such a differentiation is required to avoid intermixing of channels of different glacial period while interpolating their plan view morphology.

6.2.2 Reconstruction of plan view morphology

In order to reconstruct plan view morphology, inferences on flow direction and hydrologic parameters of each incision signature are plotted according to their period of formation on separate trackline maps. Before starting interpolation of plan view morphology of the river channel, dominant valley slope direction is determined. To decide dominant valley slope direction, seismic sections are analyzed to find out general slope direction of seismic reflectors and incision signature for flow direction. The analyses reveal that seismic reflectors, in general, dip seaward in WSW direction and more than 80% observed incisions were traversed by seismic tracklines more or less orthogonally.

Considering spatial distribution of the above incisions and general slope direction of seismic reflectors, it has been concluded that the dominant slope of the paleo shelf was more southerly as compared to WSW direction. In view of the above, it has been assumed dominant valley slope approximately in SW direction. Incision signatures of same glacial period of formation have been delineated on the trackline map with their approximate flow orientation. Taking care of other inferred correlative constraints of incisions, plan view morphologies have been interpolated. An illustration of interpolation of plan view morphology is presented in Figure 6.4. Though river channels are very active hydrologic features and very responsive to any of its governing physical parameter, river channels which had sustained for the longest time have been identified. Further, Rosgen's river channel classification system (Rosgen, 1994), which is based on the hydraulic parameter of rivers in equilibrium, may not be true for buried river channel system, therefore, computed hydraulic parameters have been compared to infer drainage type of buried channel system.

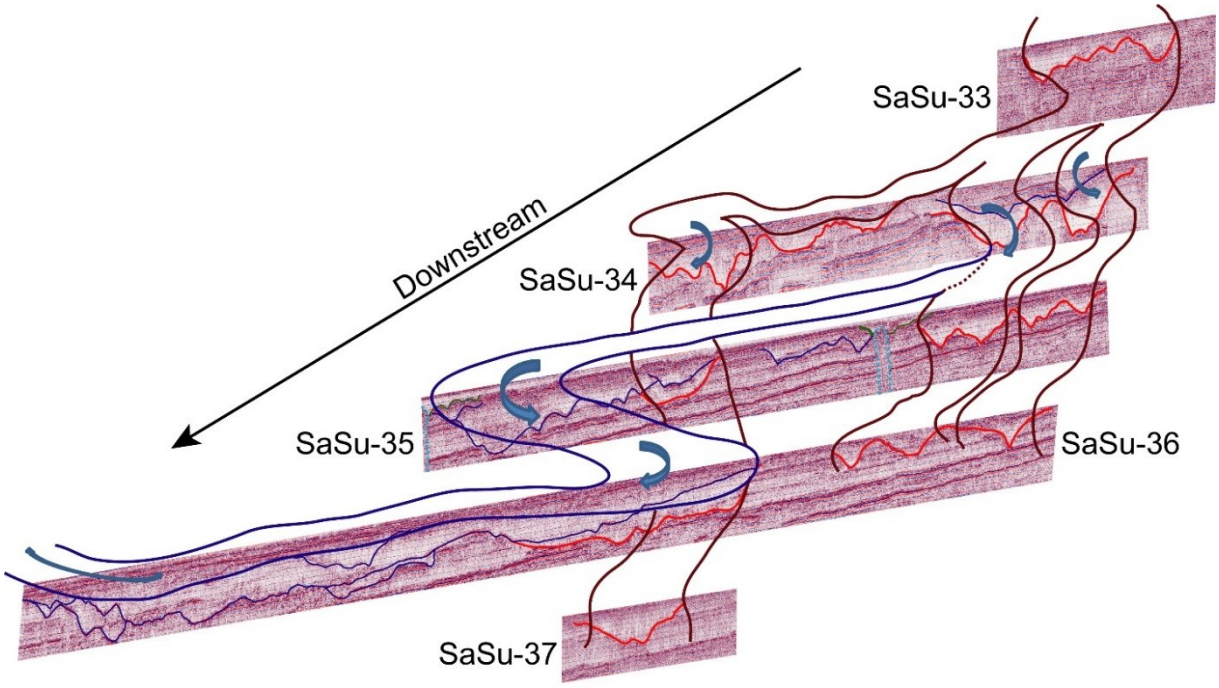

Figure 6.4 Fence diagram illustrating downstream trends of a portion of Phase-2 channel system. Blue arrows indicate flow direction. Thick blue and brown color curves represent channel boundaries of younger and older stages of Phase-2 channel system, respectively. Details of Phase-2 and its time duration are presented in Section 6.3.

6.3. Timing of formation and burial of river channels

On the basis of three distinctly identified subaerial unconformities S9, S7 and S6 (discussed in Chapter 4), cross-cutting relations and differences in morphological features, observed channel incisions are divided grossly into three phases of incision viz. Phase-1, Phase-2, and Phase-3.

Phase-3 incisions are the youngest incisions in all the recognized phases and are buried just below the Holocene_TS (S11). These signatures are reworked by wave activity during the Holocene transgression. "S9" is the stratal surface, which contains Phase-3 incisions. The nearshore region of the study area was exposed to different aerial processes for varying time-scale during the last low stand half cycle of sea-level (Fig. 6.5). Using the methodology described in Section 4.2 of Chapter 4, it is interpreted that Phase-3 incisions started at ~115 kyr BP with lowering of sea-level and later got completely buried due to rapid sea-level rise after the LGM.

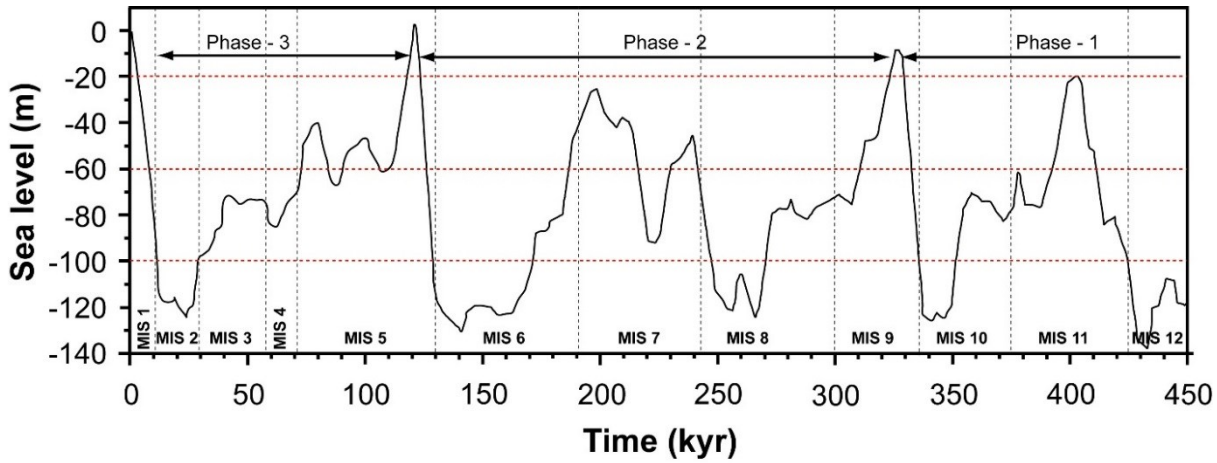

Figure 6.5. Sea-level curve of the last 450 kyr (modified by Rehak et al., 2010 from Siddal et al., 2003). Marine Isotopic Stages (MIS) have been added following Lisiecki and Raymo (2005).

Phase-2 incisions are older than the Phase-3 incisions. Seismic units S7 and S6 are the stratal surfaces at which Phase-2 incisions took place. These incisions contain clear signatures corresponding to two major half cycle of low stand (Fig. 6.3(I)). After integrating this information with sea-level curve (discussed in Chapter 4), it has been established that Phase-2 incision took place in stages. Older incisions of Phase-2 initiated in response to rapid sea-level fall at ~320 kyr BP and got matured during low stand corresponding to Marine Isotopic Stages (MIS) 8, which got partially buried in subsequent sea-level rise during ~250-215 kyr BP (Fig. 6.5). It may be mentioned here that the shallower region of the study area was not completely submerged between ~210 kyr and ~195 kyr BP. Therefore, subaerial processes which were active since ~320 kyr BP in the shallower region remained active during 210-195 kyr BP also. Younger incision of Phase-2 initiated at ~190 kyr BP in response to rapid sea-level fall during the next half cycle of low stand sea-level and got matured during the low stand corresponding to MIS 6, which got completely buried due to sea-level rise after penultimate glacial maximum. Therefore, it is concluded here that Phase-2 incisions started at ~320 kyr BP and got completely buried at ~125 kyr BP. The youngest incision of this phase corresponds to penultimate glacial period which started at ~190 kyr BP (MIS 6). Oldest incision started at ~320 kyr BP (during MIS 9) prior to penultimate glacial period.

Phase-1 incisions are the oldest incision observed on the inner continental shelf. As Phase-1 incisions are limited mostly in the submerged rocky region of the study area and sea-level had the least control over the morphological signature, it has been interpreted that Phase-1 incisions are much older than ~330 kyr BP.

6.4 Morphology of channel incisions

6.4.1 Morphology of Phase-1 incisions

Interpolated plan view morphology of the Phase-1 channel is similar to a straight river channel (Fig. 6.6). Seismic signatures of Phase-1 incisions reveal that river was flowing through natural depressions through rocky terrain on exposed the then continental shelf. Paleo-physiographical and structural features mostly controlled the morphology of the Phase-1 channel incisions. Two upstream sections of this channel can be linked with present day Mandovi and Zuari Rivers. Initially, these two sections were flowing independently and joined at 'O' (Fig. 6.6). It flowed on a sediment base like a straight river channel for ~15 km towards SW direction beyond point "O". It may be noted that seismic signatures of Phase-1 incisions are observed between coast and ~40 m water depths. The incision signatures of this phase suddenly disappear beyond ~40 m water depth, probably due to higher dominant slope of exposed the then continental shelf which restricted their longitudinal as well as lateral extent.

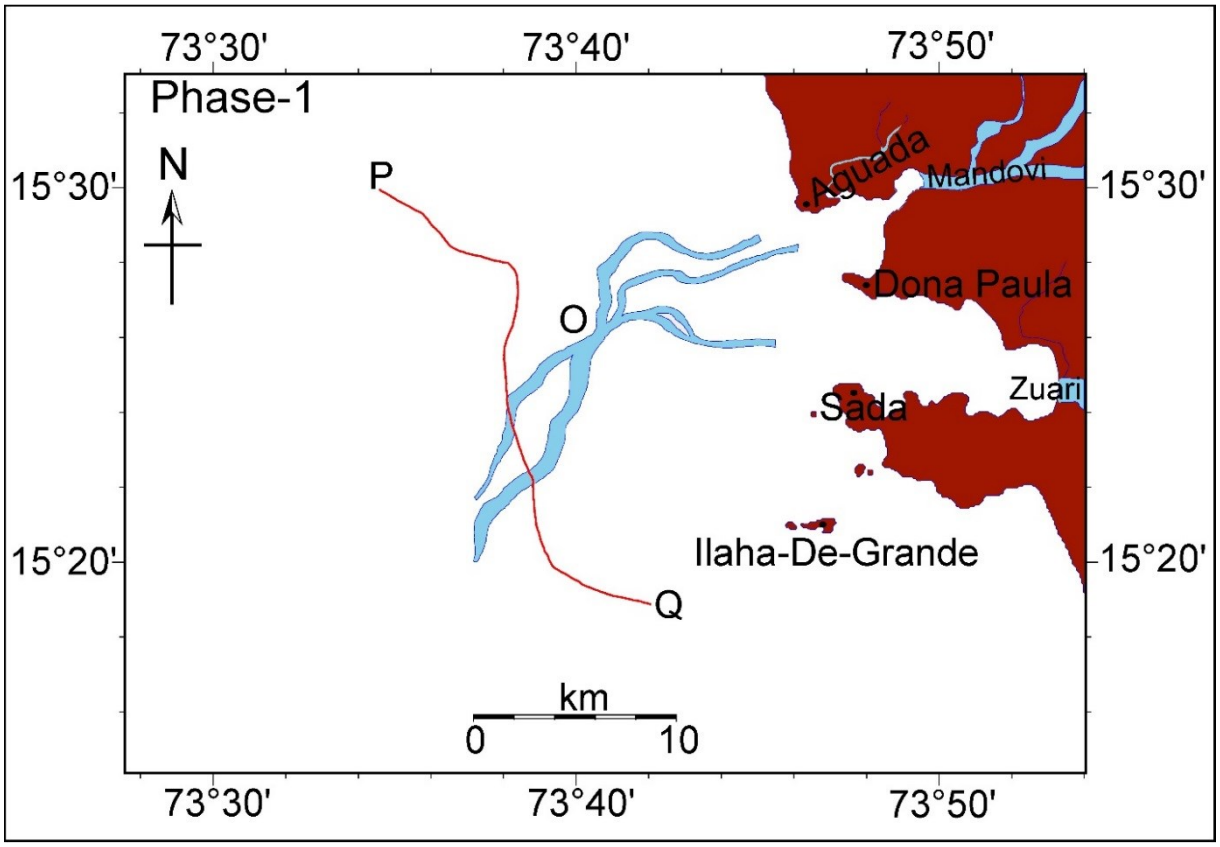

Figure 6.6 Interpolated plan view morphology of Phase-1 (>330 kyr BP) channel incision. O is the confluence point of ancestral Mandovi and Zuari rivers. PQ is the boundary line between nearshore submerged rocky region and marine sediment assemblage in offshore region.

6.4.2 Morphology of Phase-2 incisions

Phase-2 incision signatures, younger than Phase-1, are observed between coast and ~55 m water depth (Fig. 6.7). Due to the deposition of sediment in different sea cycles, a wider surface with decreased slope became available for the Phase-2 incisions, resulting an increase in areal extent of the river channel. Phase-2 incisions are ~200 m to ~1000 m wide with maximum entrenchment ranging from ~10 m to ~35 m, whereas mean depth varied between 5 m and 21 m. Cross-sectional morphology of the Phase-2 incisions revealed signatures of channel migration related to base level fluctuation as well as climatic variation. For example, shape and infill signature of incision B2 (Fig. 6.3(II)) suggest that channel migration took place in response to variation in both sea-level and hydrologic (precipitation) conditions. Whereas, transparent infill reflectors of

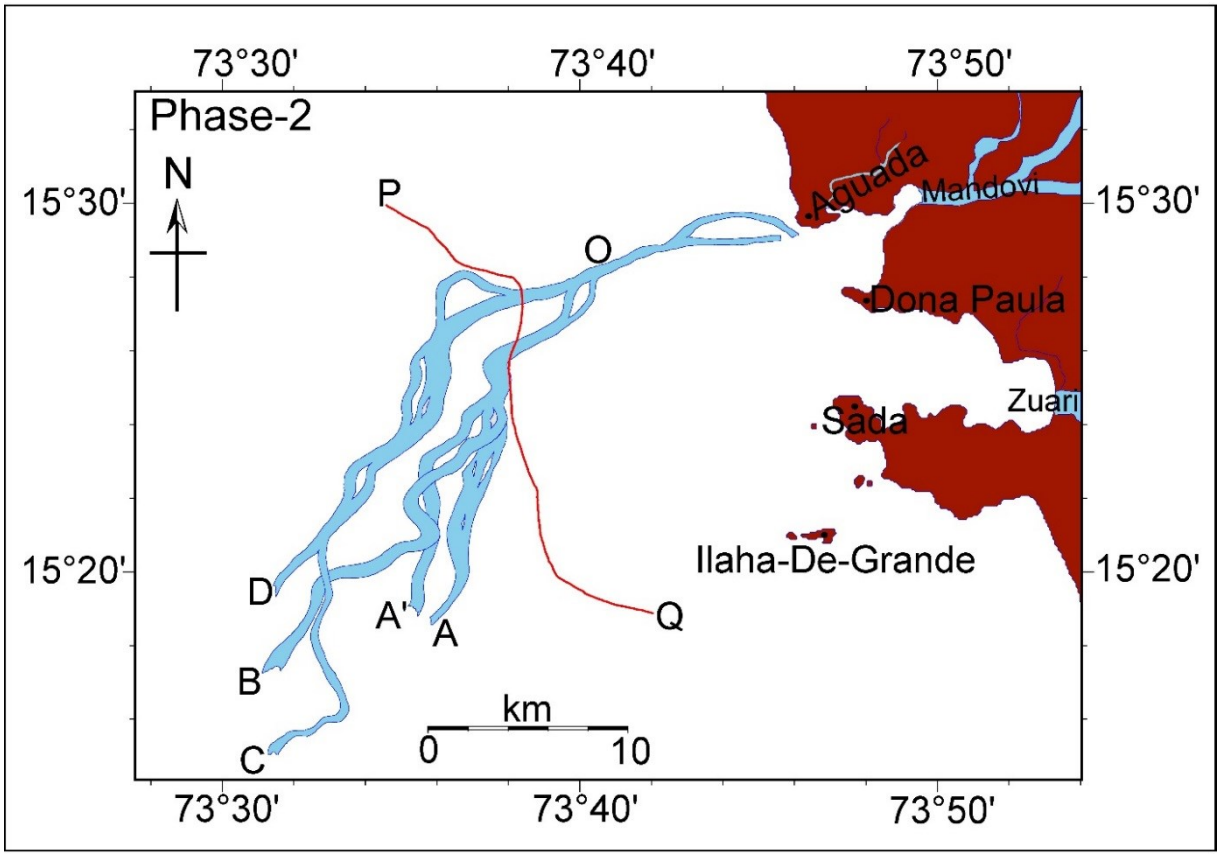

Figure 6.7 Interpolated plan view morphology of Phase-2 (320-125 kyr BP) channel incision. OA, OA', OB, OC and OD represent channel sections of Phase-2 channel. PQ is the boundary line between nearshore submerged rocky region and marine sediment assemblage in offshore region.

incision A1 (Fig. 6.3(I)) suggest that channel migration from A1 to A2 took place primarily because of sea-level changes. Interpolated plan view morphology of the Phase-2 channel

incision also shows migration corresponding to sea-level cycles. The incision in sedimentary strata became more sinuous with each passing stages (Fig. 6.7). Plan view morphology of Phase-2 incision has changed from poorly braided to ingrown meander with each passing stage (Fig. 6.7). At initial stage of the Phase-2 incision, channel was flowing through rocky region filled with poorly stratified coarse grain sediments as a poorly braided channel. At this stage, the orientation of Phase-2 channel was slightly different than that of Phase-1 channel (Figs. 6.6 and 6.7). With time, channels migrated further westward due to the availability of newer and wider shelf for incision at every stage. Results of the study reveal that the main course of river channel was primarily along the channel section OA in its initial stage at ~300 kyr BP. In response to further sea-level fall (Fig. 6.5), it migrated to channel section OA' (Fig. 6.7). The main course was again changed to OB in subsequent sea-level fall and section OA was abandoned, whereas, part of OC and OD also became active. Later, due to rise in sea-level (after 250 kyr), sections OA, OA' and OB got buried. During penultimate glacial period, the main course of the channel shifted to section OC and OD (Fig. 6.7). In summary, Phase-2 incisions are wide and very deep and mostly U-shaped. Rapid sea-level fall, low stand of sea-level for a long time (Fig. 6.5) and efficient hydrologic environmental condition during the Phase-2 incision have played significant roles for deeper, wider and U-shaped incisions.

6.4.3 Morphology of Phase-3 incisions

Phase-3 incision signatures are observed on a flood plain with a seaward slope of ~0.2%. The flood plain is marked by subaerial unconformity S9. Although Phase-3 incision signatures are most affected by wave activity during post LGM rapid sea-level rise, these signatures are still well preserved and observed in the entire study area. The preserved incisions are ~100 m to ~1200 m wide, and their maximum entrenchment varies from ~3 m to ~20 m. Mean depth of these incisions varies from ~1.5 m to ~10 m. Interestingly, deep V-shaped incisions are frequently observed in deeper water depth. Interpolated plan view morphology of Phase-3 incisions (Fig. 6.8) reveals that unlike Phase-2 and Phase-1 incisions, Phase-3 incised channel (maximum sinuosity 1.4) is similar to anastomosed river channel system which converged in deep water region. This convergence of the channel system is probably due to rapid sea-level fall during ~40-20 kyr BP (Fig. 6.5). Anastomosing channels are formed on low gradient flood plain in low hydraulic energy condition, and channel avulsion takes place either due to rapid base-level fluctuations or periodic increase in sediment load or due to both (Makaske, 2001).

Therefore, it is suggested that weak and variable hydraulic energy condition prevailed during Phase-3 incisions.

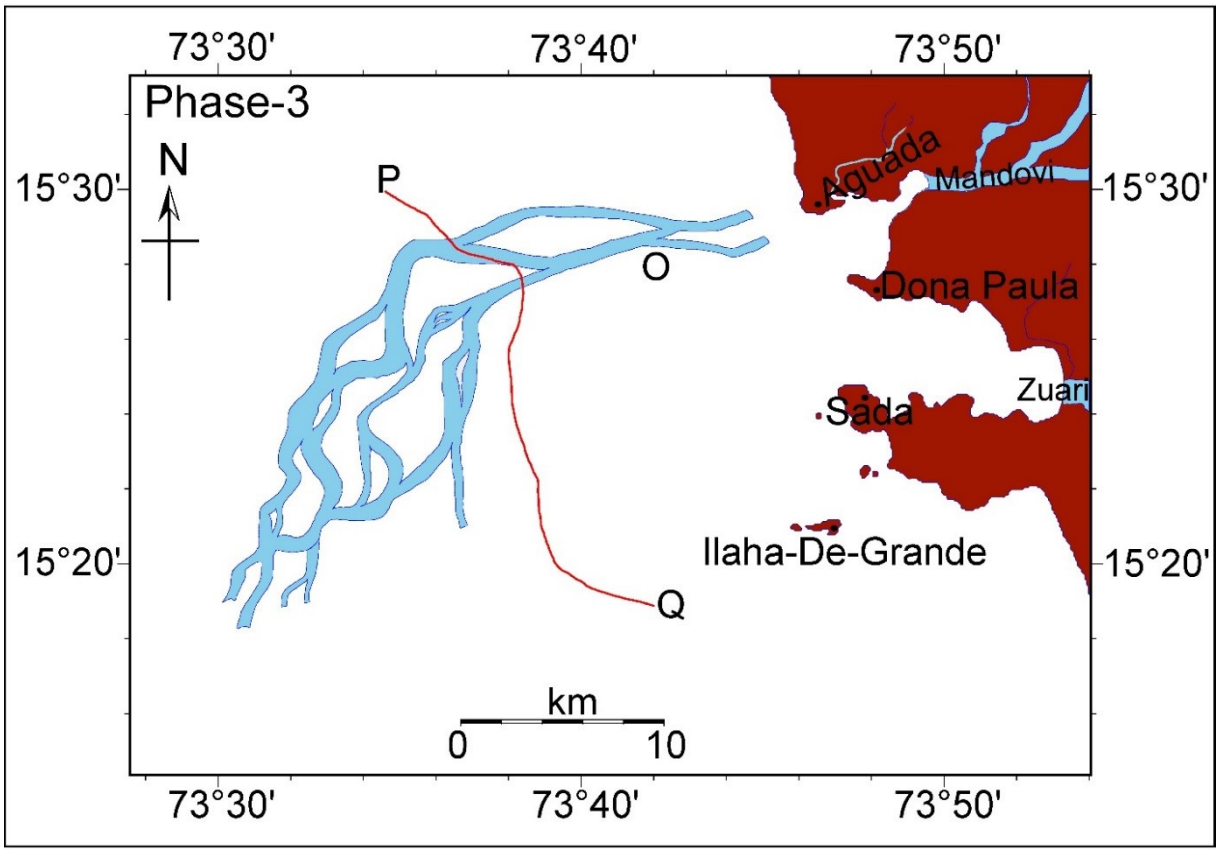

Figure 6.8 Interpolated plan view morphology of Phase-3 (110-10 kyr BP) channel incision. O is the confluence point of ancestral Mandovi and Zuari rivers. PQ is the boundary line between nearshore submerged rocky region and marine sediment assemblage in offshore region.

Sea-level fall during last glacial period is superimposed by higher order sea-level fluctuations (Fig. 6.5). Also, there were millennial scale strengthening and weakening of the Indian summer monsoon during the last glacial period (Rostek et al., 1993; Thamban et al., 2002; Patnaik et al., 2012; Marzin et al., 2013; Saraswat et al., 2013). These two factors might be responsible for the development of anastomosing type channel system in the study area. In addition, availability of thicker and heterogeneous sedimentary layer in the upper reach as well as low slope of exposed flood plain might have also played a pivotal role in developing the anastomosed channel system of this phase.

6.5 Morphometric results and Late Quaternary environmental inferences

Morphometric parameters and paleo-flow estimates are calculated based on the methodology discussed earlier and are presented in Table 6.1. The results reveal that aspect ratio of Phase-2 incisions varies between 9 and 132, indicating fluvio-estuarine environment during channel incisions. Maximum entrenchment along channel section

Table 6.1 Morphometric parameters and paleo-flow estimates of Phase-2 and Phase-3 channel systems of Mandovi-Zuari estuaries of Goa.

	Phase-2 incisions		**Phase-3 incisions**	
Morphometric Parameters				
Parameters	**Min**	**Max**	**Min**	**Max**
Width (m)	>200	<1000	>100	<1200
Mean Depth (m)	5	21	1.6 m	12
Aspect Ratio (Width /Mean Depth)	9	132	30	306
Sinuosity	1.1	1.29	1.2	1.4
Dominant Slope (%)	~0.25		<0.2	
Paleo-flow Estimates				
Mean Bank Full Discharge (m^3/s)	124	2700	187	2100
Mean Velocity (m/s)	1.5	1.7	1.4	1.5

OB, OC and OD (Fig. 6.7) is ~30 m with mean depth of ~20 m. Computed channel-belt sinuosity varies from 1.1 to 1.29 indicating an increase in sinuosity with a decrease in dominant slope of the exposed surface. These results suggest that although in each stage channel incision started with the sea-level fall in estuarine environmental condition, carving of main channel in sedimentary assemblage took place in a fluvial environment. Similarly, the aspect ratio of Phase-3 varies between 30 and 306. Channel-belt sinuosity of these incisions varies from 1.2 to 1.4. Whereas, maximum entrenchment, mostly observed in the deeper region of the study area, is ~20 m with mean depth of ~10 m. These results suggest that the main channel was developed in estuarine environment or low energy fluvial environment. Sea-level curve and paleo-environmental studies (Rostek et al., 1993, Saraswat et al., 2013) also support our inferences i.e. Phase-3 incision evolved under multiple estuarine conditions and low hydraulic energy fluvial condition. Comparison of computed hydrodynamic parameters of Phase-2 and Phase-3 incision signatures facilitated to compare prevailing hydrodynamic conditions. Mean depth of Phase-2 incisions are almost double than the Phase-3 incisions. Mean flow velocities (1.5-1.7 m/s) through Phase-2 incisions were higher than that of Phase-3 incision (1.4-1.5 m/s). Maximum mean bank full discharge through Phase-2 incisions was ~33% higher than that of

Phase-3 incisions. Higher dominant slope and rapid sea-level fall may contribute to the deeper entrenchment and higher mean flow velocity of Phase-2 incision. However it also requires sufficient higher hydrologic environmental condition. Higher mean bank full discharge suggest that Phase-2 incisions were carved in a better hydrologic environmental condition than that of Phase-3. Since the study area falls in tropical climate region and receives maximum precipitation during summer monsoon, it is suggested that the Indian summer monsoon was better during or prior to penultimate glacial periods (between ~140-195 kyr BP and ~250-320 kyr BP) than that of the last glacial period (~115-18 kyr BP).

6.6 Comparison of incised valley off Goa with other shelf settings

Late Quaternary sea-level fluctuations caused compound incised valley systems on the continental shelves all over the world. Compound valley incisions are widely investigated by ground truthing of acquired HRSS data using high cost long sediment cores. Incised valleys on the continental shelf off Hong Kong (Bahr et al., 2005), Mississippi-Alabama (Greene et al., 2007), Languedoc, Gulf of Lion (Tesson et al., 2010, 2011, 2015), and western Long Island, New York (Liu et al., 2017) are examples of compound valley incisions which are formed over tectonically passive and minimal subsidence shelf setting. Continental shelf of Goa also contains preserved signatures of compound incised valley. The channel systems investigated on the inner continental shelf of Goa are typical of those carved in similar settings. In particular, Mississippi-Alabama inner continental shelf falls in tropical climate region and contains preserved incised channel system corresponding to MIS 2 (last glacial period) and MIS 6 (penultimate glacial period). Similar to our study, Mississippi-Alabama incised channel systems are divergent seaward and older incisions were carved during the penultimate glacial period (MIS 6). These incisions were wider and deeper than the youngest incision signature. Methodology used in the present study by integrating qualitative and quantitative seismic geomorphology provides a valuable procedure for gaining insight into the evolutionary history of drainage system in the absence of long sediment core data. Moreover, this study also provides comparison of hydrologic regimes associated with prevailing environment during two glacial periods. In general, integration of base level concepts of river, stratigraphy and sea-level curve to interpret high resolution shallow seismic sections, provides an alternative of costly long core data to a certain extent.

6.7 Conclusions

Analysis of HRSS data allowed to conclude that sedimentary strata on the inner continental shelf of Goa contains preserved channel incision signatures corresponding to more than three glacial periods. Phase-1 incisions are older than ~330 kyr BP, whereas, Phase-2 incisions are carved during ~320-125 kyr BP. Youngest channel incisions are carved during the last glacial period between ~110 kyr BP and ~10 kyr BP, and belong to Phase-3 incisions. The seaward divergent channel systems were incised by confluent channel of ancestral Mandovi and Zuari rivers. With each passing sea-level cycle, channel incision became more sinuous and their areal extent increased. Buried channels evolved from straight river type (Phase-1) to ingrown meander (Phase-2) and then similar to anastomosing type (Phase-3). Unlike Phase-2 and Phase-1, Phase-3 incisions are incised in multiple estuarine and low energy fluvial conditions. Comparison of computed hydraulic parameters of Phase-2 and Phase-3 incisions reveals that Phase-3 incisions took place in lower hydraulic energy condition than the Phase-2 incisions. Phase-2 channels had ~33% more mean bank full discharge than that of the Phase-3 channels. The mean depths of the Phase-2 incision are almost double than that of Phase-3 incision. This implies that the hydrologic environment associated with penultimate and prior to penultimate glacial periods was also stronger than that of the last glacial period. The present study suggests that the Indian summer monsoon was stronger during the formative stage of Phase-2 incisions than that of Phase-3.

Chapter 7
Paleo-Coastline and Gas Charged Sediments

7.1 Introduction

This chapter deals with the significant geomorphologic/acoustic features observed in the high resolution shallow seismic sections of the study area (Fig. 7.1). It emphasizes mainly two prominent features, viz. paleo-coastline and gas charged sediments. Signature of paleo-coastline reveals information about stable sea-level conditions, whereas gas charged sediments provide clues for the origin and factors controlling its distribution pattern.

Accretion of sedimentary landforms (delta, spits, beaches, sand bars etc.) takes place in close proximity of coastline under appropriate terrigenous sediment supply, shoreline trajectory and stable sea-level condition. These geomorphologic features are very dynamic in nature and can migrate with shoreline. Beach rocks, in situ woods and peats, shore parallel sand ridges etc., especially at distal locations on continental shelf, can be considered as indicators of paleo-shoreline. Identification of these paleo-coastline landforms are important and contribute significantly for the evolutionary history of continental shelves.

Shallow gas charged sediment zones are formed due to intense oxidization of organic matter in a sedimentary environment over thousands of years (Garcia-Gil et al., 2002). Transgressive and regressive events, over geological time, change sedimentary environment and alter distribution and quantity of organic matters, which could thus provide various types of gas traps (Garcia-Gil et al., 2002). The accumulation of shallowly trapped gases may occur on or beneath surface of sedimentary column, as well as in the dissolved form in water column (Garcia-Gil et al., 2002). Shallow gas related sedimentary structures occur in the form of acoustic blanking, acoustic curtains, acoustic columns, acoustic turbidity, turbidity pinnacles and intra-sedimentary plumes in seismic sections (Hovland and Judd, 1992). Shallow gas related

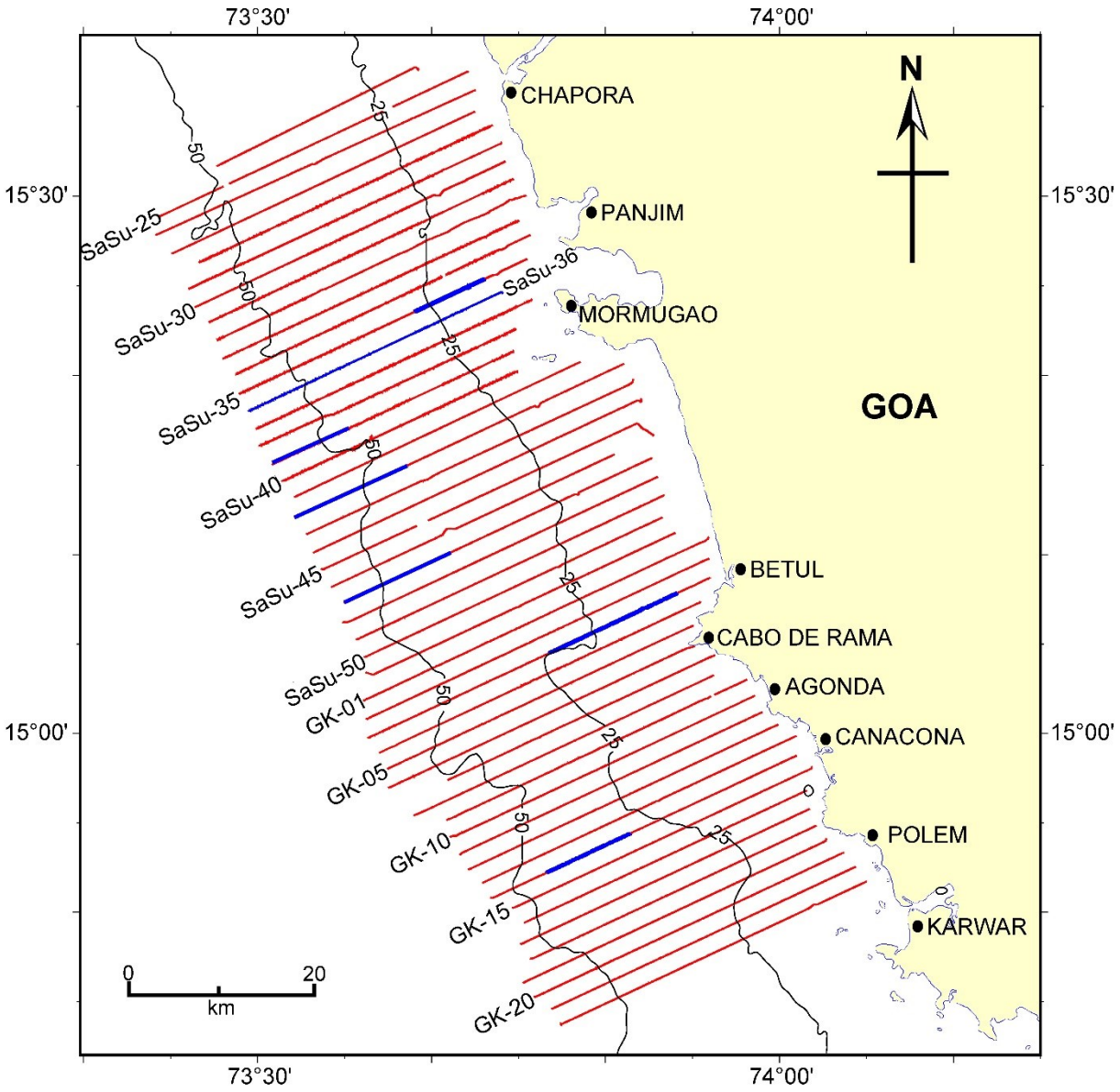

Figure 7.1 Seismic tracklines (solid red lines) used to delineate paleo-coastline and gas charged sediment zones on the inner continental shelf of Goa. Isobaths are shown with solid black contour lines and annotated values on the contours are in meter. Parts of the seismic tracklines, highlighted with blue color, refer to the locations corresponding to seismic sections used in the subsequent figures.

sedimentary structures have been reported from the western offshore region of India by several researchers (Siddiquie et al., 1981a, b; Karisiddaiah et al., 1993; Karisiddaiah and Veerayya, 1994, 2002; Subbaraju and Wagle, 1996; Veerayya et al., 1998). Further, Karisiddaiah and Veerayya (1994) reported 2.6 Tg of potential methane gas covering an area of 6500 km^2 on the western continental shelf of India.

The importance of studying shallow gas charged sediment zones has increased over recent decades. One of the reasons of growing interest is methane seepage from the seabed which alters the surrounding ecosystem and food chain supply system. On a global scale, methane seepage is involved in the biogeochemical cycling and elemental transformation of carbon, sulfur and nitrogen (Hinrichs and Boetius, 2002; Dekas et al., 2009; Boetius and Wenzhöfer, 2013). Since the gas that escapes from shallow gas charged sediments is mostly methane, these features also contribute to global warming (Best et al., 2004). Therefore, study of gas charged sediment zones has become important for climate change analysis. For example, contribution of methane emission from shallow gas structures and seepages on the continental shelf around the United Kingdom is estimated to be 40% of the total national emission (Judd et al., 1997). Additionally, shallowly trapped gas may also cause sediment instability (Premchitt et al., 1992) which poses hazards to coastal engineering works.

In the present study, analysis and interpretation of High Resolution Shallow Seismic (HRSS) data are carried out to identify sand ridges and gas charged sediment zones on the inner continental shelf of Goa (Fig. 7.1). Further, their distribution pattern are investigated to delineate paleo-coastline, origin as well as factors controlling distribution pattern of gas charged sediment zones.

7.2 Paleo-coastline

Earlier geophysical studies on the western continental shelf of India have reported the presence of sand ridges on the inner continental shelf (Nair, 1975; Wagle et al., 1994; Wagle and Veerayya, 1996). Further, Wagle et al. (1994) inferred that these sand ridges are formed in paleo-beach/barrier environment and are related with the stillstand of sea-level during the Holocene. In this study, the sand ridges are interpreted based on seismic signatures observed in the HRSS sections, which occur at ~55 m water depth. The details of their seismic characteristic properties are described in the following sections:

The HRSS data reveal an anomalous undulations on the seabed immediately after seaward pinching out of seismic unit U11 (discussed in Chapter 4) at ~55 m water depth. Mostly these undulations are marked as sudden change in gradient of the seabed and oftentimes it is caused by mounded morphologic features (Fig. 7.2). These features are up to ~4 km wide and have relief varying from ~2 to 6 m. Interestingly, most of the mounded features are located seaward

and are in proximity of an incision signature. These incision signatures are found on subaerial unconformity S9 which are interpreted as Phase-3 incisions (discussed in chapter 6). In several seismic sections, more than one mounded features have been observed. Usually, the mounded features at seaward locations are at ~4 to 5 m below the similar features at landward locations. Careful analysis of seismic data revealed that these mounded features are found only in upper part of the seismic unit 'U10' (discussed in chapter 4) and are bounded by transgressive surface S11 at the top. The seismic reflectors within the feature are characterized by low amplitude with chaotic to hummocky reflection pattern. At some places, the high amplitude bounding surface S11 hamper penetration of acoustic energy to deeper layers (Fig. 7.2).

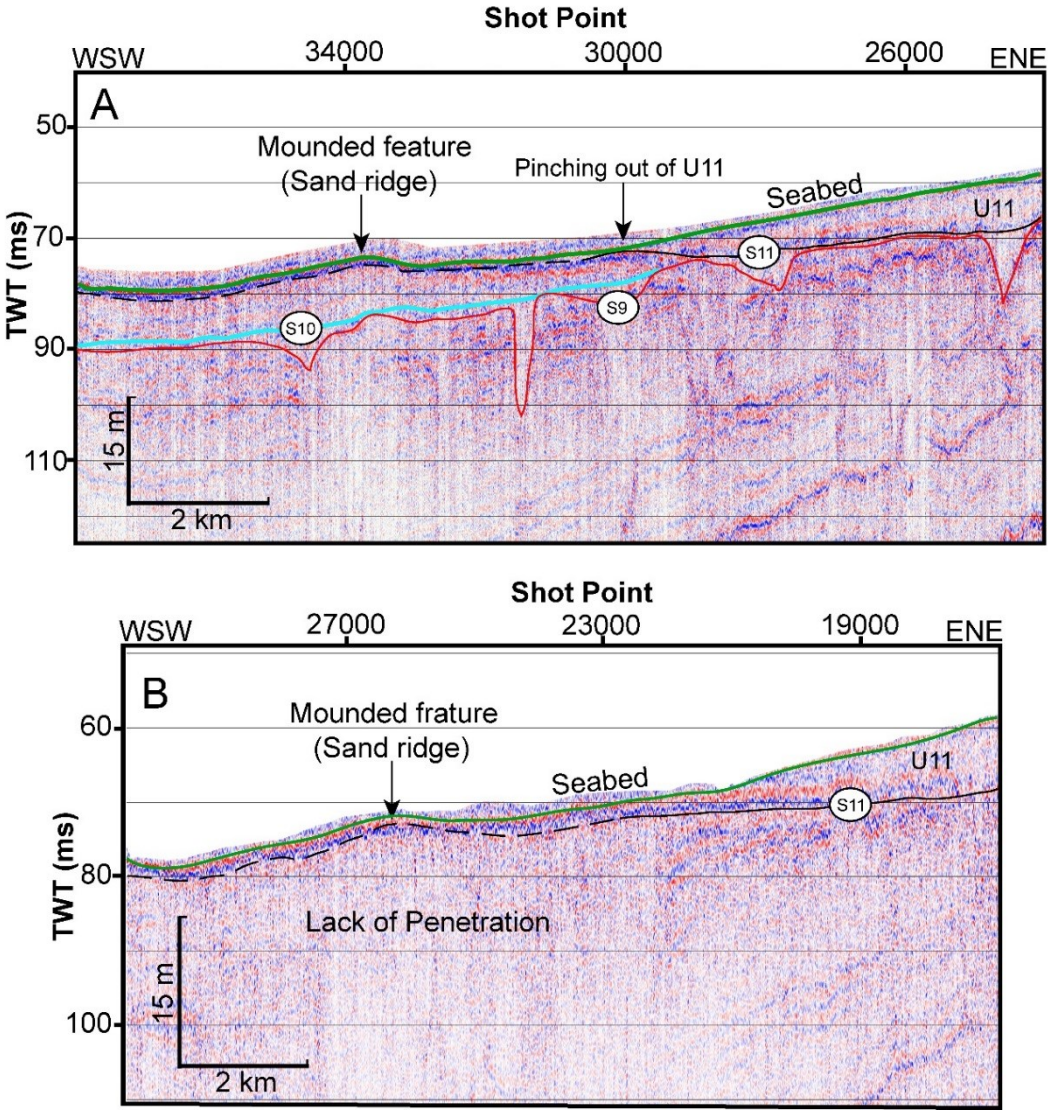

Figure 7.2 Seismic sections depicting interpreted mounded features and very-feeble/lack of sub-surface reflectors beneath it. (A) Part of seismic section along trackline SaSu-42 depicting mounded feature and seismic unit U11. (B) Part of the seismic section along trackline SaSu-39 showing lack of penetration below the interpreted mounded feature.

High amplitude reflectors refer to the high contrast in acoustic impedance which can be interpreted as the significant change in the sediment type due to change in depositional environment. Whereas, chaotic to hummocky reflection pattern within the mounded feature indicates that the sediment assemblage within the feature is not well stratified and formed in a higher energy condition, usually non-marine environment. Therefore, it is interpreted that these mounded features are made up of sand assemblage which is not well stratified and deposited in high energy non-marine condition. Further, observed sedimentary unit U10 is a strong signature of very slow rate of sea-level rise or a brief period of standstill condition of the Holocene transgressive sea at ~53 m water depth (discussed in chapter 4). Therefore location of these sand ridges on the upper part of the seismic unit U10 asserts that these ridges have formed in coastal environment (non-marine) (Fig.7.3). The sand ridges are interpreted as paleo-beaches and surf zone sand bars which are accreted along a stable paleo-coastline in a coastal depositional environment. Nearby river supplied the sediment for the accretion. It may be noted that the sand ridges at seaward locations are interpreted as surf zone sand bars, whereas, the same at landward locations are interpreted as paleo-beaches. Locations of the paleo-beaches and surf zone sand bars are plotted on a map and presented in Figure 7.4. It can be seen that the paleo-beaches are distributed at ~55 m water depth and runs parallel to the present day coastline of the study area. Based on the observed seismic signatures and their orientation with respect to the present day coastline, these paleo-beaches are inferred as the remains of a stable paleo-coastline. The length of these paleo-beaches extends up to ~10 km at places. As the signatures of paleo-beaches are not available everywhere, onlap location of U10 is also used as a coastline signature, and a paleo-coastline has been delineated and plotted on the map (Fig. 7.4). The interpreted paleo-coastline is located at ~35 km WSW of the present day coastline of the study area.

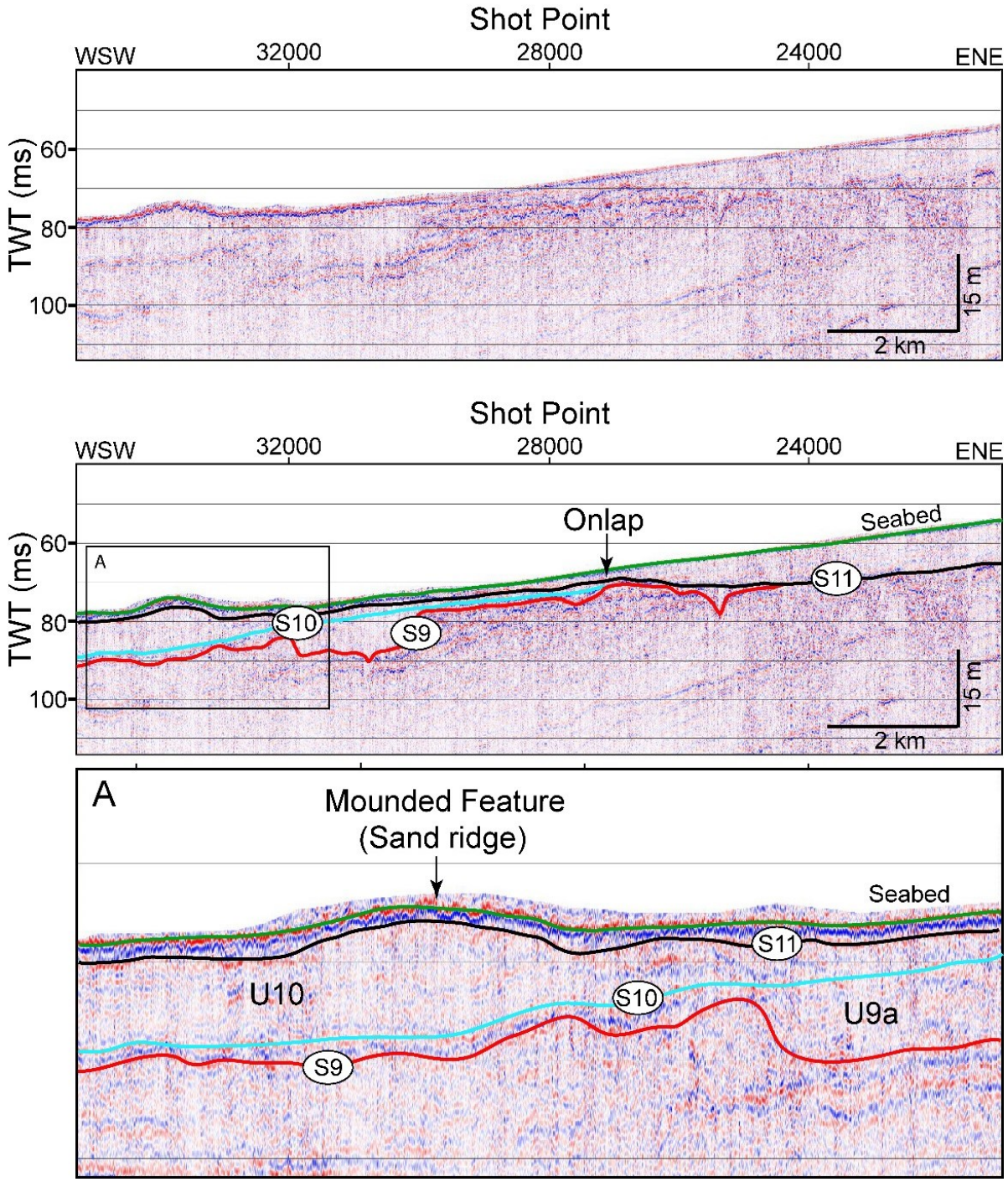

Figure 7.3 Uninterpreted and interpreted seismic section along part of the trackline SaSu-47 highlighting onlap of bounding surface S10 on the S9. (A) An enlarged section of the rectangular box (shown in interpreted seismic section) showing mounded feature interpreted as sand ridge.

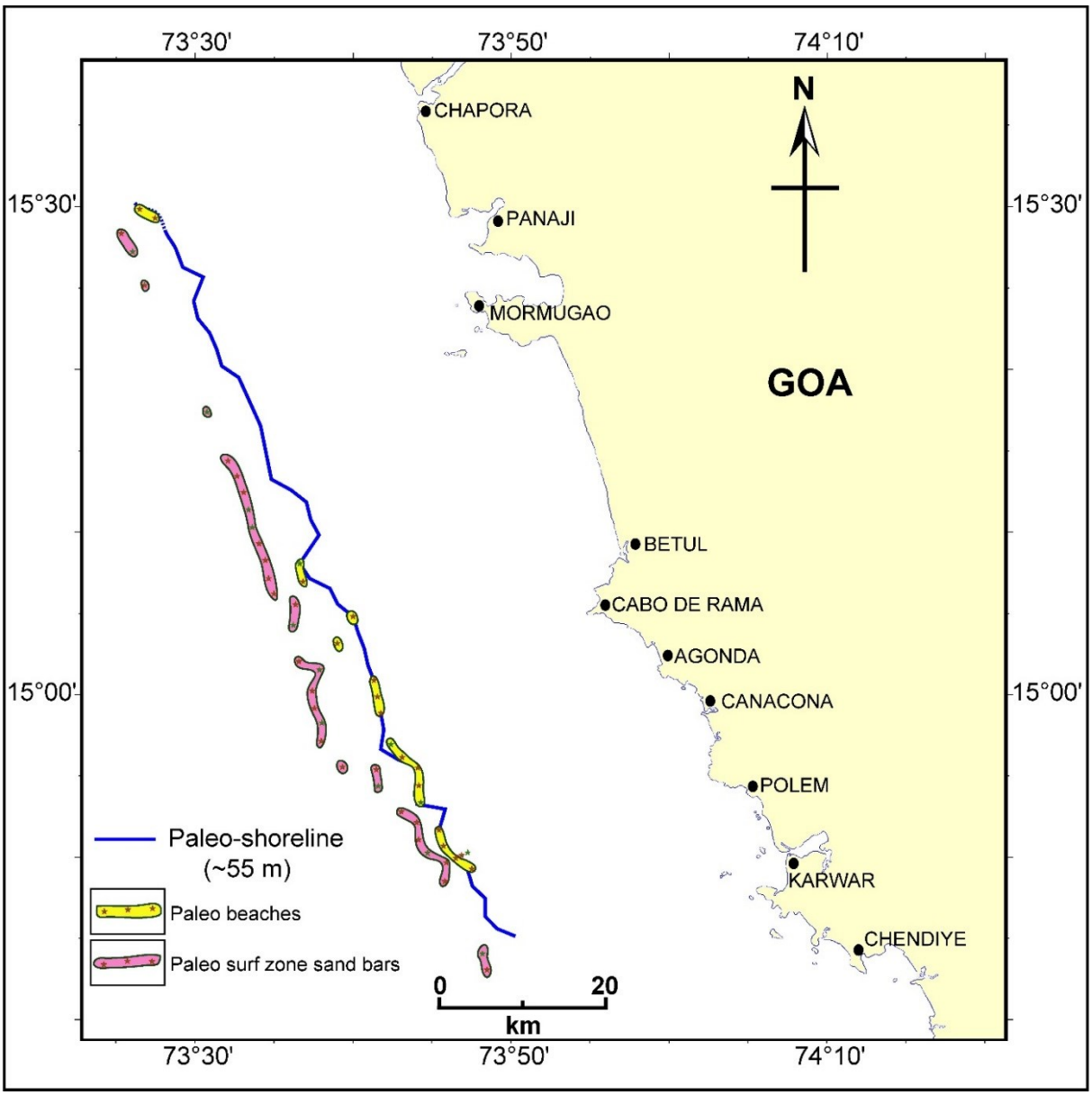

Figure 7.4 Map depicting distribution of paleo-beaches (short bars with yellow color) and paleo-surf zone sand bars (short bars with pink color) on the inner continental shelf of Goa. Solid blue line represents interpreted paleo-coastline.

7.3 Gas charged sediments

Gas charged sediments are marked by reflection free patches in the HRSS sections of the study area which are caused due to absorption of seismic energy. Acoustic blanking and acoustic turbidity are most abundant in the study area (Figs. 7.5, 7.6 and 7.7). In addition, gas chimneys are also observed at a few locations.

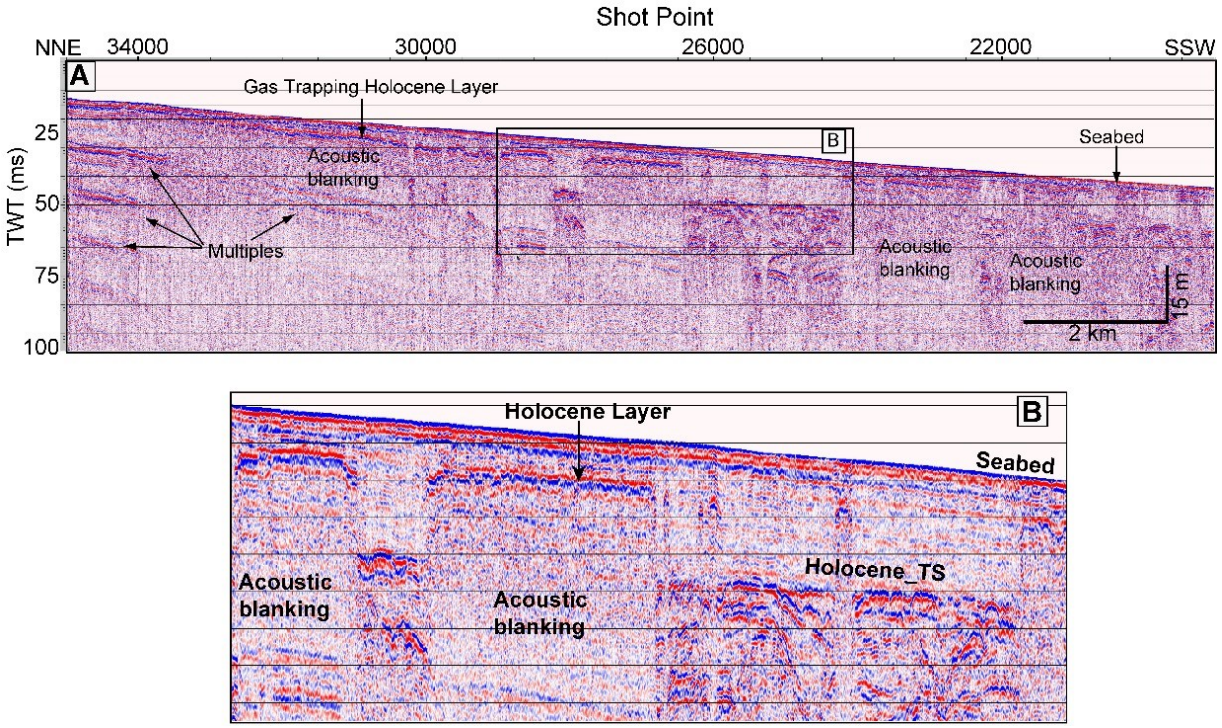

Figure 7.5 (A) Seismic section along part of trackline GK-03, showing signature of gas trapped by the Holocene sedimentary layers in Zone-1. (B) An enlarged section of the rectangular box (Fig. 7.5 A) showing acoustic blanking with distinct flanks.

Analyses of seismic profiles reveal that top of these reflection free patches are confined by different stratigraphic layers. On the basis of acoustic characteristic of gas charged sediments and confining sedimentary layers, identified gas charged sediment zones are divided into two zones viz. Zone-1 and Zone-2 (Fig. 7.8). Zone-1 is characterized by acoustic blanking with distinct flanks (Fig. 7.5). This zone is marked between ~8 and 30 m water depth and limited to southern part of the study area (Fig. 7.8). The width of acoustic blanking varies between ~150 and 12000 m. Shallow gas features are trapped at ~1.5 to 5 m below sea floor (mbsf) in the Holocene sedimentary layers underlain by the Holocene_TS. Seismic profiles do not reveal any signature of gas seepage from this zone.

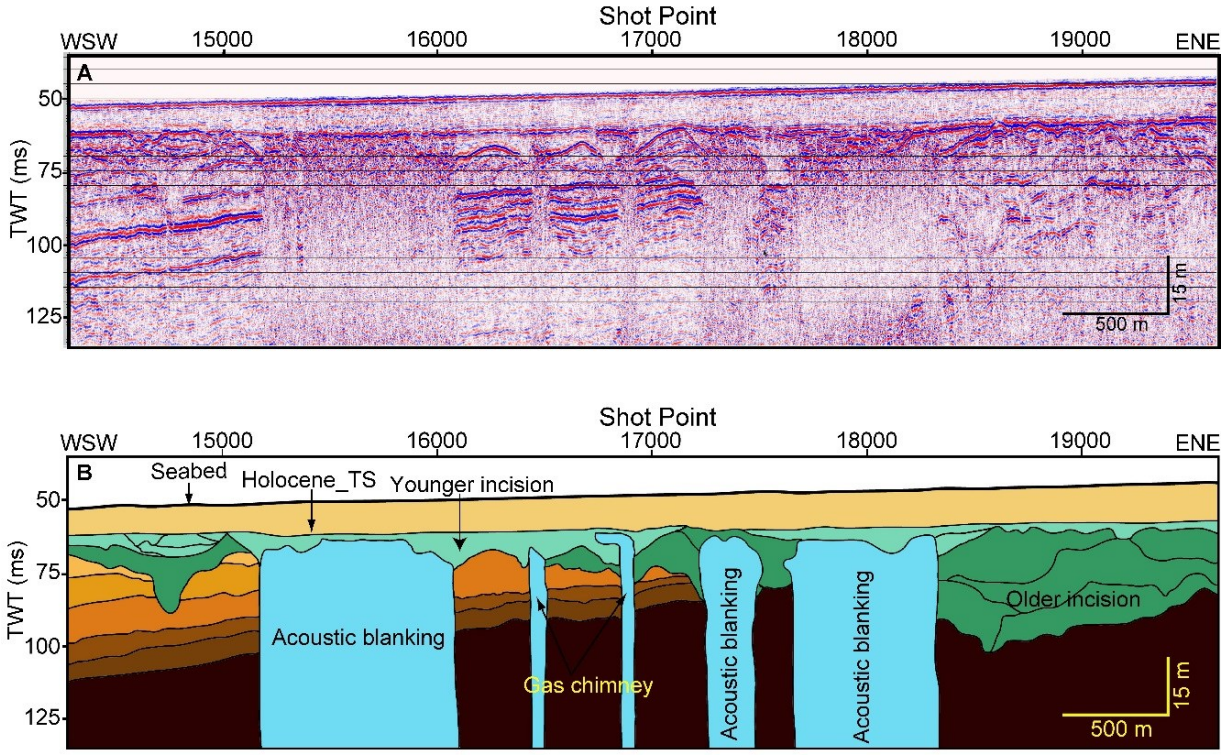

Figure 7.6 (A) Uninterpreted seismic section along part of trackline SaSu-36. (B) Interpreted seismic section showing gas trapped below Holocene_TS and buried river bed. It also depicts various seismic signatures corresponding to gas masking such as acoustic blanking and gas chimney.

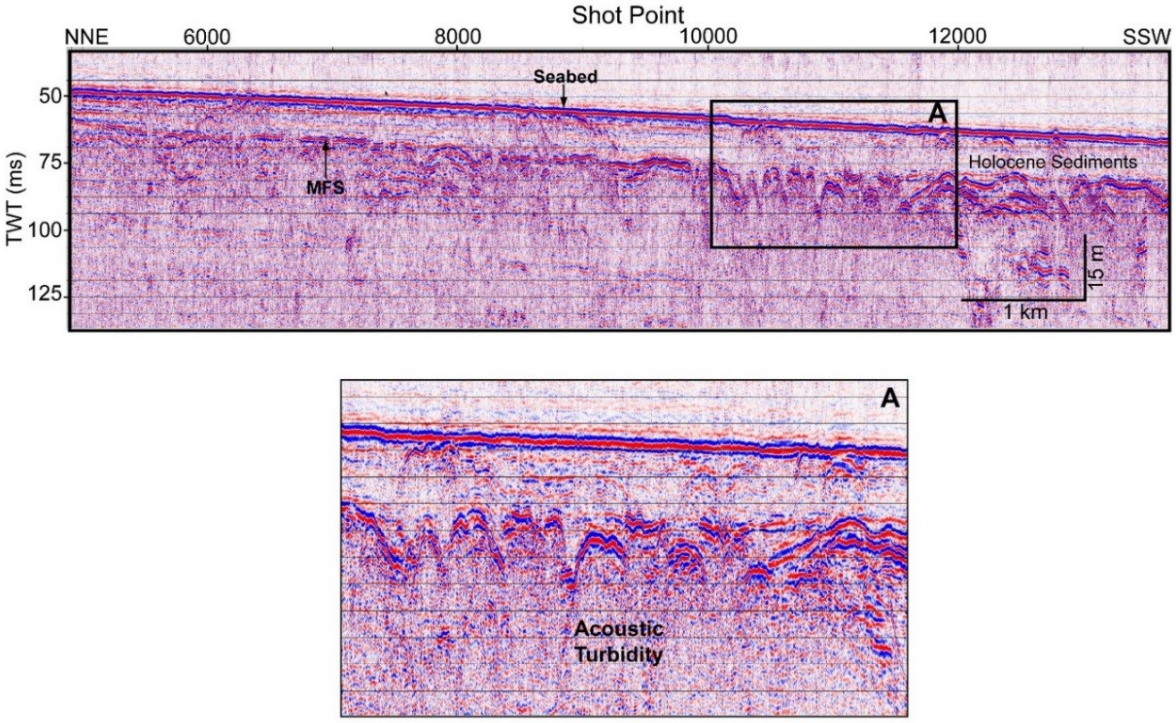

Figure 7.7 Seismic section along part of trackline SaSu-35 showing acoustic turbidity. **(A)** Enlarged seismic section of the rectangular box shown in Fig. 7.6. Holocene_TS refers to the Holocene Transgressive Surface.

Zone-2 consists of several isolated small patches of acoustic blanking, acoustic turbidity and gas chimneys which are trapped at ~6 to 15 mbsf. Unlike Zone-1, shallow gas features in Zone-2 are mostly trapped below the Holocene_TS. These features are mostly found over the Late Pleistocene channel incision and have altered the incision signatures (Fig. 7.6). The identified shallow gas features of Zone-2 are either confined by the river beds or by the layers just below Holocene_TS (Holocene_TS is discussed in Chapters 4 and 5) or by both (Fig. 7.6). Widths of shallow gas features in Zone-2 vary from ~120 m to ~2500 m and are comparatively smaller than the Zone-1 features. Interestingly, widths of observed shallow gas features in Zone-2 are always comparable or smaller than the size of river incision related to it. It may be noted that Zone-1 gas features do not show any such relation with incised channel signatures. As mentioned earlier, Zone-2 consists of several small patches of gas features, which are located off Chapora, Mandovi, Zuari, Colva, Sal, Talpona and Galgibag rivers. Also, Zone-2 gas features are mostly confined between ~20 and 45 m water depths in the entire study area. In addition, Zone-2 gas features are also found beyond ~50 m water depth off Mandovi and Zuari rivers (Fig. 7.8).

7.4 Discussion

From the study of HRSS profiles, it is obvious that the anomalous seismic reflection free patches in the inner continental shelf off Goa appear just a few meters below the seafloor. It is found that shallow gases are trapped by Holocene layers at ~1.5 to 5 mbsf in Zone-1, whereas, these are trapped below the Holocene_TS between ~6 m to ~15 mbsf in Zone-2. Trapping of these shallow gases by different stratigraphic layers reveals that the distribution and extent of the gas charged zones are not only dependent on favorable condition, such as temperature and pressure but also dependent on the lithological character of the region. The gas found in marine sediments can originate either from biogenic or thermogenic processes (Floodgate and Judd, 1992; Megonigal et al., 2004; Canfield et al., 2005; Reeburgh, 2007). The most common gas in shallow-water sediments reported globally is biogenic and is produced by microbial methanogenesis under anaerobic conditions (Judd and Hovland, 2007). In our study area, previous studies reveal that the trapped gas in the sediments is mainly methane and biogenic in nature (Mazumdar et al., 2009). Areas of fine-grained muddy sediment that receive high fluxes of organic matter provide ideal conditions for the formation of biogenic methane (Fleischer et al., 2001). The probable sources for the organic material on the inner continental shelf are (i) intertidal vegetation (mangroves) which got buried due to the sea-level rise, (ii) the terrigenous

material brought by river channels through its course during the lowered sea-level conditions, (iii) the terrigenous materials supplied by the river channels during highstand sea-level and were driven away by coastal long shore currents, and (iv) marine productivity. Since gas features in Zone-1 are not linked with any channel incision, it is interpreted that the organic material which caused gas formation in Zone-1, might have been derived from the buried intertidal vegetation (mangroves) and from the material carried by coastal longshore currents. Acoustic masking similar to the zone-1 is not observed in the entire area. Further, limited occurrence of gas charged sediment (Zone-1) off Betul-Cancona region (Fig. 7.8) might be due to its bay like coastline configuration.

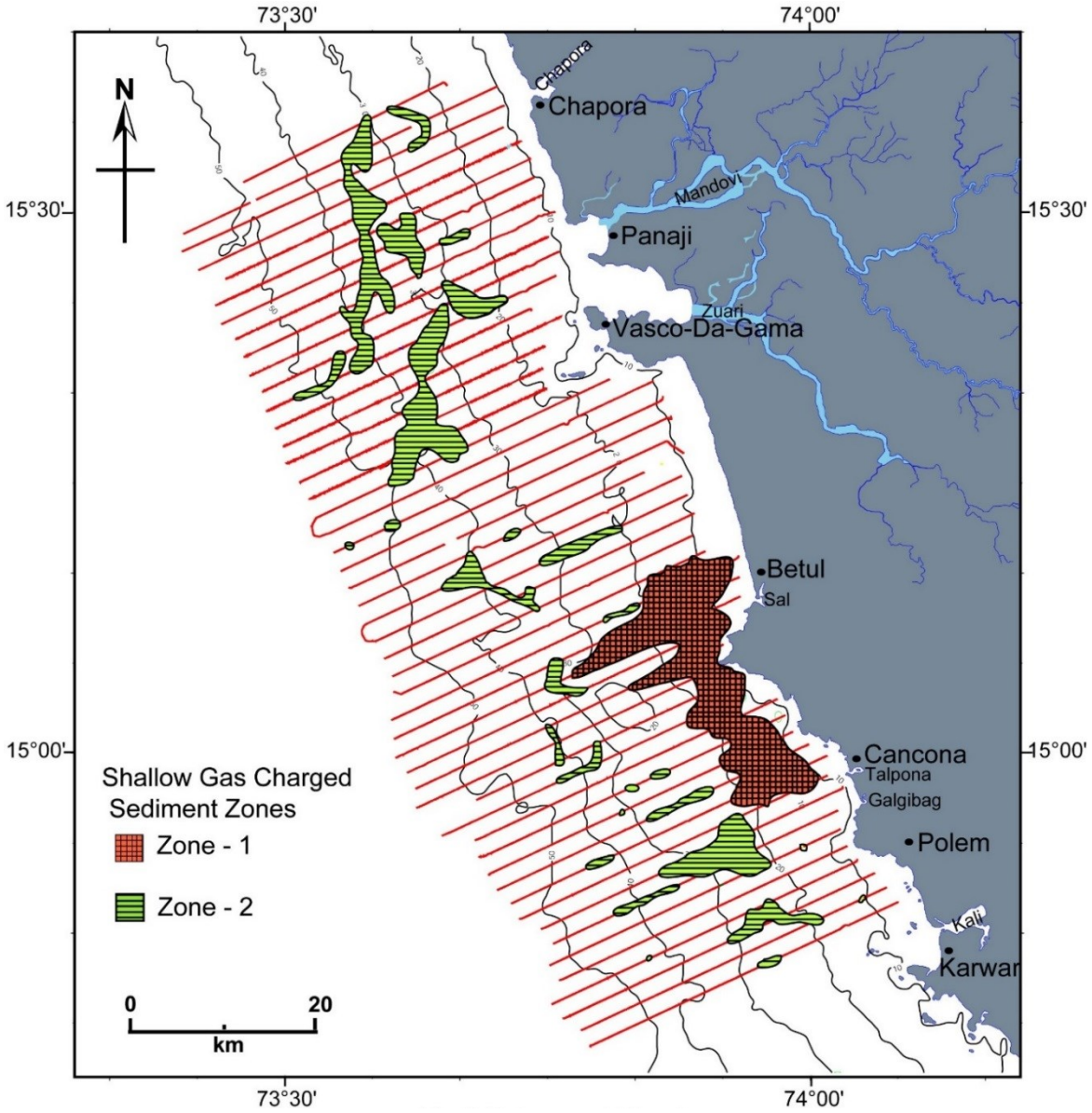

Figure 7.8 Map depicting shallow gas charged sediment zones in the study area. Bathymetric contours (10, 20, 30, 40 and 50 m) are shown with solid black color lines.

Presence of Cabo-de-Rama headland with its coast line configuration might have acted as a barrier for long shore current and made a sheltered basin for sediment deposition with low energy condition. Further, available Holocene sea-level curve of the west coast of India reveals nearly stand still condition at ~25 m below present sea-level during 10000-9000 years BP (Hashimi et al., 1995). Since, relatively stable sea-level and gently sloping intertidal areas with suitable substrate (silt and clay) provides ideal conditions for intertidal vegetation e.g. mangroves (Woodroffe, 1983). Therefore, this period was favorable for extensive mangrove growth in the then exposed intertidal zone which is presently submerged between 20 to 30 m water depth. It may be mentioned here that previous studies based on sediment core analysis revealed the presence of peat within the silty substrate from several locations of shallow water region of central west coast of India (Mascarenhas, 1997). Sediment core data off Goa-Karwar (SK-148/14) region revealed mangrove derived peats which were formed during the early Holocene. This peat dominated layer is overlain by clay layers (sticky clay). Zone-1 where the gas is trapped within the Holocene layer above the Holocene_TS is one such zone. Therefore, source of organic material in Zone-1 is interpreted to be predominantly buried mangrove remains. Cabo-de-Rama headland with its coast line configuration had provided the favorable sheltered region for the mangroves to get preserved during rapid sea-level rise (12 m/kyr) between 9000-7000 years BP. Over a period of time, these preserved mangrove remains got converted firstly to peat and later became source of gas which are trapped in sediments of Zone-1.

Zone-2 consists of several isolated patches of gas charged zones. More than 90% of the observed columnar acoustic blanking and turbidity in Zone-2 are found in the immediate vicinity of the lenticular channel incision. In Zone-2, shallow gas is trapped mostly below the Holocene_TS and buried river bed. These observations indicate that gas features in Zone-2 can be linked with the channel incisions. The organic materials, brought by these paleo-channels, subsequently got buried in the channel due to post glacial sea-level rise, are the cause of it. The channel incisions are found to be carved during different low stand half cycle of sea-level associated with different glacial periods (as discussed in chapter 6). Therefore, it can be interpreted that the organic material responsible for these gas charged zones were also brought by the rivers during different glacial periods. In the region of gentle slopes, hydraulic energy of the river channel decreases downstream. Base level (i.e. sea-level for coastal rivers) rise causes aggradations of river bed in the lower hydraulic energy condition. The loss in hydraulic energy of the incised river downstream with rising base level might be the reason of limited offshore

extent of the Zone-2 which is mostly located upto ~45 m water depth and rarely found beyond ~45 m water depth.

Although bathymetry of the study area does not show any signature related to gas escape through seabed, HRSS profiles at very few locations suggest gas seepage in Zone-2 of study area. These features are related with acoustic turbidity which is mostly confined below Holocene_TS (Fig. 5). In the absence of clear evidence of gas seepage, it is suggested that high resolution sonography of the seabed and chemical analysis of sediment and water samples need to be carried out to ascertain seepages of gas from the seabed.

7.5 Conclusions

Analysis of HRSS data revealed observed seabed undulations which are mounded features (sand ridges) depicting a sudden change in the seabed gradient. These are interpreted as paleo-beaches (landward) and surf zone sand bars (seaward). The paleo-beaches are interpreted as the remains of a stable paleo-coastline. Careful analysis of HRSS section revealed that the sand ridges are located at ~55 m water depth. The relief of these ridges varies between ~2 to 6 m and they are ~2 to 4 km wide along the tracklines. Seismic signatures of paleo-beaches reveals that they are located ~4 to 5 m higher than the surf zone sand bars. The spatial distribution of the sand ridges revealed that they are distributed at the outer flank of the study area and have oriented parallel to the present day coastline. The paleo-beaches are inferred as the remains of a stable paleo-coastline which is located at ~35 km WSW of the present day coastline of the study area.

Further, the HRSS data also allowed to mark two different types of gas charged sediment zones on the inner continental shelf off Goa, central west coast of India. Zone-1 has limited areal extent between ~8 and 30 m water depth in sheltered basin of the study area, whereas, Zone-2 is distributed in the entire study area mostly between ~20 m and ~45 m water depth. Lithological characteristics of the Late Pleistocene-Holocene sedimentary deposits controlled the distribution of gas charged sediments. The source organic material as well as sediments of Zone-1 and Zone-2 were deposited in the Holocene and Late Pleistocene respectively. The biogenic gases in Zone-1 are confined within the Holocene sedimentary layers whereas, they are confined in Zone-2 below the Holocene_TS within the paleo-river bed or a layer just below Holocene_TS or by both. Gases in Zone-1 were formed by the bio-degradation of organic material which was predominantly mangrove (intertidal vegetation) derived. Further, our study

suggests that coastline configuration, Holocene rapid sea-level rise and lithological character of exposed intertidal zone had played key role in the formation and distribution of gas charged sediment of Zone-1. On the other hand, biogenic gases in Zone-2 was formed by organic material which was predominantly derived by ancestral rivers through its course during different glacial periods of the Late Pleistocene. The distribution pattern of buried rivers and their hydraulic energy condition during the base level rise played pivotal roles in the formation and distribution of gas charged sediments in Zone-2 of the study area.

Chapter 8

Late Pleistocene-Holocene evolution of the inner continental shelf of Goa

8.1 Introduction

Analyses and interpretation of the High Resolution Shallow Seismic (HRSS) data of the present study revealed that the sedimentary architecture of inner continental shelf of Goa contains signatures of depositional and erosional features corresponding to more than three glacial periods. Further, similar to tectonically passive continental shelves of the world, the HRSS data from the study area do not show any signature related to the Quaternary tectonic activity such as faulting (subsidence or upliftment) and folding. Preserved signatures of erosion and deposition revealed potential information to reconstruct the evolutionary history of the inner continental shelf of Goa.

In previous chapters, detailed analysis of sedimentary architecture (Chapter 4), evolution of buried paleo-channels and paleo-environmental conditions (Chapter 6) and geomorphologic signatures formed during the Holocene transgression (Chapter 7) have been presented. Present chapter describes the evolution of inner continental shelf of Goa based on the results and inferences drawn in those chapters.

8.2 Evolution of inner continental shelf of Goa

High resolution sequence stratigraphic analyses of the HRSS data of the inner continental shelf of Goa facilitated to identify (i) presence of seaward dipping rocky basement up to ~35 m water depth, (ii) three subaerial unconformities which seem to terminate at the seaward edge of the rocky basement at ~35 m water depth, and (iii) presence of sediment deposits corresponding to the Holocene highstand sea-level. It is worth to mention here that the similar deposits corresponding to other past highstand sea-level are absent.

The rocky basement is interpreted (up to ~35 m water depth) as the extension of hinterland rock outcrops. The depressions within the basement rock are filled with coarse grain sediments. This rocky basement provided a platform for highstand sediment deposition. Whereas, subaerial unconformities were formed due to lowered sea-level conditions during the last three glacial periods. Detailed analysis of morphologic features and interpolation of their plan form revealed that the areal extent and erosional capacity of paleo-channels were controlled by the variation of shelf gradient, prevailing hydrologic environments and sea-level fluctuations during the last three glacial periods. The paleo-channels along with wave action activity of the sea played an important role in removal of previous highstand sediment deposits in each subsequent lowering of the sea-level. From the inferences drawn in the previous chapters, it can be concluded that the Late Pleistocene-Holocene inner continental shelf has evolved due to the interplay between fluvial channels, eustasy and climate. Integration of the analyses and interpretation presented in this study allows to propose the Late Pleistocene-Holocene evolutionary history of the inner continental shelf of Goa in three stages (Fig 8.1). Description of stage-wise evolutionary history of the inner continental shelf of Goa is presented in the following sub-sections.

8.2.1 Stage-1 (~325 kyr to 200 kyr BP)

The first stage (Stage-1) deals the evolutionary history between ~325 and 200 kyr BP. Sea-level at ~325 kyr BP was at ~5 m below the present sea-level (Fig. 8.1) and the coastline was slightly seaward as compared to the present day coastline. The then rivers were narrower and slightly deeper as compared to the present day Mandovi-Zuari rivers, and were debouching slightly westward into the Arabian Sea. The mouth zones were well within the extent of rocky basement. Since the high stand sea-level prevailed for quite long period (~5 kyrs), a highstand sediment deposit (similar to the Holocene sediment deposits) over the rocky basement is expected. These deposits along with the buried rocky basement have preserved incision signatures corresponding to older incisions. With the start of sea-level fall at ~320 kyr BP at a rate ~5 m/kyr, coastline started migrating seaward. The continental shelf which was buried previously got exposed to various subaerial processes. As a result, the highstand deposits over the rocky basement was eroded due. Initially, wave derived drift currents and later channel incisions played significant roles for erosion of the highstand sediment deposits. Channel incision started

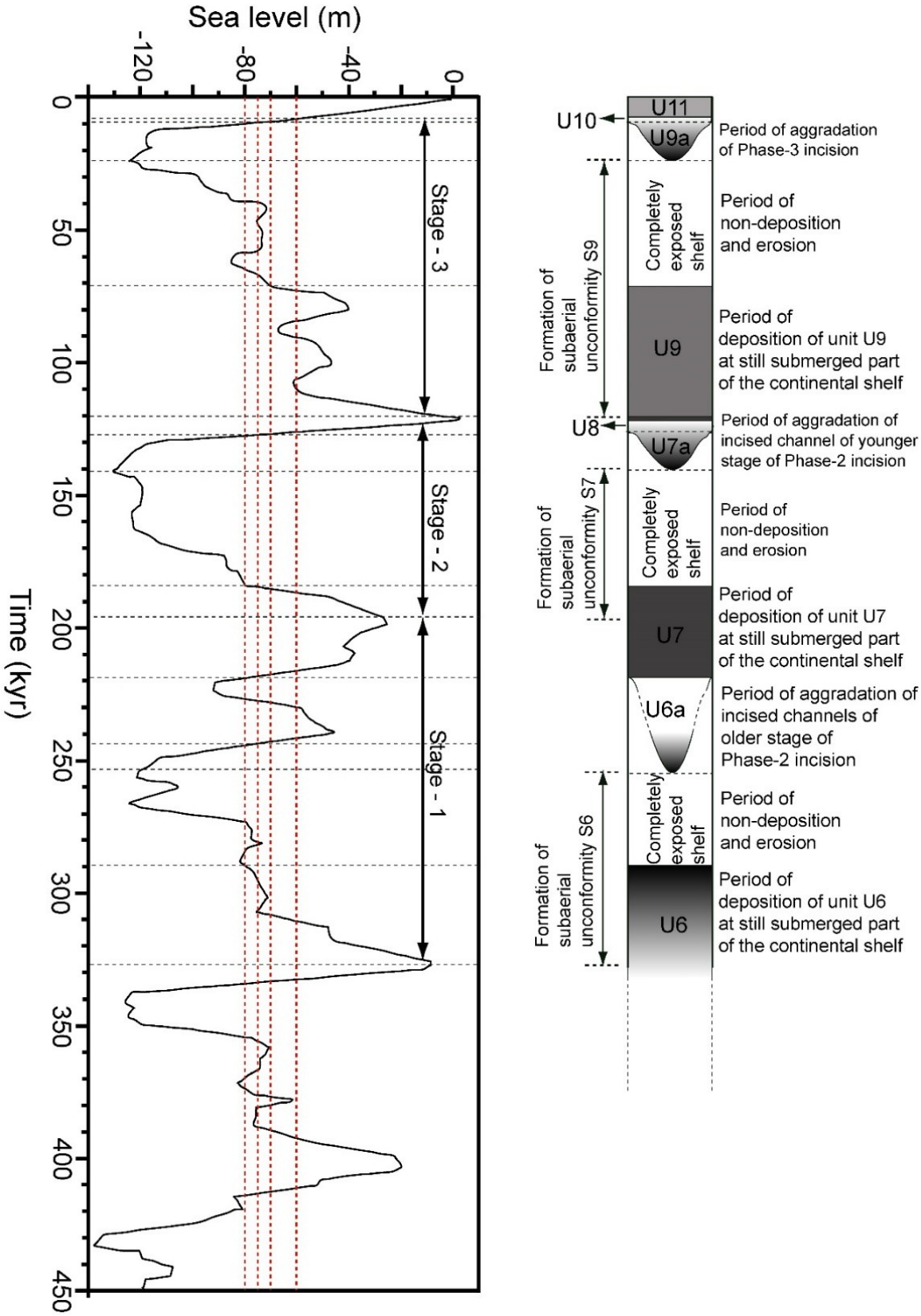

Figure 8.1. Correlation of sea-level curve of the last 450 kyr (modified by Rehak et al., 2010 from Siddal et al., 2003) with the identified sedimentary units (U6-U11).

on remnant of the highstand sediment deposits. During the incision processes, river channels through their enlarged catchment area continuously eroded the highstand deposits from the exposed region on one hand and started supplying it to still submerged region of the continental shelf on the other hand. As a result, deposition of sedimentary unit U6 beyond the rocky region commenced. During ~320 to 310 kyr BP, initially rivers might have been wider with wider flood prone area which progressively become narrower with further base level fall. The rocky basement in this region controlled the morphology of the then rivers. Later, with further sea-level fall, channel incisions started in the sedimentary region (please see Chapter 4, Section 4.3.1), away from the rocky region. In the sedimentary region, the channel morphology and its erosional capacity were controlled by the base level. At ~290 kyr BP, the study area was completely exposed and paleo-channels commenced incising sedimentary unit U6 (Chapter 4) in the deeper region of the exposed shelf (Fig. 8.1). With further sea level fall between ~270 and 255 kyr BP, the channels entrenched deeper and got matured. Their flood prone area became limited to their course in the study area from which they supplied the terrigenous sediments to further deeper region of the continental shelf. The study area remained exposed effectively between ~290 kyr BP and 220 kyr BP for a period of 50 kyrs. During this period, subaerial erosional processes working in this area caused almost complete erosion of the highstand sediment deposits of previous cycles. In subsequent sea level rise between ~220 kyr BP and 200 kyr BP, the transgressive sea might have eroded partially the sedimentary unit U6 and rose up to a level which was still ~25 m below the present sea-level. The sea-level rise caused channel filling with the terrigenous sediments. The rocky region of the study area was partially submerged and the channel retracted to the exposed part of the rocky platform. The transgression of sea resulted burial of remnant of sedimentary unit U6. Due to the transgression, the incised channel was filled with terrigenous sediment which resulted sedimentary unit U6a.

8.2.2 Stage-2 (~200 kyr to 120 kyr BP)

The second stage (Stage-2) deals with evolutionary history of the inner continental shelf of Goa between ~200 kyr and 120 kyr BP. As the sea remained ~25 m below the present sea-level between ~200 kyr BP and 195 kyr BP (Fig. 8.1), a coastline was developed on the rocky basement platform which was much inside seaward in comparison to the present day coastline. The channel which was incised during the last cycle of sea-level remained active at the partially submerged platform. The short period of highstand sea-level might have given rise to a highstand sediment deposition over the thin layer of transgressive deposit. Evolution of sedimentary unit U6 overlain by thin sedimentary layer formed due to sea-level transgression

gave rise to comparatively gentle surface which became available for fluvial incision for the next cycle of sea-level fluctuations. Commencement of sea-level fall at ~195 kyr BP restarted the whole process of migration of erosional and depositional environment. The evolution of the Late Pleistocene-Holocene continental shelf of the study area was affected severely due to rapid sea-level fall and subsequent rise during the Stage-2 as compared to the Stage-1 (Fig. 8.1). The sea-level fall during this stage took shortest time duration (~45 kyr) to reach the minimum level of sea (penultimate glacial maxima) as compared to sea-level fall during the Stage-1. The shorter duration of sea-level highstand and fall caused deposition of thin sedimentary unit U7 (see chapter 4) which got eroded during the subsequent sea level rise. Comparatively wide and gentle surface became available for the channel incision during this period. Rapid fall of the sea-level caused deep entrenched channel incisions with low flood prone area. Due to sea-level fall, the continental shelf in the study area remained exposed for a period of ~60 kyrs. During this period, the highstand sediment deposits again were almost completely eroded by the subaerial erosional processes. Sea-level transgression between ~140 kyr BP and 120 kyr BP caused evolution of sedimentary unit U7 which was buried under thin layer of transgressive sedimentary unit U8. Sea-level rise again caused channel in-filling with terrigenous sediments which resulted evolution of sedimentary unit U7a. The sea-level rose to a level which was higher than the present sea-level. It caused complete burial of the rocky platform and the incised channels. The higher sea-level generated a coastline which was located east of the present day coastline.

8.2.3 Stage-3 (~120 kyr BP to present)

Third and last stage (Stage-3) refers to the evolution of inner continental shelf of Goa between ~120 kyr BP to present. During this stage of evolution, higher order sea-level fluctuations were superimposed on sea-level fall which caused relatively slower rate of fall and multiple coastline transgression and regression events when sea-level was between ~40 and 60 m (Fig. 8.1). The rocky platform underwent partial submersion and emersion multiple times. Further, multiple incision and burial of paleo-channels took place which resulted deposition of sedimentary unit U9 and formation of a wider and gentler surface seawards, beyond the rocky platform. At ~70 kyr BP, the continental shelf was completely exposed. Channels started incising the wider and gentler exposed surface of the continental shelf. The incision during this stage was also punctuated by the higher order sea-level variations. The higher order sea-level fluctuations and weaker hydrological regime caused channel incision which were similar to anastomosed type

river channels. These channels had lower entrenchment capacity and were comparatively wider than the channel incisions of the last two stages. Later, rapid sea-level fall between ~40 kyr BP and ~20 kyr BP caused deeper entrenched incision beyond ~50 m water depth. Channels had comparatively lesser time to get matured. The subsequent sea transgression took place in steps, i.e. transgression up to some level followed by a short period of standstill. One such transgression and standstill caused partial erosion of sedimentary unit U9 and evolution of sedimentary unit U10 beyond ~55 m water depth. At several places, signature of this standstill is manifested in the form of beach ridges and sand bars at ~55 m water depth (see Chapter 7). Further rapid sea transgression at ~7.5 kyr BP caused partial erosion and burial of sedimentary unit U9 under very thin layer of transgressive deposits. From ~7 kyr BP to present, sea-level is at almost stillstand resulting highstand sediment deposit. The sea-level transgression from the early Holocene to present resulted formation of the sedimentary unit U11.

8.3 Conclusions

Integration of the results derived in the previous chapters allowed to articulate the Late Quaternary evolutionary history of the inner continental shelf of Goa. Paleo-shelf structure along with fluvial erosion and depositional processes controlled the extent and configuration of each evolving sedimentary units on the continental shelf. The inner continental shelf of the study area evolved in three major stages corresponding to last three glacial periods. First stage of evolution took place between ~325 kyr BP and ~200 kyr BP and sedimentary unit U6 and U6a were evolved. Sedimentary unit U6 evolved between ~320 kyr BP and ~220 kyr BP when the study area was exposed for subaerial erosion and deposition processes. The sedimentary unit U6 is made up of well-stratified homogeneous sediment deposits corresponding to the regressive and lowstand sea condition, whereas sedimentary unit U6a embodies mostly terrigenous sediments brought by the older channels of Phase-2 incisions during subsequent transgressive period (i.e. between 220 kyr BP and 200 kyr BP) of the sea-level.

Second stage of evolution took place between ~200 kyr BP and 120 kyr BP and sedimentary unit U7, U7a along with transgressive sedimentary unit U8 were evolved. Sedimentary unit U7 in the study area evolved between ~200 kyr BP and ~140 kyr BP. This sedimentary unit is again made up of well-stratified homogeneous sediment deposits corresponding to regressive and lowstand sea condition. Whereas sedimentary unit U7a is composed of terrigenous sediments brought by the younger channels of Phase-2 incisions during subsequent transgressive period

(i.e. between ~140 kyr BP and 120 kyr BP) of the sea-level. Rapid transgression of sea during this period generated a thin layer of transgressive sedimentary unit. The remains of this transgressive unit is referred as U8.

The third and final stage of evolution started at ~120 kyr BP with the subsequent sea-level fall. The sea-level fall in this stage of evolution was superimposed by higher order sea-level variations. The sea-level fall took place in stages which allowed multiple incisions and burial of river channels, and cyclic deposition and erosion of new sedimentary strata. The cyclic formation and subsequent erosion of strata is one of the reason for the preservation of sedimentary unit U8 deposited during the last transgression. The sedimentary unit U9, U9a, U10 and U11 evolved in the third stage of evolution. Sedimentary unit U9 in the study area, deposited during the sea-level fall between ~120 kyr BP and ~70 kyr BP. Whereas, sedimentary unit U9a contains terrigenous sediment deposits ranging from ~22 kyr BP to ~7 kyr BP. Sedimentary unit U10 deposited during episodic sea-level transgression in the early Holocene. Whereas, sedimentary unit U11 deposited during the sea-level rise between the early Holocene and present. It contains sediment deposits corresponding to initial transgressive to highstand sediment deposits.

Chapter 9
Summary and Conclusions

Present research work is based on analysis and interpretaion of High Resolution Shallow Seismic (HRSS) data to decipher the Late Pleistocene-Holocene evolutionary history and roles of endogenous and exogenous processes for the evolution of the inner continental shelf of Goa. It illustrates the role of paleo-fluvial channel incision process and fourth order sea-level fluctuations in the development of sedimentary architecture and paleo-basin. It significantly contributes to the high resolution seismic sequence stratigraphic analysis by providing a new and an alternate methodology to find out the period of formations of subaerial unconformities in the absence of costly long sediment cores. The results of the study provide new insights for the Holocene sedimentation processes and depositional rates on the inner continental shelf of Goa. Summary of the research work reported in the thesis and major conclusions derived are as follows.

9.1 Sedimentary architecture of inner continental shelf of Goa

The HRSS investigations provided reasonably sufficient information of sedimentary architecture for ~125 m thick sediment assemblage of the inner continental shelf of Goa. The important conclusions derived in the present study on the sedimentary architecture of the inner shelf of Goa are as follows:

(i) The continental shelf of Goa is a moderately sediment-starved type continental shelf. The terrigenous sediment supply ceases to a bare minimum at ~50 m water depth. Beyond this depth, a highly reflective sea bed is observed which doesn't allow penetration of high frequency acoustic waves. This low penetration is mainly attributed to the presence of increased amount of calcareous sand.

(ii) Entire sedimentary assemblage can be divided into eleven distinct stratigraphic units and three sub units corresponding to the eleven distinctively visible seismic units (U1 to U11)

and three sub-seismic units (U6a, U7a and U9a). The seismic units are bounded by their corresponding bounding surfaces (S1 to S11). Application of the concept of river base level on buried channels and correlation of incision depth with sea-level curve allowed to assign period of formation of some of the bounding surfaces and seismic units.

(iii) Out of eleven bounding surfaces, three surfaces were formed during the last three consecutive glacial periods. The surfaces represent subaerial unconformities S6, S7 and S9. The youngest unconformity (S9) was formed during the last glacial period between ~115 kyr BP and 10 kyr BP (MIS 5e to MIS 2). Whereas, the oldest subarerial unconformity (S6) was formed between ~320 kyr BP and 215 kyr BP. The subaerial unconformity (S7) was formed during penultimate glacial period between ~195 kyr BP and 125 kyr BP.

(iv) The subaerial unconformities were formed due to channel incisions during low stands of sea-level. The sedimentary strata on the inner continental shelf contains preserved channel incision signatures corresponding to more than three glacial periods. The results of the study allowed to conclude that the Late Quaternary inner continental shelf of Goa was evolved as a compound incised valley under the influence of glacio-eustatic sea-level variations. During each low stands of sea-level, ancestral rivers of Goa alongwith initial wave based scouring reworked the exposed continental shelf to such an extent that the entire highstand sediment assemblage was eroded.

9.2 Holocene sediment thickness on the inner continental shelf of Goa

Sequence stratigraphic analysis of the HRSS data allowed to infer that the youngest seismic unit U11 embodies most of the Holocene sediment assemblage. Correlation of seismic units with available Holocene sea-level curve of the west coast of India reveals that this sediment assemblage in the study area started depositing from the early Holocene. Maps depicting sediment thickness and mean sedimentation rates for the Holocene sediments are prepared, for the first time, using gridded data generated from the HRSS data and available Holocene sea-level curve. A gridded data and corresponding map for the Holocene transgressive surface is also generated in this study. Later, this gridded data was used to evaluate the roles of various coastal processes and paleo-basin structure for the observed Holocene sediment thickness distribution pattern on the inner continental shelf of Goa. The important conclusions on spatial distribution of the Holocene sediment thickness are as follows:

(i) Gridded data for sediment thickness revealed that a total of ~32.09 km^3 volume of sediments were deposited on the inner continental shelf between Chapora in the north and Ankola in the south from the early Holocene to the present.

(ii) The Holocene sediment thickness varies from 0.78 to 15.67 m. The thickness increases from coast to ~20 m water depth and thereafter decreases to ~2 m at ~50 m water depth. It remains almost constant (~2 m) beyond ~50 m water depth.

(iii) Sediment thickness along the coast (between the coast and 40 m water depth) initially increases from offshore Chapora to Canacona and then decreases sharply further southward. Beyond 45 m water depth, it does not show any significant trend.

(iv) Sediment thickness map revealed two conjoint high sedimentation zones between off Betul and Canacona.

(v) Analysis of paleo-basin structure and sediment distribution pattern revealed that there is no major role of distant terrigenous sediment source and longshore current in deposition of the Holocene sediment. Further, it establishes hinterland sediment source, present coastline configuration, basin structure along with paleo-fluvial process as major players for the observed sediment distribution pattern.

(vi) The gridded data for sediment thickness and sedimentation rates provide a clear picture of the sedimentation pattern of the study area. Comparison of sedimentation rates estimated in this study with previous sedimentological studies revealed that the sedimentation rates estimated from the gridded data are consistent and reliable.

9.3 Paleo-river channels

Analysis of HRSS data allowed to map buried channels on the inner continental shelf of Goa, carved by the ancestral rivers of the present day Mandovi and Zuari rivers. It revealed that the sedimentary assemblage on the inner continental shelf contains preserved channel incision signatures corresponding to more than three glacial periods. These buried channels were carved during the lowstands of the sea-level and were buried during each subsequent sea-level rise. Paleo-hydrologic environmental and glacio-eustatic sea-level variations alongwith evolving continental shelf had major control on the geomorphology of these buried channels. With each passing glacial period on comparatively wider continental shelf, the areal extent of the buried channels increased. The important conclusions derived from the study of buried channels are as follows:

(i) Observed channel incisions have been differentiated into three phases of incisions based on their period of formation and geomorphological character. Phase-1 incisions are older than ~330 kyr BP, whereas Phase-2 incisions are carved during ~320-125 kyr BP. Youngest channel incisions are sculptured during the last glacial period between ~110 and 10 kyr BP and belong to Phase-3 incisions.

(ii) With each passing sea-level cycle, channel systems became more sinuous and divergent seaward, and their areal extent increased. Thus, they evolved from straight river type (Phase-1) to ingrown meander (Phase-2) and then similar to anastomosing type (Phase-3). Unlike Phase-2 and Phase-1 incisions, Phase-3 incisions are incised in multiple estuarine and low energy fluvial conditions.

(iii) Comparison of computed hydraulic parameters of Phase-2 and Phase-3 incisions reveals that Phase-3 incisions were developed in lower hydraulic energy condition than the Phase-2 incisions.

(iv) Phase-2 channels had ~33% more mean bank full discharge than that of the Phase-3 channels. The mean depths of the Phase-2 incisions are almost double than that of Phase-3 incisions. This implies that hydrologic environment associated with penultimate and prior to penultimate glacial periods was stronger than that of the last glacial period. This also suggests that the Indian summer monsoon was stronger during the formative stage of Phase-2 incisions (~320-125 kyr BP) than that of Phase-3 (~110-10 kyr BP).

9.4 Other geomorphological features

HRSS data of the study area revealed signatures corresponding to paleo-coastline which might have been formed during a brief standstill period of transgressive sea during the Holocene. It also revealed the presence of geo-acoustic signatures corresponding to gas charged sediment zones. Analysis of HRSS data allowed to mark two different types of gas charged sediment zones on the inner continental shelf of Goa and facilitated to investigate the origin and distribution of these zones. The important conclusions drawn in the present study on the paleo-coastline and gas charged sediment zones are as follows:

(i) Observed seabed undulations which are marked with a sudden change in the seabed gradient are interpreted as sand ridges. These sand ridges are the remains of a stable paleo-coastline.

(ii) Careful analysis revealed that the sand ridges are located at ~55 m water depth and are ~2 to 4 km wide along the tracklines with relief ranging from ~2 to 6 m.

(iii) The sand ridges are further divided into two types of formation, (a) paleo-beaches, and (b) surf zone sand bars. Signatures of paleo-beaches are found at ~2 to 4 m higher level landward as compared to surf zone sand bars located seaward.

(iv) The paleo-beaches are inferred as the remains of a stable paleo-coastline which is located at ~35 km WSW of the present day coastline of the study area.

(v) Spatial distribution of gas charged sediment zones revealed two zones. Zone-1 has limited areal extent between ~8 and 30 m water depth in sheltered basin of the study area, whereas Zone-2 is distributed in the entire study area mostly between ~20 m and ~45 m water depth.

(vi) Lithological characteristics of the Late Pleistocene-Holocene sedimentary deposits controlled the distribution of gas charged sediments.

(vii) The source organic material as well as sediments of Zone-1 and Zone-2 were deposited in the Holocene and Late Pleistocene, respectively.

(viii) The biogenic gases in Zone-1 are confined within the Holocene sedimentary layers whereas, they are confined in Zone-2 below the Holocene-TS within the paleo-river bed or a layer just below the Holocene_TS or by both.

(ix) Gases in Zone-1 were formed by organic matter which was predominantly mangrove (intertidal vegetation) derived. The results of the study suggest that coastline configuration, long term longshore drift current pattern, Holocene rapid sea-level rise and lithological character of exposed intertidal zone had played a pivotal role in the formation and distribution of gas charged sediments in the Zone-1.

(x) Biogenic gases in Zone-2 were formed by organic matter which was predominantly derived by ancestral rivers through their course during different glacial periods of the Late Pleistocene. The distribution pattern of paleo-rivers and their hydraulic energy condition during the base level rise played an important role in the formation and distribution of gas charged sediments in Zone-2.

9.5 Evolution of inner continental shelf of Goa

Integration of inferences drawn from the sequence stratigraphic and geomorphologic analysis of the sedimentary architecture of the study area allowed to articulate the Late Quaternary evolutionary history of the inner continental shelf of Goa. The inner continental shelf of Goa was evolved under the combined effect of glacio-eustatic sea-level and paleo-environmental variations along with coastal erosion and depositional processes. Paleo-basin structure along

with fluvial erosion and depositional processes controlled the extent and configuration of each evolving sedimentary unit. The important conclusions drawn in the present study on the Late Quaternary evolutionary history of the inner continental shelf are as follows:

(i) The inner continental shelf of the study area was evolved from last 330 kyr in three major stages. These stages correspond to last three glacial periods.

(ii) First stage of evolution took place between ~325 and ~200 kyr BP. During this period, sedimentary unit U6 and U6a were evolved.

(iii) Sedimentary unit U6 in the study area evolved between ~320 kyr BP and 220 kyr BP when the study area was exposed. The sedimentary unit U6 is made up of well-stratified homogeneous sediment deposits corresponding to the regressive and lowstand sea condition, whereas sedimentary unit U6a embodies mostly terrigenous sediments brought by the older channels of Phase-2 incisions during subsequent transgressive period (i.e. between 220 kyr BP and 200 kyr BP) of the sea-level.

(iv) Second stage of evolution took place between ~200 kyr BP and 120 kyr BP. During this period sedimentary unit U7, U7a and transgressive sedimentary unit U8 were evolved.

(v) Sedimentary unit U7 in the study area evolved between ~200 and ~140 kyr BP. The sedimentary unit U7 is again made up of well-stratified homogeneous sediment deposits corresponding to regressive and lowstand sea condition. Whereas, sedimentary unit U7a is composed of terrigenous sediments brought by the younger channels of Phase-2 incisions during subsequent transgressive period (i.e. between ~140 and 120 kyr BP) of the sea-level. Rapid transgression of the sea during this period generated a thin layer of transgressive sedimentary unit. The remains of this transgressive unit is referred as U8.

(vi) Third and final stage of evolution started at ~120 kyr BP with the subsequent sea-level fall. The sea-level fall in this stage of evolution was superimposed by higher order sea-level variation which resulted in a relatively slower rate of sea-level fall. The sea-level fall took place in stages which allowed multiple incision and burial of river channels and also cyclic deposition and erosion of the newer sedimentary strata. The cyclic formation and subsequent erosion of strata is one of the reasons for the preservation of sedimentary unit U8 deposited during the last transgression.

(vii) The sedimentary units U9, U9a, U10 and U11 were deposited during the third stage of evolution.

(viii) Sedimentary unit U9 in the study area, deposited during the sea-level fall between ~120 and ~70 kyr BP. Whereas, sedimentary unit U9a contains terrigenous sediment deposit ranging from ~22 kyr BP to ~7 kyr BP. Sedimentary unit U10 deposited in the early

Holocene during the episodic Holocene sea-level transgression. Whereas, sedimentary unit U11 is deposited during the sea-level rise between the early Holocene to the present. It contains sediment deposits corresponding to initial transgressive to highstand sediment deposits during the Holocene.

References

Agrawal, A., 1990. Structure and tectonic evolution of western continental margin of India, Ph.D. dissertation, Univ. of N. C. at Chapel Hill, 117 pp.

Agrawal, A., Rogers, John J. W., 1992. Structure and tectonic evolution of the western continental margin of India: Evidence from subsidence studies for a 25-20 Ma plate reorganization in the Indian Ocean In: Bartholomew, M. J., Hyndman, D. W., Mogk, D. W., Mason, R. (Eds.), Basement Tectonics 8: Characterization and Comparison of Ancient and Mesozoic Continental Margins - Proceedings of the 8th International Conference on Basement Tectonics (Butte, Montana, 1988), Kluwer Academic Publishers, Dordrecht, The Netherlands, pp. 583-590.

Almeida, F., 1977a. Seabed survey of Angria Bank in the vicinity of proposed site for jacking of DV Sagar Samrat. Unpublished report, National Institute of Oceanography, 5 pp.

Almeida, F., 1977b. Survey of the proposed submarine pipeline route from Bombay floating light to Karanja-Butcher island and Trombay (Part I) 2. Unpublished report, National Institute of Oceanography, 69 pp.

Bahr, A., Wong, H.K., Yim, W.S., Huang, G., Ludmann, T., Chan, L.S., Thomas, W.R., 2005. Stratigraphy of quaternary inner-shelf sediments in Tai O Bay, Hong Kong, based on ground-truthed seismic profiles. Geo-Marine Letters, 25, 20-33.

Banakar, V.K., Mahesh, B.S., Burr, G. and Chodankar, A.R., 2010. Climatology of the Eastern Arabian Sea during the last glacial cycle reconstructed from paired measurement of foraminiferal δ 18 O and Mg/Ca. Quaternary Research, 73, 535-540.

Barrie, J.V., Conway, K.W., 2012. Paleogeographic reconstruction of Hecate Strait, British Columbia: changing sea levels and sedimentary processes reshape a glaciated shelf. Sediments, Morphology and Sedimentary Processes on Continental Shelves. International Association of Sedimentologists, 44, 29-46.

Bastia, R. and Radhakrishna, M., 2012. Chapter 6 - Subsurface geology, depositional history, and petroleum systems along the western offshore basins of India. In: R. Bastia and M. Radhakrishna (Eds.), Developments in Petroleum Science. Elsevier, 59, 269-317.

Beerbower, J.R., 1964. Cyclothems and cyclic depositional mechanisms in alluvial plain sedimentation. Kansas Geological Survey Bulletin, 169, 31-32.

Begin, Z.E.B., Meyer, D.F., Schumm, S.A., 1981. Development of longitudinal profiles of alluvial channels in response to base-level lowering. Earth Surface Processes and Landforms, 6, 49-68.

Besse, J., Courtillot, V., 1988. Paleogeographic maps of the continents bordering the Indian Ocean since the early jurassic. Journal of Geophysical Research, Solid Earth, 93, 11791-11808.

Best, A.I., Tuffin, M.D., Dix, J.K., Bull, J.M., 2004. Tidal height and frequency dependence of acoustic velocity and attenuation in shallow gassy marine sediments. Journal of Geophysical Research, Solid Earth, 109, 1-17.

Bhattacharya, G.C., Chaubey, A.K., 2001. Western Indian Ocean - a glimpse of the tectonic scenario. In: Sengupta, R., Desa, E. (Eds.). The Indian Ocean - A Perspective, Oxford & IBH Pub. Company Ltd., 691-729.

Bhattacharya, G.C., Chaubey, A.K., Murty, G.P.S., Srinivas, K., Sarma, K.V.L.N.S., Subrahmanyam, V., Krishna, K.S., 1994. Evidence for seafloor spreading in the Laxmi Basin, northeastern Arabian Sea. Earth and Planetary Science Letters, 125, 211-220.

Bhattacharya, G.C., Subrahmanyam, V., 1986. Extension of the Narmada-Son lineament on the continental margin off Saurashtra, Western India as obtained from magnetic measurements. Marine geophysical researches, 8, 329-344.

Bhattacharya, G.C., Yatheesh, V., 2015. Plate-tectonic evolution of the deep ocean basins adjoining the Western Continental Margin of India - A proposed model for the early opening scenario. In: Mukherjee S. (Ed.), Petroleum Geosciences: Indian Contexts, Springer International Publishing, Switzerland, 1-61.

Biswas, S.K., 1982. Rift basins in western margin of India and their hydrocarbon prospects with special reference to Kutch basin. American Association of Petroleum Geologists Bulletin, 66, 1497-1513.

Biswas, S.K., 1987. Regional tectonic framework, structure and evolution of the western marginal basins of India. Tectonophysics, 135, 307-327.

Biswas, S.K., Singh, N.K., 1988. Western continental margin of India and hydrocarbon potential of deep sea basins. 7th Offshore South Asia conference, Singapore. 170-181.

Blum, M. D., Tornqvist, T. E., 2000. Fluvial responses to climate and sea-level change: a review and look forward. Sedimentology, 47, 2-48.

Boetius, A., Wenzhöfer, F., 2013. Seafloor oxygen consumption fuelled by methane from cold seeps. Nature Geoscience, 6, 725.

Borole, D.V., Krishnaswami, S., Somayajulu, B.L.K., 1982. Uranium isotopes in rivers, estuaries and adjacent coastal sediments of western India: their weathering, transport and oceanic budget. Geochimica et Cosmochimica Acta, 46, 125-137.

Brizga, S.O., Finlayson, B.L., 1990. Channel avulsion and river metamorphosis: the case of the Thomson river, Victoria, Australia. Earth Surface Processes and Landforms, 15, 391-404.

Canfield, D.E., Kristensen, E., Thamdrup, B., 2005. Aquatic Geomicrobiology. Advances in marine biology. 48, 656 pp.

Canfield, D.E., Kristensen, E., Thamdrup, B., 2005. Aquatic Geomicrobiology. Advances inmarine biology. 48, 638.

Caratini, C., Bentaleb, I., Fontugne, M., Morzadec-Kerfourn, M.T., Pascal, J.P., Tissot, C., 1994. A less humid climate since ca. 3500 yr BP from marine cores off Karwar, western India. Palaeogeography, Palaeoclimatology, Palaeoecology, 109, 371-384.

Catuneanu, O., 2002. Sequence stratigraphy of clastic systems: concepts, merits, and pitfalls. Journal of African Earth Sciences, 35, 1-43.

Catuneanu, O., Abreu, V., Bhattacharya, J.P., Blum, M.D., Dalrymple, R.W., Eriksson, P.G. and others, 2009. Towards the standardization of sequence stratigraphy. Earth-Science Reviews, 92, 1-33.

Catuneanu, O., Galloway, W.E., Kendall, C.G.S.C., Miall, A.D., Posamentier, H.W., Strasser, A., Tucker, M.E., 2011. Sequence stratigraphy: methodology and nomenclature. Newsletters on Stratigraphy, 44, 173-245.

Cenki, B., Kriegsman, L.M., 2005. Tectonics of the Neoproterozoic Southern Granulite Terrain, South India. Precambrian Research, 138, 37–56.

Chand, S., Subrahmanyam, C., 2003. Rifting between India and Madagascar-mechanism and isostasy. Earth and Planetary Science Letters, 210, 317-332.

Chaubey, A.K., Bhattacharya, G.C., Murty, G.P.S., Srinivas, K., Ramprasad, T., Rao, D.G., 1998. Early tertiary seafloor spreading magnetic anomalies and paleo-propagators in the northern Arabian Sea. Earth and Planetary Science Letters, 154, 41-52.

Chaubey, A.K., Dyment, J., Bhattacharya, G.C., Royer, J.Y., Srinivas, K., Yatheesh, V., 2002a. Paleogene magnetic isochrons and palaeo-propagators in the Arabian and Eastern Somali basins, NW Indian Ocean. Geological Society of London, 195, 71-85.

Chaubey, A.K., Rao, D.G., Srinivas, K., Ramprasad, T., Ramana, M.V., Subrahmanyam, V., 2002b. Analyses of multichannel seismic reflection, gravity and magnetic data along a regional profile across the central-western continental margin of India. Marine Geology, 182, 303-323.

Chaumillon, E., Tessier, B., Reynaud, J.Y., 2010. Stratigraphic records and variability of incised valleys and estuaries along French coasts. Bulletin de la Societe geologique de France, 181, 75-85.

Chiocci, F. L. & Chivas, A. R., 2014. An overview of the continental shelves of the world. In: Chiocci, F.L., Chivas, A.R. (Eds.), Continental Shelves of the World: Their Evolution During the Last Glacio-Eustatic Cycle. Geological Society, London, Memoirs, 41, 1-5.

Clift, P.D., Hodges, K.V., Heslop, D., Hannigan, R., Van Long, H., Calves, G., 2008. Correlation of Himalayan exhumation rates and Asian monsoon intensity. Nature geoscience, 1, 875.

Davis, W.M., 1902. Baselevel, grade and peneplain. The Journal of Geology, 10, 77-111.

Dekas, A.E., Poretsky, R.S., Orphan, V.J., 2009. Deep-sea archaea fix and share nitrogen in methane-consuming microbial consortia. Science, 326, 422-426.

Dessai, A.G., 2011. The geology of Goa Group: revisited. Journal of the Geological Society of India, 78, 233.

Devaraju, T.C., Huhma, H., Sudhakara, T.L., Kaukonen, R.J., Alapieti, T.T., 2007. Petrology, geochemistry, model Sm-Nd ages and petrogenesis of the granitoids of the northern block of western Dharwar craton. Journal of the Geological Society of India, 70, 889.

Devaraju, T.C., Sudhakara, T.L., Kaukonen, R.J., Viljoen, R.P., Alapieti, T.T., Ahmed, S.A., Sivakumar, S., 2010. Petrology and geochemistry of greywackes from Goa-Dharwar sector, western Dharwar craton: implications for volcanoclastic origin. Journal of the Geological Society of India, 75, 465-487.

Devey, C.W., Stephens, W.E., 1991. Tholeiitic dykes in the Seychelles and the original spatial extent of the Deccan: Journal of the Geological Society, 148(6), 979-983.

Dury, G.H., 1976. Discharge prediction, present and former, from channel dimensions. Journal of Hydrology, 30, 219-245.

Dyment, J., 1998. Evolution of the Carlsberg ridge between 60 and 45 Ma: Ridge propagation, spreading asymmetry, and the Deccan-reunion hotspot. Journal of Geophysical Research: Solid Earth, 103, 24067-24084.

Faruque, B.M., Ramachandran, K.V., 2014. The continental shelf of western India. In: Chiocci, F.L., Chivas, A.R. (Eds.), Continental shelves of the world: their evolution during the last Glacio-Eustatic cycle. Geological Society of London, Memoirs 41, 213-220.

Fernandes, O. A., 2009. The evolving coast of Goa: a geological perspective. In: Mascarenhas. A., Kalavampara. G. (Eds.), Natural resources of Goa: A geological perspective, Geological Society of Goa, Goa, India, 25-34.

Fielding, C.R., Trueman, J.D., Dickens, G.R., Page, M., 2003. Anatomy of the buried Burdekin River channel across the Great Barrier Reef shelf: how does a major river operate on a tropical mixed siliciclastic/carbonate margin during sea level lowstand? Sedimentary Geology, 157, 291-301.

Fisk, M.R., Duncan, R.A., Baxter, A.N., Greenough, J.D., Hargraves, R.B., Tatsumi, Y., 1989. Reunion hotspot magma chemistry over the past 65 my: results from Leg 115 of the ocean drilling program. Geology, 17, 934-937.

Fleischer, P., Orsi, T., Richardson, M., Anderson, A., 2001. Distribution of free gas in marine sediments: a global overview. Geo-Marine Letters, 21, 103-122.

Flemings, P.B., Jordan, T.E., 1989. A synthetic stratigraphic model of foreland basin development. Journal of Geophysical Research, Solid Earth, 94, 3851-3866.

Floodgate, G.D., Judd, A.G., 1992. The origins of shallow gas. Continental Shelf Research, 12, 1145-1156.

Friedrichs, C.T., 1995. Stability shear stress and equilibrium cross-sectional geometry of sheltered tidal channels. Journal of Coastal Research, 11, 1062-1074.

Garcia-Gil, S., Vilas, F., Garcia-Garcia, A., 2002. Shallow gas features in incised-valley fills (Rıa de Vigo, NW Spain): a case study. Continental Shelf Research, 22, 2303-2315.

GSI (Geological Survey of India), 1996. Geological and Mineral Map of Goa. Government of India.

Gokul, A.R., Srinivasan, M.D., Gopalakrishnan, K., Viswanathan, L.S., 1985. Stratigraphy and structure of Goa. Proceeding of Seminar, Earth Resources for Goa's Development. Geological Survey of India, 1-13.

Gombos Jr, A.M., Powell, W.G., Norton, I.O., 1995. The tectonic evolution of western India and its impact on hydrocarbon occurrences: an overview. Sedimentary Geology, 96, 119-129.

Gopalkrishnan, K., 1976. Canacona granite and its relation to the schistose rocks, Canacona taluka, Goa. Proceeding of Seminar Precambrian geology of the peninsular India, Geol. Surv. India Misc. Publ, 23, 375-379.

Goswami, B.N., Shukla, J., Schneider, E.K., Sud, Y.C., 1984. Study of the dynamics of the intertropical convergence zone with a symmetric version of the GLAS climate model. Journal of the Atmospheric Sciences, 41, 5-19.

Grasby, S.E., Chen, Z., Issler, D., Stasiuk, L., 2009. Evidence for deep anaerobic biodegradation associated with rapid sedimentation and burial in the Beaufort-Mackenzie basin, Canada. Applied Geochemistry, 24, 536-542.

Green, A.N., 2009. Palaeo-drainage, incised valley fills and transgressive systems tract sedimentation of the northern KwaZulu-Natal continental shelf, South Africa, SW Indian Ocean. Marine Geology, 263, 46-63.

Greene Jr, D.L., Rodriguez, A.B., Anderson, J.B., 2007. Seaward-branching coastal-plain and piedmont incised-valley systems through multiple sea-level cycles: late quaternary examples from Mobile bay and Mississippi sound, U.S.A. Journal of Sedimentary Research, 77, 139-158.

Gunnell, Y., Fleitout, L., 2000. Morphotectonic evolution of the Western Ghats, India. In: Summerfield, M. (Ed.), Geomorphology and global tectonics. Chichester: John Wiley & Sons, 321-338.

Hanebuth, T.J.J., Stattegger, K., Bojanowski, A., 2009. Termination of the last glacial maximum sea-level lowstand: the Sunda-shelf data revisited. Global and Planetary Change, 66, 76-84.

Harinadha Babu, P., Vidyadharan, K.T., Jayaprakash, A.V., 1981. Geology and mineral resources of Karnataka and Goa. Miscellaneous Publication. Geological Survey of India, 30, 1-68.

Harris, P.T., Alo, B., Bera, A., Bradshaw, M., Coakley, B.J., Grosvik, B.E., Lourenço, N., Moreno, J.R., Shrimpton, M., Simcock, A., Singh, A., 2015. Offshore hydrocarbon industries. In: The first global integrated marine assessment world. Ocean Assessment I. United Nations World Ocean Assessment, Oxford University Press, Oxford, Ch-21, 1-38.

Harris, P.T., Macmillan-Lawler, M., 2016. Global overview of continental shelf geomorphology based on the SRTM30_PLUS 30-Arc Second Database. In: Finkl, C.W., Makowski, C. (Eds.), Seafloor mapping along continental shelves. Springer International Publishing Switzerland, 169-190.

Harris, P.T., Macmillan-Lawler, M., Rupp, J., Baker, E.K., 2014. Geomorphology of the oceans. Marine Geology, 352, 4-24.

Hashimi, N.H., Kldwai, R.M., Nair, R.R., 1978. Grain-size & Coarse-fraction Studies of Sediments between Vengurla & Mangalore on the Western Continental Shelf of India. Indian Journal of Marine Sciences, 7, 231-238.

Hashimi, N.H., Nigam, R., Nair, R.R., Rajagopalan, G., 1995. Holocene sea level fluctuations on western Indian continental margin: an update. Journal of the Geological Society of India, 46,157-162.

Hathaway, J.C., Poag, C.W., Valentine, P.C., Manheim, F.T., Kohout, F.A., Bothner, M.H., Miller, R.E., Schultz, D.M., Sangrey, D.A., 1979. US Geological Survey core drilling on the Atlantic shelf. Science, 206, 515-527.

Hinrichs, K.U., Boetius, A., 2002. The anaerobic oxidation of methane: new insights in microbial ecology and biogeochemistry. In: Wefer, G., Billett, D., Hebbeln, D., Jorgensen, B.B., Schluter, M., Van, W.T. (Eds.), Ocean margin systems. Springer-Verlag, Berlin, Heidelberg, 457-477.

Hovland, M., Judd, A.G., 1992. The global production of methane from shallow submarine sources. Continental Shelf Research, 12, 1231-1238.

Iwuoha, P.O., Adiela, P.U., Nwannah, C.C., Okeke, O.C., 2016. Sediment source and transport in river channels: Implications for river structures. The International Journal of Engineering and Science, 5, 19-26.

IHO (International Hydrographic Organization), 2008. IHO Standards for Hydrographic Surveys, 5th edition, February 2008. Monaco, International Hydrographic Bureau, 28pp.

Johnston, R.H., 1983. The saltwater-freshwater interface in the tertiary limestone aquifer, southeast Atlantic outer-continental shelf of the U.S.A. Journal of Hydrology, 61, 239-249.

Judd, A., Davies, G., Wilson, J., Holmes, R., Baron, G., Bryden, I., 1997. Contributions to atmospheric methane by natural seepages on the UK continental shelf. Marine Geology, 137, 165-189.

Judd, A., Hovland, M., 2007. Seabed fluid flow: the impact on geology, biology and the marine environment. Cambridge University Press, New York.

Kale, V.S., Rajaguru, S.N., 1985. Neogene and Quaternary transgressional history of the west coast of India: an overview. Bulletin of the Deccan College Research Institute, 44,153-167.

Kale, V.S., Shejwalkar, N., 2008. Uplift along the western margin of the Deccan Basalt Province: Is there any geomorphometric evidence? Journal of Earth System Science, 117, 959-971.

Karisiddaiah, S.M. and Veerayya, M., 1994. Methane-bearing shallow gas-charged sediments in the eastern Arabian Sea: a probable source for greenhouse gas. Continental Shelf Research, 14(12), pp.1361-1370.

Karisiddaiah, S.M., Veerayya, M., Vora, K.H. and Wagle, B.G., 1993. Gas-charged sediments on the inner continental shelf off western India. Marine Geology, 110(1-2), pp.143-152.

Karisiddaiah, S.M., Veerayya, M., Vora, K.H., 2002. Seismic and sequence stratigraphy of the central western continental margin of India: late-quaternary evolution. Marine Geology, 192, 335-353.

Karisiddaiah, S.M. and Veerayya, M., 2002. Occurrence of pockmarks and gas seepages along the central western continental margin of India. Current Science, 82(1), 52-57.

Kastner, M., Elderfield H., Martin, J.B., Suess, E., Kvenvolden, K.A., Garrison, R.E., 1990. Diagenesis and interstitial water chemistry at the Peruvian continental margin - major constituents and strontium isotopes. Proceedings of the Ocean Drilling Program, Scientific Results. 112, 413-440.

Kessarkar, P.M., Rao, V.P., Ahmad, S.M., Babu, G.A., 2003. Clay minerals and Sr–Nd isotopes of the sediments along the western margin of India and their implication for sediment provenance. Marine Geology, 202, 55-69.

Khare, N., Nigam, R., Hashimi, N. H., 2008. Revealing monsoonal variability of the last 2,500 years over India using sedimentological and foraminiferal proxies. Facies, 54, 167-173.

Kolla, V., Coumes, F., 1990. Extension of structural and tectonic trends from the Indian subcontinent into the eastern Arabian Sea. Marine and petroleum Geology, 7, 188-196.

Kong, X., Liu, J., Du, Y., Wen, C., Xu, G., 2011. Seismic geomorphology of buried channel systems in the western south Huanghai sea: retrodiction for paleoenvironments. Acta Oceanologica Sinica, 30, 47-58.

Krishna, K.S., Rao, D.G., Murty, G.P.S., Ramana, Y.V., 1989. Sound velocity, density, and related properties along a transect across the Bay of Bengal. Geo-Marine Letters, 9, 95-102.

Krishnan, M.S., I968. Geology of India and Burma. Higginbotham (P) Limited, Madras, 536 pp.

Kumar, P., Chaubey, A.K., 2019. Extension of flood basalt on the northwestern continental margin of India. Journal of Earth System Science, 128, 81.

Kumar, R., 1985. Fundamentals of historical geology and stratigraphy of India. Wiley 524 pp.

Labaune, C., Tesson, M., Gensous, B., Parize, O., Imbert, P., Delhaye-Prat, V., 2010. Detailed architecture of a compound incised valley system and correlation with forced regressive wedges: example of Late Quaternary Têt and Agly rivers, western Gulf of Lions, Mediterranean Sea, France. Sedimentary Geology, 223, 360-379.

Leopold, L.B., Wolman, M.G., Miller, J.P., 1964. Fluvial processes in geomorphology. Freeman, W.H. and Company, San Francisco, California, 522 pp.

Lericolais, G., Auffret, J.P., Bourillet, J.F., 2003. The quaternary channel river: seismic stratigraphy of its palaeo-valleys and deeps. Journal of Quaternary Science, 18, 245-260.

Levy, J-P., 2000. The United Nations convention on the law of the sea. In: Cook, P. J., Carleton, C., (Eds.), Continental shelf limits: The scientific and legal interface. Oxford, Oxford University Press, 8-16.

Lisiecki, L.E., Raymo, M.E., 2005. A pliocene-pleistocene stack of 57 globally distributed benthic δ18O records. Paleoceanography, 20, 1-17.

Liu, S., Goff, J.A., Austin Jr, J.A., 2017. Seismic morphology and infilling structure of the buried channel system beneath the inner shelf off western Long island, New York: accessing clues to palaeo-estuarine and coastal processes. Marine Geology, 387, 12-30.

Mahadevan, T.M., 1994. Deep continental structure of India: a review. Geological Survey of India, Memoir 28, 348.

Makaske, B., 2001. Anastomosing rivers: a review of their classification, origin and sedimentary products. Earth-Science Reviews, 53, 149-196.

Malod, J.A., Droz, L., Kemal, B.M., Patriat, P., 1997. Early spreading and continental to oceanic basement transition beneath the Indus deep-sea fan: northeastern Arabian Sea. Marine Geology, 141, 221-235.

Malone, M.J., Claypool, G., Martin, J.B., Dickens, G.R., 2002. Variable methane fluxes in shallow marine systems over geologic time: the composition and origin of pore waters and authigenic carbonates on the New Jersey shelf. Marine Geology, 189, 175-196.

Manjunatha, B.R., Shankar, R., 1992. A note on the factors controlling the sedimentation rate along the western continental shelf of India. Marine Geology, 104, 219-224.

Marr, J.G., Swenson, J.B., Paola, C., Voller, V.R., 2000. A two-diffusion model of fluvial stratigraphy in closed depositional basins. Basin Research, 12, 381-398.

Marzin, C., Kallel, N., Kageyama, M., Duplessy, J.C., Braconnot, P., 2013. Glacial fluctuations of the Indian monsoon and their relationship with North Atlantic climate: new data and modelling experiments. Climate of the Past, 9, 2135-2151.

Mascarenhas, A., 1997. Significance of peat on the western continental shelf of India. Journal Geological Society of India, 49, 145-152.

Mazumdar, A., Peketi, A., Dewangan, P., Badesab, F., Ramprasad, T., Ramana, M. V., Patil, D.J., Dayal, A., 2009. Shallow gas charged sediments off the Indian west coast: genesis and distribution. Marine Geology, 267, 71-85.

McKenzie, D., Sclater, J.G., 1971. The evolution of the Indian ocean since the late cretaceous. Geophysical Journal International, 24, 437-528.

Megonigal, J.P., Hines, M.E., Visscher, P.T., 2004. Anaerobic metabolism: linkages to trace gases and aerobic processes. In: Schlessinger, W.H. (Ed), Elsevier-Pergamon, Oxford, UK, 317-424.

Menier, D., Tessier, B., Proust, J. N., Baltzer, A., Sorrel, P., Traini, C., 2010. The holocene transgression as recorded by incised-valley infilling in a rocky coast context with low sediment supply (southern Brittany, western France). Bulletin de la Societe Geologique de France, 181, 115-128.

Menier, D., Estournès, G., Mathew, M., Ramkumar, M., Briend, C., Siddiqui, N., Traini, C., Pian, S., Labeyrie, L., 2016. Relict geomorphological and structural control on the coastal sediment partitioning, north of Bay of Biscay. Z. für Geomorphologie 60, 67–74.

Michael, L., Rao, D. G., Krishna, K. S., Vora, K. H., 2009. Late quaternary seismic sequence stratigraphy of the gulf of Kachchh, northwest of India. Journal of Coastal Research, 25, 459-468.

Miles, P.R., Roest, W.R., 1993. Earliest sea-floor spreading magnetic anomalies in the north Arabian Sea and the ocean-continent transition. Geophysical Journal International, 115, 1025-1031.

Miller, M.C., McCave, I.N., Komar, P., 1977. Threshold of sediment motion under unidirectional currents. Sedimentology, 24, 507-527.

Mohan, M., 1985. Geohistory analysis of Bombay high region, Mar. Pet. Geol., 2,350-360.

Mora, G., 2005. Isotope-tracking of pore water freshening in the fore-arc basin of the Japan Trench. Marine Geology, 219, 71-79.

Morgan, L.K., Werner, A.D., Patterson, A.E., 2018. A conceptual study of offshore fresh groundwater behaviour in the Perth basin (Australia): modern salinity trends in a prehistoric context. Journal of Hydrology, Regional Studies, 19, 318-334.

Naini, B.R., Talwani, M., 1983. Structural framework and the evolutionary history of the continental margin of western India. In: Watkins, J.S., Drake, C.L. (Eds.), Studies in continental margin geology. American Association of Petroleum Geologists Memoir, 34, 167-191.

Nair, R.R., 1975. Nature & origin of small scale topographic prominences on the western continental shelf of India. Indian Journal of Geo-Marine Sciences, 4, 25-29.

Nair, R.R., Hashimi, N.H., Kidwai, R.M., Guptha, M.V.S., Paropkari, A.L., Ambre, N.V., Muralinath, A.S., Mascarenhas, A., D'Costa, G.P., 1978. Topography & sediments of the western continental shelf of India - Vengurla to Mangalore. Indian Journal of Geo-Marine Sciences, 7, 224-230.

Nair, R.R., Pylee, A., 1968. Size distribution and carbonate content of the sediments of the western shelf of India. Bulletin of National Institute of Sciences of India, 38, 411-420.

Nambiar, A.R., Rajagopalan, G., 1995. Radiocarbon dates of sediment cores from inner continental shelf off Taingapatnam, southwest coast of India. Current Science, 68, 1133-11137.

Nambiar, A.R., Rajagopalan, G., Rao, B.R.J., 1991. Radiocarbon dates of sediment cores from inner continental shelf off Kaiwar, West coast of India. Current Science, 61, 353-354.

Nigam, R., 1988. Fluctuating monsoonal precipitation as revealed by foraminiferal variations in a core from shelf regime off Karwar (India). Current Science, 57, 490-491.

Nigam, R., Khare, N., 1995. Significance of correspondence between river discharge and proloculus size of benthic Foraminifera in paleomonsoonal studies. Geo-Marine Letters, 15, 45-50.

Nigam, R., Khare, N., Borole, D. V., 1992. Can benthic foraminiferal morpho-groups be used as indicators of paleomonsoonal precipitation? Estuarine, Coastal and Shelf Science, 34, 533-542.

Nigam, R., Khare, N., Nair, R. R., 1995, Foraminiferal evidences for 77-year cycles of droughts in India and its possible modulation by the gleissberg solar cycle. Journal of Coastal Research, 11, 1099-1107.

Nigam, R., Nair, R. R. 1989. Cyclicity in monsoon. Bulletin of Sciences, 5, 42-44.

Nordfjord, S., Goff, J.A., Austin Jr, J.A., Sommerfield, C.K., 2005. Seismic geomorphology of buried channel systems on the New Jersey outer shelf: assessing past environmental conditions. Marine Geology, 214, 339-364.

Nordfjord, S., Goff, J.A., Austin Jr., J.A., Gulick, S.P.S., Galloway, W.E., 2006. Seismic facies of incised valley-fills, New Jersey continental shelf: implications for erosion and preservation processes acting during late Pleistocene/Holocene transgression. Journal of Sedimentary Research, 76, 1284–1303.

Norton, I.O., Sclater, J.G., 1979. A model for the evolution of the Indian Ocean and the breakup of Gondwanaland. Journal of Geophysical Research, Solid Earth, 84, 6803-6830.

Oteri, A.U., 1988. Electric log interpretation for the evaluation of salt water intrusion in the eastern Niger delta. Hydrological Sciences Journal, 33, 19-30.

Pandarinath, K., Narayana, A.C., Yadava, M.G., 1998. Radiocarbon dated sedimentation record up to 2 ka BP on the inner continental shelf off Mangalore, south-west coast of India. Current Science, 75, 730-732.

Pandarinath, K., Shankar, R., Yadava, M.G., 2001. Late quaternary changes in sea level and sedimentation rate along the SW coast of India: evidence from radiocarbon dates. Current Science, 81, 594-600.

Pandarinath, K., 2009. Clay minerals in SW Indian continental shelf sediment cores as indicators of provenance and palaeomonsoonal conditions: a statistical approach. International Geology Review, 51, 145-165.

Pant, G.B., Parthasarathy, S.B., 1981. Some aspects of an association between the southern oscillation and Indian summer monsoon. Archives for Meteorology, Geophysics and Bioclimatology, 29, 245-252.

Paola, C., 2000. Quantitative models of sedimentary basin filling. Sedimentology, 47, 121-178.

Paola, C., Heller, P.L., Angevine, C.L., 1992. The large-scale dynamics of grain-size variation in alluvial basins, 1. Theory. Basin Research, 4, 73-90.

Patnaik, R., Gupta, A.K., Naidu, P.D., Yadav, R.R., Bhattacharyya, A., Kumar, M., 2012. Indian monsoon variability at different time scales: marine and terrestrial proxy records. Proceedings of the Indian National Science Academy, 78, 535-547.

Person, M., Dugan, B., Swenson, J.B., Urbano, L., Stott, C., Taylor, J., Willett, M., 2003. Pleistocene hydrogeology of the Atlantic continental shelf, New England. Geological Society of America Bulletin, 115, 1324-1343.

Person, M., Marksamer, A., Dugan, B., Sauer, P.E., Brown, K., Bish, D., Licht, K.J., Willett, M., 2011. Use of a vertical Δ 18 O profile to constrain hydraulic properties and recharge rates across a glacio-lacustrine unit, Nantucket Island, Massachusetts, USA. Hydrogeology Journal, 20, 325-336.

Post, V.E., Groen, J., Kooi, H., Person, M., Ge, S., Edmunds, W.M., 2013. Offshore fresh groundwater reserves as a global phenomenon. Nature, 504, 71-78.

Premchitt, J., Rad, N.S., To, P., Shaw, R., James, J.W.C., 1992. A study of gas in marine sediments in Hong Kong. Continental Shelf Research, 12, 1251-1264.

Ramana, M.V., Desa, M.A., Ramprasad, T., 2015. Re-examination of geophysical data off northwest India: Implications to the late cretaceous plate tectonics between India and Africa. Marine Geology, 365, 36-51.

Rao, D.G., 1984. Marine magnetic anomalies off Ratnagiri, Western continental shelf of India. Marine geology, 61,103-110.

Rao, P.S., 1989. Sonograph patterns of the central western continental shelf of India. Journal of Coastal Research, 5, 725-736.

Rao, T. C. S., 1977. Survey of the proposed submarine pipeline route from Bombay floating light to Karanja Island (Part II) 2. Unpublished report, National Institute of Oceanography, 54 pp.

Rao, V. P., Montaggioni, L., Vora, K. H., Almeida, F., Rao, K. M., Rajagopalan, G., 2003. Significance of relic carbonate deposits along the central and southwestern margin of India for late quaternary environmental and sea level changes. Sedimentary Geology, 159, 95-111.

Rao, V.P., 1991. Clay mineral distribution in the continental shelf and slope o! Saurashtra, west coast of India. Indian Journal of Marine Sciences, 20, 1-6.

Rao, V.P., Rao, B.R., 1995. Provenance and distribution of clay minerals in the sediments of the western continental shelf and slope of India. Continental Shelf Research, 15, 1757-1771.

Rao, V.P., Veerayya, M., 1996. Submarine terrace limestones from the continental slope off Saurashtra-Bombay: evidence of late quaternary neotectonic activity. Current Science, 71, 36-41.

Rao, V.P., Wagle, B.G., 1997. Geomorphology and surficial geology of the western continental shelf and slope of India: a review. Current Science, 73, 330-350.

Reeburgh, W.S., 2007. Oceanic methane biogeochemistry. Chemical Reviews, 107, 486-513.

Rehak, K., Niedermann, S., Preusser, F., Strecker, M.R., Echtler, H.P., 2010. Late Pleistocene landscape evolution in south-central Chile constrained by luminescence and stable cosmogenic nuclide dating. Bulletin, 122, 1235-1247.

Reimer, P.J., Bard, E., Bayliss, A., Beck, J.W., Blackwell, P.G., Ramsey, C.B., Buck, C.E., Cheng, H., Edwards, R.L., Friedrich, M., Grootes, P.M., 2013. IntCal13 and Marine13 radiocarbon age calibration curves 0–50,000 years cal BP. Radiocarbon, 55(4), 1869-1887.

Reimer, P.J., Bard, E., Bayliss, A., Beck, J.W., Blackwell, P.G., Ramsey, C.B., Buck, C.E., Cheng, H., Edwards, R.L., Friedrich, M., Grootes, P.M., 2013. IntCal13 and Marine13 radiocarbon age calibration curves 0–50,000 years cal BP. Radiocarbon, 55, 869-1887.

Ribberink, J.S., Van der Sande, J.T.M., 1985. Aggradation in rivers due to overloading-analytical approaches. Journal of Hydraulic Research, 23, 273-283.

Rijil. K., 2011. Shelf-slope configuration along the Western Continental Margin of India. Unpublished report, National Institute of Oceanography, 50 pp.

Roberts, C.M., Hawkins, J.P., 1999. Extinction risk in the sea. Trends in Ecology & Evolution, 14, 241-246.

Rosgen, D.L., 1994. A classification of natural rivers. Catena, 22, 169-199.

Rostek, F., Ruhlandt, G., Bassinot, F.C., Muller, P.J., Labeyrie, L.D., Lancelot, Y., Bard, E., 1993. Reconstructing sea surface temperature and salinity using δ18O and alkenone records. Nature, 364, 319-321.

Royer, J.Y., Chaubey, A.K., Dyment, J., Bhattacharya, G.C., Srinivas, K., Yatheesh, V., Ramprasad, T., 2002. Paleogene plate tectonic evolution of the Arabian and eastern Somali basins. Geological Society of London, 195, 7-23.

Saraswat, R., Lea, D.W., Nigam, R., Mackensen, A., Naik, D.K., 2013. Deglaciation in the tropical Indian ocean driven by interplay between the regional monsoon and global teleconnections. Earth and Planetary Science Letters, 375, 166-175.

Schumm, S.A., 1968. River adjustment to altered hydrologic regimen, Murrumbidgee river and paleochannels, Australia. U.S Government Printing Office, 598, 1-65.

Schumm, S.A., 1993. River response to baselevel change: implications for sequence stratigraphy. The Journal of Geology, 10, 279-294.

Schwab, W.C., Gayes, P.T., Morton, R.A., Driscoll, N.W., Baldwin, W.E., Barnhardt, W.A. and others, 2009. Coastal change along the shore of northeastern South Carolina-The South Carolina coastal erosion study. U.S. Geological Survey. 87pp.

Shareef, N. M., Mukhopadyay R., Sivasamy, A., Neelakantarama, J. M., Prasad, P. D., Varghese, S., 2016. Delineation of buried channels of Bharathappuzha by single-channel shallow seismic survey. Current Science, 110, 153-156

Shetye, S.R., Gouveia, A.D., Shenoi, S.S.C., Sundar, D., Michael, G.S., Almeida, A.M., Santanam, K., 1990. Hydrography and circulation off the west coast of India during the southwest monsoon 1987. Journal of Marine Research, 48, 359-378.

Shetye, S.R., Gouveia, A.D., Singbal, S.Y., Naik, C.G., Sundar, D., Michael, G.S., Nampoothiri, G., 1995. Propagation of tides in the Mandovi-Zuari estuarine network. Proceedings of the Indian Academy of Sciences-Earth and Planetary Sciences, 104, 667-682.

Shetye, S.R., Shankar, D., Neetu, S., Suprit, K., Michael, G.S., Chandramohan, P., 2007. The environment that conditions the Mandovi and Zuari estuaries. In: Shetye, S.R., Kumar, M.D., Shankar, D. (Eds.), The Mandovi and Zuari estuaries. National Institute of Oceanography, India, 1-27.

Shetye, S.R., Shenoi, S.S.C., Gouveia, A.D., Michael, G.S., Sundar, D., Nampoothiri, G., 1991. Wind-driven coastal upwelling along the western boundary of the Bay of Bengal during the southwest monsoon. Continental Shelf Research, 11, 1397-1408.

Siddall, M., Rohling, E.J., Almogi-Labin, V., Hemleben, Ch., Meischner, D., Schmelzer, I., Smeed, D.A., 2003. Sea-level fluctuations during the last glacial cycle. Nature 423, 853-858.

Siddiquie, H.N., 1976a. Survey of the proposed submarine pipeline route from Bombay High to Bombay. Unpublished report, National Institute of Oceanography, 128 pp.

Siddiquie, H.N., 1976b. Location of lost well heads in the Bombay High oil felds. Unpublished report, National Institute of Oceanography, 9 pp.

Siddiquie, H.N., Rao, D.G., Veerayya, M., Wagle, B.G., 1980. Acoustic masking due to gases in shallow seismic profiling on the shelf off Bombay.

Siddiquie, H.N., Rao, D.G., Vora, K.H., Topgi, R.S., 1981b. Acoustic masking in sediments due to gases on the western continental shelf of India. Marine Geology, 39, M27-M37.

Siddiquie, H.N., Rao, D.G., Wagle, B.G., Vora, K.H., Gujar, A.R., Karisiddaiah, S.M., 1981a. The continental shelf in the southern Gulf of Khambhat-an evaluation of the seabed for constructions. Proceedings of First Indian Conference in Ocean Engineering, IIT Madras, India, 1, 35-42.

Singh, N. K., Lal, N. K., 1993. Geology and petroleum prospects of the Konkan-Kerala basin. In: Biswas S. K. et al. (Eds), Proceeding second seminar on petroliferous basins of India, Indian Petroleum Publishers, Dehra Dun, India, 2,461-469.

Singh, P., Jammu, B., 2008. A Textbook of Engineering and General Geology. S.K. Kataria & Sons, 591 pp.

Sinha, R., Sripriyanka, K., Jain, V., Mukul, M., 2014. Avulsion threshold and planform dynamics of the Kosi River in north Bihar (India) and Nepal: A GIS framework. Geomorphology 216, 157–170.

Smith, R. W., Taft, G., 2000. Legal aspects of the continental shelf. In: Cook, P. J., Carleton, C., (Eds.), Continental shelf limits: The scientific and legal interface. Oxford, Oxford University Press, 17-24.f

Sternberg, R.W., 1972. Predicting initial motion and bedload transport of sediment particles in the shallow marine environment. In: Swift, D.J.P., Duane, D.B., Pilkey, O.H., Eds.), Shelf Sediment Transport. Dowden, Hutchinson and Ross, Stroudsberg, Pa., 61-82.

Stuiver, M., Reimer, P.J., Reimer, R.W., 2017. CALIB 7.1 [WWW program] at http://calib.org. Last accessed, 8-24.

Subba Raju, L.S., Krishna, K.S., Chaubey, A.K., 1991. Buried late pleistocene fluvial channels on the inner continental shelf off Vengurla, west coast of India. Journal of Coastal Research, 7, 509-516.

Subba Raju, L.V., Wagle, B.G., 1996. Shallow seismic and geomorphic expression of buried wave-cut terrace and erosional valleys off Redi, west coast of India. J. Coast. Res., 12(1), 205-210.

Subrahmanya, K.R., 1987. Evolution of the Western Ghats, India-a simple model. Journal of Geological Society of India, 29, 446-449.

Subrahmanya, K.R., 1998. Tectono-magmatic evolution of the west coast of India. Gondwana Research, 1, 319-327.

Subrahmanyam, V., Ramana, M.V., Rao, D.G., 1993. Reactivation of Precambrian faults on the southwestern continental margin of India: evidence from gravity anomalies. Tectonophysics, 219,327-339.

Subrahmanyam, V., Rao, D.G., Ramana, M.V., Krishna, K.S., Murty, G.P.S., Gangadhara, M., 1995. Structure and tectonics of the southwestern continental margin of India. Tectonophysics, 249(3), 267-282.

Symonds, P. A., Eldholm, o., Mascle, J., Moore, G. F., 2000. Characteristics of continental margins. In: Cook, P. J., Carleton, C., (Eds.), Continental shelf limits: The scientific and legal interface. Oxford, Oxford University Press, 25-63.

Tesson, M., Labaune, C., Gensous, B., Delhaye-Prat, V., 2010. Quaternary compound incised valleys of the Roussillon coast (SE France): correlation of seismic data with core data. Bulletin de la Societe Geologique de France, 181, 183-196.

Tesson, M., Labaune, C., Gensous, B., Suc, J.P., Melinte-Dobrinescu, M., Parize, O., Imbert, P., Delhaye-Prat, V., 2011. Quaternary "compound" incised valley in a microtidal environment, Roussillon continental shelf, western gulf of Lions, France. Journal of Sedimentary Research, 81, 708-729.

Tesson, M., Posamentier, H., Gensous, B., 2015. Compound incised-valley characterization by high-resolution seismics in a wave-dominated setting: example of the Aude and Orb rivers, languedoc inner shelf, gulf of Lion, France. Marine Geology, 367, 1-21.

Thamban, M., Rao, V.P., Schneider, R.R., 2002. Reconstruction of late quaternary monsoon oscillations based on clay mineral proxies using sediment cores from the western margin of India. Marine Geology, 186, 527-539.

Torsvik, T.H., Amundsen, H., Hartz, E.H., Corfu, F., Kusznir, N., Gaina, C., Doubrovine, P.V., Steinberger, B., Ashwal, L.D. and Jamtveit, B., 2013. A Precambrian microcontinent in the Indian Ocean. Nature Geoscience, 6, 223.

Traini, C., Menier, D., Proust, J. N., Sorrel, P., 2013. Transgressive systems tract of a ria-type estuary: The Late Holocene Vilaine River drowned valley (France). Mar. geol. 337, 140-155, doi:10.1016/j.margeo.2013.02.005

Vail, P. R., Mitchum, R. M. Jr., Thompson, S., III, 1977. Seismic stratigraphy and global changes of sea level, part four: global cycles of relative changes of sea level. American Association of Petroleum Geologists Memoir 26, 83–98.

Vail, P.R., Mitchum, R.M., Jr., 1977, Seismic stratigraphy and global changes of sea level, part 1: overview: in Payton, C.E. (Ed.), Seismic stratigraphy- applications to hydrocarbon

exploration, American Association of Petroleum Geology, Memoir 26, Tulsa, Oklahoma, 51-52.

van Geldern, R., Hayashi, T., Bottcher, M.E., Mottl, M.J., Barth, J.A., Stadler, S., 2013. Stable isotope geochemistry of pore waters and marine sediments from the New Jersey shelf: methane formation and fluid origin. Geosphere, 9, 96-112.

Varadachari, V.V.R., Sharma, G.S., 1967. Circulation of the surface waters in the North Indian Ocean. Journal of Indian Geophysical Union, 4, 61-73.

Varma, S., Michael, K., 2012. Impact of multi-purpose aquifer utilisation on a variable-density groundwater flow system in the Gippsland basin, Australia. Hydrogeology Journal, 20, 119-134.

Veerayya, M., Almeida, F., 1996. Acoustic basement: Its relevance to Karwar port development. Proceeding International conference on Ocean Engineering (COE), IIT Madras, India, 404-409.

Veerayya, M., Karisiddaiah, S. M., Vora, K. H., Wagle, B. G., Almeida, F., 1998. Detection of gas-charged sediments and gas hydrate horizons along the western continental margin of India. Geological Society, London, Special Publications, 137, 239-253.

Veerayya, M., Murty, C.S., Varadachari, V.V.R., 1981. Sediment distribution in the offshore regions of Goa. Indian Journal of Marine Sciences, 10, 332-336.

Vora, K.H., Almeida, F., 1990. Submerged reef systems on the central western continental shelf of India. Marine Geology, 91, 255-262.

Vora, K.H., Wagle, B.G., Veerayya, M., Almeida, F., Karisiddaiah, S.M., 1996. 1300 km long late pleistocene-holocene shelf edge barrier reef system along the western continental shelf of India: occurrence and significance. Marine Geology, 134, 145-162.

Vora, k. H., 1997. Past sea level changes along the western continental margins of India: evidences from morphology of the sea bed. Lecture note, CSIR-NIO, 5pp.

Vora, K.H., 2007. Past sea level changes along the western continental margins of India: Evidences from morphology of the sea bed. Lecture Notes, Refresher Course in Marine Geology and Geophysics, National Institute of Oceanography, Dona Paula, India, 97-101.

Wadia D.N., 1975. Geology of India (4th Edn.). Tata McGraw-Hill Publishing Company Limited, New Delhi.

Waelbroeck, C., Labeyrie, L., Michel, E., Duplessy, J. C., McManus, J. F., Lambeck, K., Balbon, E., Labracherie, M., 2002. Sea-level and deep water temperature changes derived from benthic foraminifera isotopic records. Quaternary Science Reviews, 21, 295-305.

Wagle, B.G., Veerayya, M., 1996. Submerged sand ridges on the western continental shelf off Bombay, India: evidence for late pleistocene-holocene sea-level changes. Marine geology, 136, 79-95.

Wagle, B.G., Vora, K.H., Karisiddaiah, S.M., Veerayya, M., Almeida, F., 1994. Holocene submarine terraces on the western continental shelf of India; implications for sea-level changes. Marine Geology, 117, 207-225.

Weatherall, P., Marks, K.M., Jakobsson, M., Schmitt, T., Tani, S., Arndt, J.E., Rovere, M., Chayes, D., Ferrini, V., Wigley, R., 2015. A new digital bathymetric model of the world's oceans. Earth and Space Science, 2, 331-345.

White, R., McKenzie, D., 1989. Magmatism at rift zones: the generation of volcanic continental margins and flood basalts. Journal of Geophysical Research, Solid Earth, 94, 7685-7729.

Whiting, B.M., Karner, G.D., Driscoll, N.W., 1994. Flexural and stratigraphic development of the West Indian continental margin. Journal of Geophysical Research: Solid Earth, 99, 13791-13811.

Widdowson, M., 1997. Tertiary palaeosurfaces of the SW Deccan, western India: implications for passive margin uplift. Geological Society of London, 120, 221-248.

Woodroffe, C.D. 1983. Development of mangrove forests from a geological perspective. In: Teas, H.J. (Ed.), 1983. Biology and Ecology of Mangroves. Dr. W. Junk, The Hague, 1-17.

Yilmaz, Ö., 2001. Seismic data analysis: Processing, inversion, and interpretation of seismic data. Society of exploration geophysicists, Tulsa.

Zaitlin, B.A., Dalrymple, R.W., Boyd, R., 1994. The stratigraphic organization of incised-valley systems associated with relative sea-level change. In: Dalrymple, R.W., Boyd, R., Zaitlin, B.A. (Eds.), Incised-valley systems: Origin and sedimentary sequences. Sedimentology and Paleontology Special Publication, 51, 45-60.

Zecchin, M., Catuneanu, O., 2013. High-resolution sequence stratigraphy of clastic shelves I: units and bounding surfaces. Marine and Petroleum Geology, 39, 1-25.

Zhang, Z.Z., Zou, L., Cui, R.Y., Wang, L.B., 2011. Study of the storage conditions of submarine freshwater resources and the submarine freshwater resources at north of Zhoushan sea area. Marine Science Bullettin, 30, 47-52.

Zheng, S., Wu, B., Wang, K., Tan, G., Han, S., Thorne, C.R., 2017. Evolution of the Yellow River delta, China: Impacts of channel avulsion and progradation. International Journal of Sediment Research, 32, 34-44.

List of Publications of the Author

• Research articles

1. **Dubey, K.M.**, Chaubey, A.K., Mahale, V.M. and Karisiddaiah, S.M., 2019. Buried channels provide keys to stratigraphic and paleo-environmental changes: a case study from the west coast of India. Geoscience Frontiers, 10, 1577-1595.

2. **Dubey, K.M.**, Chaubey, A.K., 2019. Origin and distribution of gas charged sediment over inner continental shelf off Goa. Current Science, 116 (8), 1410-1417.

3. Kumar P., Mishra A.**,** Kumar P.V., Kumar, S., **Dubey, K.M.**, Singh, D., Chaubey A.K. 2018. Integrated Geophysical Appraisal of Crustal Structure and Tectonic Evolution of the Angria Bank, Western Continental Margin of India. Marine Geophysical Research doi:10.1007/s11001-019-09383-9.

• Conference (abstracts)

1. **Dubey, K.M**., Chaubey, A.K. Seismic Signatures of Shallow Gas Charged Sediments and their Distribution Pattern on the inner continental shelf of central west coast of India. 40th Annual Convention, Seminar and Exhibition of AEG, 1-3rd November 2018, held at IIT-Bombay. Abst. 80.

2. Jacob, J., Vinay Kumar P., **Dubey K.M**., Mishra A., Kumar P., Kumar S. and Chaubey A.K. Integrated geophysical analysis for identifying tectonic elements in the mid Thane creek. 40th Annual Convention, Seminar and Exhibition of AEG, 1-3rd November 2018, held at IIT Bombay, Mumbai. Abst. 8.

3. **Dubey, K.M.,** Chaubey, A.K. A tool to decipher the total period of non-deposition and erosion over a subaerial unconformity using base level concept. International conference on Recent Trends in Multi-Disciplinary Research (ICRTMDR), held at V.O. Chidambaram College, Thoothukudi, Tamilnadu, during 19-20th April 2018. pp.161.

4. Vinay Kumar P., Jacob J., **Dubey K.M**., Mishra Akhil, Kumar Shravan, Kumar, P., Chaubey A.K. Integrated geophysical investigation of offshore extension of Alibag-Uran fault, Mumbai, India. International Conference on Recent Trends in Multi-Disciplinary Research (ICRTMDR) held at V.O. Chidambaram College, Thoothukudi, Tamilnadu, during 19-20th April 2018, page no-142.

5. **Dubey, K.M.**, Chaubey, A.K. Extent and formation of buried channels on the continental shelf off Goa, central west coast of India. Emerging Trends in Geophysical Research for Make in India held at IIT, Dhanbaad during 9-11 March 2018.

6. Chaubey, A.K., **Dubey, K.M.**, Singh, D., Mishra, A. Identification and Mapping of submarine ground water discharge zone due to tidal pumping using geophysical techniques:

A case study off Udupi, Karnataka. National Seminar on 'Approaches to clean and sustainable development in coastal zones of India- Present status and future need', held at CSIR-National Institute of Oceanography, Regional Centre, Mumbai during 25-26 August 2016, pp. 18.

7. Chaubey, A.K., **Dubey, K.M.**, Mahale, V.M. and Karisiddaiah, S.M. Seismic geomorphology of buried channel system off Goa, central west coast of India. International Symposium on the Indian Ocean on 'Dynamics of the Indian Ocean: Perspective and Retrospective', held at CSIR-National Institute of Oceanography, Goa during 30 November-4 December, 2015, pp. 565.